Vibrational spectroscopic studies on some intermolecular complexes of the halogens.

George William Brownson

UNIVERSITY OF DURHAM

A THESIS

entitled

VIBRATIONAL SPECTROSCOPIC STUDIES ON SOME INTERMOLECULAR COMPLEXES OF THE HALOGENS

Submitted by

GEORGE WILLIAM BROWNSON, B.Sc.
(UNIVERSITY COLLEGE)

A candidate for the degree of Doctor of Philosophy

1975

ACKNOWLEDGEMENTS

I wish to express my gratitude to Dr. D. Steele for the use of his normal co-ordinate program 'LINDA' without which it would have been impossible to complete Chapter 6. My thanks are also due to Dr. R.N. Jones of N.R.C. Ottawa for the use of his band shape analysis programmes.

It has been both a joy and a privilege to work in the Science Laboratories at Durham. In particular, I would like to thank my Supervisor, Dr. J. Yarwood, for his constant encouragement and enthusiasm, Mrs. Eileen Duddy for her good nature and patience in typing this manuscript, and last, but by no means least, Mrs. Kay Jones and Mr. Dave Hartshorn for drawing and photographing (respectively) many of the diagrams and spectra.

TO MY MOTHER

MEMORANDUM

The work described in this thesis was carried out in the University of Durham between September 1969 and October 1974. This work has not been submitted for any other degree and is the original work of the author except where acknowledged by reference.

Part of this work has been the subject of the following publications:-

G.W. Brownson and J. Yarwood, J. Mol. Struct., 10, 147 (1971).

G.W. Brownson and J. Yarwood, Spect. Lett., 5, 193 (1972).

G.W. Brownson and J. Yarwood, Adv. Mol. Rel. Processes, 5, 1 (1973).

ABSTRACT

The work described in this thesis may be divided into three parts.

The first part is an investigation into the changes which occur in the pyridine spectrum when the molecule complexes with the halogens or ICN. It has been shown that intensity changes are due to charge transfer and other (electrostatic) interactions. Normal co-ordinate calculations show only minor changes in vibrational mixing on complexation (see below).

The second part of this work is a detailed investigation of the changes in the IX acceptor spectra on complexation with pyridine, dioxan, and other donor solvents. Studies on the variations of temperature and concentration were carried out to determine the nature of the absorptions in the very far-infrared (<150 cm.$^{-1}$) for these complexes. It has been shown that for the 'weaker' interactions (*e.g.* dioxan-I_2) the bands arise from a 'collisional' mechanism. However, for the longer-lived pyridine-X_2 complexes the band is composite. This is partly due to a well-defined $\nu_{(D-I)}$ mode broadened by vibrational relaxation in a polar medium of excess donor. There is also a contribution from the Poley-Hill 'libration' of the complex dipole in solution. Band shape studies show that the rotation of the pyridine donor in solution is considerably restricted by intermolecular forces. The acceptor band profile reflects only vibrational and/or translational effects.

The third part describes normal co-ordinate calculations for the 'triatomic' (D-X-Y) and 'whole molecule' models of the pyridine-IX (X = Cl, Br) complexes. The pyridine-d_5-IX complexes were used to calculate the interaction constant for the D-X-Y system. This information was used with the pyridine force field to calculate the frequencies and normal co-ordinates for the 'whole complex' molecule. It is shown that the frequency shifts observed on complexation are caused largely by the G matrix changes when the X-Y molecule is complexed. It was found that some mixing between the

essentially D-I-X vibrations and the 'ring' modes does occur. The pyridine normal co-ordinates, however, change little on going to the complex, and the massive intensity changes thus appear to be due to electronic re-distribution during vibration.

CONTENTS

CHAPTER 1

Introduction

A. Scope and Objectives of this Work.

The work described in this thesis can be divided into four main sections.

The first section deals with the effect of the formation of a donor-acceptor complex on the vibrational spectra of the donor and acceptor molecules. A series of halogens, interhalogens and the 'pseudo' halogen, iodine cyanide, were used as acceptors complexing with both strong and weak donors. In particular, the effects which the 'strong' donor pyridine and the 'weak' donor p-dioxan have on the vibrational spectra were investigated.

In the case of the p-dioxan-iodine complex a study was made to try and establish if a 'rigid' or 'well-defined' complex existed in solution. The pyridine-iodine monochloride complex is usually considered a 'well-defined' stable complex. A stable complex might be defined as a complex which does not change chemically over the period it takes to make the measurement. Whilst the iodine chloride molecules will interchange, the equilibrium constant is large (about 146 litre $mole^{-1}$) and the equilibrium

$$Py + ICl \rightleftharpoons PyICl$$

will be far over to the right. The complex will thus have a long lifetime relative to the period it takes to make vibrational measurements. The dioxan-iodine complex, on the other hand, has a much smaller equilibrium constant (about 0·89 litre $mole^{-1}$) and will have a much shorter lifetime than the pyridine-iodine chloride complex. A search was made for bands due to the oxygen-iodine stretching mode. The absorption band found in this region did not seem to behave like a normal vibrational band.

This resulted in the second part of this work, a systematic variation of temperature, donor concentration, and acceptor concentration observing

the change in band shape, intensity and frequency. This information was then interpreted in terms of a collisional model.

The third part of this thesis deals with a normal co-ordinate study on pyridine and the pyridine complexes to find out how much the changes in vibrational spectra were due to the mass effect, how much due to force constant (chemical) changes and how much due to mixing of the donor and acceptor vibrations.

Finally, the inorganic chemistry of halogen complexes is very interesting and the fourth part deals with the preparation of a number of ionic complexes not mentioned in the literature. Unfortunately, most of the complexes prepared decomposed in solution. However, the vibrational spectra in the solid were observed and an attempt made to explain the structure in terms of the spectra.

B. Instrumentation in the Far-Infrared Region.

(i) Fourier Theory.

The far-infrared spectra recorded over the region 50-400 $cm.^{-1}$ were obtained using a Beckman-RIIC Ltd. FS720 Interferometer. The interferogram was recorded on eight track paper tape and then analysed using the computer program given in Appendix A. The computation was carried out using the I.B.M. 360/67 computer jointly owned by the Universities of Newcastle and Durham.

Fourier theory was originally developed by J.B.J. Fourier[1] to solve the one-dimensional heat-diffusion equation. However, this theory has applications far beyond the bounds of heat transmission. Michelson[2] discovered that the interference pattern from a two beam interferometer as a function of the path difference between the two beams is the Fourier transform of the optical power spectrum of the source illuminating the interferometer. Before the advent of optical detectors and electrical

data recording the technique was impracticable because the intensity and number of fringes had to be estimated visually.

The full theory of the application of Fourier theory to interferometric spectroscopy is beyond the scope of this thesis. There are, however, a number of excellent papers on this topic in the literature.[3-6] Only a general outline of the technique will be discussed here.

It is first important to understand the meaning of some of the mathematical expressions and theorems frequently encountered.

(a) Fourier's Theorem.

Any periodic function f(x) can be expressed as the sum of a series of sinusoidal functions which have wavelengths which are integral sub-multiples of the wavelength λ of f(x).

$$f(x) = C_o + C_1\cos(\frac{2\pi x}{\lambda} + \alpha_1)\ldots. + C_n\cos(\frac{2\pi xn}{\lambda} + \alpha_n) \quad \cdots\cdot \quad [1.1]$$

The n's are called 'orders of the terms' which are harmonics.

(b) Fourier Analysis.

This is the name given to the determination of amplitude C_n and the phase angle α_n in Eqn. [1.1]. Fourier theory has an extension to non-periodic functions based upon the concept of the Fourier transform. A beam of light is a periodic function, so expressing a beam of light in terms of a Fourier series, would be to express it as a sum of waves each with a particular C_n and λ/n corresponding to the frequencies of the component beams.

(c) The Fourier Transform.

Fourier's theorem refers to periodic functions. By definition the function f(x) is periodic, if f(x+p) = f(x), for every x, where p is the period.

The Fourier series must be modified to cover the case of a continuous spectrum of wavelengths of light. Since an integral is the limit of a sum, the Fourier series (i.e. a sum of terms) is replaced by a Fourier integral.

The Fourier integral represents a continuous spectrum of frequencies.

The Fourier transform of a function f(x) is defined as,

$$a(k) = \int_{-\infty}^{+\infty} f(x)\exp(ikx)dx \qquad \ldots\ldots \quad [1.2]$$

The Fourier transform of a Fourier transform is the original function multiplied by 2π.

(d) The Convolution Theorem.

The convolution of two functions (f(x) and g(x)) is defined by the function

$$F(x) = \int_{-\infty}^{+\infty} f(x')g(x - x')dx' \qquad \ldots\ldots \quad [1.3]$$

where F(x) is called the convolution of f(x) and g(x) and x' is the 'dummy' variable. It is the sum of the product of the two functions over the region where they both have values. The Fourier transform of the convolution of two functions is the product of their individual transforms.

Functions which can be most easily Fourier-transformed with the help of the convolution theorem, include functions which can be expressed as the product of two simple functions, and whose transforms are therefore written as a convolution. An observed spectrum is the true optical spectrum, convoluted with the slit function.

(e) The δ Function.

The δ function is the limit of a square pulse as its width h goes to zero, but its enclosed area Hh (H is the height) remains at unity. It is therefore zero everywhere except at x = 0, where it has infinite value. The transform of a δ function at the origin in one dimension is a constant.[7]

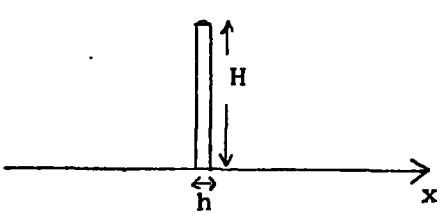

(2) Fourier Transform Spectroscopy.

Fourier transform spectroscopy is dependent upon the fact that in a two beam interferometer the intensity of the central light fringe is the Fourier transform of the incident original power spectrum. The spectral intensity $G(\bar{\nu})$ at any frequency $\bar{\nu}$ cm.$^{-1}$ with the measured interferogram intensity I(x) is given (neglecting the imaginary part) by,

$$G(\bar{\nu}) = \sum_{x=0}^{x=\infty} [I(x) - \frac{I(o)}{2}]\mathrm{Cos}(2\pi\bar{\nu}x)dx \quad \ldots\ldots \quad [1.4]$$

where x is the optical path difference of the two terms and I(o) is the interferogram intensity at zero path difference. The intensities of the interferogram are measured at discrete values of optical path difference $n\Delta x$ up to some maximum value $N\Delta x$ where n is an integer equal to 0,1,2,3,4 ... N and Δx is the interferogram sampling interval. The value of Δx must be such that

$$\Delta x \leqslant \frac{1}{2(\bar{\nu}_1 - \bar{\nu}_2)} \quad \ldots\ldots \quad [1.5]$$

where $(\bar{\nu}_1 - \bar{\nu}_2)$ is the total range of frequencies incident upon the detector. Special filters (e.g. black polythene) are used to restrict the range of frequencies incident upon the detector from 0 to $\bar{\nu}_{max}$, where $\bar{\nu}_{max}$ is the high frequency cut off, i.e. $\bar{\nu}_2 = 0$.

$$\Delta x \leqslant \frac{1}{2\bar{\nu}_{max}} \quad \ldots\ldots \quad [1.6]$$

This ensures that the highest frequency present is sampled at least once every half cycle.

Equation [1.4] becomes approximated to the sum,

$$G(\bar{\nu}) = \sum_{n=0}^{n=N} [I(n\Delta x) - \tfrac{1}{2}I(o)]\mathrm{Cos}(2\pi\bar{\nu}n\Delta x)\Delta x \quad \ldots\ldots \quad [1.7]$$

when n = 0

$$G(\bar{\nu}) = \frac{I(o)\Delta x}{2}$$

The output of the detector is amplified and converted to binary numbers. The range of the digitiser is from 2^0 to 2^{12}. The value of $\frac{1}{2}I(o)$ is obtained by taking the average value of the interferogram and must be subtracted from all values of I(x) before Fourier transform computations begin. The computed spectral intensities $G(\bar{\nu})$ are directly proportional to the measured amplitudes of the interferogram function, i.e.

$$\left[I(n\Delta x) - \frac{I(o)}{2}\right]$$

and the first term in the summation makes a constant contribution to the whole spectrum and is independent of $\bar{\nu}$. However, the Fourier transform depends only upon the oscillation of the function and there is no theoretical reason why $I(o)/2$ should be subtracted. However, in practice subtracting $I(o)/2$ reduces the size of the figures in the array to be transformed and saves computing time. The transform program will only transform arrays which are of the size 2^n where n is an integer. This is because our program uses the Cooley-Tukey Algorithm[16] (see below).

Because a finite sampling interval is involved all interferograms will contain a phase error depending upon how near the sampling point has come to the exact zero path position. Corrections for phase error due to this must be made.

The optical resolution $\Delta\bar{\nu}$ of the interferometer is related to the distance (D) travelled by the moving mirror.

$$\Delta\bar{\nu} = 2D\left[\frac{\sin[2\pi(\bar{\nu}-\bar{\nu}'_{max})D]}{[2\pi(\bar{\nu}-\bar{\nu}'_{max})D]}\right] \quad \ldots\ldots \quad [1.8]$$

where the total path difference $D = N\Delta x$, $\bar{\nu}'_{max}$ is the frequency of the peak at its maximum and the width at half height is $(\bar{\nu} - \bar{\nu}'_{max})$.

This equation has the limiting condition that the smallest interval resolved is approximately

$$\Delta\bar{\nu} \approx {}^{0.7}/D \text{ usually further approximated to } {}^{1}/D \quad \ldots\ldots \quad [1.9]$$

Since the computed spectrum is the convolution of the actual spectrum with the instrumental function, the subsidiary side lobes of the latter cause oscillations to be seen near regions where rapid changes in absorption are occurring. These oscillations give rise to 'noise' which should be eliminated as far as possible. The process of weighting the interferogram values $[I(n\Delta x) - \frac{1}{2}Io]$ so that the modulation of the interferogram goes to zero at maximum path difference D, $(N\Delta x)$ is known as 'apodisation'. Apodisation usually involves modifying the scanning function so that it takes no negative values and the side lobes are reduced. Although the central band is made much broader, i.e.

$$\Delta\bar{\nu} = 2D\left[\frac{\sin^2[2\pi(\bar{\nu}-\bar{\nu}'_{max})D]}{[2\pi(\bar{\nu}-\bar{\nu}'_{max})D]^2}\right] \qquad \ldots\ldots \quad [1.10]$$

and the price of reducing side bands is lower resolution. The resolution is reduced to

$$\Delta\bar{\nu} \approx {}^2/D \qquad \ldots\ldots \quad [1.11]$$

In this work normal runs were 1024 points with a sampling interval of 8 microns. This gave a resolution of 2·5 $cm.^{-1}$ since all the interferograms were apodised.

The angular beam spread of off axis rays due to imperfect collimation of the finite source aperture will also reduce the resolution. If the source subtends a solid angle Ω at the collimating mirror then the maximum value[4] of R is given by

$$R = \frac{2\pi}{\Omega} \approx 8\left(\frac{f}{d}\right)^2 \approx \frac{\bar{\nu}}{\Delta\bar{\nu}} \qquad \ldots\ldots \quad [1.12]$$

where d is the source diameter and f is the focal length of the collimating mirror.

The FS720 has source apertures of 3, 5 and 10 mm. which give resolving powers of 10^4, 4×10^3 and 10^3 respectively.

The fact that the source beam has a finite width results in the off axial rays of light having to travel slightly further than the axial rays. This leads to all the calculated frequencies being over-estimated by a factor of the order of $(1 + \frac{\Omega}{4\pi})$. The true frequencies can be obtained from the calculated frequencies by the formula,

$$\bar{\nu}_{true} = \frac{\bar{\nu}_{(calc.)}}{(1 + \frac{\Omega}{4\pi})} \quad \ldots\ldots \quad [1.13]$$

In practice this factor is only of the order of $10^{-4}\bar{\nu}_{(calc.)}$ and only becomes important where high resolution is required at high frequencies. In this research this was not a problem as most of the work was carried on broad bands at low frequency.

The region over which measurements can be made depends on the thickness of the beam splitter. Unfortunately a beam splitter with a transmittance and reflectance of 50% does not exist. In practice a Melinex (polyethylene terephthalate) beam splitter is used because it has a high permittivity and a refractive index of 1·85 in the far infrared.[8] The beam splitter efficiencies at various thicknesses are shown in Figure 1.1.

If 50% of the light were reflected and 50% transmitted the beam splitter would reach its theoretically ideal value of 25% (i.e. the product). In practice multiple internal reflections reduce the beam splitter efficiency.[9,10]

The overall efficiency of the beam splitter is given by

$$E \alpha (2\pi\bar{\nu}d') \quad \ldots\ldots \quad [1.14]$$

where E is the efficiency

$\bar{\nu}$ is the frequency of incident radiation

d' is the apparent thickness of the beam splitter material.

In the FS720 where the beam splitter is at 45^{o} to the two Michelson mirrors d' is given from the refractive index n and true thickness d.

$$d' = d\sqrt{n^2 - \tfrac{1}{2}} \quad \ldots\ldots \quad [1.15]$$

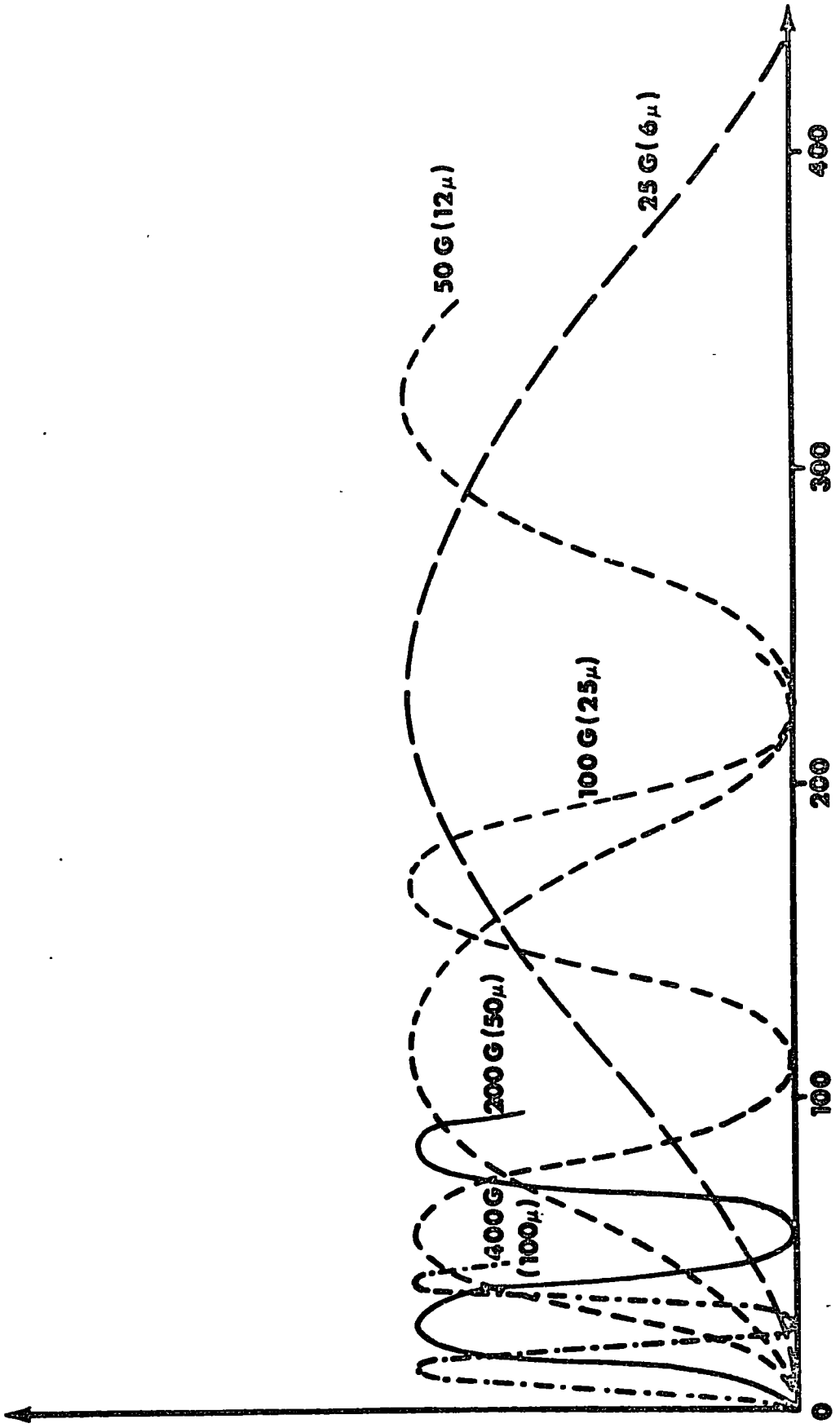

Fig 11 RELATIVE BEAM SPLITTER EFFICIENCIES

By choosing the beam splitter of appropriate thickness it is possible to obtain spectra throughout the far-infrared region.

It is advisable to use optical filters to restrict the energy falling on the detector to the frequency range of interest. The table below lists some typical beam splitter and optical filter combinations.

Table 1.1.

'Frequency' Range/ $cm.^{-1}$	Beam Splitter Thickness	Filter
140-350	6 microns (25 gauge)	Black lens
300-500	$4\frac{1}{2}$ microns (15 gauge)	Yoshinaga filter, white lens
20-220	12 microns (50 gauge)	Black lens

The detector in the FS720 was a Golay pneumatic detector.[11] A chamber containing gas of low thermal conductivity is sealed at one end with a diamond window through which radiation reaches a thin absorbing film. The absorbing film has a low thermal capacity and responds readily to infrared radiation, in turn warming the gas with which it is in contact. A rise in temperature of the gas in the chamber produces a corresponding rise in pressure and therefore a distortion of the mirror membrane with which the other end of the gas chamber is sealed. To prevent changes in room temperature from affecting the detector a fine leak is provided which connects the detector chamber with a ballasting reservoir of gas on the other side of the mirror membrane. In the absence of a changing radiation signal pressures are the same on both sides of the membrane which remains flat.

An alternating radiation of f cycles per second will produce a corresponding deformation of the mirror membrane at f cycles per second

which by a suitable optical system and photocell can be converted into an alternating voltage.

Golay detectors[13] have a signal to noise ratio of 30 - 50 on grating instruments but this is increased to over 150 on interferometers for a resolution of 2 $cm.^{-1}$

Therefore it is clear that the grating instrument has few advantages over the interferometer except that the interferogram requires computation before a spectrum can be obtained. However, this poses few problems where good computing facilities are available.

3. Advantages of Interferometers over Grating Instruments.

(i) Sources in the far-infrared region are very weak. The source used in this work was a high pressure mercury discharge in a silica envelope. Since silica absorbs above 70 $cm.^{-1}$ the lamp is just a hot silica rod for most of the far-infrared region (40-400 $cm.^{-1}$). Using an interferometer the whole spectral range falls simultaneously upon the detector at a given time rather than a single resolution width as with a grating instrument. Thus the interferometer receives information about the full spectral range during an entire scan while a grating instrument receives information only in a narrow band at a given time. (This is the Fellgett advantage[7]).

(ii) To cover the far-infrared region several gratings would be required with a series of filters for removing unwanted orders of diffracted radiation and 'stray' light. With a monochromator it is also necessary to halve the slit widths in order to double the resolution and this reduces the signal to noise level by a factor of four. Thus, it would take sixteen times as long to maintain the same signal to noise ratio by increasing the time constant on a grating instrument as an interferometer. In order to double the resolution on an interferometer one has only to double the distance travelled (i.e. double the time taken).

The fact that the spectrum is calculated does in itself have some advantages because certain mathematical improvements can be made in the data to produce a more accurate spectrum.[12] These include:-

(i) Apodisation. This smoothes out noise ripples giving more accurate transmission data. (For a further discussion see the following section on Computing).

(ii) Aliasing. The equation [1.7] for $G(\bar{\nu})$ does not give the true spectrum $G_T(\bar{\nu})$ because a finite sampling interval Δx has been used. It has been shown that[14]

$$G(\bar{\nu}) = G_T(\bar{\nu}) \times D' \quad \ldots\ldots \quad [1.16]$$

where D' is the transform of the dirac comb function D. $D' = f(\bar{\nu}, \Delta x, \delta)$.

However if $\bar{\nu}_{max} < \frac{1}{2\Delta x}$

$$G(\bar{\nu}) = G_T(\bar{\nu}) \quad \ldots\ldots \quad [1.17]$$

Therefore by filtering off all frequencies greater than $\bar{\nu}_{max}$ the computed spectrum is made identical with the true spectrum.

The FS720 interferometer used in this work had 2 sampling intervals available (i.e. 4 and 8 microns) with aliasing frequencies of 1250 and 625 $cm.^{-1}$ respectively. In most cases the 4 micron sampling interval was used because of the 'oversampling advantage' making the approximation of $G(\bar{\nu})$ more accurate. In practice little difference was observed using the two sampling intervals. Filtering out frequencies above 450 $cm.^{-1}$ was done using a black polythene filter. For work between 400-550 $cm.^{-1}$ a Yoshinaga filter was used to remove frequencies above 550 $cm.^{-1}$ No measurements have been done in this work above 550 $cm.^{-1}$ using the FS720.

(iii) Truncation. The effect of only being able to integrate to a maximum path difference D instead of to infinity may be expressed[14] as

$$G_T(\bar{\nu}) = G(\bar{\nu})C'$$

C is a crenel function which is unity for $|x| < n\Delta x$ and zero for $x > n\Delta x$. C' is the transform of the crenel function. This means that any fine structure in the spectrum $G(\bar{\nu})$ comparable in magnitude to the resolution will be blurred out. The maximum travel allowed on the FS720 is 10 cms. which gave a theoretical resolution of 0·1 $cm.^{-1}$ In fact since the bands studied were > 20 $cm.^{-1}$ wide a resolution[17] of 0·2 x 20 = 4 $cm.^{-1}$ is all that is required. Computation using 1024 points gives a travel distance of 0·82 cms. (sampling interval 8 microns) giving a theoretical resolution of about 1·2 $cm.^{-1}$

(iv) Normalisation. As explained in the section on Computation (see p. 14) the normalisation corrections is used to give the true percentage transmission, correcting for the normalisation of sample and background.

(v) Noise in the Interferogram. A large 'spike' transforms to give a sine wave and this spectrum must be rejected. There is also a danger of normalising to 'peak' noise level rather than 'mean' noise level. The effects of noise can be reduced by removing frequency components outside the range over which the spectrum is required.[15]

(vi) Autocorrelation Procedure. This is explained in the Computation Section (p. 14), it eliminates the problem of phase error.

(vii) Padding. Transforming a padded interferogram is sometimes valuable when the number of padded points added is small. The number of points transformed can only be multiples of 2^n with the Cooley-Tukey algorithm.[16]

Thus if 1012 points were present on a tape, 1024 or 512 points would have to be analysed. To add on extra 12 points would allow all the data to be used. However to add further points is a waste of computing time since the padded points contain no extra information.

From the above discussion it can be seen that interferometric data can be analysed to a high degree of precision. The raw interferogram does at least

indicate whether reaction or cell leakage has occurred. High frequency bands give sharp ripples and low frequency bands broad ripples. This is because the interferogram is the Fourier transform of the power spectrum. In other words the interferogram is the time domain of the optical spectrum. Fast oscillations represent fast variations (sharp ripples) i.e. high frequency, slow oscillations (broad ripples) represent low frequency bands. (This is shown in Figs. 1.2A and 1.2B).

4. Computation.

The interferogram, in pure binary form, is recorded on 8 track paper tape. The tape is spooled on to a magnetic disc using program DCL99SPY. This program converts the binary numbers to decimal numbers (format I4) and then stores these in arrays of 20 as card images on a magnetic disc.

The program most frequently used in this work was filed as DCH05277. This employed an autocorrelation phase correction and a Cooley-Tukey transformation.[16] For convenience the program was written as a series of sub-routines linked to a main program.

A brief description of the program will now be given explaining the main function of each section. The program is listed in Appendix A.

The Main Program.

This section defines the size of the arrays and calls the various sub-routines. Further information is self-evident from the comment cards in the program.

The Sub-routines.

(i) Sub-routine TPREAD (Tape Read).

This sub-routine reads the M decimal numbers of the interferogram from the disc into array A(J) where J = 1,M. Arrangements are provided to read a second tape if a ratioed spectrum is required.

(ii) Sub-routine AMX.

This routine finds the maximum value of the input data i.e. the nearest point to the top of the interferogram central fringe. It then prints out the

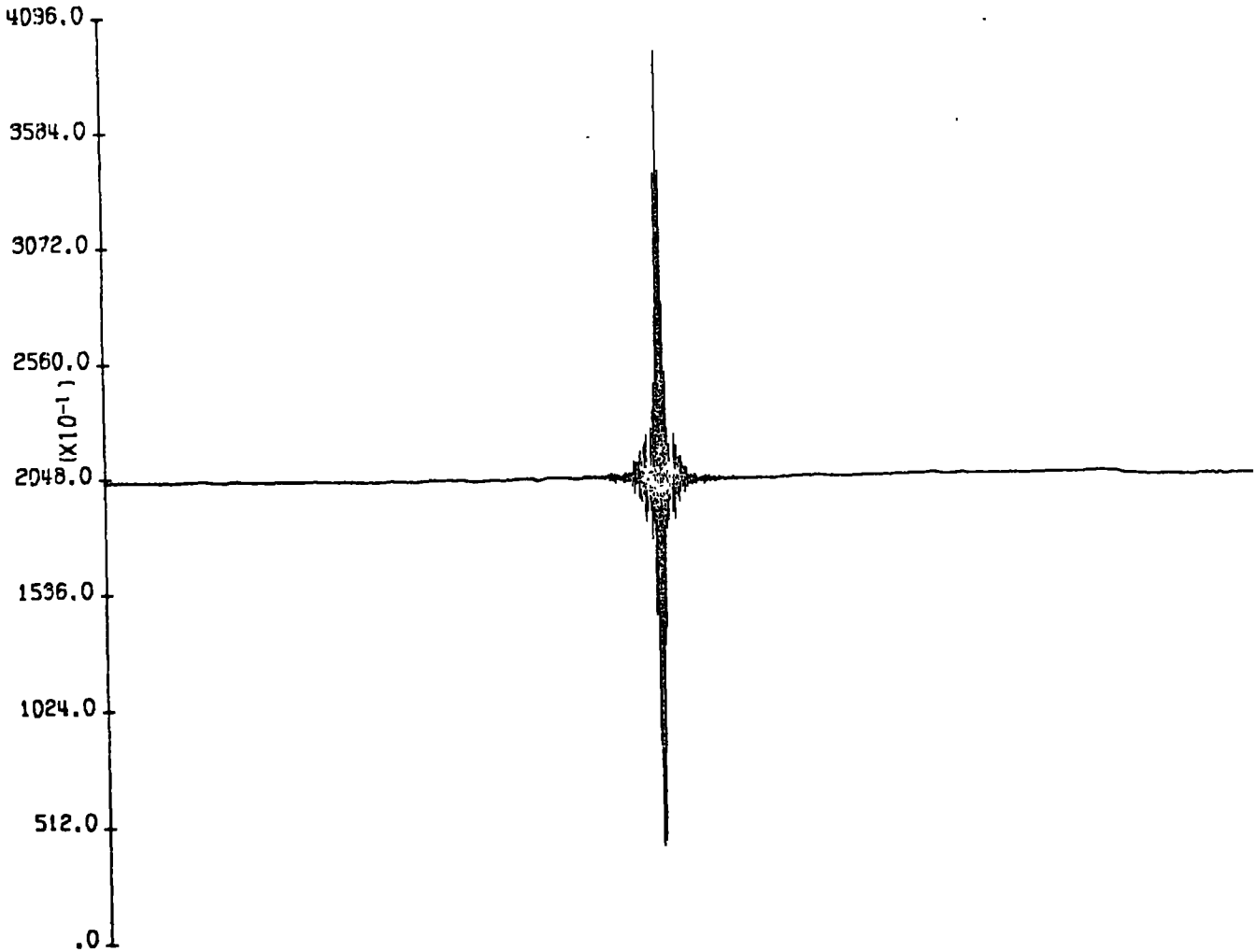

Fig. 1.2A. Interferogram produced by FS720 when only frequencies higher than 450 $cm.^{-1}$ are allowed to fall on the detector.

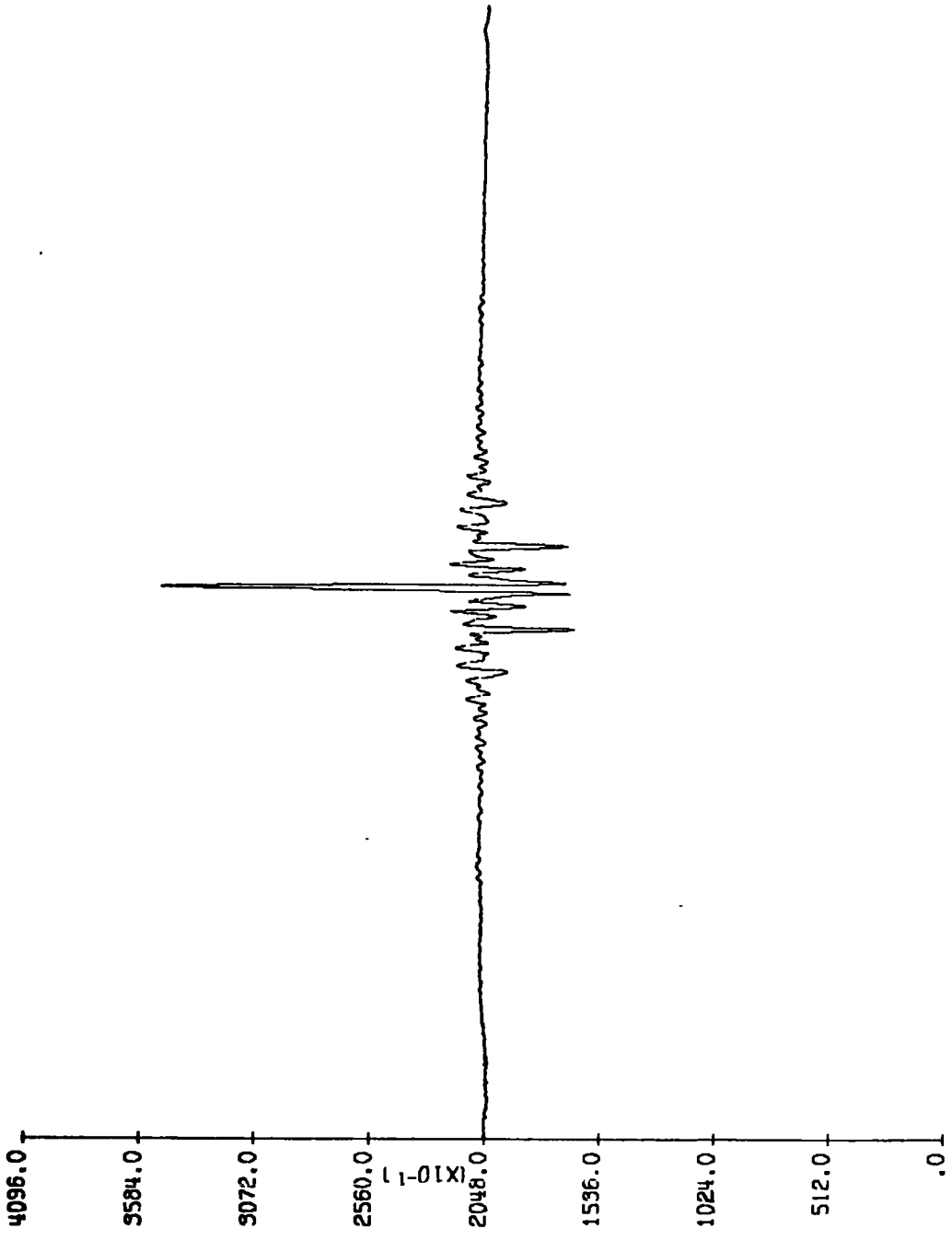

Fig. 1.2B. Interferogram produced by the FS720 when only frequencies below 130 $cm.^{-1}$ are allowed to fall on the detector.

maximum value of the interferogram and the values close to it. If the number of points M is less than the number N to be transformed the program puts in N-M points equal to the M^{th} value. AMX also calculates the average value of the array by summing all the elements of the interferogram and dividing by the number of points.

(iii) Sub-routine SUBDH (Data Handling).

This routine calls AMX (array A maximum value) which gives the maximum value in the array and the average value. The routine there selects $^{N}/_{2}$ points on each side of the maximum value. The copied interferogram is then printed out. The array is reduced by removing the average value from each data point. The reduced interferogram is then printed out as C(K) - K going from 1 to N.

The reduced interferogram is next autocorrelated to remove phase error. Autocorrelation is a process of displacement multiplication of the interferogram C(K) followed by summation of the series. This process always results in a function which is symmetrical about the maximum value and hence phase errors are eliminated. This produces a function as in Figure 1.3.

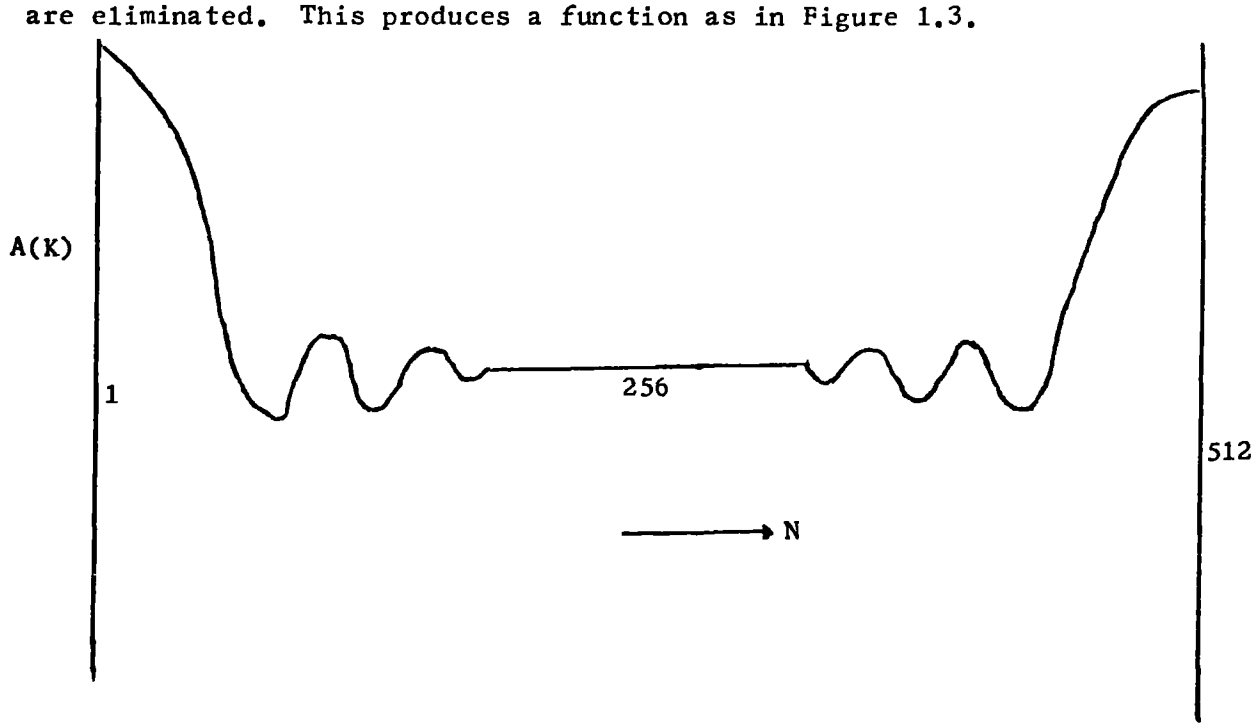

Fig. 1.3.

Initially the large central values of the interferogram are in phase with each other and are thus multiplied by each other, hence at small values of N the summation has a maximum value. As N increases the function reaches a minimum as the maximum values are now multiplied by what is essentially $I(o)/2$. As $N \rightarrow K$ the two arrays are nearly 360^{o} out of phase and the function approaches a maximum again.

Taking 512 points as an example the array is almost symmetrical when one plots A257 → A512 and A1 → 256. The interferogram maximum value is A(1).

The routine AMX is then recalled to find the largest value in the array and to check its position. The interferogram is normalized by dividing by the largest value A(1) and the normalized array is printed out. The autocorrelated interferogram is stored with the largest number in element 1 of the array.

The interferogram must be apodised before transformation otherwise a sinusoidal ripple appears on the computed spectrum.[12] The apodisation function used in this work was,

$$\text{APOD} = \text{Cos}^{2}\pi\left(\frac{K-1}{N-2}\right) \qquad \ldots\ldots \quad [1.18]$$

where K goes from 1 to $N/2$.

The maximum at zero path difference is not affected since if K = 1, then APOD = 1. The apodisation function reaches a very small value at its extremes as illustrated by Table 1.2.

(iv) Sub-routine TM (Transformation).

This carries out a Fourier transform by the Cooley Tukey Algorithm.[16] The spectral distribution is obtained from a 'one-sided' Fourier cosine transform and hence must consist of a symmetric function about zero path difference. This is why the autocorrelation procedure by convolution of the interferogram with itself giving a completely symmetric interferogram is used

Table 1.2.

N	K	APOD
512	1	1
512	35	0•9574
512	86	0•750
512	137	0•448
512	171	0•250
512	205	0•095
512	239	0•0108
512	256	0

in SUBDH. The spectrum was not computed using a double-sided power transform because it has the disadvantage that the signal/noise ratio is poorer in regions of low energy.

(v) Sub-routine PT (Plot).

The results of the Fourier transform over the spectral region are selected, the square root of the intensities taken (since the autocorrelation procedure effectively squares the intensity data) and the transmission value is normalized by dividing by the maximum value. The sub-routine calls the sub-routine LP (line printer) which prints the scale on the transmission axis prior to printing the spectrum on the line printer using sub-routine GP (graph plot).

(vi) Sub-routine GP.

A plot of the spectrum on the line printer is produced together with cards.

(vii) Sub-routine COR.

This deals with the gain corrections. Before the normalized single beam spectrum can be ratioed it is necessary to correct for the normalization constants employed and the different gain settings used. The ratioed transmission values are multiplied by a normalization factor NF given by

$$NF = \frac{NC(T_o)}{NC(T) \times NC(R)} \quad \ldots\ldots \quad [1.19]$$

$NC(T_o)$ = normalization constant in background array

$NC(T)$ = " " " sample "

$NC(R)$ = " " " ratioed "

NF gives the ratio of the original transmission values.

In order to compensate for the different gains employed to obtain T and T_o a gain correction which depends on the differences in gain settings is used.

$$1db = 20\log_{10}(\frac{V_1}{V_2})$$

or

$$\frac{V_1}{V_2} = \exp(\frac{2{\cdot}303 \text{ dB}}{20}) = \text{amplification} \quad \ldots\ldots \quad [1.20]$$

where V_1 and V_2 are the amplifier output and input voltages.

The gain correction factor is the reciprocal of the gain increase calculated.

Thus a reading of 5 dB corresponds to an amplification of 1·776, and reading of 10 dB corresponds to an amplification of 1·40 (3·17 - 1·77) so the gain correction to multiply by the ratioed transmission values would be $^1/1{\cdot}40 \approx 0{\cdot}71$.

A typical example in this work would be for pyridine-iodine monobromide in chloroform which had gains of about 35·15 dB and 36·60 dB for the solvent and solution respectively. This results in a gain correction factor of 0·848. It is to be noted that, as the detector aged, the gains had to be increased in order to bring the interferogram level (far from zero path) to 50% on the recorder. However, the difference in gain between sample and background is independent of the age of the detector since it only represents the variation in absorption of sample to background.

C. Instrumentation in the Near Infrared Region.

The Grubb-Parson's GS2A. Near infrared measurements were carried out using a Grubb-Parson's model GS2A. This instrument covers the spectral region between 2 and 25 microns and is fully described in the appropriate Grubb-Parson's Spectrometer Manual. This is a conventional grating (12,000 lines per inch) double beam spectrometer with a Nernst glower source. Vertically oscillating mirrors act as a chopper separating reference and sample beams so that they fall alternately on the detector. The detector is a thermocouple. Potassium bromide and calcium fluoride prisms are used to select the orders of the grating.

The GS2A works on the principal of the optical null balance. A metal comb with 'v-shaped' teeth is provided in the reference beam. This comb is automatically adjusted by means of a servo system to produce at the wavelength selected absorption equal to that of the sample in the other beam.

As long as the energy received by the spectrometer from each beam is equal there will be no change in energy received by the detector while the mirrors are reciprocating. When the sample absorbs energy, more energy is received from the reference than from the sample beam so that as the mirrors reciprocate there is an alternating component produced in the energy reaching the thermal detector in the spectrometer. The resulting A.C. output from the detector is amplified and used to control the servo motor which drives the comb into the reference beam until balance is restored. If the sample absorption now becomes less, an A.C. output is again produced but of opposite polarity, and this drives the servo motor in the opposite direction until balance is again restored. As the absorption produced by the comb is a linear function of its displacement its position at balance provides a direct measure of the absorption of the sample. The pen of the recorder is mechanically coupled to the comb so that a direct record of sample absorption is obtained

on the chart. Any non-linearity of the scale is due to non-linearity of the comb and is usually small.[16a]

(i) Instrumental Factors to be Optimised to Obtain the most Accurate Results Possible in the Near-Infrared Region.

The response time of the spectrometer is the time it takes the chart recorder to record the signal from the detector. The optical null system has the disadvantage that the motor driving the pen goes progressively slower as balance point is reached. Further, the pen takes a finite time to reach the 'proper' transmission value and this leads to 'tracking' error. The 'tracking' error can be checked by switching off the grating and chart drive on the side of a band. The distance the pen moves before it comes to a step is the 'tracking' error. However, switching on or off caused an electrical 'spike' to appear on the chart so tracking error is difficult to assess. The 'tracking' error was reduced to a minimum by adjusting the gain and the grating speed so that the time taken to scan the steepest part of the band was at least twice the time it takes the pen to rise or fall that distance, when the beam is suddenly blocked off. Normally, speeds of one micron in 30 minutes were adequate. Each band was scanned twice and the difference in peak height should be no more than the tracking error. In most cases the 'tracking' error seemed to be of the order of 0·5% transmission value at transmission value 30%. At 5% transmission the error was about 0·8% and at 50% transmission the error was less than 0·5%.

The formulae for calculating the intensity are strictly only correct if the slit is assumed to be of zero width - which is experimentally impossible.

Normally the resolution is adequate[17] if the slit width is less than $0{\cdot}2\Delta\bar{\nu}_{\frac{1}{2}}$ where $\Delta\bar{\nu}_{\frac{1}{2}}$ is the observed half-band width.

The instrument may be operated with a programmed slit and in this mode of operation the energy falling on the detector is kept approximately constant. However, for the narrow bands in the pyridine complexes it was necessary to

go to the narrowest slit width available consistent with a satisfactory amount of noise-free energy falling on the detector. The optical width (S) is larger than the geometric slit width (d) because the light is not a point source so it has a solid angle at the sample larger than the slit area; in fact $S \approx 400d/n\lambda^2$

where d = geometrical slit width in mm.

λ = wavelength in microns

n = the order of the grating defined below:-

Order	Range	Prism
1	5 - 25 mμ	KBr prism
2	3·6 - 5 mμ	CaF_2 "
3	2·5 - 3·7 mμ	CaF_2 "
4	2 - 2·5 mμ	CaF_2 "

In the case of the 1012 $cm.^{-1}$ band[18] in the pyridine-ICl complex the intensity is constant up to slit widths of 0·5 $\Delta\bar{\nu}_{\frac{1}{2}}$ although the shape changes considerably as the slit is narrowed. For larger slit widths the intensity falls and the band-width increases considerably.

The Ramsay procedure[17] was followed; decreasing the slit width manually until the peak height of the band reaches a maximum showing that S is lower than $\Delta\bar{\nu}_{\frac{1}{2}}$. As the slit is closed the gain must be increased so a compromise must be reached between increased noise and small slit.

Electrical drift was minimised by blocking both beams and adjusting the balance so that over a period of 10 minutes (the time to run a band) transmission variations were less than 1%.

(ii) The Perkin-Elmer 577

A number of measurements were made using the Perkin-Elmer 577 in 1974 for the following reasons:-

(a) Measurements in the 500 $cm.^{-1}$ (twenty micron) region are difficult with the GS2A or the FS720.

Both the polythene and melinex have strong absorptions in this region so using the FS720 little energy was available in this region. The detector in the GS2A is not accurate enough for intensity measurements over about 17 microns.

(b) The GS2A is linear in microns. Since absorption bands are expressed in wave-numbers, and many of the bands overlapped for the systems studied, it is far easier to fold over the non-overlapped portion of the band to determine the band profile and intensity if the measurements are made in wave-numbers.

(c) The PE577 is fitted with a nitrogen 'flush' which eliminates water vapour absorption, this facility is absent in the GS2A.

(d) Measurements on a second machine will give some indication of the systematic error and the reproducibility of the results.

The slit = 2 was used as the compromise between slit width and energy reaching the detector. In all cases for the measurement of intensity the expansion 25, gain division 5 and automatic time constant were used.

The source does not emit the same amount of energy at all wavelengths. To compensate for this and other instrumental factors the slit widths are programmed, to maintain the energy falling on the detector at approximately constant signal-to-noise ratio. At slit = 2 half the normal program slit width and one quarter the normal program energy is used.

The transmission values at 2000 $cm.^{-1}$ (approximately the average frequency studied) were checked using linearty discs. The results are tabulated below.

Theoretical Value Disc	Observed Value
6•3	6•0
13•6	13•1
25•1	25•4
50•0	50•0
70•0	70•0

D. Intensity Measurements in the Near- and Far-Infrared Regions.

The apparent integrated intensity can be obtained from

$$\Gamma_i^a \text{(apparent)} = \frac{1}{C1} \int_{band} Ln(\frac{T}{T_o})_{Ln\nu} d(Ln\bar{\nu}) \quad \ldots\ldots [1.21]$$

or

$$B_i \text{(apparent)} = \frac{1}{C1} \int_{band} Ln(\frac{T}{T_o})_{\nu} d\bar{\nu} \quad \ldots\ldots [1.22]$$

where C is the concentration, 1 the path length, T_o the apparent transmitted radiation intensity of the reference material or cell, T the apparent transmitted radiation intensity of the sample and where the two intensities are related by[19]

$$B_i \approx \Gamma_i^a \bar{\nu}_i \quad \ldots\ldots [1.23]$$

The best value of B_i or Γ_i^a is obtained by plotting the band area against C1 followed by a least squares analysis if sufficient data are available. To obtain a value of the true integrated intensity one must use

$$\Gamma_i^t = \frac{1}{C1} \int Ln(\frac{I_o}{I})_{Ln\bar{\nu}} d(Ln\bar{\nu}) \quad \ldots\ldots [1.24]$$

or

$$A_i = \frac{1}{C1} \int_{band} Ln(\frac{I_o}{I})_{\bar{\nu}} d\bar{\nu} \quad \ldots\ldots [1.25]$$

[where I_o is the incident radiation intensity and I the transmitted radiation intensity] it is then necessary to plot B_i against C1 and extrapolate to C1 = 0.[19,20] This extrapolation is only strictly valid for constant incident radiation and resolving power over the width of the band.[19]

1. Using the GS2A.

Output from the chart recorder (0-50 millivolt scale) was monitored on a Solartron digital voltmeter, model LM1450.

A Solartron data transfer unit measured this voltage every 4 seconds and printed the time and voltage out on a Westroe ASR33 teletype unit. These voltages were also recorded on paper tape. These tapes were then stored on a

magnetic disc in the usual manner. The GS2A program filed as DCHO514 had read into it the starting value in microns, the speed of the wavelength drive in microns per second and the values from the tape. It was then able to calculate the ratioed spectrum.

This method was used to reduce the tedium of feeding in data by hand. A number of band areas were calculated by the program and by hand using a planimeter, the values were in agreement up to about one decimal place.

Table 1.3.

1010 $cm.^{-1}$ (Band PyrIBr/$CHCl_3$)				
Area (from tape)	Area (hand-done)	% Difference	No. of points (hand)	No. of points (tape)
2•81	2•63 2•78	8%	10 15	30
2•90	2•75 2•85	6%	10 15	32
6•84	6•85	0•4%	27	48

The table above compares hand values and tape values. The tape values were slightly more accurate because more points were taken. However, estimation by hand is equally as good if enough points are taken near the central maximum. For hand values to be meaningful the separation between two points must be approximately a straight line otherwise the Simpson's rule calculation for the area is not valid.

2. Using the 577.

The transmission of sample and background read off at one wave-number intervals was written on to NUMAC sheets, typed out onto cards and fed into program DCHO514. This program then worked out the area and (if required) plotted out the ratioed spectra in a similar manner as for the GS2A. This method had the advantage that the base line could be better estimated by eye than with

the tape output where editing of the tapes is extremely difficult.

A displacement of 1% in the base line (T_o) curve can result in a change of band area of between 3 and 10%[21] depending on the total band area and the shape of the base line. For solution work it is normal to employ the pure solvent as reference. Sometimes, however, the pure solvent does not fit the wings of the complex band. This is because:-

(i) Absorption by the complex in the wings due to other bands in the same region.

(ii) Changes in solvent concentration due to the presence of complex in solution. This is probably most important with strong solute bands.

(iii) Small changes in the refractive index which leads to different reflective properties when the complex is removed.[22]

(iv) Changes in the solvent band intensity due to interaction with the donor, acceptor or complex species.

e.g. The large solubility of pyridine-iodine monobromide in the 'inert solvent' chloroform is partially due to hydrogen bonding with chloroform; this causes an increase of the C-H intensity. This perturbation is of the order of, or greater than, the intensity of the C-H vibrations of a saturated solution of the complex. (The $\nu_{(C-H)}$ band intensities in the complexes are low). For this reason it is impossible to carry out any measurements of the C-H pyridine-halogen complex bands in chloroform.

3. Using the FS720.

Card output containing the percentage transmission and wavelength at suitable intervals (usually 2·5 $cm.^{-1}$) was fed into DCHO514 and the intensities evaluated in the usual way.

In conclusion it can be said that if the precautions outlined in the above discussion are taken, intensities can be evaluated to better than 90% of the 'true' value.

CHAPTER 2

Theoretical Background

A. Infrared Spectral Studies on Donor-Acceptor Complexes.

1. Intensity Changes Due to Charge Transfer from Donor to Acceptor on Complexing.

The extreme case of charge transfer occurs when an electron on the donor is transferred to the acceptor to produce two independent ions:

$$D: + A \longrightarrow D^{+}_{solv} + A^{-}_{solv}$$

Intermediate cases occur when partial transfer occurs resulting in partial bonding. The degree of charge transfer will depend upon the:

(i) ionization potential of the donor,

(ii) the electron affinity of the acceptor,

(iii) the polarity of the solvent.

A polar solvent will encourage the formation of ionic species.

However, the above discussion assumes a static situation. As the molecule vibrates the ionization potential of the donor and electron affinity of the acceptor will change. The effective centres of gravity of positive and negative charge will change. The sizes of the charges may also vary. The dipole moment is given by the charge multiplied by the distance separating the charge. Since both these quantities are changing the dipole moment will change, which results in an absorption intensity. Furthermore, the larger the initial charge transfer, the larger the dipole moment change (assuming the same charge displacement takes place on vibration), so one would expect that the stronger the complex, the greater the observed intensity.

According to Mulliken[23] the dipole moment change determines the extent of charge transfer from base to acid which is in turn a function of the ionization energy of the base. This was verified by plotting the frequency of charge transfer absorption bands against ionization energy of the bands.[24,25]

Since,

$$I^V = V' - V = \tfrac{1}{2}K'(Q-Q'_o)^2 - \tfrac{1}{2}K(Q-Q_o)^2 \quad \ldots\ldots [2.1]$$

I^V = vertical ionization energy.

Q_o = normal co-ordinate for the particular vibration under consideration in the isolated donor.

Q'_o = normal co-ordinate for the particular vibration under consideration in the donor cation.

K' = force constant for the vibration under consideration in the donor cation.

K = force constant for the vibration in the isolated donor.

$$\left(\frac{\partial I}{\partial Q}\right)_{Q = Q_o} = K'(Q_o - Q'_o) \quad \ldots\ldots [2.2]$$

Thus from measurements on the first electronically excited state the values for the donor cation may be estimated and an approximate value of the variation in vertical ionization energy (i.e. dI) obtained.

Mulliken[23] assumes a wavefunction ψ_N for the ground state of the complex

$$\psi_N = a\psi_o + b\psi_1 \quad \ldots\ldots [2.3]$$

$$a \approx 1 \qquad b \ll a$$

ψ_o = wave function for a non bonded state.

ψ_1 = " " " " dative state in which an electron has been transferred from the base to the acid.

Neglecting overlap and setting the energy of the no bond state equal to zero, perturbation theory gives,

$$\frac{b}{a} = -\frac{H_{o1}}{W_1} \quad \ldots\ldots [2.4]$$

where $H_{o1} = \int \psi_o \hat{\mathcal{H}} \psi_1 dt$

$$W_1 = I^V - E_A^V - C \quad \ldots\ldots [2.5]$$

E_A^V = vertical electron affinity of the acceptor.

C = Coulomb energy of the pair.

Assuming H_{o1} and C are fairly constant with respect to changing acceptor, these quantities can be estimated from the electronic spectra of complex. Substituting values of H_{o1}, C and the equilibrium value of the ionization energy, the equilibrium value of the mixing coefficients $\frac{b_e}{a_e}$ may be obtained and since

$$b_e = \frac{1}{[a_e^2/b_e^2 + 1]} \quad \ldots\ldots [2.6]$$

the equilibrium value b_e can be evaluated. Re-substituting with the perturbed value of the ionization energy (I + dI) a new value of b i.e. b' is evaluated.

Thus $db = b_e - b'$ which is the change of mixing coefficient on vibration.

The dipole moment of the complex is given by,

$$\mu = b_e^2 \mu_1 \quad \ldots\ldots [2.7]$$

where μ_1 is the dipole moment of the dative state.

$$d\mu = 2b_e db\mu_1 \quad \ldots\ldots [2.8]$$

The integrated intensity A_i is given by

$$A_i = \frac{N\pi g_i}{3c^2}\left(\frac{\partial\mu}{\partial Q}\right)^2 \quad \ldots\ldots [2.9]$$

where

$$\left(\frac{\partial\mu}{\partial Q}\right)^2 = \left(\frac{\partial\mu_x}{\partial Q}\right)^2_{yz} + \left(\frac{\partial\mu_y}{\partial Q}\right)^2_{xz} + \left(\frac{\partial\mu_z}{\partial Q}\right)_{xy}$$

substituting [2.8] into [2.9].

$$A_i = 4b_e^2\mu_1^2 \frac{N\pi g_i}{3c^2}\left(\frac{\partial b}{\partial Q}\right)^2 \quad \ldots\ldots [2.10]$$

Thus it can be seen that the intensity depends upon:-

(i) The variation in vertical ionization energy of the donor.

(ii) The equilibrium value of the mixing coefficient b which is in turn controlled by the electron affinity of the acceptor, the ionization energy of the donor and the resonance integral H_{o1}.

(iii) The change in overlap during vibration.

Ferguson[26] et al. have shown that, since the resonance integral H_{o1} will be to a first approximation proportional to the overlap integral S_{o1},

$$\text{where } S_{o1} = \int \psi_o \psi_1 d\tau \qquad \ldots\ldots [2.11]$$

then the mixing coefficient b_e will be proportional to the overlap integral S_{o1}. Hence a variation of donor and acceptor wavefunctions during vibration will give rise to absorption. He also observed that variations in the Coulombic term in equation [2.5] will be negligible if the variation in mean donor acceptor distance is not varied by donor vibration (for donor bands). It is interesting to note that the overlap integral depends on the geometry of the complex unlike the ionization energy and electron affinity variations.

In view of the high electronegativity of the halogens it is believed that in donor-halogen complexes the electron affinity of the acceptor and orbital overlap seems certain to increase with increasing halogen inter-nuclear distance so that the two effects should be additive in the infrared intensity, i.e.

$$A_{obs} \propto db^2 = [db(\text{overlap}) + db(E_A^v)]^2 \qquad \ldots\ldots [2.12]$$

The intensity of donor vibrations will also depend upon db^2 which is in turn dependent on the change in ionization energy. The ionization energy of the donor varies when the size of the molecule is varied.[26,27] Thus vibrations where the form of the normal co-ordinates involve a change in molecule size will be perturbed in intensity.

Some donor molecules will be able to delocalize the positive charge over the constituent atoms. This movement of charge will cause a variation of the transition dipole moment resulting in a change of intensity. Vibrational modes of the donor which involve a variation of overlap between the donor and acceptor molecule during vibration will also be perturbed in intensity. This would be expected to be more important for 'strong' complexes than weak ones since in a weak complex one would expect no relative movement of the donor and

acceptor molecules should occur during vibrations of the donor.

Finally, from equation [2.5] it can be seen that db will be dependent on the change of Coulomb energy (dC) of the pair. Mulliken and Person[28] have shown that $\partial C/\partial Q$ should be zero if there is no change in the donor acceptor distance during vibration. Mulliken and Person[28] take the view that for weak complexes the D-A distance does not change and that $\partial C/\partial Q$ will only affect the D-A low frequencies in the 'stronger' complexes.

2. Frequency Changes on Complexation.

The structure of the complex between the donor molecule D and the inter-halogen acceptor IX can be described in terms of two structures:

$$D \cdots\cdots I - X \qquad (A)$$

$$[D - I]^+ X^- \qquad (B)$$

For weak complexes the no bond structure (A) is important but as the strength of interaction increases the ionic structure (B) becomes more important. This model predicts a fall in $k_{(I-X)}$ and a rise in $k_{(D-I)}$. The increase of charge-transfer (which oscillates during the vibration) with increasing interaction points to an increase in intensity for the $\bar{\nu}_{(D-I)}$ and $\bar{\nu}_{(I-X)}$ bands.

Person et al.[29] pointed out a second model which explains the observed situation equally well.

$$D \cdots\cdots I - X \qquad (A')$$

$$D^+ \cdots\cdots [I - X]^- \qquad (B')$$

The solid line represents a covalent bond; the dotted line represents van der Waals forces.

The electron in B' spends part of its time in an $a\sigma$ (or $a\sigma^*$) molecular orbital of the halogen, and hence reduces the I - X bond order and the observed force constant and frequency. The intensity is explained by the iodine vibrating towards a $[D - I]^+ \cdots\cdots X^-$ state. Person et al.,[29] using a very crude model, have estimated that pyridine-iodine monochloride has a structure which is highly ionic.

A better estimate of the electronic charge distribution may be obtained from N.M.R. and N.Q.R. studies. N.M.R. studies on the substituted pyridine iodine monochloride complexes[30] indicate the electronic redistribution is not influenced by steric effects and therefore by the extent of overlap between the molecules. Assuming that the double bond character and s orbital hybridisation of the halogen molecule are zero the charge distributions for iodine chloride and the pyridine complex have been estimated from N.Q.R. studies.[31]

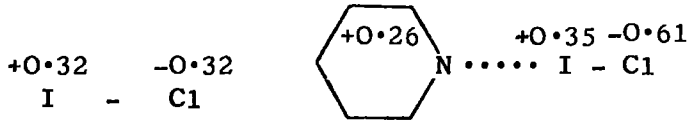

Classical electrostatic forces thus appear to play a dominant role in complex stabilisation. Fleming and Hanna[31] have also given an interesting discussion on the charge transfer structure of pyridine-iodine chloride which will be referred to in Chapter 3.

A recent study[32] has been made on pyridine-iodine monochloride using E.S.C.A. These results suggest a transfer of 0·1 electrons from the nitrogen to iodine atom in the C.T. complex. However, the difference from the N.Q.R. data can be explained as due to the fact that the E.S.C.A. measurements were made in the vapour phase.

To summarise, the vibrational spectra of the complex are interpreted from the spectra of the isolated molecules and from the predicted spectra of D^+ and A^-.

3. Changes in the Acceptor Spectra on Complexation.

Where the electron is accepted into a localised orbital involving the X - Y bond of acceptor X - Y - Z then changes should occur mainly in the X - Y frequency with much less change in the Y - Z frequency.

Electronic rearrangements occur for vibrations which

(i) change the vertical electron affinity E_A^v,

(ii) Change the overlap between donor and acceptor atomic orbitals.

The value of the mixing coefficient b is related approximately to the relative change of force constant $\Delta k/k$ by the expression[33a]

$$\Delta k/k \approx b^2 + a_b S_{ol} \quad \ldots\ldots [2.13]$$

where S_{ol} is the overlap integral.

Thus a change in b will produce an increase in intensity of the acceptor $\bar{\nu}_{(X - Y)}$ band and a reduction of the band frequency.

4. Changes in the Donor Spectra on Complexation.

The spectra of D and D^+ would be expected to be similar, the loss of part of one bonding electron is spread over several bonds in aromatic donors or the electron comes from non-bonding orbitals (in the case of pyridine or dioxan for example).

Electronic rearrangements occur for vibrations which:

(i) Change the vertical ionization energy I^v. For donor-acceptor interaction the ionization energy interaction is directional so only totally symmetric (i.e. on the axis of X - Y interaction) vibrations will do this.

(ii) Change the overlap between donor and acceptor atomic orbitals.

Vibrations of the donor which have displacement co-ordinates along the axis of interaction between donor and acceptor in their respective symmetry co-ordinates will be expected to be the most perturbed on complexation.

5. Hydrogen Bonding and Charge-Transfer Complexes.

Since chloroform was frequently used as a solvent in these studies and chloroform is known to interact with pyridine forming a hydrogen bonded complex[33b] it is important to make some mention of hydrogen bonding. In the hydrogen-bonded complex the light hydrogen atom is moving whilst the heavy donor and atoms attached to the hydrogen atom are approximately stationary.

Tsubomura[34] estimated the intensification of O-H bond stretching vibration and reached the conclusion that charge transfer (as a vibronic contribution) is the most important factor determining the change in ionization energy dI. Thus, a variation of the vertical electron affinity with respect to the internal co-ordinate is also to be expected for the X-H bond just as for halogen complexes, so the explanation for the intensification of the X-H stretching vibration upon hydrogen-bond formation is probably exactly the same as for the halogen stretching vibration.

Chloroform will stabilize semi-polar species of the type $D^{\delta+} \cdots I \cdots Cl^{\delta-}$ by hydrogen bonding but this is usually just considered as a general solvent effect.

6. Reasons for the Appearance of Infrared Inactive Bands on Complexation.

After the discovery of the Cl-Cl stretching band in the infrared spectrum of a solution of chlorine in benzene by Collin and D'Or[35] it was assumed that the chlorine molecule was in an unsymmetrical location. However, this is not necessarily the case as Ferguson and Matsen[26] pointed out. The chlorine molecule may be in a symmetrical environment and the electron vibration causes the appearance of the bands. Hence there is no information to be gained about the geometry from the appearance of a halogen-halogen stretching band.

Apart from ensuring that no new bands formed on complexation were due to impurities, no studies were made on the Raman bands of the donor which were observed on complexation.

7. Intensity Changes Due to Changes in Symmetry and Normal Co-ordinates on Complexation.

Only a brief mention will be made here as this intensity change will be explained fully in Chapter 6 on normal co-ordinates. The normal co-ordinates of D or A may change from their values in the free molecule causing intensity changes to occur. These changes may be due to mixing of internal D (or A) co-ordinates with the new DA co-ordinates. In the event of a symmetry change

on complexation mixing of internal D (or A) co-ordinates together may occur.

The appearance of a band (in e.g. the donor) which appears in the complex will obey an intensity sum rule mixing with an allowed band to gain intensity at the expense of the allowed band. However polarization and vibronic effects will also affect the intensities so a reduction in intensity may not be observed.

8. Intensity Changes Due to Electrostatic Interactions Other than Charge Transfer.[36]

Even though D and A may be non-polar molecules, D and A may become polarized in the complex so that stretching causes a dipole moment change. Also, the polarization is expected to change sharply with changing D-A distance causing a further large electrostatic contribution to $\partial\mu/\partial Q$. The bending vibrations will be expected to be affected to a lesser effect by these perturbations. Vibrations which occur along the axis of interaction should be the ones most enhanced by this process.

The polarization forces in order of strength are[37] (i) ionic; (ii) ion-dipole; (iii) dipole-dipole; (iv) dipole-induced dipole; (v) London dispersion.

(i) Ionic.

This is the attraction of ions due to the Coulomb energy of attraction E

$$E = -\frac{q_1 q_2}{r} \qquad \ldots\ldots [2.14]$$

q_1 and q_2 are the ionic charges.

r is the separation.

Repulsive forces proportional to $\frac{1}{r^9}$ prevent coalition.

(ii) Ion-Dipole Attraction.

This is the attraction of a charged ion to a molecular dipole.

The energy of interaction E is given by

$$E = -\frac{e\mu}{r^2} + \frac{\alpha e^2}{r^4} \qquad \ldots\ldots [2.15]$$

charge-dipole polarised molecule

α = polarizability of the molecule.

e = charge of the ion.

(iii) Dipole-Dipole Attraction.

The energy of interaction of two dipoles μ_1 and μ_2 is given by

$$E = -\frac{2\mu_1\mu_2}{r^3} \qquad \ldots\ldots [2.16]$$

The orientation of the dipoles should be linear, i.e. + - + - etc.

(iv) Dipole-Induced Dipole Attraction.

The interaction energy E is given by,

$$E = -2\alpha\mu^2/r^6 \qquad \ldots\ldots [2.17]$$

μ is the permanent dipole moment and α is the polarizability of the molecule in which the dipole is induced.

(v) London-Dispersion Forces.

An instantaneous dipole due to vibration in the donor induces an instantaneous dipole in the acceptor and vice-versa. The net effect is a tendency to synchronize the electron motion in both atoms.

$$E = -3/2\ (\alpha_1\alpha_2/r^6)\ [I_1I_2/(I_1 + I_2] \qquad \ldots\ldots [2.18]$$

α_1 and α_2 are the polarizabilities of donor and acceptor.

I_1, I_2 are the respective ionization potentials of donor and acceptor.

Thus it can be seen that even without charge transfer considerable electrostatic forces may be operative between molecules.

9. Solvent Effects on Absorption Intensity and Frequency.

The ground states of most 'charge-transfer' complexes appear to involve very little transfer of charge when the complexes exist in solution in a solvent of low ionizing power. If a solvent of high ionizing power is chosen ionization of the essentially non-ionic complex will occur. The driving force is the solvation of ions,[38,39]

$$DA + \text{solvent} \rightleftharpoons D^{+}_{solv} + A^{-}_{solv}$$

When the D - A complex forms in solution it may be considered as the desolvation of D and A followed by the formation of DA (solvated).

$$D(S) + A(S) \rightleftharpoons DA(S)$$

The properties of the complex measured in solution give the difference between the D,A interaction and the D,S and A,S interactions.

For the D - X - Y complexes the two low frequency bands (see Chapter 3) are solvent sensitive getting closer together[40,41,42] as the permittivity of the solvent increases. This effect has been attributed to the increase of the polar $D^{+}[X - Y]^{-}$ contribution to the ground state of the complex. If this were the case one would expect the band intensities to increase by the appropriate amount.

Where an increased intensity is not observed increased vibrational coupling of the low frequency modes may have resulted in an intensity redistribution. Part of the frequency shift may be due to an increase in 'bulk dielectric' effect due to non-specific interactions. However, the frequency shifts predicted[45] by the Kirkwood-Bauer-Magat[43,44] equation:

$$\frac{\Delta\bar{\nu}}{\bar{\nu}} = \left(\frac{\bar{\nu}_g - \bar{\nu}_s}{\bar{\nu}_g}\right) = C(\epsilon - 1)/(\epsilon + 2) \approx \frac{C(n^2 - 1)}{(n^2 + 2)} \quad \ldots\ldots \quad [2.19]$$

(where

$\bar{\nu}_g$ is the wavenumber in the gas phase

C is proportional to the intensity of the vibrational band

$\bar{\nu}_s$ is the wavenumber in solution

ϵ is the permittivity of the solvent, and

n is the refractive index of the solvent)

due to a change of refractive index is very small (about 3 $cm.^{-1}$) compared with the observed shifts.

A great deal of empirical work has been done on solvent shifts; relating the solvent shift to (i) the separation of the interacting species[46], (ii) the heat of formation of the complex[47,48,49], (iii) the association constant[48], (iv) the pK_a of the donor[50], (v) the pK_b of the acceptor[51], (vi) Taft and Hammett[52] parameters.

Since good correlation is usually only observed provided comparison is restricted to a particular chemical type of donor and acceptor discussion on this will be left to the appropriate chapters. It seems clear that solvent effects depend to some extent on all the standard thermodynamic properties which are indicative of bond formation because of the very diffuse nature of the interaction. Only by considering which thermodynamic property is most susceptible to variation under the conditions studied can some sort of semi-empirical relationship between frequency shift and the physical property be built up.

B. Band Shape Studies.

1. Introduction.

Interest in band shape analysis arose in this work from the need to interpret changes in half band width and shapes observed in the studies of band intensities of pyridine-halogen complexes. For example the 1586 $cm.^{-1}$ band of pyridine in chloroform has an apparent half band width of 11 $cm.^{-1}$; in the iodine-bromide complex the band has shifted up to 1601 $cm.^{-1}$, the intensity is practically unchanged and the half band width is halved at 6 $cm.^{-1}$ For iodine chloride in cyclohexane (presumably a 'non-complexing' solvent) the $\bar{\nu}_{(I-Cl)}$ has a half band width of 15 $cm.^{-1}$ In the pyridine complex the $\bar{\nu}_{(I-Cl)}$ band has a

half band width of 25 $cm.^{-1}$, an increase of 10 $cm.^{-1}$

It was also found that in the case of p-dioxan-iodine the band frequency, shape and intensity (assuming the equilibrium law holds) had a dependence on the concentration of dioxan (see Chapter 5).

These effects are not due to a change in bulk electrical permittivity (i.e. increasing medium polarity) because dioxan exists 98% in the chair form[53] and cyclohexane is generally regarded as an 'inert' non-polar solvent.

However, cyclohexane is not 'inert' compared to n-heptane, it has been shown in a recent publication[54] that the intensity in cyclohexane for IBr and ICl is considerably larger than in n-heptane, this can only be accounted for by the lower ionization potential of cyclohexane indicating that cyclohexane does to some extent compete with the dissolved donor to interact with the acceptor. This is also supported by the higher value for the benzene-iodine equilibrium constant in n-hexane as opposed to cyclohexane.[55]

However, an individual dioxan molecule as it vibrates in solution will, due to the distortions produced by vibrations, lose its symmetry and have a considerable transient dipole moment. This implies that local field effects on the environment of the 'average molecule' as it moves through solution will have an effect on the characteristics of the band.

Therefore a systematic study of the experimental variables i.e. concentration, incident energy (e.g. microwave, Raman, far-infrared etc.) on the characteristics of the observed bands should throw some light on which mechanisms are predominant.

Thus, in order to understand these effects it is first necessary to discuss the various models and mechanisms that have been put forward to explain band shapes and intermolecular interactions in the gas-phase and solution.

2. Effects on Band Shape of Condensation from Gas-Phase to Liquid.

For a diatomic molecule in the gas-phase the nuclear energy is given by[56]

$$\epsilon_{total} \approx \epsilon_{rot} + \epsilon_{vib} \quad \ldots\ldots \quad [2.20]$$

Where,

$$\epsilon_{total} = BJ(J + 1) + (v + \tfrac{1}{2})\bar{\nu}_e - x_e(v + \tfrac{1}{2})^2\bar{\nu}_e$$

Figure 2.1. shows the situation diagrammatically.

Fig. 2(i)

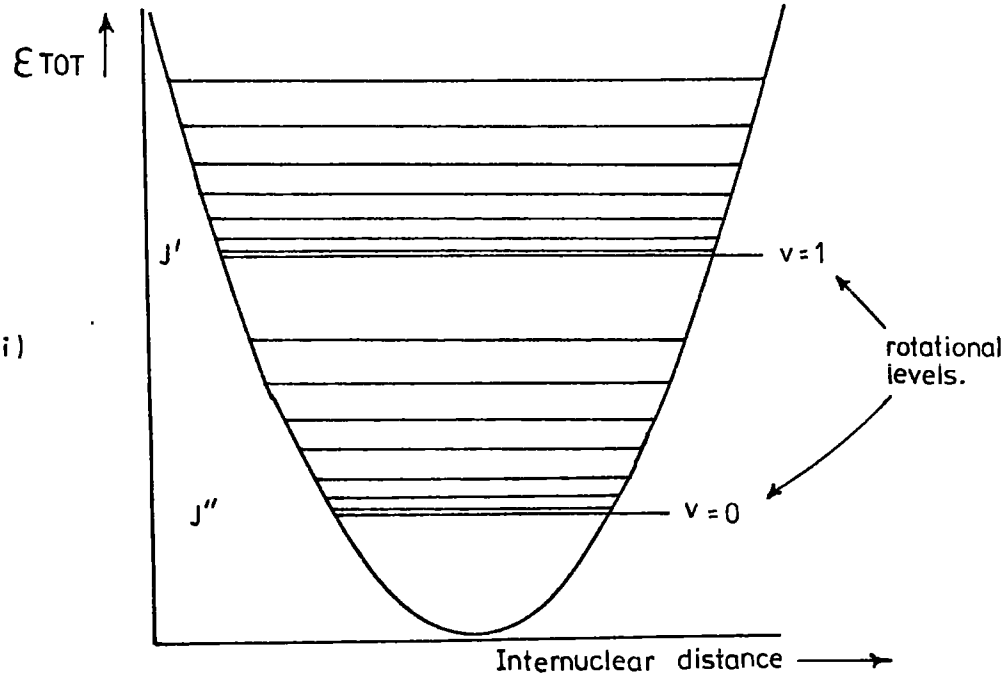

$$\Delta v = 0, \pm 1, \pm 2 \qquad \Delta J = \pm 1$$

$$\text{and } \Delta\bar{\epsilon}_{J,v} = \bar{\nu}_{spec} = \bar{\nu}_o + 2\bar{B}m \qquad \text{..... [2.21]}$$

$$m = \pm 1, \pm 2$$

$\bar{\nu}_o$ is the band centre. (2.21 neglects the anharmonicity factor x_e).

Hence the gas spectrum has a band centre at frequency $\bar{\nu}_o$ and a rotational fine structure of separation $2\bar{B}$, $\bar{B}$ being the rotational constant.

On going to the solution the fine structure is generally lost and a broad band is observed. The molecules in solution perturb one another so strongly that they are unable to rotate freely and this leads to a collapse of the rotational fine structure making the bands much sharper. Sometimes a residual rotational structure[57] is retained if there is a weak interaction with the solvent. Jones and Sheppard,[57] in the case of methyl chloride in carbon tetrachloride, observed that certain bands were considerably broader than others.

This was due to a residual rotational structure showing that the methyl chloride had retained its ability to rotate about a particular axis, i.e. the y

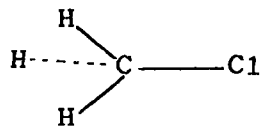

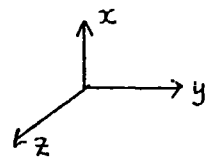

axis in this case.

It is necessary to divide the vibrations into those which change the dipole into:

(i) parallel to

and (ii) perpendicular to the main symmetry axis which is the C_3 axis about which the top rotates.

Accordingly Jones and Sheppard[57] observed that bands due to 'parallel' modes were much narrower than those due to 'perpendicular' modes due to suppression of rotation about an axes perpendicular to the C-Cl axis of symmetry. The top will in any case spin more easily about the C-Cl axis due to inertial effects.

3. Relaxation Processes in Solution.

Relaxation may be defined as the lag in response of a system to changes in the forces to which it is subject. These external forces are of the form of A.C. fields, whether this be a conventional A.C. field between the poles of a magnet or an oscillating electromagnetic wave e.g. infrared radiation.

(i) Microwave Region.

The dielectric properties of polar materials arise from the ability of their dipoles to re-orientate in an applied electric field. This ability is normally retained in the gaseous or liquid states even when the field reverses 10^6 times per second. On solidification the molecules normally become anchored in the solid lattice so that they can no longer rotate. This leads to the marked fall in permittivity shown by most polar materials on freezing.[58]

Another means exists for eliminating dipole orientation in the liquid; if the frequency of the electromagnetic field is raised sufficiently ($\approx 10^{12}$ s^{-1}) the molecules will no longer be able to rotate appreciably before the field direction is reversed. Accordingly there will be a fall in the permittivity as the frequency increases from 10^6 to 10^{12} s^{-1}. From this it can be seen that 'the average molecule requires more than one picosecond (10^{-12} s) to rotate 180°'.

A low frequency field causes the molecules to partly re-orientate before the field reverses. This re-orientation of the dipoles transmits the energy through the medium and so constitutes an electric current (displacement current). For no lag between molecular re-orientation and applied voltage variations the displacement current will be 90° ahead of the applied voltage. This follows because the displacement current is at a maximum when the applied e.m.f. changes the most rapidly. In an ideal dielectric there is no joule heating effect as the current has no component with the e.m.f.

As the frequency is increased up to microwave values the rotation of the molecules will lag behind the voltage oscillations. Thus the phase

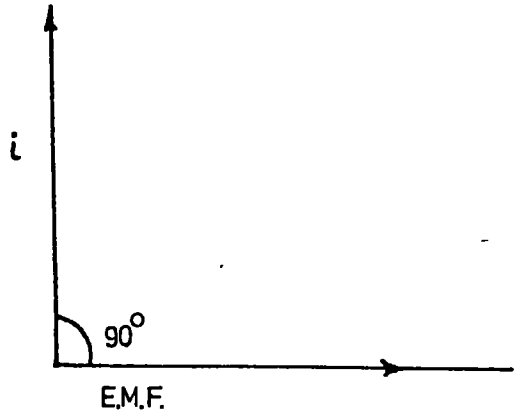

Ideal Dielectric

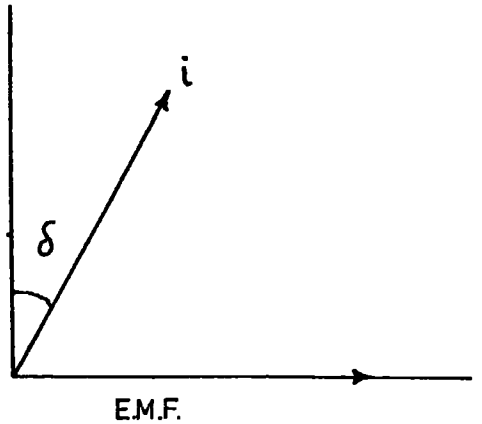

High Frequencies

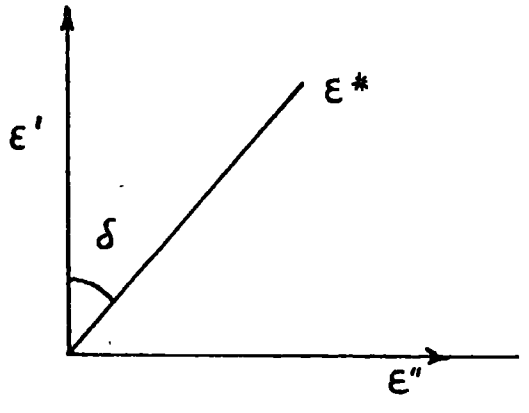

Fig. 2.2.

displacement delta (δ) causes the current to acquire a component ($i\sin\delta$) in phase with the voltage and so dissipation of energy as joule heating. Also the permittivity falls at very high frequencies to that of a non-polar molecule.

Under these conditions the permittivity is expressed by a complex quantity ϵ^*

$$\epsilon^* = \epsilon' + i\epsilon'' \quad \ldots\ldots [2.22]$$

ϵ' = real part of the permittivity.

ϵ'' = the dielectric loss factor.

In order to calculate the permittivity as a function of frequency the relationship between the susceptibility $\chi(\bar{\nu})$ - also a function of frequency is used.

$$\epsilon(\bar{\nu}) = \epsilon_o + 4\pi\chi(\bar{\nu}) \quad \ldots\ldots [2.23]$$

To calculate $\chi(\bar{\nu})$ the variation of $\mu(t)$-the dipole moment as a function of time-must be considered. It is assumed that the rate of approach of $\mu(t)$ to equilibrium will be proportional to the deviation from equilibrium. When a steady field E has been applied for a long time the dipole moment will be related by E to the static susceptibility, that is, for zero frequency

$$\mu(\infty) = \chi(o)E \quad \ldots\ldots [2.24]$$

At time t $\mu(t)$ will not have reached the steady state so

$$\frac{\partial\mu(t)}{\partial t} = \frac{\mu(\infty) - \mu(t)}{\tau} \quad \ldots\ldots [2.25]$$

$1/\tau$ is the constant of proportionality. τ is called the RELAXATION TIME. If the field is now made alternating

$$E(t) = E_o\exp(i\bar{\nu}t) \quad \ldots\ldots [2.26]$$

$$\frac{\partial\mu(t)}{\partial t} + \frac{\mu(t)}{\tau} = \frac{\chi(o)E_o\exp(i\bar{\nu}t)}{\tau}$$

Hence solving for $\mu(t)$

$$\mu(t) = \frac{\chi_o E_o \exp(i\bar{\nu}t)}{(1 + i\bar{\nu}t)} \quad \ldots\ldots [2.27]$$

Since $\chi(\bar{\nu}) = \frac{\chi(o)}{(1 + i\bar{\nu}t)}$

$$\mu(t) = \chi(\bar{\nu})E(t)$$

Since $\epsilon^* = \epsilon_{obs} = \epsilon_o + 4\pi\chi = \epsilon' + i\epsilon''$

$$\epsilon' = \epsilon_o + \frac{4\pi\chi_{(o)}}{1 + \bar{\nu}^2\tau^2} \quad \ldots\ldots [2.28]$$

$$\epsilon'' = -\frac{4\pi\chi_{(o)}\bar{\nu}t}{1 + \bar{\nu}^2\tau^2} \quad \ldots\ldots [2.29]$$

At very low frequency the observed permittivity tends towards the static dielectric constant.

$$\epsilon' \to \epsilon_o + 4\pi\chi_{(o)} \quad \ldots\ldots [2.30]$$

$$\epsilon'' \to o \quad \text{as} \quad \bar{\nu} \to o \quad \ldots\ldots [2.31]$$

At very high frequency the molecule is completely unable to respond to the rapidly changing field and

$$\epsilon' \to \epsilon_o \quad \text{as} \quad \bar{\nu} \to \infty$$

$$\epsilon_2 \to o$$

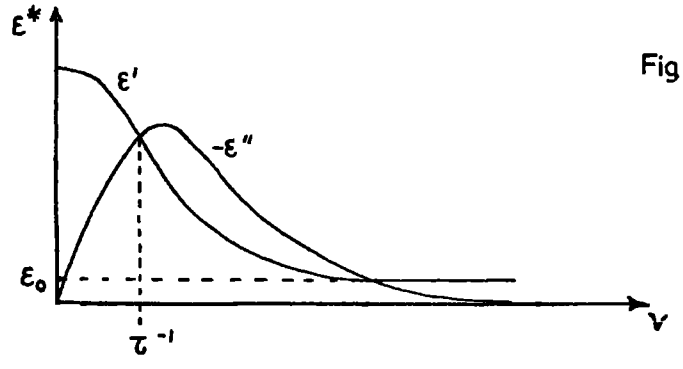

Fig.2.3.

Frequency dependence of the dielectric constant in a medium dominated by relaxation processes.

In between these two limits there is a gradual change in ϵ' and an absorption band around a frequency.

$$\bar{\nu} = \frac{1}{\tau} \qquad \ldots\ldots \quad [2.32]$$

The Effect of Temperature on the Relaxation Dispersion in the Microwave Region.

Debye[59] has shown, assuming a solution of polar molecules in a non-polar solvent rotating against the viscous drag of the surroundings that,

$$\tau = \frac{4\pi\eta a^3}{kT} \qquad \ldots\ldots \quad [2.33]$$

η = viscosity of fluid at temperature T.

a = the radius of the hard sphere which experiences the same frictional couple as the molecule under the same conditions. In order to overcome the local viscous forces the molecule must overcome the potential 'hump' V_R in order to rotate. The value of V_R depends on the degree of interaction with the polar molecule. The variation of viscosity with temperature fits the equation,[60]

$$\eta \approx \text{const} \exp(^{-V_R}/kT) \qquad \ldots\ldots \quad [2.34]$$

Plots of relaxation time against the ratio of viscosity to temperature are linear also supporting the above theory.

(ii) Relaxation Processes Observed in the Infrared Region.

The intensity of absorption in the infrared depends on the change in dipole moment with normal co-ordinate. This change depends upon a vibrational transition which occurs very rapidly compared to the time taken to align in an electric field. Therefore one would expect that relaxation processes observed in the infrared to be rapid compared to the microwave region.

From the previous discussion it is clear that the shape of an infrared absorption depends upon the processes leading to absorption. These are:-

(a) a rotational contribution,
(b) a vibrational contribution,
(c) a translational contribution.

In the infrared it is not possible to split these three components.

However, non-polar inert molecules would be expected to have a greater freedom and hence a greater rotational part than molecules experiencing electron donor-acceptor forces, or dipole-induced dipole interactions. In the case of iodine complexes with lighter molecules the sheer mass of the atoms would seriously reduce the rate of orientation causing the bands to be dominated by vibrational and/or translational effects.

Bratos et al.[61] has given a mathematical treatment to explain the profile of a diatomic molecule as influenced by a particular mechanism, the most important mechanisms are:-

(a) Vibrational Relaxation Via Translational Diffusion.

This is one of the mechanisms by which the vibrational energy is relaxed into the medium. The motion consists of jumps between sites separated by an energy barrier V_T. It is necessary to decide whether the environment of the molecule changes during the vibration. As explained previously, relaxation correlation times are a measure of the rate of change from the steady state. In this case the translational correlation time τ_T gives the rate of change of environment of the molecule. If this is much greater than the life-time of the vibration (i.e. the reciprocal frequency converted to picoseconds) the solvent action will be statistical. Estimates[61] for τ_T from diffusion coefficients indicate that $\tau_T \approx 10^{-10}$ s for HCl in CCl_4 where weak interaction occurs (if the frequency of absorption is 10 cm.$^{-1}$ the life-time is about 3×10^{-12} s).

$$\therefore \quad \tau_T \gg \text{the vibrational life-time}$$

Hence the above hypothesis is confirmed where weak solvent interactions occur.

It seems clear that for a statistical treatment to work one must assume a large number of independent solvent molecules modulating the vibration. Bratos[61] et al. found for a large number of solvent molecules interacting in the absence of vibrational mixing that the vibrational contribution should be Gaussian. If the number of solvent molecules interacting is small the situation is much more complex.

The function G_V describes the relaxation of the vibrational energy and is called the vibrational relaxation function. Morowitz and Eisenthal[62] showed that one can write

$$G_V = \exp(-\beta_v t) \quad \ldots\ldots [2.35]$$

where β_v is the vibrational damping constant.

The band half-width for pure vibrational relaxation based on translational diffusion is about $\beta_v^{\frac{1}{2}}$. If a large Gaussian component is present then vibrational effects must be important. However the converse is not true.

(b) Rotational Diffusion.

The mathematical treatment of Bratos[61] et al. considers the rotational relaxation function G_R as well as the vibrational relaxation function G_V.

The form of G_R is determined by two factors:

(i) Two types of rotational movement are possible depending on the height of the potential barrier opposing rotation V_R. If $V_R \ll kT$ the molecule executes a motion similar to free rotation. If $V_R \gg kT$ the molecule does not have the energy to rotate and the molecule tumbles through solution executing random 'flips'; this is rotational diffusion. If $V_R \approx kT$ the motion is complex although it can be approximately likened to a fraction freely rotating and a fraction undergoing rotational diffusion.

(ii) Whether the re-orientational correlation time (the time it takes for the molecule to dissipate its energy throughout the system) is long compared with the time taken for one complete rotation of the molecule. (The time for one rotation being the reciprocal of the angular velocity.) This also controls whether the orientational motion is similar to a 'free' rotation or a rotational diffusion process.

If $\tau_R \gg$ time for one rotation, free rotations occur,

If $\tau_R \ll$ time for one rotation, rotational diffusion occurs.

For a linear molecule it has been shown that[62]

$$G_R = 1 - at^2 + bt^4 \quad \ldots\ldots [2.36]$$

where $a = {}^{kT}/_{I}$

$$b = \frac{1}{3}(\frac{kT}{I})^2 + (24I^2)^{-1} < (OV)^2 >$$

k = Boltzmann constant

T = absolute temperature

I = moment of inertia

$< (OV)^2 >$ is the mean square torque due to the other molecules.

Allowing for vibrational relaxation brings in two new coefficients:

$$a' = a + \frac{\beta_v^2}{2} \quad \ldots\ldots [2.37]$$

$$b' = b + a(\frac{\beta_v^2}{2}) + (\frac{\beta_v^2}{4}) \quad \ldots\ldots [2.38]$$

At $t = O$, $G_R = 1$

When[61] $t \ll \tau_R$ (free rotation correlation time)

$$G_R = \exp[(-{}^{kT}/_{I})t^2] \quad \ldots\ldots [2.39]$$

which is Gaussian in form, i.e. free rotation gives a Gaussian component.

If $t \gg \tau_R$ (free rotation correlation time)

$$G_R = \exp(-\alpha_R t) \quad \ldots\ldots [2.40]$$

α_R = damping constant for rotational diffusion.

If rotational diffusion is predominant the band profile is Lorentzian in the centre and exponential in the wings. The strongly temperature dependent half band width is double the diffusion coefficient.

Free rotation would, of course, give a spectra similar to the gas-phase with side bands and a halfband width of the order of $(\frac{4kT}{I})^{\frac{1}{2}}$.

(c) The Litovitz Model for Collisional Complexes Undergoing Rotational Diffusion

Litovitz et al.[63] have given a somewhat different model for the picture of the mechanism of re-orientation. He denotes some liquids as 'structure limited' where a molecule remains in a fixed position for a 'Residence time' τ_{res} and then re-orientates in a time of flight τ_{fl}. The residence time being much larger than the time of flight. He describes other liquids as 'collisional limited' the molecule re-orientates continuously the individual steps being limited by collisions with neighbours. The average time duration of the individual steps is the time between collisions, τ_{bc}. Liquids composed of hydrogen-bonded or strong sterically hindered molecules are 'structure limited'. Liquids composed of spherical or small symmetric top molecules are collision limited, e.g. CCl_4, CS_2, CH_3CN, C_6H_6 and C_6H_{12}.

Litovitz interpreted the fall in frequency with increasing temperature (as observed by Pardoe[64] for polar liquids) as being due to the density dependence on τ_{bc}.

$$\tau_{bc} = \frac{1}{\bar{\nu}(\bar{r} - \sigma)} \qquad \ldots\ldots \quad [2.41]$$

where $\bar{\nu} = \left(\frac{8kT}{\pi m}\right)^{\frac{1}{2}}$ ..... [2.42]

k = Boltzmann constant

T = absolute temperature

m = mass of the molecule

$\bar{r}$ = average distance between neighbours

σ = the diameter of the molecule

$$\bar{r} = \left(\frac{V}{N}\right)^{1/3} \text{ for } CS_2 \qquad \ldots\ldots \quad [2.43]$$

V = molar volume

N = Avogadro number

$$\bar{r} = \left[\frac{\sqrt{2}V}{N}\right]^{\frac{1}{3}} \text{ for } CCl_4 \text{ and } C_6H_{12} \qquad \ldots\ldots \quad [2.44]$$

τ_{max} is the reciprocal of the observed frequency

since $\tau_{max} \propto \tau_{bc}$

or $\tau_{max} = \text{constant} \cdot \tau_{bc} = \frac{\text{constant}}{\bar{\nu}_o}$

$\bar{\nu}_o \propto \frac{1}{\sqrt{T}}$ thus as the temperature falls the frequency rises which is what was observed by Pardoe.[64]

For non-polar liquids Litovitz calculated that for a collisional mechanism $\bar{\nu}_o \leq \text{const} \sqrt{T}$.

Therefore if the main cause of the far-infrared absorption in non-polar liquids is the collision mechanism only a slight shift of $\bar{\nu}_o$ will be exhibited with increase in temperature.

The Litovitz model has been used in a recent paper[65] to calculate the approximate retardation of velocity of an IBr molecule on interaction with benzene. The most probable retardation mechanism is a 'sticky' collision. The retardation is found to be severe and would effectively reduce the velocity by about 50% during the first picosecond of interaction. A similar sort of retardation is expected for ICl. The difference in behaviour of the auto-correlation functions of ICl and IBr were then interpreted as being due to the fact that the $\bar{\nu}_{(I-Br)}$ band profile is controlled by non-rotational processes and collisional broadening with some vibrational relaxation contribution to the band shape. In the ICl case rotational diffusion also contributes to the band profile.

4. The Calculation of Correlation Functions by the Fourier Transformation of the Observed Absorption.

From the previous discussion it can be seen that an observed absorption in the infrared can arise from mechanisms which individually would have given rise to a Gaussian or a Lorentzian band contour. A Lorentzian band has the relationship,

$$\mathrm{Log}_{10}\left(\frac{I_o}{I}\right)_{\bar{\nu}} = \frac{a}{(\bar{\nu} - \bar{\nu}_o)^2 + b^2} \qquad \ldots\ldots \quad [2.46]$$

where $2b = \Delta\bar{\nu}_{\frac{1}{2}}$; $\frac{a}{b^2} 2 = \mathrm{Log}_{10}\left(\frac{I_o}{I}\right)_{\bar{\nu}_o}$

I_o = intensity of incident radiation

I = intensity of emergent radiation

Mathematically a Gaussian Curve is described by

$$\mathrm{Log}\left(\frac{I_o}{I}\right) = \frac{a}{b^2} 2\left\{\exp - \frac{[(\bar{\nu} - \bar{\nu}_o)^2 1n2]}{b^2}\right\} \qquad \ldots\ldots \quad [2.47]$$

If A(t) and B(t + τ) are any two vectors describing some states of the system at times t and t + τ and t + τ respectively then the correlation function ϕ_{AB} is given by the vector product.

$$\phi_{AB}(t,\tau) = < A(t).B(t + \tau) > \qquad \ldots\ldots \quad [2.48]$$

The brackets indicating an ensemble average. If A and B refer to the same vector property $\phi_{AB}(t,\tau)$ is an autocorrelation function. If the vector property is a property of the molecule and not the system as a whole there will be no cross terms due to molecular interactions and ϕ_{AA} is of the type $< A_i(t)A_i(t + \tau) >$. If the autocorrelation function is defined for a given environment the distribution will not vary with time and

$$\phi(t,\tau) = \phi(o,\tau) = \phi(\tau) = < A(o).A(t)) > \qquad \ldots\ldots \quad [2.49]$$

Gordon and Shimizu[66,67] (later extended by Bratos and his co-workers)[61] have established that the Fourier transform of the frequency spectrum yields a transition dipole time autocorrelation function $\phi(t)$ from which the nature and rate of molecular relaxation processes in principle may be inferred. This is defined by,

$$\phi(t) = < \vec{u}(o).\vec{u}(t) > = \int_{-\infty}^{\infty} k(\omega)\exp[i\bar{\omega}t]d\omega \qquad \ldots\ldots \quad [2.50]$$

where $\bar{\omega} = \bar{\omega} - \bar{\omega}_o$

$\vec{u}$ = unit vector pointing along the direction of the transition moment.

ω = angular frequency.

Normally only the real part of the autocorrelation function is calculated, the imaginary part being very small.[68]

Substituting wavenumber $\bar{\nu}$ for angular frequency and normalising by dividing by the band intensity one obtains,

$$\phi(t) = \langle \vec{u}(o).\vec{u}(t) \rangle = \frac{\int_{band} k(\bar{\nu})\cos[2\pi c(\bar{\nu} - \bar{\nu}_o)t]d\bar{\nu}}{\int_{band} k(\bar{\nu})d\bar{\nu}} \quad \ldots\ldots [2.51]$$

It may be seen that at low values of t the main contribution to $\phi(t)$ comes from values of $(\bar{\nu} - \bar{\nu}_o)$ which are large (and vice versa at high values of t). Thus at low t values the $\phi(t)$ value is controlled by data in the wings of the band.

A Lorentzian absorption transforms to give a $\phi(t)$ curve which falls exponentially with t and the slope from the Log$\phi(t)$ v. t graph is proportional to the half band width. A Gaussian frequency curve transforms to a Gaussian time correlation function whose decay rate is proportional to the quarter band width of the frequency curve. Hence a Gaussian curve of equivalent half band width and maximum absorption will have a Log$\phi(t)$ v. t curve which falls off twice as fast as that in the Lorentzian case.

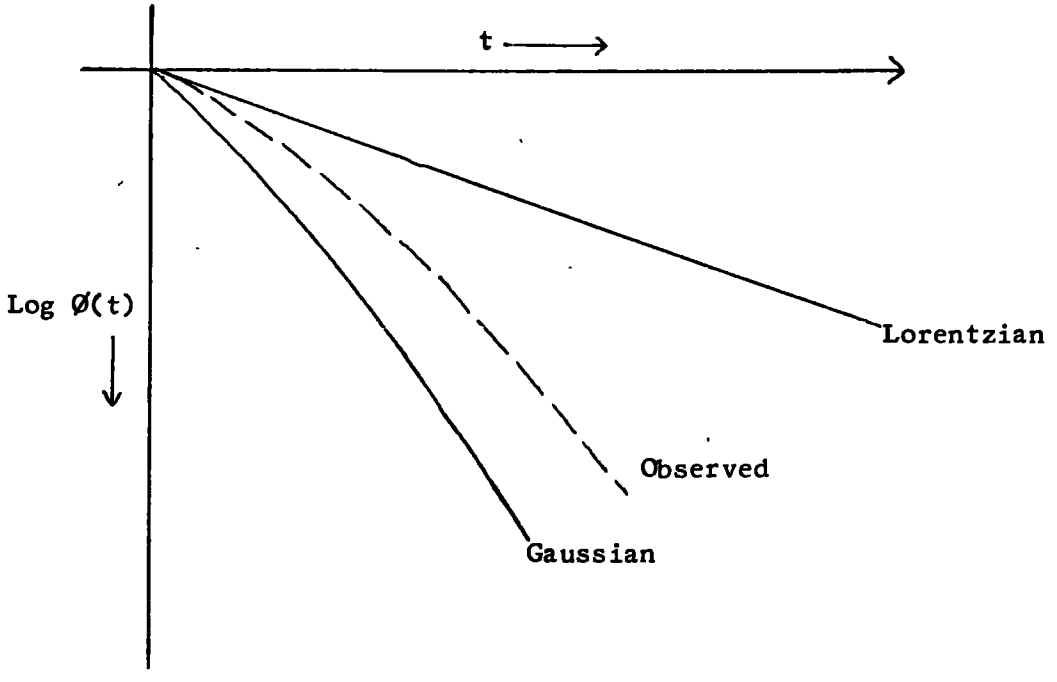

Fig. 2.4.

Figure 2.4. shows the real situation where there is a mixture of Gaussian and Lorentzian components.

The physical interpretation of the autocorrelation function is as follows. For a specific molecule at time t = 0 the transition dipole $\vec{u}(o)$ will be aligned at a specific direction. For a brief initial period free rotation will determine the kinetics of the dipole rotation and $\phi(t)$ will be governed by the inertial properties of the molecule. Gordon and Shimuzu[66,67] showed $\phi(t)$ should follow a Guassian decay rate. At longer times disruptive collisions occur and the orientation of the specific molecular dipole will be governed by molecular collisions as developed by Debye.[59] Here the orientation is characterised by an exponential decay constant and a Lorentzian frequency spectrum. The correlation function describes the decay of knowledge about a system as it approaches a random statistical distribution.

During the vibrational transition period of about 3 ps (at 1000 $cm.^{-1}$) the molecule will 'move' via translational and rotational diffusion. Thus, the resulting collisions allow the excited vibrational state to be coupled to the other degrees of freedom in the system. Accordingly $\phi(t)$ has two contributions one vibrational and one rotational, and can be written[61]

$$\phi(t) = G_R . G_V \qquad \ldots\ldots \quad [2.52]$$

Now Equation [2.35] $G_V = \exp(-\beta_v t)$

and Equation [2.40] $G_R = \exp(-\alpha_R t)$

These equations assume the translational correlation time is much larger than the vibrational life-time, and the time scale involved is much larger than the 'free rotation' correlation time.

Combining Equations [2.35] and [2.40] we get

$$\begin{aligned} \phi(t) &= \exp(-\alpha_R t).\exp(-\beta_v t) \\ &= \exp[-(\alpha_R + \beta_v)t] \qquad \ldots\ldots \quad [2.53] \end{aligned}$$

In the solid $\alpha_R \approx 0$, since most solid bands are very much sharper than in solution. It is often assumed that for the liquid phase,

$$\alpha_R \gg \beta_v$$

In most cases the I.R. band profile is dependent on both vibrational and rotational effects which are inseparable. By studies on the isotropic and anisotropic parts of the scattered light it is possible to separate these effects in the Raman,[68] since molecular re-orientation contributes only to the depolarised scattering so that the spectral distribution of the polarised part is used as a basis for removing all other effects on the band shapes. Since no Raman band shape studies were made in this work no further discussion will be made on the very interesting accounts published to-date.[70-72]

5. Mechanisms for Broadening of Vibrational Bands.

In view of the extreme broadness of the bands studied it seems worthwhile to review the theory to-date on this topic.

The Bratos dephasing mechanism described in the section on translational diffusion (p. 56) results in a broadening of the band because the vibrational transition takes place much faster than the molecular motion. The changing environment slightly alters the shape of the vibrational state energy curve which leads to a range of frequencies and hence band broadening. This is a relatively slow process because the average molecule has to go through all the different environments returning to the original one before correlation is lost. The extent of this interaction depends on its strength (i.e. the change in intermolecular potential) and the susceptibility of the vibration to interaction (i.e. a symmetry or ∂Q term) (Figure 2.5b).

In fact according to Bratos[73] the energy of interaction is proportional to $\left(\frac{\partial V}{\partial Q}\right)$ where V is the intermolecular potential. Since Q changes from one mode to another this contribution is expected to be different from one

absorption band to another. The orientational contribution, on the other hand is expected to be the same for each vibration of the same class (in the absence of vibration/rotation interaction).[74a,b]

Figure 2.5. Mechanisms of Vibrational Broadening

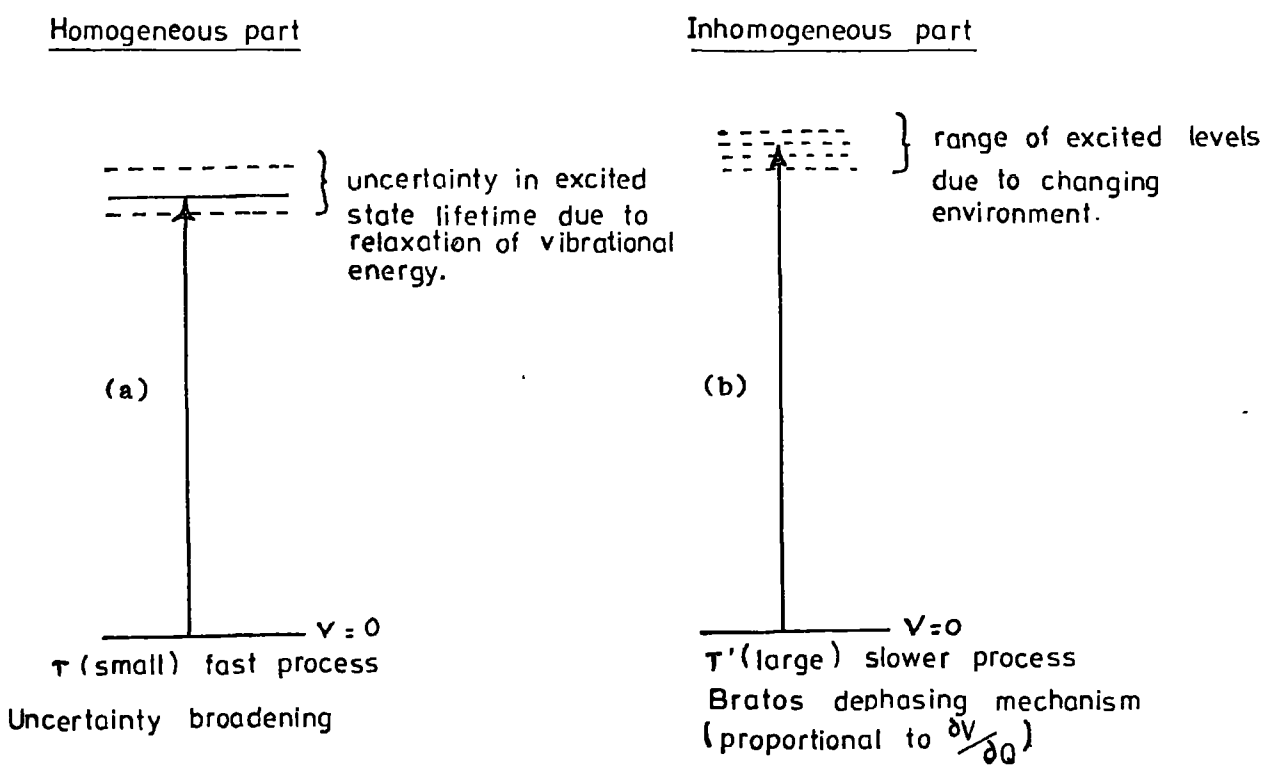

This is not an energy relaxation. The effect is one of phase loss due to the dynamic nature of the interactions, the potential V being different for each configuration.

Uncertainty Broadening (Fig. 2.5a).

In order to make any measurement on a system it is necessary to disturb that system in some way. A vibrating molecule will be changing slightly. It will take a finite time for the incident radiation to be absorbed and the re-emitted radiation to be transmitted to the detector.

The uncertainty principle states that we cannot simultaneously measure exactly both position and momentum of an object but rather $\Delta p_x \Delta x \geq \hbar$

where Δx is the uncertainty in position of an object and Δp_x is the corresponding uncertainty in the momentum along the x direction, $\Delta p_x \Delta x \geqslant h$.

A similar relationship holds between ΔE and Δt, viz,

$$\Delta E \Delta t \geqslant \hbar \qquad \ldots\ldots \quad [2.54]$$

where ΔE is the uncertainty in energy and Δt the time uncertainty.

In vibrational spectroscopy uncertainty broadening may occur because of the finite life-time of the excited vibrational state, e.g. a vibrationally excited state life-time (Δt) of 1 p.s. leads to a broadening (ΔE) of ≈ 5 cm.$^{-1}$ This is an entirely feasible broadening process if the complex studied has a life-time of the same order (1 - 2 p.s.).

Another way to consider this is to consider that if bonding alters slightly due to electron vibration then the vibrational profile of the Morse function will change, since the Morse function depends on the dissociation energy and amplitude of vibration. One would expect the $\bar{\nu}_{(D-X)}$ absorption to be the most susceptible to this fluctuation. This may be part of the reason why $\bar{\nu}_{(D-X)}$ absorption is always much broader than $\bar{\nu}_{(X-Y)}$ absorption.

If there is more than one complex present each with a slightly different absorption frequency (in general we may have n:m complexes present) this will lead to band broadening. In this situation the overlapping of several Lorentzian bands leads to a band which is more Gaussian.[74c]

A reduction of rotation due to intermolecular forces ought to lead to a reduction in band width (rotational relaxation gets longer). The fact that complex formation in this work always caused band broadening underlines the importance of vibrational effects.

Rotational Broadening.

For a 'rigid' complex an increase in moment of inertia should lead to slower rotation and the autocorrelation function will decay more slowly. The band will become narrower. The fact that this is not always observed supports the possibility in many cases of a collisional mechanism where each collision totally destroys the correlation causing a very rapid drop in $\emptyset(t)$ and hence

the half band width will increase in size.

Doppler Broadening.

Due to the Doppler effect[75] the observed frequency will rise when a molecule is travelling towards the detector and fall when it is travelling away. Townes and Schawlow[76] deduced from a consideration of the resolved components of velocities that

$$\frac{\Delta\bar{\nu}}{\bar{\nu}} = \sqrt{\frac{2kT\ln 2}{mc^2}} \qquad \ldots\ldots [2.55]$$

Chantry[77] quotes a value of 0·2 $cm.^{-1}$ for a typical infrared absorption.

From equation [2.55] it can be seen that it will be smaller in the low frequency infrared region. Since the resolution is at best 1 $cm.^{-1}$ it can safely be ignored in these studies.

6. Predictions of Variations in Band Shape Due to Alterations in the Intermolecular Forces.

(i) An increase of mass or moment of inertia will lead to slower rotational diffusion and to a $\log\emptyset(t)$ slope which is decreased. The overall band width decreases. (Since the diffusion coefficient depends upon the slope).

(ii) Increase in intermolecular forces acting on the molecules will lead to a slower rotational diffusion and hence slower decay of the correlation function, since if broadening effects are predominant this rotational (and translational) motion is hindered and the band width decreases.

(iii) Gordon et al.[66] has pointed out that vibrational relaxation leads to a shortening of the vibrational state life-time and a broadening of the band. The slope of the $\log\emptyset(t)$ plot is proportional to the half band width of the absorption and much faster decay of the autocorrelation function occurs.

Vibrational relaxation damping is caused by the coupling of the excited vibrational state with the other degrees of freedom in the system (e.g. by collision with other molecules).

7. Analysis of Observed Band Shapes.

A series of computer programmes (in Fortran IV) for the analysis of vibrational band shapes using the techniques described previously were supplied by the courtesy of Dr. Norman Jones of the National Research Council of Canada in Ottawa. These are contained in N.R.C. Bulletins 11, 12 and 13 published by Dr. R.N. Jones and his co-workers.

By feeding in the band frequency and absorbance at constant wavenumber intervals the $\emptyset(t)$ and $\text{Log}\emptyset(t)$ curves were plotted out directly.

Another program was available to generate pure Lorentzian and Gaussian band shapes by inputing the observed maximum intensity and half band width. From the mathematical functions the curves were calculated and plotted out, and output from this program could then be fed into the autocorrelation program and the calculated autocorrelation curves compared with the observed ones.

C. Models Used to Describe the Systems Studied.

In spite of a great deal of work on donor-halogen systems[78] a suitable model has not been developed which is applicable to all regions of the spectrum. This appears to be due to the differing time scales involved.

In the ultra-violet region satisfactory Benesi-Hildebrand[79] plots on the charge-transfer band have been obtained for dioxan iodine solutions in normal heptane to evaluate the equilibrium constant of the 1:1 'complex'.[80]

$$D + A \rightleftharpoons DA$$

$$K = \frac{[DA]}{[D][A]}$$

At equilibrium the rate of the forward reaction equals the rate of backward reaction

$$\therefore \quad V_{forward} = k_1[D][A]$$

$$V_{backward} = k_2[DA]$$

and $K = \frac{k_1}{k_2}$ the ratio of two rate constants.

If the forward rate constant is equal to the collision frequency about 10^{+12} sec.$^{-1}$ then, since the equilibrium constant for the dioxan iodine[80] reaction is known to be about 1 l.mol.$^{-1}$, we have,

$$1 = \frac{10^{-12}}{k_2}$$

$$\text{and} \quad k_2 = 10^{-12} \text{ sec.}$$

This indicates that the dioxan/iodine complex has a life-time of one pico-second. In the ultraviolet region where these measurements were made at, say, 20,000 cm.$^{-1}$ the observation time is about $0{\cdot}16 \times 10^{-14}$ sec. If 10^{-12} sec. is available before the complex disintegrates, then 600 transitions may take place in the complex life-time. In the far-infrared region at e.g. 200 cm.$^{-1}$ only 6 vibrations may take place during the complex lifetime. Hence it is not really surprising that a 'complex' may appear to have a very different 'stability' from measurements in the ultraviolet region as opposed to the far-infrared.

It is difficult to describe the term 'complex' because of its wide and varied usage. Sometimes it is used to describe the product of the weak reversible interaction between two or more components, and at other times it has described the product of strong interactions where new covalent (σ) bonds are formed.

(1) Charge Transfer Complexes.

The theory[81-83] uses a valence bond structure involving only charge-transfer forces even though dispersion, dipole and similar forces may be important. In many so-called 'charge-transfer' complexes charge-transfer forces do not provide the major contribution to the binding forces in the ground state. Measurements of halogen pure-electrical quadrupole resonances for complexes of benzene-bromine suggest that there is little or no transfer of charge in the ground state of these complexes.

Charge-transfer complexes usually involve simple integral ratios of the components; the enthalpy of formation is a few kilojoules per mole, the rates of formation and decomposition appear to be instantaneous by normal techniques. An extra absorption from the donor to acceptor is usually observed.

(2) Collisional Complexes.

Whilst the charge transfer model works for the high frequency spectra the collisional model explains the far-infrared spectra.[84] High resolution Raman studies[85] show no trace of a 'free' iodine band in the benzene/iodine system although somewhat better donors e.g. mesitylene/iodine[85] have a free iodine band.

This implies only one type of iodine is present since from the equilibrium constant of the benzene/iodine complex an appreciable amount of 'free' iodine should have been present under the conditions used. The only possibility is a collisional complex. Hanna's calculations[86] show that both classical electrostatic and charge-transfer forces are important.

However the existence of a doublet for benzene-ICl at 375 and 355 $cm.^{-1}$ would seem to indicate the presence of free and uncomplexed iodine chloride so that perhaps the life-time in this case is large enough for one to talk about a complex - although not necessarily a charge-transfer one.

In conclusion a complex can only be described with respect to the time-scale one is considering. Thus in the ultraviolet region a stable long-lived complex may exist, as regards the charge-transfer transition, whilst in the far-infrared region a donor- and acceptor-molecule may not interact together long enough to give rise to conventional absorption. It is generally held that at least 10 vibrations should occur in the time-scales involved. Otherwise the detector will only pick-up a blurred average. Furthermore, a normal infrared vibration is part of a rigid system during the time-scales involved. For this reason vibrational spectroscopy has been explained in terms of masses connected together by springs. If the complex is non-rigid it is not surprising that the normal laws of vibrational spectroscopy no longer hold because the concept of a force constant becomes untenable.

CHAPTER 3

Infrared Spectral Studies on Pyridine and its Complexes with the Acceptors XY (X = I, Br; Y = Cl, Br, I, CN)

I. The Donor Vibrations.

A. Introduction.

In this chapter, we shall deal mainly with the changes which occur in the infrared spectrum of the pyridine molecule when it is complexed with the molecules IX (X = Cl, Br, CN). Such 'complexes' are usually formed by the reaction Pyr + IX $\rightleftharpoons$ Pyr-IX in solution, in a non-polar solvent, and are regarded as being 'strong' complexes, for the following reasons:

(a) They can usually be isolated as solids.

(b) The equation above has for X = Cl, Br a large equilibrium constant ($\approx 10^5$ l.mol.$^{-1}$).

(c) The complex has a relatively long life-time, which, must (on the basis of the equilibrium constant) be of the order of 10^{-6} - 10^{-7} sec. (see Section 2).

As explained in Chapter 2, both the vibrational spectrum of the donor and the acceptor change on complexation with a halogen or 'pseudo' halogen. A great deal of work has been carried out on the changes of band frequency of the pyridine molecule,[87-94] but only two papers have (partially) dealt with the donor band intensities.[95,96]

B. Purification of Chemicals and Preparation of Complexes.

'Analar' pyridine was dried thoroughly over molecular sieves, but was not further purified. The infrared spectrum was identical with the spectrum quoted in 'Selected Infrared Spectral Data', published by the American Petroleum Institute, showing no impurity bands. The iodine bromide and iodine chloride were reagent grade from Hopkin and Williams Ltd., and the

complexes were prepared by the published method.[97,98]

The method used was to burette slowly the stoichiometric amount of the halogen to the pyridine solution (in the flask), with constant stirring. The solvent normally used was carbon tetrachloride, in which the complexes are only slightly soluble. The complexes precipitated out in about 90% yield. The complexes were recrystallised from carbon tetrachloride. A carbon, hydrogen, and nitrogen analysis was carried out to determine the purity, and the melting point taken for each complex. Typical values found are recorded in Table 3.1.

Table 3.1.

Analytical Data for Pyridine-IBr and Pyridine-ICl

Complex	% Carbon	% Nitrogen	% Hydrogen	m.p./ °C	Reference
Pyridine-ICl					
Expected	24•81	5•73	2•07	133	97
Observed	24•84	5•72	2•16	132	
Pyridine-IBr					
Expected	20•97	4•91	1•83	116	101
Observed	20•93	4•89	1•75	115	

Solutions of the complex were made up by weighing into a small volumetric flask; and making up with the appropriate volume of dried solvent. All measurements were made within 3 hours of making up the solution. Usually, during this time, no special changes were observed. If the spectrum changed in intensity during the time of scanning it was discarded and the results not used. The cell used in the near-infrared was a demountable solution cell with KBr plates. The path length was determined using the interferometric method.[16a] As an additional check, the path length was also measured using a micrometer. The interferometric value was normally used as it should be more accurate. The precautions concerning the use of

the instrument, such as slit width etc. were carried out as outlined in Chapter 1. The iodine cyanide used was obtained from B.D.H. Ltd. It was recrystallised from carbon tetrachloride to give white crystals. M.p. in a sealed tube = 142°C (Lit. 144-146°C, J. Chem. Phys., 1957, 27, 1211).

The infrared spectra of the solvents used were confirmed to agree with the spectra quoted in 'Selected Infrared Spectral Data', published by the American Petroleum Institute. The main impurity bands occur in the spectrum of 'Spectrosol' chloroform, supplied by Hopkin and Williams Ltd. Before drying over type 4A molecular sieves (these are small porous beads of sodium alumino silicate) the spectrum showed very strong absorptions at 1015 and 1100 $cm.^{-1}$ This is due to the ethanol (about 2%), added to the chloroform to prevent the formation of phosgene.

$$CHCl_3 + \tfrac{1}{2}O_2 \xrightarrow{\text{sunlight}} COCl_2 + HCl$$

The exact function of the ethanol is not quite clear. According to some authors it retards the decomposition of the chloroform. This is supported by the fact that infrared measurements[99] of chloroform/oxygen/ethanol mixtures show the absence of the carbonyl frequency.

However, after a few days of standing over molecular sieves the impurity bands at 1100 and 1015 $cm.^{-1}$ disappear.

C. The Systems Studied and Experimental Points of Special Importance.

1. Pyridine in Chloroform.

Chloroform absorbs strongly in the regions 3000 - 3200 $cm.^{-1}$, 1150 - 1250 $cm.^{-1}$ and 650 - 820 $cm.^{-1}$ at a thickness of 0·5 mm. For this reason, it was not possible to make measurements on pyridine $\nu_{(C-H)}$ stretching modes in chloroform. Initially, in this thesis, the pyridine assignments quoted by J.C. Duinker[113] (Ph.D. Thesis, Amsterdam, 1964) will be used. The chloroform absorption also prevented measurements on the ν_6 (a_1), ν_{16} (b_1), and ν_{26} (b_2),

ν_{25} (b_2) absorptions at 1217, 1212, 698 and 745 cm.$^{-1}$ respectively.

2. Pyridine-ICl Solutions.

Yarwood[12] has advocated the use of pyridine-ICl as an intensity standard. A few runs were made on this system, mainly to establish the reproducibility of the results, and to carry out measurements on $\nu_{(C-H)}$ stretching modes. These modes have not been examined to date.

3. Pyridine-IBr Solutions.

Apart from being more soluble than the pyridine-ICl, the pyridine-IBr complex in solution was very similar to the pyridine-ICl. There were no problems with reactions, and no significant changes in the spectrum over a period of 4 hours. Because both complexes have very large association constants, all the pyridine was complexed with the acceptor. No 'free' pyridine bands were observed in the donor spectrum in chloroform solutions.

4. Pyridine-ICN.

The pyridine vibrations are only slightly perturbed in frequency, although quite considerably in intensity, on complexation. Because of the overlap of the 'free donor', and 'complexed donor' bands, it is difficult to separate them. For this reason an attempt was made to complex as much as possible of the donor, with the acceptor, by keeping the acceptor concentration in excess. The equilibrium constant has been estimated to be about 51 litre mole^{-1} (see Table 3.2.). However, the solubility of

Table 3.2.

Association Constants for the Pyridine-Halogen Complexes

Complex	Solvent	Association Constant K_c/litre mole^{-1}	Reference
Pyridine-ICl	CCl_4	$4{\cdot}8 \times 10^5$	97
Pyridine-IBr	CCl_4	$1{\cdot}3 \times 10^4$	97
Pyridine-I_2	CCl_4	105	97a
Pyridine-ICN	CCl_4	51	121
Pyridine-Br_2	C_6H_6	97	137

ICN in a 4% pyridine solution in chloroform, estimated using a burette, is about 40 grams/litre (i.e. 0·24M). Therefore one is limited by the ICN solubility, and it is only possible to vary the path length l over a limited range of values.

Furthermore, it is important not to increase the concentration of ICN too much, as reaction may take place with the KBr plates. At the end of a series of runs on intensity measurements the whole region was scanned to ensure that no reaction had occurred.

5. Pyridine-Cl_2.

The stoichiometric quantities of pyridine and chlorine, dissolved in carbon tetrachloride, were mixed in a glove-box to give a white solid. This rapidly began to change to yellow and the appearance of the HCl vibrational spectrum indicated that the chlorine had attacked the pyridine ring. The probable reaction[100] is:

$$C_5H_5N + Cl_2 \longrightarrow [C_5H_5NCl]^+ + Cl^-$$

$$[C_5H_5NCl]^+ \longrightarrow C_5H_5N + Cl^+$$

$$C_5H_5N + Cl^+ \longrightarrow C_5H_4ClN + H^+$$

$$H^+ + Cl^- \longrightarrow HCl$$

Hence, the HCl spectrum is observed.

Weak solutions of chlorine in carbon tetrachloride, did not appear to react (no evidence of HCl spectrum). Apart from noting the frequencies of the shifted bands (for a possible normal co-ordinate calculation) no further work was carried out on this system.

6. The Pyridine-Br_2 Complex in Carbon Tetrachloride.

Certain 'sensitive modes' are the most perturbed on complexation. These are, as usual, the ν_4, ν_6, ν_7, ν_9, ν_{10}, ν_{14} and ν_{16} modes. The C-H stretching frequencies are reduced in intensity. However, the lack of

frequency shift makes studies on these bands more difficult. Most of the studies will be limited to the 'sensitive' modes.

Great care must be taken with bromine as it is extremely volatile, and escapes slowly from the cell. If the peak maxima on fast scan differed by more than 2% from the maxima on 25X expansion, the spectrum was rejected, and the cell refilled. It was not possible to get all the pyridine complexed, as the high concentration of bromine required would result in reaction taking place. Band shape studies are thus only possible on shifted bands. It is important to point out that whilst carbon tetrachloride is regarded as an inert solvent, this is very much a relative term. For any molecule to dissolve in solution there must be some interaction. Anderson and Prausnitz[102] showed that carbon tetrachloride forms a weak charge-transfer complex with benzene and with mesitylene. For 1:1 complexes the association constants are, respectively, 9×10^{-3} and $1{\cdot}13 \times 10^{-1}$ litre mole^{-1}.

In order to avoid the precipitation of insoluble ionic bromide complexes, when the pyridine solution was added to the bromine, the bromine solution was made up in carbon tetrachloride and added to the pyridine solution in carbon tetrachloride.

7. Pyridine-I_2 Complexes in Carbon Tetrachloride.

A known weight of pyridine, in a known volume of carbon tetrachloride, was added to iodine weighed out in a volumetric flask. The flask was made up to the mark with the pyridine/carbon tetrachloride solution. Iodine being the least reactive of the halogens, no problems of side reactions were encountered. Since the pyridine was in such a vast excess, the pyridine in carbon tetrachloride was used as background.

A more complete description of the inorganic chemistry of the pyridine-halogen complexes, will be given in Chapter 7. The intensities were

determined as described in Chapter 1.

8. Deuterated Pyridine with Acceptors.

It was important to carry out studies on the vibrational spectrum of pyridine-d_5 complexes to determine the frequencies for the normal co-ordinate calculation (Chapter 6). Intensity studies are also of value to confirm the assignments since one would expect the pyridine-d_5 bands to behave in a similar manner to the pyridine-h_5 ones. This assumes, of course, that the changes in normal co-ordinates between the complexed pyridine, and complexed pyridine-d_5 are small.

In the case of pyridine-ICl and pyridine-d_5-ICl the highest intensities were observed for the ν_{14}, ν_9, ν_7, ν_4, ν_{10}, ν_6 bands and thus this confirmed the assignments for these bands. The frequency results are summarised in Table 3.3.

By substituting the atomic weight of deuterium for hydrogen in the G matrix, and using the same F matrix it should be possible to calculate the frequencies of the vibrations in the pyridine-d_5-halogen complexes. Since 'chemically' deuterium, and hydrogen, are identical, one would expect the force constants to be identical in the two complexes. The deviation of the calculated, from the observed frequencies, in the pyridine-d_5-halogen complexes, should give an extra check on the accuracy of the force field.

9. Studies on the b_2 Modes.

The halogen complexes are prepared from solutions in carbon tetrachloride. A contact film of carbon tetrachloride shows two very intense absorptions at 785 and 795 $cm.^{-1}$ Even the smallest trace of carbon tetrachloride (< 0·01%) will give spurious absorptions at these frequencies. For this reason, the complex was recrystallised from carbon disulphide, before use, when measurements are made in the 600 - 700 $cm.^{-1}$ region. The carbon

tetrachloride impurity did not affect the melting point, because its boiling point at 77°, resulted in it being distilled out of the melting point tube, long before the complex melts. It is not advisable to store pyridine-IBr in a vacuum desiccator, which would remove the carbon tetrachloride, because pyridine-IBr loses IBr on pumping. (For further details see the experiment discussed in Chapter 7).

D. Frequency and Intensity Changes on Complexation.

1. Frequency Changes.

The frequency data are summarised in Table 3.4.

Whilst a number of attempts have been made to assign the bands in the pyridine spectrum,[103,105,105a] no-one has proved the assignment to be correct. Since quite dramatic changes occur in frequency, and intensity, on complexation some evidence may be obtained to confirm, or reject, a particular assignment. Furthermore, the pyridine-d_5 vibrations would be expected to give exactly the same pattern of frequency and intensity shifts as pyridine-h_5 on complexation, provided vibrational mixing (Chapter 6), is not a major influence on the intensities.

The infrared spectrum of pyridine and pyridine-d_5 has been assigned by Corrsin, Fax and Lord.[103] Long, Murfin and Thomas[104] have carried out a force field calculation on pyridine and the mixed deuterated derivatives. They transferred Whiffen's[105] internal force constants from benzene directly to pyridine. Zerbi et al.[105a] have analysed the planar normal co-ordinates of the same molecules using a Urey Bradley[106] force field. Both Long et al., and Zerbi et al., disagree with the Wilmshurst and Bernstein assignment,[107] which was derived using both infrared and Raman spectra. McCullough[108] calculated thermodynamic properties and reassigned some of the fundamental frequencies in order to get a better fit between calculated and observed frequencies. Although, of course, the fit will, to a large extent, depend upon the original frequencies used in the calculation.

Table 3.3.

Near-Infrared Spectral Data for the Pyridine-d_5-Halogen Complexes

Mode	'Free' Pyridine-d_5					Pyridine-d_5-ICN		Pyridine-d_5-ICl	
	Solvent	Band posn./ $cm.^{-1}$	Intensity ($CHCl_3$)	Solvent	Band posn./ $cm.^{-1}$	Solvent	Band posn./ $cm.^{-1}$	Solvent	Band posn./ $cm.^{-1}$
a_1 modes									
ν_1	Pure liquid	2293	m	$CHCl_3$	2295				
ν_2	"	2270	s	"	2269				
ν_3	"	2254	Not Observed	"	-				
ν_4	"	1530	$CHCl_3$ absorbs	"	1539	$CHCl_3$	1552	$CHCl_3$	1555
ν_5	"	1340	w	"	1338	"	1345	"	1340
ν_6	"	1006	m	"	1015	"	1020	"	1018
ν_7	"	962	s	"	965	"	972	"	975
ν_8	"	886	m	"	878	"	877	"	
ν_9	"	823	$CHCl_3$ absorbs	"	≈823	"	830	"	
ν_{10}	"	582	m	"	585	"	599	"	605
b_1 modes									
ν_{11}	Pure liquid	2293	m	$CHCl_3$	2295	$CHCl_3$			
ν_{12}	"	2285	m	"	2288	"			
ν_{13}	"	1542	$CHCl_3$ absorbs	"	1542	"	1570	$CHCl_3$	1585
ν_{14}	"	1322	w	"	1325	"	1330	"	1322
ν_{15}	"	1301	s	"	1302	"	1311	"	
ν_{16}	"	908	vvw	"	908	"	925	"	
ν_{17}	"	887	vw	"	889	"	889	"	885
ν_{18}	"	833	m	"	833	"	833	"	832
ν_{19}	"	625	$CHCl_3$ absorbs	"	625	"	625	"	

Table 3.4.

Near-Infrared Spectral Data for the Vibrations of Pyridine and Pyridine-Halogen Complexes

	Pyridine							Pyridine-I_2	
Mode	Solvent	Band posn./ $cm.^{-1}$	Intensity	Solvent	Band posn./ $cm.^{-1}$	Solvent	Band posn./ $cm.^{-1}$	Solvent	Band posn./ $cm.^{-1}$
a_1 class									
ν_1	Liquid	3054	m	CCl_4	3062	$CHCl_3$	3061	CCl_4	
ν_2	"	3054	m	"	3062	"	3061	"	
ν_3	"	3036	s	"	3025	"	3034	"	
ν_4	"	1580	s	"	1583	"	1585	"	1595
ν_5	"	1482	s	"	1484	"	1484	"	1482
ν_6	"	1218	m	"	1217	"	1220	"	1212
ν_7	"	1068	s	"	1070	"	1069	"	1068
ν_8	"	1029	s	"	1029	"	1031	"	1032
ν_9	"	992	m	"	997	"	991	"	1005
ν_{10}	"	605	s	"	604	"	605	"	621
b_1 class									
ν_{11}	"	3083	s	"	3086	"	3085	"	
ν_{12}	"	3054	m	"	3062		3061	"	
ν_{13}	"	1572	m	"	1578			"	
ν_{14}	"	1439	vs	"	1439		1440	"	1448
ν_{15}	"	1375	w	"	1378		1375	"	1355
ν_{16}	"	1217	m	"	1215		1217	"	1212
ν_{17}	"	1148	s	"	1152		1149	"	1150
ν_{18}	"	1068	s	"	1062				1070
ν_{19}	"	652	vw	"	655		652	"	
b_2 class									
ν_{20}	"	675	w	"	668			"	678
ν_{21}	"	942	vw	"	942			"	
ν_{22}	"	749	m	"	CCl_4 absorbs			"	CCl_4 absorbs
ν_{23}	"	703	w	"	CCl_4 absorbs			"	CCl_4 absorbs
ν_{24}	"	405	s	"	409			"	415
a_2 class infrared inactive Raman spectrum									
ν_{25}	liquid	886							
ν_{26}	liquid	374							
ν_{27}	liquid	981							

Table 3.4. (cont.)

Mode	Pyridine-Br_2		Pyridine-Cl_2		Pyridine-IBr		Pyridine-ICl		Pyridine-ICN	
	Solvent	Band posn./ $cm.^{-1}$	Solvent	Band posn./ $cm.^{-1}$	Solvent	Band posn./ $cm.^{-1}$	Solvent	Band posn. $cm.^{-1}$	Solvent	Band posn. $cm.^{-1}$
a_1 class										
ν_1	CCl_4		CCl_4		$CHCl_3$	Solvent absorbs	$CHCl_3$		$CHCl_3$	
ν_2	"		"		"		"		"	
ν_3	"		"		"		"		"	
ν_4	"	1595	"	1605	"	1602	"	1602	"	1595
ν_5	"	1484		1491	"	1478	"	1478	"	1482
ν_6	"	1210			"	1212	"	1212	"	
ν_7	"	1070		1070	"	1068	"	1068	"	1070
ν_8	"	1032		1031	"	1033	"	1035	"	1035
ν_9	"	1010		997	"	1010	"	1013	"	1005
ν_{10}	"	625		609	"	628	"	631	"	619
b_1 class										
ν_{11}	"		"		"					
ν_{12}	"		"		"					
ν_{13}	"		"	1576	"	1578	"	1578	"	1578
ν_{14}	"	1449	"	1436	"	1450	"	1452	"	1445
ν_{15}	"		"	1375	"	1355	"	1355	"	
ν_{16}	"	1212	"		"	1212	"		"	
ν_{17}	"	1148	"	1150	"	1155	"	1156	"	1152
ν_{18}	"		"	1068	"	1068	"	1066	"	1069
ν_{19}	"		"		"	952	"	952	"	
b_2 class										
ν_{20}	"	675			"	978	"	972		
ν_{21}	"				"	955	"	955		
ν_{22}	"				"	$CHCl_3$ absorbs	"	$CHCl_3$ absorbs		
ν_{23}	"				"	"	"			
ν_{24}	"				"	430	"	425		415

As explained in Chapter 2, the enormous intensity perturbation on complexation is due to 'electron vibration'. Because of the $\left(\frac{\partial_I}{\partial_Q}\right)$ contribution to the charge-transfer mechanism (see Chapter 2), one would expect the a_1 class vibrations to be the most affected in intensity on complexation. This, of course, assumes that the geometry of the solid complex[109] is the same as that in solution.

It is extremely difficult to make measurements on the C-H stretching bands in the case of the complexes with iodine, bromine, chlorine and iodine cyanide, because it is impossible to ensure that all the pyridine is complexed. Any free pyridine present would have a much greater intensity than the complexed pyridine. Only in the pyridine-ICl and pyridine-IBr cases was it possible to look at the C-H stretching bands.

When a spectrum of a pyridine solution was compared with a spectrum of the same pyridine solution with a known weight of acceptor added, important differences were observed between the two spectra. The bands arising from the ν_6, ν_7, ν_9, ν_{10}, ν_6 (also ν_{16}), and ν_7 (also ν_{18}) modes were considerably increased in intensity. The bands arising from the ν_1, ν_2, ν_3, ν_5 modes are considerably reduced in intensity. This is in good agreement with the expected large perturbation for the a_1 modes, and supports the assignment. The bands arising from the ν_4 and ν_8 modes are only slightly increased in intensity. The ν_4 band does at least show a considerable frequency perturbation. The ν_8 band, however, shows only a small frequency and intensity perturbation. The normal co-ordinate calculation (see Chapter 6) shows that this band has about 90% contribution from the $\Delta\alpha$ co-ordinates, in the free pyridine and the complex. This shows that the ν_8 vibration involves ring distortion. Further discussion of this band will be left to Chapter 6.

The corresponding pyridine-d_5 band, at 877 $cm.^{-1}$, is similarly unperturbed in intensity on complexation. This does at least indicate that

the two bands have similar orientation of their transition dipoles. The assignment of the ν_{10} band at about 720 cm.$^{-1}$, as suggested by McCullough[108] is neither confirmed, nor rejected, by these studies.

The lack[33] of complex bands near 1139 and 884 cm.$^{-1}$ rules out the assignment of these bands to a_1 modes, as suggested by Kline and Turkevich.[110] There is no evidence to suggest that the ν_{16} band appears at 1200 or 1288 cm.$^{-1}$ as suggested by McCullough[108] or Wilmshurst and Bernstein, respectively.

The out-of-plane b_2 class of vibrations contains two ring vibrations giving rise to bands at 675 and 405 cm.$^{-1}$. The 405 cm.$^{-1}$ band shows a considerable perturbation on complexation in frequency but not in intensity. The 675 cm.$^{-1}$ absorption is less affected. The frequency is not changed.

The b_2 class also contains three bands arising from C-H out-of-plane bending at 942, 749 and 703 cm.$^{-1}$ respectively. The reason for the extreme weakness of the 942 cm.$^{-1}$ absorption is not clear. It is slightly increased in intensity in the complex.

2. Studies on the Intensity Changes of the Pyridine Band on Complexation with the Halogens.

(i) a_1 + b_1 Vibrations of Pyridine-IBr and Pyridine-ICl.

A full intensity study was made on the perturbed bands of pyridine-IBr. Work on the other halogen complexes was restricted to a less rigorous survey, to see if they followed the same trend as pyridine-IBr.

In view of the great care needed to obtain intensity results, and the fact that pyridine-ICl has been suggested as an intensity standard, the author felt it to be worthwhile to measure the intensity of a few of the bands in the pyridine-ICl spectrum. Provided the results agreed with the literature values,[96] this would ensure that the correct experimental procedure was being carried out.

The intensity results for pyridine-ICl in chloroform are listed in Table 3.5. The results agree within the error of the literature values[96] in

Table 3.5.

Summary of the Infrared Intensities of Pyridine-ICl in Chloroform

Band posn./ $cm.^{-1}$	[Complex] moles/litre	Path Length/ mm.	10^6 Cl (mole $cm.^{-2}$)	Area/ $cm.^{-1}$	Intensity[a] (Darks)	$\Delta\bar{\nu}_{\frac{1}{2}}/cm.^{-1}$	Literature value intensity	Literature value $\Delta\bar{\nu}_{\frac{1}{2}}$
1604	$6{\cdot}492 \times 10^{-2}$	0·502	3·2959	9·68	2940	4·0	2950 ± 0·300	4·2
1453			3·2959	12·97	3940	3·5	4300 ± 400	4·2
1355			3·2959	0·7848	240	3·5	250	Not quoted
1155			3·2959	1·800	550	4·0	450 ± 50	5·0
1070			3·2959	9·75	2960	3·0	3350 ± 400	2·5
1036			3·2959	2·231	680	2·8	750 ± 150	2·8
1014			3·2959	9·887	2990	3·5	3430 ± 500	3·5
631			3·2959	5·932	1800	3·5	1940 ± 500	4·0
422			6·9	1·38	200	6·0		

[a] The 'Dark' intensity unit (used throughout this work) is 1 litre $mole^{-1}$ $cm.^{-2}$

intensity. The bands are slightly narrower. This could be due to instrumental factors, e.g. narrower slit and a different instrument, or a solvent concentration effect, since the Cl value used is twice the highest value in the literature.[96] Studies on the broader pyridine bands are in better agreement since there were fewer problems due to slit width (see Table 3.6.). The intensity values of pyridine in carbon tetrachloride and chloroform were confirmed (see Table 3.6.). The intensity of the $\nu_{(C-H)}$ stretching modes in carbon tetrachloride were measured for the first time. It was not possible to make intensity measurements on the $\nu_{(C-H)}$ bands in chloroform because the solvent absorbs strongly and masks the C-H absorption.

As can be seen from Table 3.6. the pyridine intensities in chloroform agree within 20% of the values in carbon tetrachloride. It would seem reasonable to assume that this would also be the case for the $\nu_{(C-H)}$ band intensities in chloroform and carbon tetrachloride. Unfortunately, it is not possible to measure the intensities of $\nu_{(C-H)}$ bands of the pyridine-IBr and pyridine-ICl complexes in carbon tetrachloride because of their very low solubility. The $\nu_{(C-H)}$ band intensities for the pyridine-IBr complex in chloroform-d was measured. Chloroform-d does not absorb in the 3000 - 3150 $cm.^{-1}$ region and thus allowed measurements on the $\nu_{(C-H)}$ bands to be made.

As can be seen from Tables 3.6 and 3.7. there is a dramatic drop in intensity on complexation of the $\nu_{(C-H)}$ bands. The band at 3010 $cm.^{-1}$ has been interpreted as a combination band (i.e. $\nu_{13} + \nu_{14}$).[103] However, one would expect this band to have moved up in frequency to (1578 + 1452) = 3030 $cm.^{-1}$ on complexation (assuming the anharmonicity is the same). The nearest band to this is the band at 3025 $cm.^{-1}$ which is very weak. If this is the correct interpretation, the combination band has fallen in intensity by over 100% and this would appear to be unlikely. The assignment is not easily explained by the perturbation on complexation. Group theory predicts five $\nu_{(C-H)}$ vibrations ($3a_1 + 2b_1$). None of the a_1 or b_1 fundamentals should

Table 3.6.

Summary of the Infrared Intensities of Pyridine in: (A) Carbon Tetrachloride; (B) Chloroform

(A)								(B)				
Band posn./ $cm.^{-1}$	[Pyridine] moles/litre^{-1}	10^6 Cl/ mole $cm.^{-2}$	Area/ $cm.^{-1}$	Intensity/ Darks	$\Delta\bar{\nu}_{\frac{1}{2}}$/$cm.^{-1}$	Lit. value intensity	Lit. value $\Delta\bar{\nu}_{\frac{1}{2}}$	Band posn/ $cm.^{-1}$	Cl $\times 10^3$	Area/ $cm.^{-1}$	Intensity/ Darks	$\Delta\bar{\nu}_{\frac{1}{2}}$/$cm.^{-1}$
3088	$7{\cdot}4227 \times 10^{-2}$	3·72	5·49	1470	10·0	None	None					
	$36{\cdot}7 \times 10^{-2}$	18·89	27·44	1450	10·0							
		11·31	15·72	1390	10·0							
		7·39	10·80	1460	10·0							
		13·86	20·01	1450	10·0							
3011	$7{\cdot}4227 \times 10^{-2}$	3·72	3·55	950	11·0	None	None					
	$36{\cdot}7 \times 10^{-2}$	18·89	14·54	770	9·0							
		11·31	10·82	960	10·0							
		7·39	7·12	960	9·6							
		13·86	12·87	930	9·0			1606	2·06	0·8798	430	7·0
								1589	2·06	6·99	3390	10·0
1484		18·89	8·68	460		430	Not quoted					
1218		18·89	6·98	370		390	Not quoted					
1071		18·89	9·44	500		430	Not quoted	1072	2·06	0·6935	340	4·0
1031		18·89	12·84	680		700	Not quoted	1034	2·06	1·258	610	3·6
991		18·89	8·68	460		530	Not quoted	996	2·06	1·5002	730	4·5
605		18·89	8·67	460		480	Not quoted	606	2·06	0·833	410	6·0
1147		18·89	7·56	400		340	Not quoted	406	9·72	20·9	215	6·0
								406	10·19	19·4	200	7·0

Table 3.7.

Intensity Studies on the $\nu_{(C-H)}$ Bands of Pyridine-IBr

Band Position/ $cm.^{-1}$	[Complex] moles/litre	10^6 Cl/mole $cm.^{-2}$	Area/ $cm.^{-1}$	Intensity/ Darks	$\Delta\bar{\nu}_{\frac{1}{2}}/cm.^{-1}$	Pyridine Absorption		Band Position/ $cm.^{-1}$	Solvent
						Intensity/ Darks	$\Delta\bar{\nu}_{\frac{1}{2}}/cm.^{-1}$		
3110		5·589	≈0·27	5	Too weak				$CDCl_3$
3080	$11·17 \times 10^{-2}$	5·589	2·25	402	9·0	1400	10·0	3088	$CDCl_3$, CCl_4
3045		4·589	0·5567	19	10·0			3042*	$CDCl_3$ CCl_4
3025		5·589	≈0·200	4	Too weak			3032	$CDCl_3$ CCl_4
3010		5·589	≈1·30	200	On top of $CDCl_3$ band	900	9·5	3011†	$CDCl_3$, CCl_4

* Overlaps with 3032 $cm.^{-1}$ band.

† Overlaps with 3032 $cm.^{-1}$ band.

be degenerate, but the normal co-ordinate calculation predicts that the $\nu_{(C-H)}$ vibrational frequencies are quite close together. So it seems possible that two vibrations occur at the same frequency by chance.

In any event, one thing is certain. There is an enormous drop in intensity on complexation. If the 3010 and 3080 $cm.^{-1}$ bands are $\nu_{(C-H)}$ fundamentals, two bands are far more intense than the other three. Spectrum 3.1. shows pyridine-IBr in chloroform-d and carbon disulphide illustrating this decrease in intensity, while Spectra 3.2A. and 3.2B. show the 3000 $cm.^{-1}$ region in more detail.

As explained in Chapter 2, the intensity depends upon the change in dipole moment with normal co-ordinate. Since the frequency perturbation on complexation is small, one would expect the normal co-ordinates not to change very much on going from the 'free' donor to the complexed donor. (This is confirmed by the calculations described in Chapter 6). Also the ν_1, ν_2, ν_3, ν_4, ν_{12} vibrations are at much higher energy than the highest band positions of those which arise from ring modes. Whilst the symmetry co-ordinates of the five vibrations mix with each other, our calculations show that mixing with the other symmetry co-ordinates is less than 5% (see Chapter 6).

Chapter 2 showed that enormous intensity perturbations are best interpreted in terms of the 'electron vibration' i.e. the change in dipole moment due to changes in charge transfer with atomic displacement, determines the intensity. The dipole moment μ is the charge C multiplied by the separation, s.

$$\mu = C.s \qquad \ldots\ldots [3.1.]$$

$$\therefore \quad d\mu = Cds + sdC \qquad \ldots\ldots [3.2.]$$

In other words, the above equation means that the intensity depends on the size of the charge vibrating C, and the change of charge dC, during the

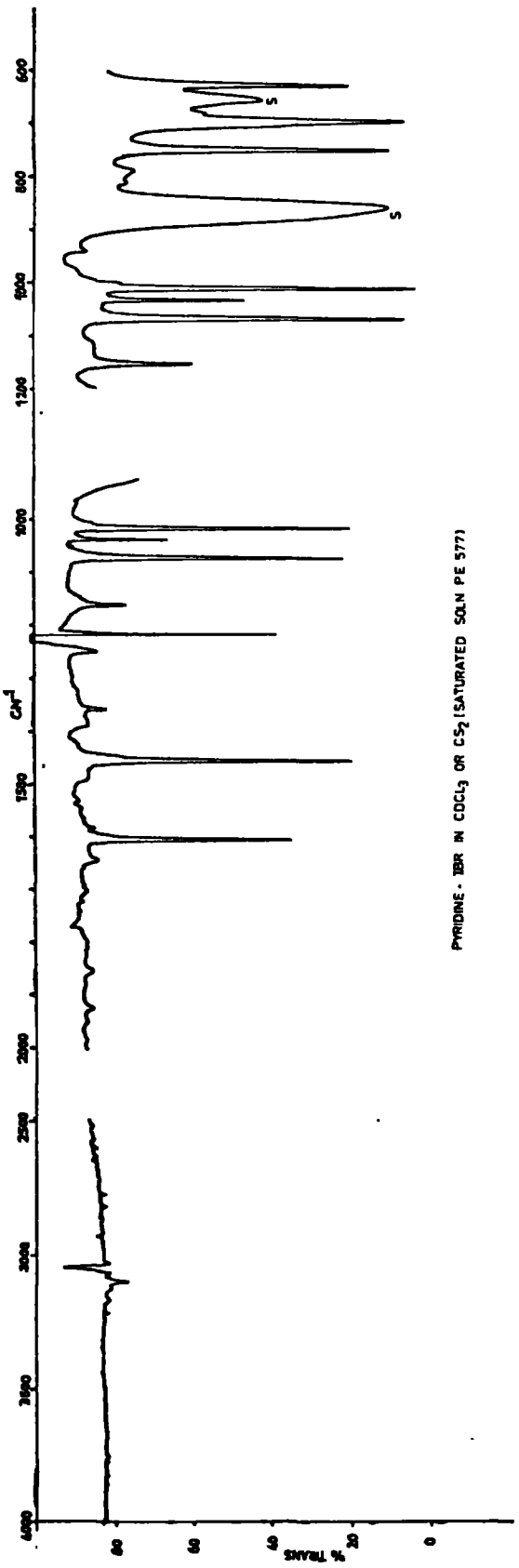
PYRIDINE - TBR IN $CDCl_3$ OR CS_2 (SATURATED SOLN PE 577)
CM^{-1}
% TRANS
S
S

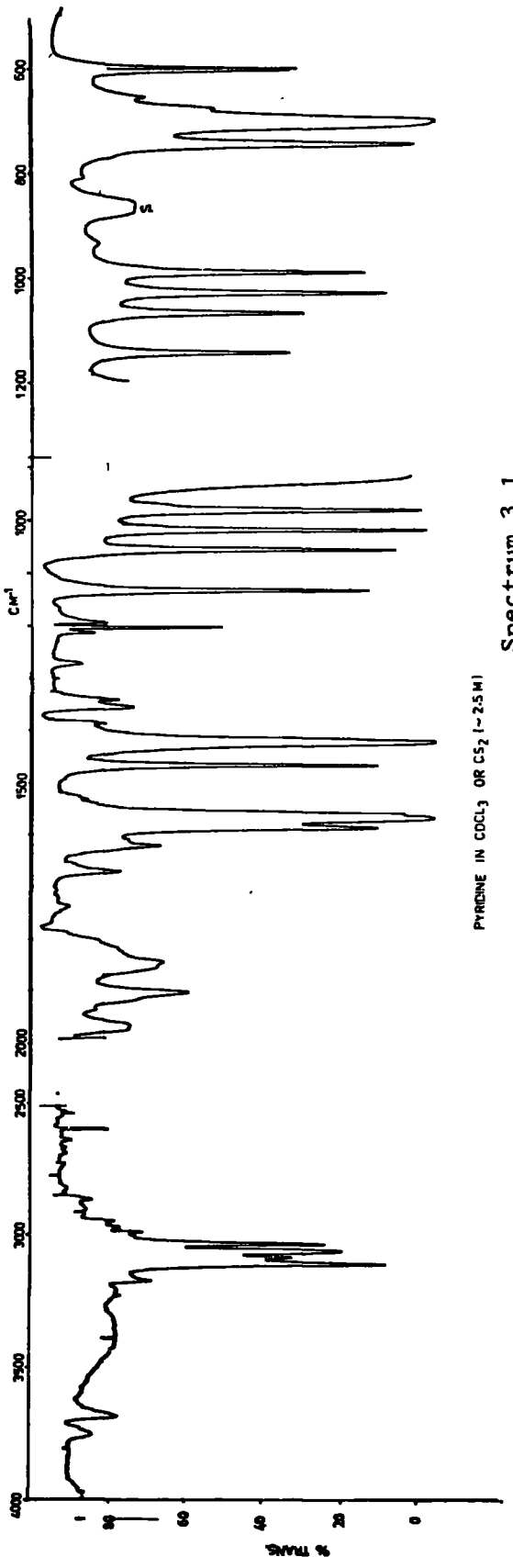
PYRIDINE IN $CDCl_3$ OR CS_2 (~2.5 M)
CM^{-1}
% TRANS
S

Spectrum 3.1.

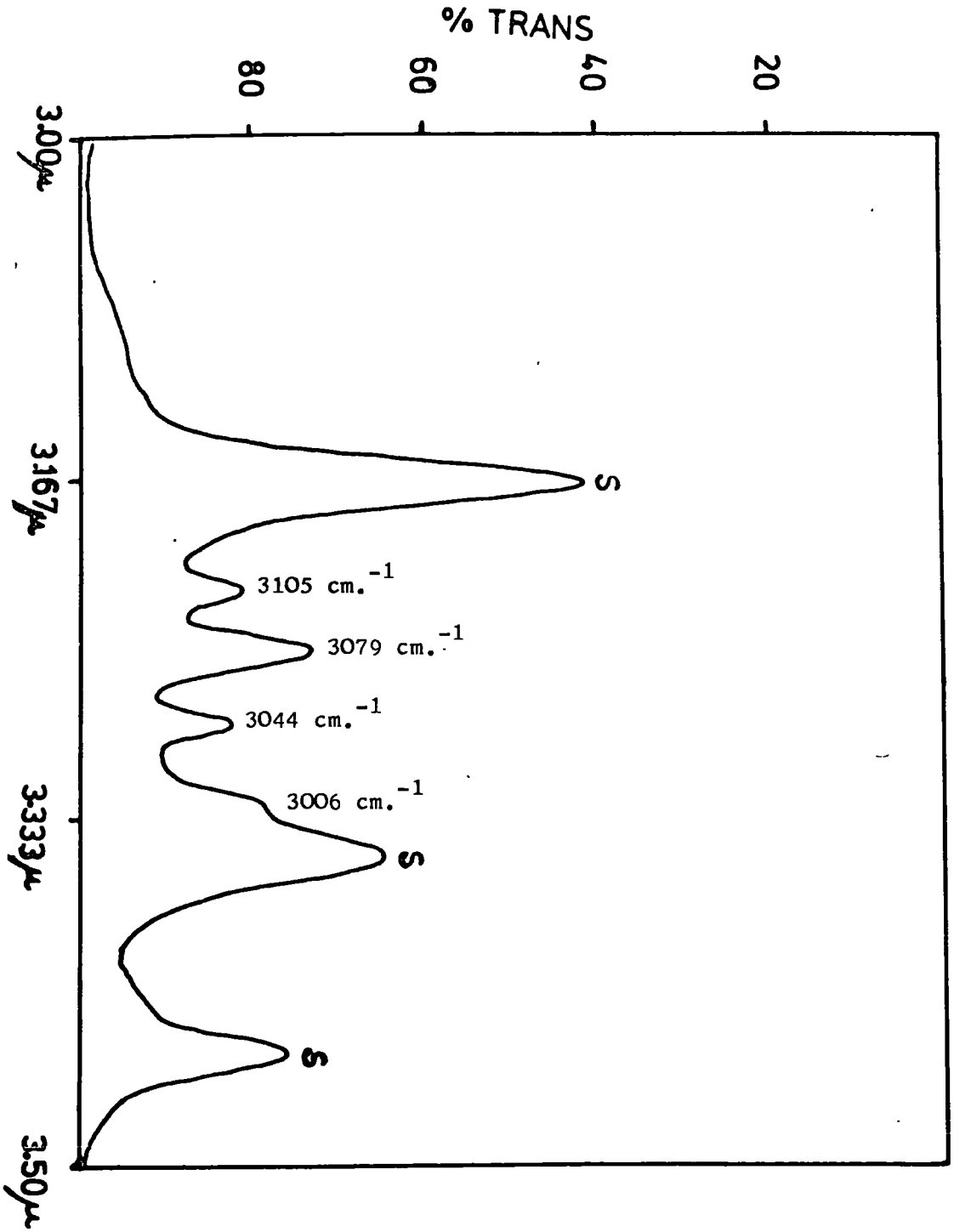

Spectrum 3.2A. Pyridine-ICl in chloroform-d. Solution is saturated at a path length of 0·5 mm. S indicates a solvent absorption.

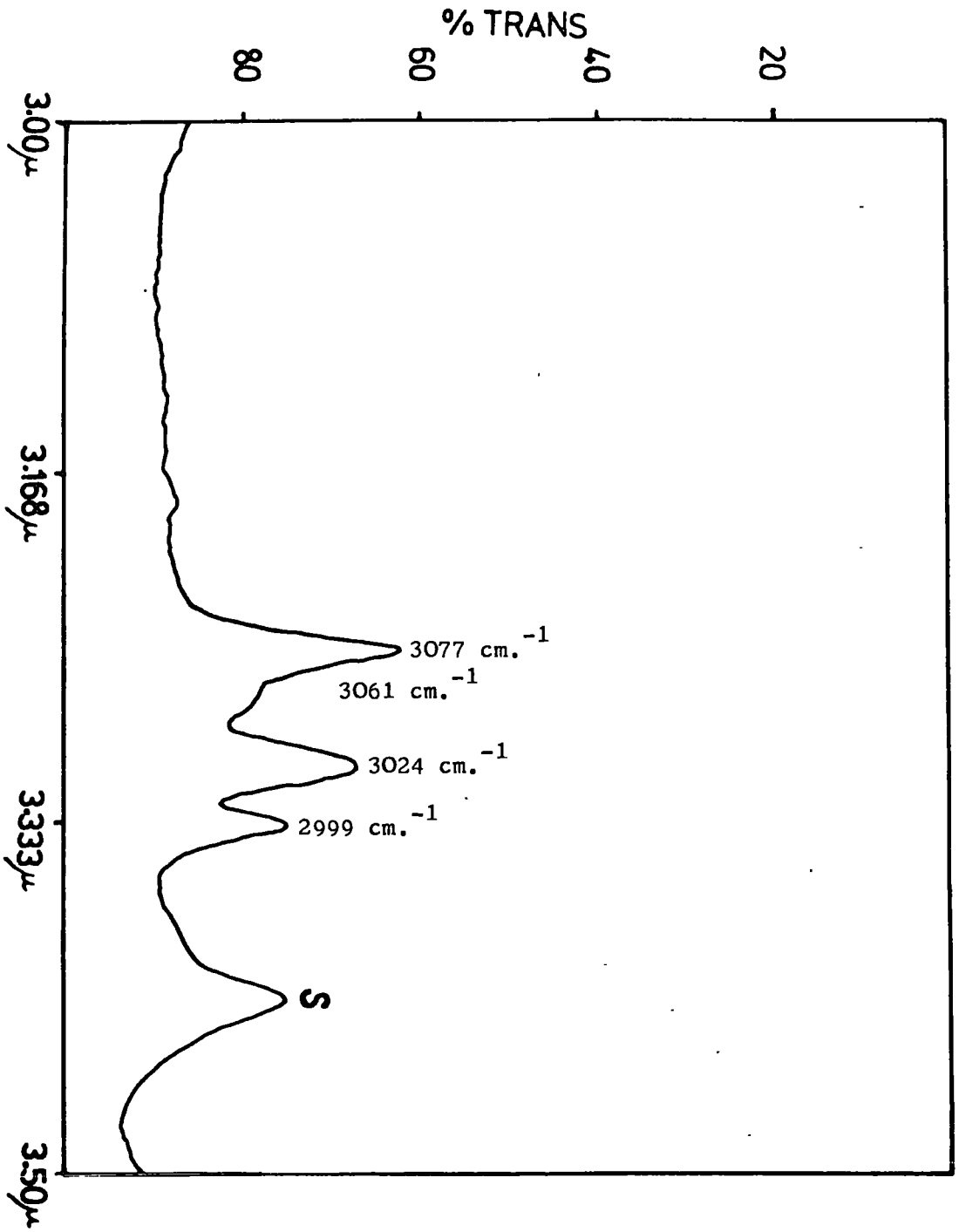

Spectrum 3.2B. Pyridine-ICl in carbon disulphide. Solution is saturated at a path length of 0·5 mm. S indicates a solvent absorption.

course of the vibration. Assuming the change of charge dC is not very different in pyridine and the complex, then the intensity change will depend upon the charge C on the atoms in the free donor, compared with those on the complexed donor. The size of the total charge C donated from pyridine can be estimated from n.q.r. studies.[31] However, in order to assess the trend in intensity, one requires to know the charge distribution in pyridine-IBr and pyridine-ICl. Whilst the n.q.r. of pyridine-ICl has been determined, the pyridine-IBr n.q.r. has only been partly established[114] at the time of writing.

In any case, the n.q.r. data would only determine the total charge on the donor. No information on the charge distribution in the ring would be given. However, if the charge donated from the pyridine ring was greater for the ICl complex than for the IBr complex, one would expect the frequencies in the ICl complex to be the most perturbed.

However, the fall in intensity of the five $\nu_{(C-H)}$ bands (ν_1, ν_2, ν_3, ν_{11}, ν_{12}), on complexation, can be explained by the following very crude model. Pyridine has a similar structure to benzene with the same 'aromatic' structure. However, the lone-pair on the nitrogen, to a first approximation, is not involved in bonding. Hückel theory predicts the following electronic arrangement in benzene and pyridine.

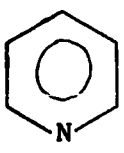

— $\alpha - 0{\cdot}84\beta$

— $\alpha + 0{\cdot}84\beta$

— $\alpha + 1{\cdot}17\beta$

— $\alpha + 2{\cdot}11\beta$

—— $\alpha - 2\beta$

— — $\alpha - \beta$

— — $\alpha + \beta$

—— $\alpha + 2\beta$

α = Coulomb integral, H_{11}

β = Resonance integral, H_{12}

π-e Charge Distribution

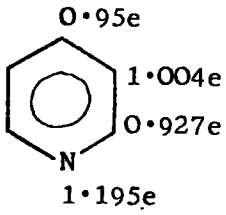

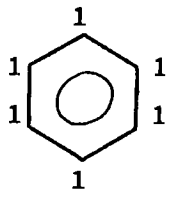

I_p, Benzene = 9·24 eV

I_p, Pyridine = 9·27 eV

In the free pyridine the C-H bonds will be polarised according to the atomic electronegativities[115] i.e. $C^{\delta-}\leftarrow H^{\delta+}$. This polarity will be reduced due to the positive charge delocalised in the ring on complexation (see Fig. 3.1.).

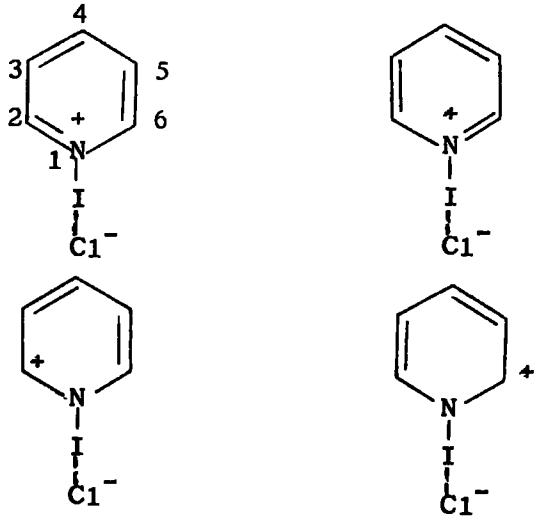

Fig. 3.1.

Bond	No. of Canonical Forms with Double Bond Character
1-2	1
2-3	3
3-4	2
4-5	2
5-6	3
6-1	1

Table 3.8.

This model uses the mesomeric effect to explain the influence of the positive charge on the ring vibrations. If the positive charge was more localised on the nitrogen atom, then the electron density on the carbon atoms would be more influenced by the inductive (distance) effect.

The n.m.r. spectra should give some information on this question. This is because, when placed in a magnetic field, the electrons surrounding the nucleus tend to circulate, to produce a field opposing that applied.

In fact, it can be shown that:

(ref. 56, p.248)

$$H_i = H_z (1 - \sigma_i) \quad \ldots\ldots \quad [3.3.]$$

where H_i is the field experienced by a particular nucleus i, whose shielding constant is σ_i and H_z is the field applied.

In the complex, one would expect from the mesomeric mechanism, that the electron density about the hydrogen atom, in the $\alpha + \gamma$ C-H bonds should be lower, than in the β C-H bonds. It would thus be expected that the shielding constants should be such that,

$$\sigma CH\ (\beta) > \sigma CH\ (\alpha + \gamma)$$

Thus the field experienced by the hydrogen nucleus in the $\alpha + \gamma$ positions is greater than at the nucleus in the β position. Equation 3.3. shows that, in order to come to resonance with radiation of a particular frequency, an α and γ C-H hydrogen requires a greater applied field, than a β C-H hydrogen.

It should be noted that electron density is not the only factor determining the value of the shielding constant. The field-induced circulation of electrons in neighbouring parts of the molecule may give rise to small magnetic fields acting in opposition or in the same direction as the applied field. Thus, changes in the magnetic anisotropy of the nitrogen should cause an upfield shift of the α protons,[147] when the nitrogen lone pair electrons take part in a specific interaction, i.e. the nitrogen lone pair effectively deshields the α carbon atoms in the free pyridine.

In the absence of reaction field effects,[148] it would appear to be reasonable to interpret an α-proton downfield shift, as arising from the deshielding effect of electron density redistribution in the complex, which is greater than the predicted relative shielding effects caused by nitrogen atom magnetic anisotropy and nitrogen atomic dipole changes.

Thus, Yarwood[30] observed a downfield shift of the pyridine protons on complexation with ICl. The downfield shifts of the α-, β-, and γ-protons were 11, 19, and 30 c/s respectively. So, allowing for the lone pair electrons becoming involved in a specific interaction the α value is really larger than 11 c/s. The γ-value is definitely larger than the β-value. Therefore, the n.m.r. data tends to support the predominance of the mesomeric mechanism although inductive effects are clearly operative as well.

Whilst the resonance structure makes a large contribution to the intensity, the contribution to the frequency is very much smaller. Considering as an example the band arising from the ν_7 vibration in pyridine, the intensity is increased by 700%, whilst the frequency is only changed by 0·2% on complexation with ICl. One would expect the resonance structures in Table 3.8. to alter the $f_{(C-C)}$ and $f_{(C-N)}$ force constants (see Chapter 6). However a change of 0·2 millidynes/A^o of the $f_{(C-C)}$ and $f_{(C-N)}$ force constants does not significantly affect the frequencies of the $a_1 + b_1$ vibrations. It would thus appear that the resonance structures are not very important in perturbing the donor frequencies.

The low intensity of the $\nu_{(C-H)}$ bands, and the fact that the pyridine-ICl complex is only a third as soluble as the pyridine-IBr complex in chloroform-d, meant that work was initially confined to the pyridine-IBr complex, in the 3000 - 3100 $cm.^{-1}$ region. Measurements made in 3000 - 3100 $cm.^{-1}$ region at the time of writing indicate (in carbon disulphide where very large path lengths may be used (about 4 mm.)) that the absorptions are very weak, i.e. similar to the pyridine-IBr absorptions. (Spectrum 3.2.).

It is interesting to note that in the benzene case bonding electrons are directly involved in the complex. The perturbation of the benzene vibrations on complexation will be weaker than the pyridine case because:

(a) the ionisation potential of benzene is higher[116] (less charge transfer),

(b) the positive charge will not be localised on the ortho and para positions, so the intensity perturbation will be less concentrated on particular modes.

At the present time only two groups of papers (partially) deal with the benzene halogen complex donor vibrations.[117,118] These support the above prediction; however, no measurements have been made on the C-H stretching modes in the benzene-halogen complexes.

As can be seen from Table 3.9. the intensities of pyridine-IBr and pyridine-ICl in chloroform are very similar. The bands obey Beer's Law, a typical Beer-Lambert Law graph is shown (for the ν_{10} band of pyridine-IBr in benzene) in Figure 3.2. Provided a large number of points are taken the intensities are reproducible to within 10%.

Apart from the ν_1, ν_2, ν_3, ν_{11}, ν_{12}, ν_5, ν_{13} bands the other bands in the donor bands arising from the $a_1 + b_1$ vibrations are increased in intensity, and narrowed on complexation. The IBr complex bands are slightly broader and slightly weaker in intensity, but the difference is only about 10% for the most sensitive bands. The frequencies of the two complexes are also practically identical. The chloroform interacts with the pyridine complexes to some extent, presumably with the overall dipole of the molecule by hydrogen bonding to the negative end (see Chapter 4). For this reason the complexes are more soluble in chloroform than carbon tetrachloride.

The bands are narrowed by the suppression of orientational motion about the two axes perpendicular to the C_2 axis. If orientational motion controls

Table 3.9.

The Infrared Band Intensities for Pyridine-IBr and Pyridine-IC1 (Donor Bands)

Mode	Solvent	Pyridine-IBr					Pyridine-IC1		
		Band Position/cm.$^{-1}$	$\Delta\nu_{\frac{1}{2}}$/ cm.$^{-1}$	10^6c.l/ mole cm.$^{-2}$	Area/ cm.$^{-1}$	Intensity/ 'darks'	Band Position/cm.$^{-1}$	$\Delta\nu_{\frac{1}{2}}$/ cm.$^{-1}$	Intensity/ 'darks'
ν_4	$CHCl_3$	1602	5·5	3·382	8·13	2120	1604	4·0	2940
				5·559	15·10	2700			
				0·949	2·77	2900			
				0·605	1·82	2980			
				0·606	1·81	2970			
				1·603	4·17	2600			
				1·319	3·36	2557			
				0·863	2·78	3200			
				1·854	4·42	2400			
				1·417	3·67	2600			
				0·984	3·00	3050			
				0·303	0·85	2790			
				Average value = 2700 ± 300 darks					
ν_6	$CHCl_3$-d	1213	3·5	5·589	6·72	1200	1070	2·5	3350
ν_7	$CHCl_3$	1070	3·5	5·589	16·7	3010			
				3·824	12·8	3350			
				0·613	2·03	3300			
				1·319	4·20	3200			
				0·802	2·37	3000			
				1·854	5·19	3800			
				6·613	2·18	3500			
				0·303	1·12	3710			
				0·949	3·32	3500			
				0·962	3·48	3600			
				1·870	5·80	3100			
				Average value = 3300 ± 400 darks					

/cont.

Table 3.9. cont.

Mode	Solvent	Pyridine-IBr					Pyridine-ICl		
		Band Position/cm.$^{-1}$	$\Delta\nu_{\frac{1}{2}}$/ cm.$^{-1}$	10^6c.l/ mole cm.$^{-2}$	Area/ cm.$^{-1}$	Intensity/ 'darks'	Band Position/cm.$^{-1}$	$\Delta\nu_{\frac{1}{2}}$/ cm.$^{-1}$	Intensity/ 'darks'
ν_8	$CHCl_3$	1035	3·5	1·854	1·24	670	1036	2·8	680
				5·589	2·84	510			
				1·302	0·708	550			
				1·87	1·320	700			
				0·962	0·644	670			
				0·949	0·651	690			
				0·611	0·351	580			
				0·620	0·355	580			
				0·401	0·291	725			
				Average = 700 ± 100 darks					
ν_9	$CHCl_3$	1011	3·5	3·824	12·2	3190	1011	3·5	3430
				0·612	2·12	3460			
				1·854	6·83	3700			
				1·319	4·24	3210			
				0·949	3·07	3200			
				1·116	3·90	3500			
				0·962	3·19	3320			
				0·303	1·04	3450			
				Average 3,300 ± 300 darks					
ν_{10}	$CHCl_3$	630	5·5	3·824	6·823	1780	631	3·5	1800
				1·116	1·96	1760			
				5·589	9·78	1750			
				Average = 1,760 ± 100 darks					

/cont.

Table 3.9. cont.

Mode	Solvent	Pyridine-IBr					Pyridine-IC1		
		Band Position/cm.$^{-1}$	$\Delta\nu_{\frac{1}{2}}$/ cm.$^{-1}$	10^6c.l/ mole cm.$^{-2}$	Area/ cm.$^{-1}$	Intensity/ 'darks'	Band Position/cm.$^{-1}$	$\Delta\nu_{\frac{1}{2}}$/ cm.$^{-1}$	Intensity 'darks'
ν_{15}	$CHCl_3$	1355	3·7	5·589	0·896	160	1355	3·5	240
				3·824	0·44	120			
				1·417	0·197	140			
				1·319	0·174	130			
				Average 140 ± 20 darks					
ν_{17}	$CHCl_3$	1155	5·0	1·417	0·79	560	1155	4·0	550
ν_{14}	$CHCl_3$	1451	3·5	3·824	14·10	3600	1453	3·5	3940
				5·589	18·15	3250			
				0·802	3·21	4000			
				0·613	2·52	4110			
				1·319	4·47	3400			
				1·854	7·06	3800			
				1·529	5·66	3700			
				0·854	3·55	4150			
				0·949	3·84	4040			
				Average = 3,800 ± 300 darks					
ν_{10}	C_6H_6	630	6·5	0·962	2·32	2410	629	5·0	2500
				0·613	1·40	2290			
				1·854	3·93	2120			
				1·319	3·14	2380			
				1·116	2·73	2300			
				0·949	2·53	2660			
				0·303	0·76	2510			
				1·417	3·40	2400			
				0·984	2·26	2260			
				0·605	1·33	2300			
				Average = 2,300 ± 300 darks					

/cont.

Mode	Solvent	Pyridine-IBr					Pyridine-ICl		
		Band Position/cm.$^{-1}$	$\Delta\nu_{\frac{1}{2}}$/ cm.$^{-1}$	10^6 c.l/ mole cm.$^{-2}$	Area/ cm.$^{-1}$	Intensity/ 'darks'	Band Position/cm.$^{-1}$	$\Delta\nu_{\frac{1}{2}}$/ cm.$^{-1}$	Intensity/ 'darks'
ν_{26}	$CHCl_3$	693		0·6128	2·98	4900	-	-	-
				1·319	6·21	4700			
				1·417	7·96	5600			
				Average = 5,100 ± 100 darks					
ν_{27}	$CHCl_3$	421	6·5	18·45	4·281	230	422	6·0	200

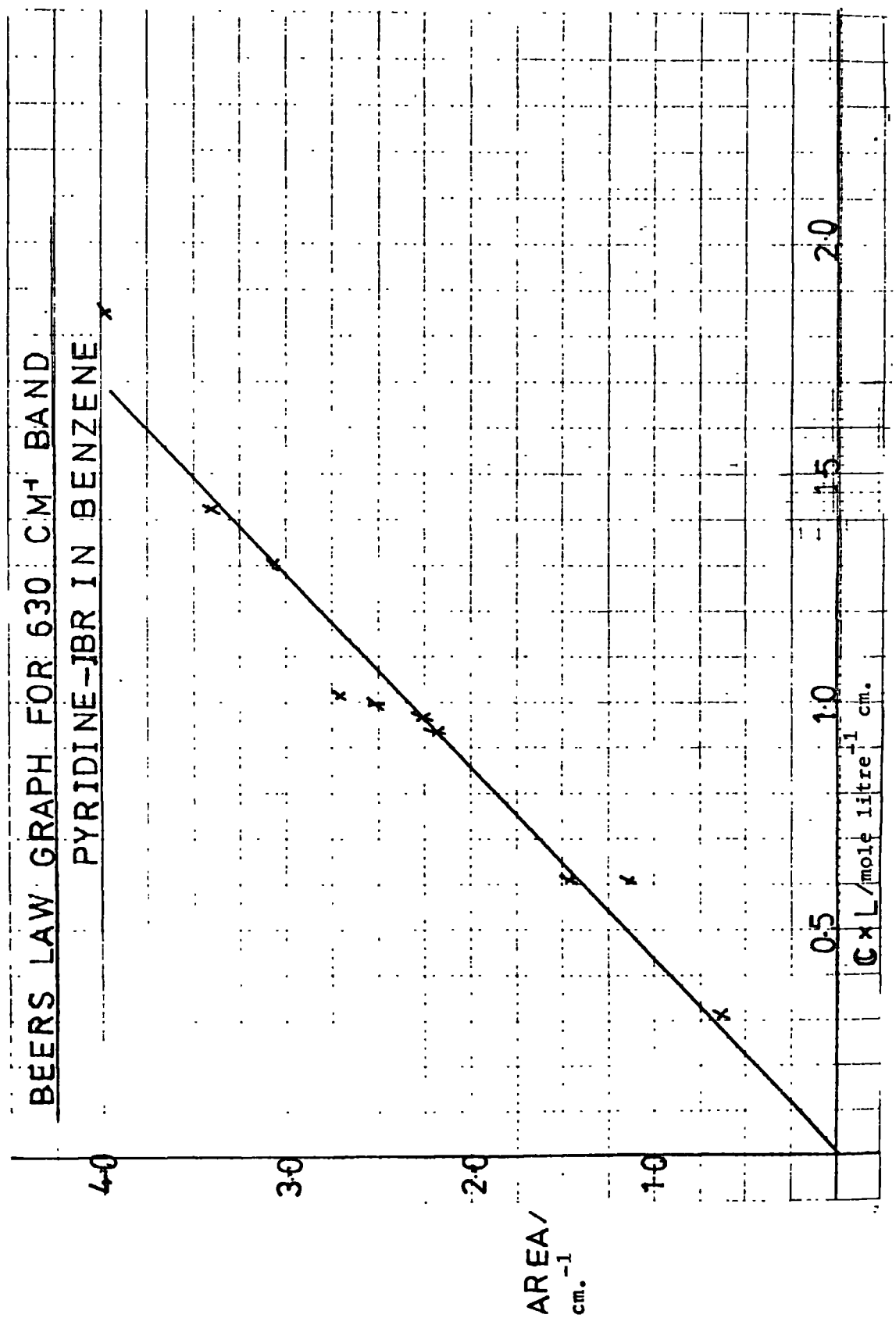
BEERS LAW GRAPH FOR 630 CM⁻¹ BAND
PYRIDINE-IBR IN BENZENE
AREA/ cm.⁻¹
4·0
3·0
2·0
1·0
0·5
1·0
1·5
2·0
C×L/mole litre⁻¹ cm.

Fig. 3.2.

Table 3.10.

Bands Observed in Pyridine-I_2/CS_2 Solutions Not Assigned to Fundamentals

Band Position/cm^{-1} Pyridine-CS_2	Intensity	With Iodine[a]	Band Position/cm^{-1} Pyridine-CS_2	Intensity	With I_2	Comments
3720	w	3720 ↑	1915	m	1912 ↑	
3675	w	3675 ↑	1815	m	1815	
3125	w	3125 ↑	1805	m	1804 ↑	
3080	s	3078	1680	m	1680 ↑	
3058	m	3058	1635	m	1630 ↑↑	
3028	m	3038	1218	s	1238 ↑↑	Suspect splitting of 1216 - other nearest band is 1275cm^{-1}
3024	m	3036	1525		1525	
					1375	
3002	s	3002			1250	
2905	w					
2925	w					
2815	w					
2790	w					
1970						
1980						

a ↑ indicates an increase in intensity on adding iodine.

the band shape, expressions such as Chapman's equation[119b] show that the diffusion coefficient D falls as the molecular mass increases.

Hence fall in value of the diffusion coefficient causes a reduction in α and hence a reduction in band width (see section 2).

In solution the complex experiences dipole-dipole, dipole-induced dipole and electron donor-acceptor forces between the molecules. However, if the molecule (and the dipole) rotate about the C_2 axis, then these forces will be unaffected to a first approximation.

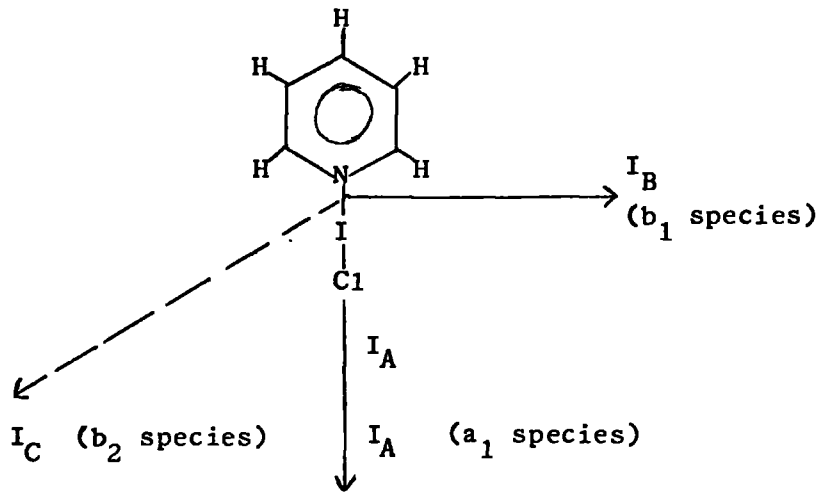

	I_A	I_B	I_C
Pyridine	85·36 amu Å^2	88·04	173·4
			$I_C > I_A \approx I_B$ OBLATE
Pyridine-ICl	88·04 amu Å^2	1189·80	1277·84
			$I_A < I_B \approx I_C$ PROLATE

Figure 3.3.

Since the moment of inertia about the C_2 axis is practically unaltered on complexation one would expect a similar rate of reorientational motion about the C_2 axis. The sheer bulk of the molecule combined with the intermolecular forces will hinder the rotational diffusion about axes perpendicular to the C_2 axis.

On going from pyridine to pyridine-IBr, the greatest narrowing appears to occur for most of the a_1 vibrations. This is probably because the transition moment for the a_1 modes lies along the C_2 axis. The b_1 modes show variable narrowing as the transition dipole is at an angle to the I_B axis (see Figure 3.3.).

However, it must be noted that two opposing effects are probably occurring. Firstly, narrowing will occur due to the reduction of the orientational contribution to the band shape. Secondly, broadening due to vibrational relaxation. Our normal co-ordinate analysis (see Chapter 6), shows that the ν_{10} band at 603 cm.$^{-1}$ shows a large Q change in the complex. Since the Bratos mechanism[73] predicts that vibrational broadening is dependent on $\left(\frac{\partial_V}{\partial_Q}\right)$ this explains why this band shows the least narrowing (assuming that the change in ∂_V on complexation affects all modes in a roughly similar fashion).

(ii) Other Bands Observed Not Assigned to Fundamentals.

The non-restrictive nature of the selection rules for the C_{2v} point group, together with the large number of fundamental frequencies and uncertainty about the amount of anharmonicity, makes it impossible to explain the observed combination bands without difficulty. Table 3.10. indicates the large number of combination bands observed, most of which are perturbed in intensity to some extent. This was observed by running sample and background on the same chart on slow scan. Mention will only be made of those combination bands which show the largest perturbation. They are all within an order of magnitude of the intensity of the 1355 cm.$^{-1}$ band. These are listed in Table 3.11.

The band at 1242 cm.$^{-1}$ may be a fundamental. One would expect the frequencies of the pyridine vibrations to be perturbed on complexation. The band is not observed in the uncomplexed pyridine at the concentrations used. The band at 1212 cm.$^{-1}$ has been assigned to both an a_1 (ν_6) and a b_1 (ν_{16}) vibrational mode.

Table 3.11.

Pyr/I_2 in Carbon Disulphide

Frequency	Assignment	Calculated	Comments
1635	$\nu_{10} + \nu_8$ or $\nu_9 + \nu_{19}$	1650, 1610	
1525	Observed. Not assigned		In CCl_4
1375	$\nu_{10} + \nu_{22}$	1364	
1260	$\nu_{19} + \nu_{10}$	1272	
1242	$\nu_{10} + \nu_{20}$	1295	Large intensity increase on complexation
1285	$\nu_{10} + \nu_{20}$	1295	
810	$2\nu_{24}$		CS_2 obscures ν_{24}

The nearest assignment quoted[103] to 1242 cm.$^{-1}$ for overtones in pyridine gives a calculated frequency 30 cm.$^{-1}$ too high, and a weak absorption is found only 12 cm.$^{-1}$ from the calculated frequency.

Green et al.[112] assigned the ν_{16} vibrational mode a band at 1288 cm.$^{-1}$ He made the proposed change to bring the value of ν_{16} into line with that for benzene and the monosubstituted benzenes. The same arguments hold for increasing the value of ν_{16} from 1217 to 1242 cm.$^{-1}$ Furthermore, the values obtained from the unrefined zero order force field calculations[113] give a value of 1291 cm.$^{-1}$ The least accurate value where the assignment is not open to doubt was the ν_{15} mode which was in error by 59 cm.$^{-1}$ So ν_{16} = 1291 $\pm$ 59 cm.$^{-1}$ taking a value of 1242 cm.$^{-1}$ is well within the error especially as this is a band which may be perturbed in frequency on complexation.

It is worth noting that the ν_6 absorption has a shoulder at about 1205 cm.$^{-1}$ in both the complex and 'free' pyridine in CCl_4. However, this may be a hot band and not a fundamental. The ν_7, ν_{18} band showed no shoulders. This is possibly partly why it is narrower than the ν_6, ν_{16} band.

(iii) Summary.

We can summarise the findings from this part of the work as follows:

(a) The intensities of the ν_1, ν_2, ν_3, ν_{11} and ν_{12} bands, due to primarily $\nu_{(C-H)}$ stretching, have been explained by electronegativity effects alone. This is because the effects of a change of ionisation potential and normal co-ordinate effects are lower for the $\nu_{(C-H)}$ modes.

(b) The a_1 modes are more perturbed in intensity than the b_1 modes because they have two extra contributions to the intensity.

(1) The transition moment of the a_1 modes lies along the C_2 axis so does the molecular dipole moment. There will thus be a larger contribution to the intensity from dipole-induced dipole interactions. The b_1 modes lie along the I_B axis (see Fig. 3.3.)

and should be much less perturbed than the a_1 modes.

2. A contribution from the $\left(\frac{\delta_I}{\delta_Q}\right)$ term to the intensity.

Apart from the five $\nu_{(C-H)}$ bands most of the other bands arising from the a_1 and b_1 fundamentals were increased in intensity. There were exceptions however, the ν_5 band at 1484 $cm.^{-1}$ in pyridine appears at 1478 $cm.^{-1}$ in the complex. The band was too weak and no intensity measurements could be made. The ν_8 band at 1035 $cm.^{-1}$ is unchanged in intensity, but is considerably sharpened on complexation.

(c) There is some evidence for the assignment of the ν_{16} mode to a band at 1242 $cm.^{-1}$

(iv) Studies on the b_2 Modes of Pyridine-IBr.

The b_1 and b_2 modes are expected to have the smallest rotational correlation times (greatest values of α), and the a_1 modes to have the largest rotational correlation times. This is because as Figure 3.3. shows, the transition moment of the b_2 modes lies along the I_C axis. Thus it can still be affected by motion about the C_2 axis.

The b_2 bands arise at 942, 882, 745, 698 and 400 $cm.^{-1}$ for liquid pyridine. Most studies on the pyridine-IC1 complex have been made in chloroform and carbon tetrachloride. Solvent absorption prevents measurements on the 698 and 745 $cm.^{-1}$ bands. Table 3.4. shows that the ν_{27} mode is unaltered in intensity on complexation. The frequency is shifted to 421 $cm.^{-1}$ This is presumably due to mixing of the extra out-of-plane vibrations with the original donor vibrations. The intensity of the ν_{27} band is unchanged on complexation (Table 3.4.).

Both carbon disulphide and dioxan are free of absorption in the 700 - 800 $cm.^{-1}$ region. However, solutions of pyridine-IBr in dioxan decomposed to give a doublet of almost equal intensity for the ν_{26} band. This shows that the pyridine-IBr equilibrium constant is much lower in dioxan. See Spectra 3.3. and 3.4.

$$PyrIBr \rightleftharpoons Pyr + IBr$$

The experiment was repeated in carbon disulphide. A doublet was again observed for the ν_{26} band but this time the free pyridine absorption had a peak maximum only about 10% of the complexed pyridine (see Spectrum 3.5.). Assuming the bands are symmetric about the central maximum, it was possible to estimate the intensity of the complexed pyridine by doubling the half band area.

It can be seen from Table 3.12. that the b_2 modes have a large perturbation on complexation. The ν_{26} band is drastically narrowed and reduced in intensity. Whilst the ν_{25} band is increased in intensity and only slightly narrowed. However, by careful inspection of the bands it could be seen that the wings fell off more quickly in the complexed bands, i.e. the bands became more gaussian.

The lack of dependence on the direction of the transition moment, and large gaussian component for these bands indicates that: the results do not fit in with those expected on the basis of orientational relaxation making a predominant contribution. It is therefore clear that vibrational effects predominate for the pyridine-IBr complex. The decomposition into free pyridine and IBr prevented any studies on the $\nu_{(C-H)}$ stretching modes.

In conclusion it can be seen that although Raman data are necessary before rotational and vibrational effects can be unambiguously separated infrared data alone can provide valuable information on the relative importance of these factors.

(v) Intensity studies on the a_1 and b_1 vibrations of pyridine with some of the weaker halogen acceptors.

Table 3.12.

Studies on the b_2 Modes

Mode	Solvent	Acceptor	Band posn./ $cm.^{-1}$	$\Delta\bar{\nu}_{\frac{1}{2}}$/ $cm.^{-1}$	Intensity/ darks
ν_{23}	CS_2		942		Very Weak
		IBr	940		" "
	Dioxan	IBr	940		" "
ν_{24}	CS_2		Not observed		
		IBr	Not observed		
	Dioxan	Solvent has 0% transmission 850 - 910 $cm.^{-1}$			
ν_{25}	Dioxan	IC1	756	Broad as two bands overlap	
	CS_2		746	4·5	1200
	CS_2	IBr	750	40	2870
	Dioxan	Dioxan	752		
	Dioxan	IBr	758		
ν_{26}	CS_2		702	8·0	6500
	CS_2	IBr	696	4·0	3809
	Dioxan		711		
	Dioxan	IBr	700		
	Dioxan	IC1	695	('Free' pyridine at 709 $cm.^{-1}$)	
ν_{27}	Dioxan		408	6·0	

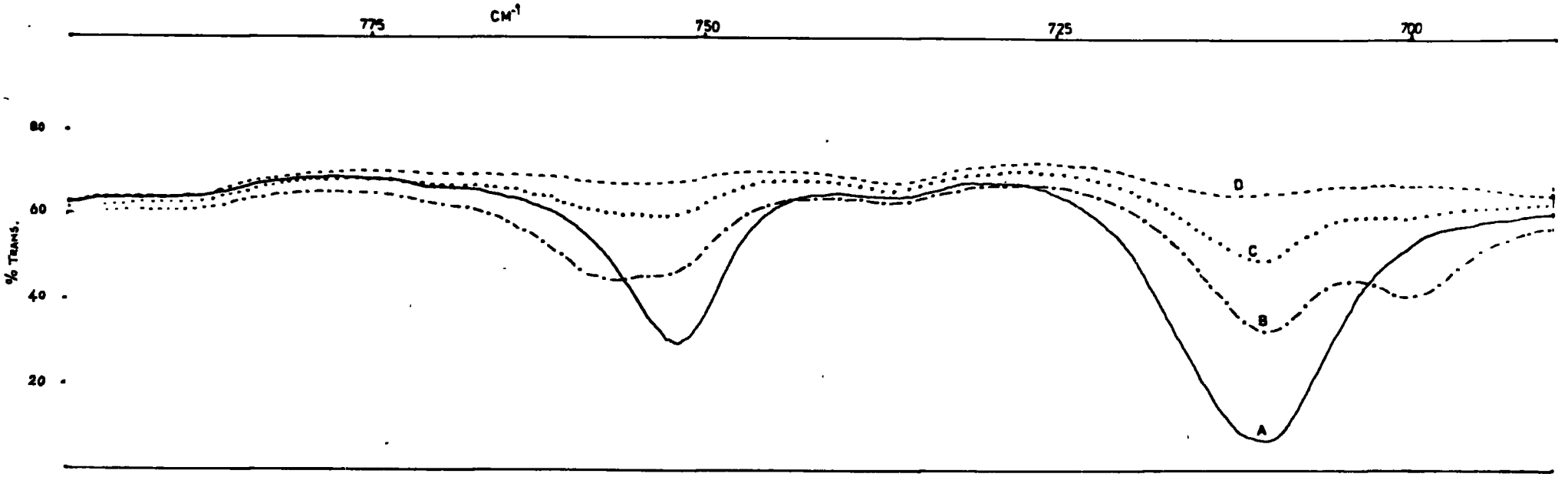

Spectrum 3.3. (A) Pyridine in dioxan (O·O2M); (B) pyridine-IBr in dioxan (O·O8M); (C) pyridine-IBr in dioxan (O·O3M); (D) dioxan background. The path length is O·2 mm.

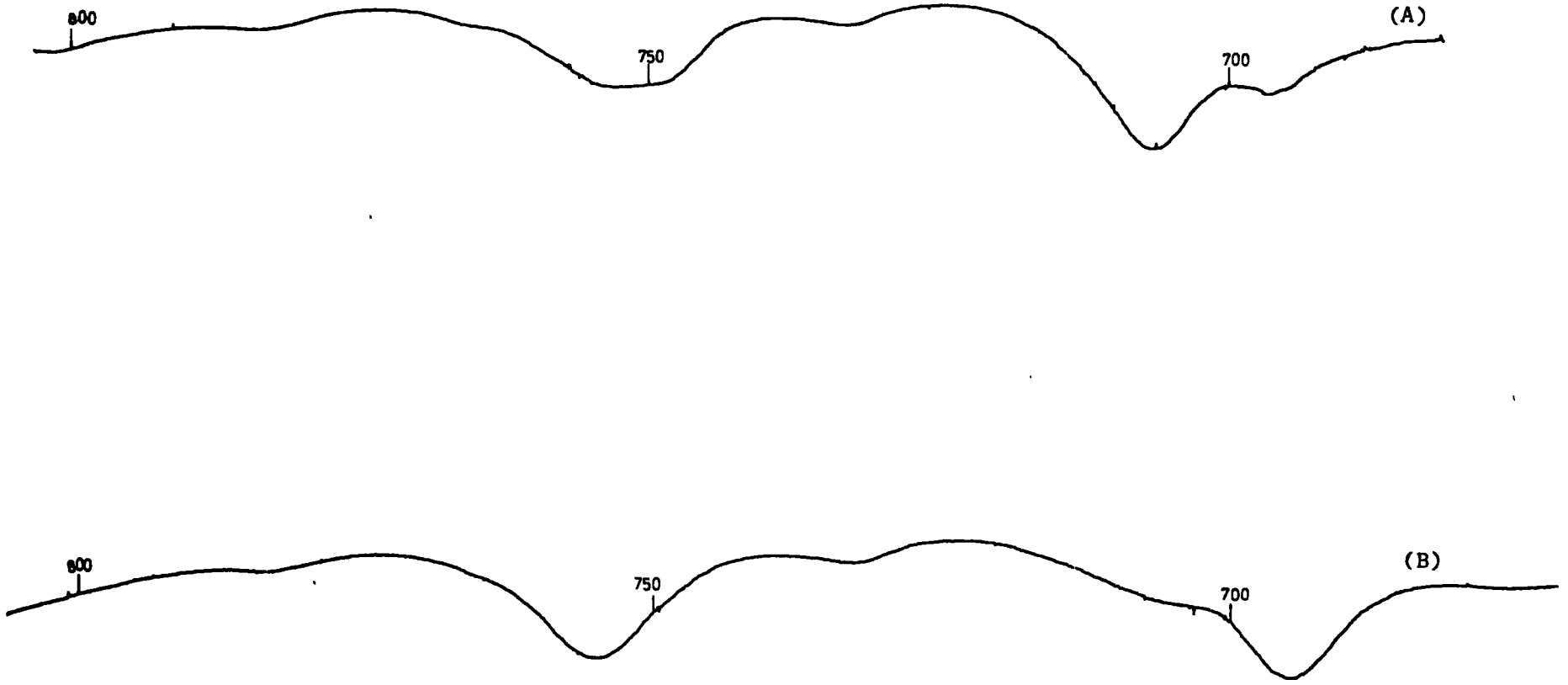

Spectrum 3.4. Pyridine-IBr (A) and pyridine-IC1 (B) in dioxan solution showing decomposition of complex and presence of 'free' pyridine bands.

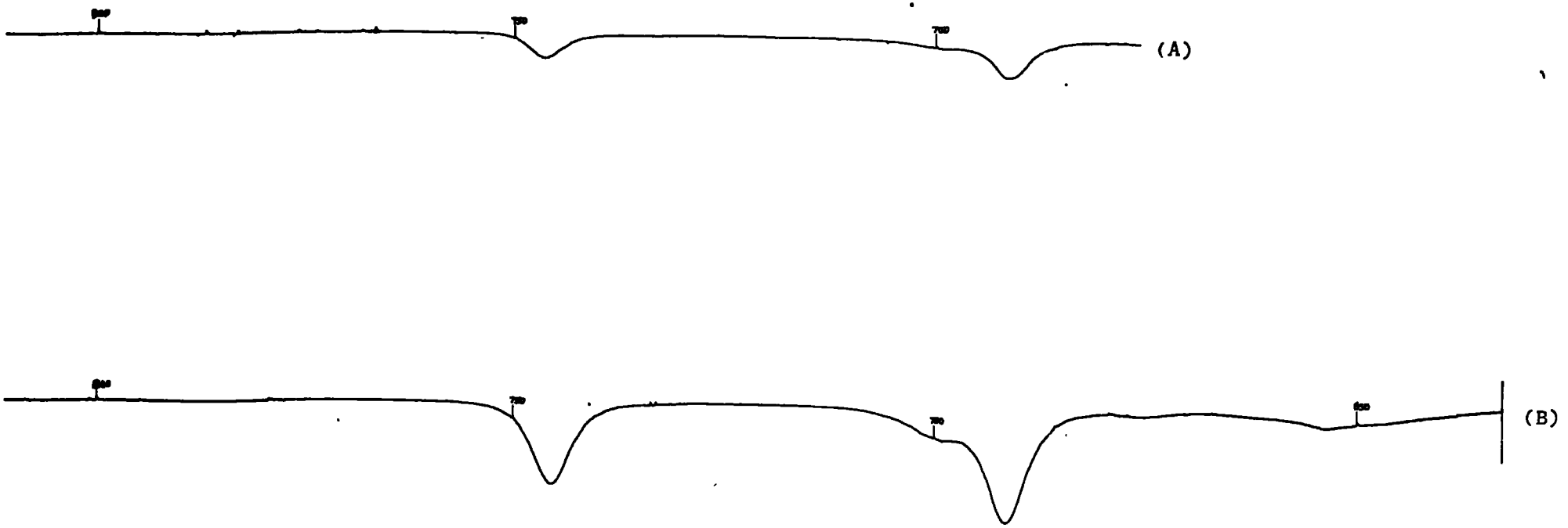

Spectrum 3.5. Pyridine-ICl (A) and pyridine-IBr (B) in CS_2 showing effects of much lower complex decomposition (compared with dioxan).

Introduction.

In view of the small difference in intensity and frequency on complexation of the pyridine-IBr and pyridine-ICl donor spectra, it was decided to limit this work to a brief survey of the pyridine-Br_2, pyridine-ICN and pyridine-I_2 donor spectra.

The similarity in intensity indicates, assuming charge transfer is the predominant mechanism, that the electron affinity of IBr and ICl are about equal. The electron affinity of IBr has not been measured.

Table 3.13.

Halogen	Electron Affinity/eV
I_2	$1{\cdot}7 \pm 0{\cdot}5$
Br_2	$1{\cdot}2 \pm 0{\cdot}5$
Cl_2	$1{\cdot}3 \pm 0{\cdot}4$
ICl	$1{\cdot}7 \pm 0{\cdot}6$

However, the electron affinities available[120] (see Table 3.13.) show no definite trend and do not disprove this suggestion.

(a) Pyridine-Br_2 in Carbon Tetrachloride.

Unfortunately no studies have been made on pyridine-ICl in carbon tetrachloride. However, the band intensities in chloroform should be similar since the band intensities of pyridine in chloroform and carbon tetrachloride agree within 20% (see Table 3.6.).

Table 3.14. shows that (i) the pyridine-bromine bands are considerably broader and weaker than they are for pyridine-ICl. The lower intensity can be accounted for because of the lower electron affinity of bromine as opposed to ICl (see Table 3.13.).

The normal co-ordinate calculation described in Chapter 6 on the pyridine-ICl and pyridine-IBr complexes explains the frequency shifts in terms of the mass effects and vibrational mixing. This is probably also true for the pyridine-Br_2 complex.

Table 3.14. shows the donor vibrations for the pyridine-Br_2 complex. The bands arising from the ν_9 and ν_{14} vibrations are stronger than in the pyridine-I_2 complex. Some of the other bands appear to be weaker, but this is probably a 'solvent' effect, since the ν_{10} band in particular is very sensitive to the pyridine concentration. However, a full study on the variation of band intensity with different pyridine and halogen concentrations would be necessary to confirm this.

In spite of the lower electron affinity and polarisability of bromine than iodine, the pyridine-Br_2 complex is stronger than the pyridine-iodine complex. The far-infrared and dipole moment data (see Chapter 5) are decisive in confirming this. The frequency shifts of the ν_9 and ν_{10} bands and intensities of the ν_{14} and ν_9 support this. More data on solvent effects etc. are necessary before the perturbations of the other vibrations can be interpreted. Rather surprisingly the absorption at 1033 $cm.^{-1}$, assigned to ν_7, was reduced in intensity in the pyridine-Br_2 complex. This was observed by running the spectrum on expansion X25, and comparing it with the spectrum of the uncomplexed pyridine. Since pyridine was present in large excess, and the frequency shift was very small, intensity measurements were not attempted on this band. The concentration of bromine could not be increased because of the dangers of reaction with the pyridine and the KBr plates.

(b) The Pyridine-I_2 Complex in Carbon Tetrachloride.

The pyridine-IBr and pyridine-ICl complexes have high equilibrium constants and can be considered as rigid complexes. On the other hand, the pyridine-I_2 and pyridine-Br_2 complexes have much smaller equilibrium constants, and are less rigid and have lower life-times.

Since the band shape is controlled by the factor $\left(\frac{\partial_V}{\partial_Q}\right)$ where vibrational relaxation is important, one would expect ∂_V to be quite different in a weak complex to a strong one. This accounts for the width of the bands.

Table 3.14.

Mode	Pyridine-Br_2 complex in CCl_4							PyrICl/$CHCl_3$		Comments
	Band posn./ $cm.^{-1}$	[Pyridine] moles/litre	[Bromine] moles/litre	10^6 Cl $mole/cm.^{-2}$	Area	Intensity/ Darks	$\Delta\bar{\nu}_{\frac{1}{2}}/cm.^{-1}$	Intensity/ Darks	$\Delta\bar{\nu}_{\frac{1}{2}}$ $cm.^{-1}$	
	3100-3000	Considerable fall in intensity in this region								
ν_{14}	1448	0·9463	$9·9 \times 10^{-2}$	0·99	4·748	4820	4·5	4300	4·2	
ν_6	1212	0·3718	$4·2 \times 10^{-2}$	2·1084	2·5037	1200	4·0	1800	3·5	
		0·9463	$9·9 \times 10^{-2}$	0·99	1·285	1280	3·5			
ν_7 ν_8	1070	On the wing of pyridine band (increased in intensity)								
ν_8	1033	Significantly reduced in intensity and slightly broadened.								
ν_9	1010	0·3718	$4·2 \times 10^{-2}$	2·1084	5·6519	2680	6·0	3430	3·5	Broadened on complexation
		0·9463	$9·9 \times 10^{-2}$	0·99	2·222	2200	6·0			
		0·4721	$9·72 \times 10^{-3}$	2·93	6·533	2230	6·0			
ν_{10}	625	0·3718	$4·2 \times 10^{-2}$	2·1084	2·696	1300	6·0	1940	4·0	
		0·4721	$9·72 \times 10^{-3}$	2·93	4·688	1600	6·0			

The ν_{10} band at 622 cm.$^{-1}$ in the pyridine-I_2 complex has a higher intensity than the ν_{10} band at 631 cm.$^{-1}$ in the pyridine-ICl complex. This is probably accounted for by the polar solvent effect (see Chapter 4), since the pyridine is present in a large excess. In the pyridine-ICl complex the pyridine:acceptor ratio is, of course, 1:1.

(c) Pyridine-ICN in Carbon Tetrachloride.

The previous discussion has shown that weak acceptors perturb the a_1 and b_1 modes less in intensity than the strong acceptors. If the same trend follows one would expect that the $\nu_{(C-H)}$ stretching modes would be correspondingly larger with a weak acceptor.

Accordingly a 6:1 excess of iodine cyanide with pyridine in carbon tetrachloride was used. From the intensity of the free pyridine, and the intensity observed for the complexed and free pyridine a very approximate estimation of the intensities of the absorptions at 3088 cm.$^{-1}$ and 3010 cm.$^{-1}$ were made. The intensities are estimated in calculations 3.1. and 3.2.

Calculation 3.1.

Complex band at 3088 cm.$^{-1}$

Area observed = 5·2 cm.$^{-1}$

[ICN] = 44·83 x 10^{-3} mole litre^{-1}

[Pyridine] = 7·5947 x 10^{-3} mole litre^{-1}

Since K = 51[121] [Pyridine]comp = 5·08 x 10^{-3} mole litre^{-1}

[Pyridine]uncomp = 2·51 x 10^{-3} mole litre^{-1}

C1(comp) = 3·556 x 10^{-3} mole litre^{-1} cm.

C1(uncomp) = 1·757 x 10^{-3} mole litre^{-1} cm.

as 1 = 7 mm.

The intensity of free pyridine = 1·47 x 10^3 darks

Area due to uncomplexed pyridine ≈ 2·55 cm.$^{-1}$

" " " complexed " ≈ 2·65 cm.$^{-1}$

as area observed = 5·2 cm.$^{-1}$

$\therefore$ Intensity of complexed pyridine with ICN $\approx 0{\cdot}7 \times 10^{-3}$ darks

Intensity of complexed pyridine with IBr $\approx 0{\cdot}2 \times 10^{-3}$ darks (calculated previously)

Calculation 3.2.

Complex band at 3010 $cm.^{-1}$

Area observed = 2·497 $cm.^{-1}$

Area due to uncomplexed pyridine $\approx$ 1·35 $cm.^{-1}$ as

$$B_i \approx 0{\cdot}77 - 0{\cdot}90 \text{ darks} \times 10^{-3}$$

Area due to complexed pyridine $\approx$ 1·14 $cm.^{-1}$

Intensity of complexed pyridine $\approx 0{\cdot}3 \times 10^{-3}$ darks (with ICN)

Intensity of complex pyridine with IBr $\approx 0{\cdot}1 \times 10^{-1}$ darks (calculated previously)

These calculations are in reasonable agreement with the above prediction. However, it must be noted that the 3010 $cm.^{-1}$ band has been assigned to a combination mode ($\nu_{13} + \nu_{14}$).

No intensities are quoted for the other donor absorptions because, whilst they seemed to be somewhat less than the pyridine-I_2 complex, the inconsistency between results was more than 10% (the expected error). This is probably partly due to the fact that no reliable equilibrium constant is available. The value of $K_c = 51 \pm 5$ litres/mole quoted by Person et al.[121] is calculated from three values of the $\nu_{(I-C)}$ absorbance with pyridine concentrations ranging from $7{\cdot}5 \times 10^{-2}$ - 12×10^{-2} moles $litre^{-1}$. It is probably only within the error 51 ± 5 litres/mole for the range of pyridine concentrations $7{\cdot}5 \times 10^{-2}$ - 12×10^{-2} moles $litre^{-1}$. Whilst it is very easy to complex all the ICN by keeping the pyridine in excess, the reverse is extremely difficult due to the low solubility of ICN. Furthermore, solvent perturbations of the intensities seem to be more important for the pyridine-ICN complex than for the pyridine-I_2 complex. This is possibly because:

(a) ICN interacts with the solvent (it definitely does in the chloroform case (see Chapter 4)). The $\nu_{(C-H)}$ absorption of chloroform in a mixture of chloroform/carbon tetrachloride is considerably increased in intensity and broadened when ICN is added. In this case the chloroform is acting as the acceptor and the ICN as the donor.

(b) Solvent effects due to changing the pyridine concentration appear to be more important in this complex. This seems to be because ICN can behave as a donor, or an acceptor and the solvent competes for the ICN molecules. However, without further information the discussion must cease here.

In conclusion, the order of complex 'strength' using the donor frequency and intensity perturbation appears to be:

Pyridine-ICl ≈ Pyridine-IBr > Pyridine-Br_2 ≈ Pyridine-I_2 > Pyridine-ICN

This follows the equilibrium constants which are $4{\cdot}8 \times 10^5$, $1{\cdot}3 \times 10^4$, $1{\cdot}46 \times 10^2$, 90*, 56 litre $mole^{-1}$ (see Table 3.1.). The narrowing of the a_1 and b_1 modes has been explained as due to suppression of orientation about the two axes perpendicular to the C_2 axis. Some information is given about the direction of the transition moment. However, this rigid molecule model appears to break-down for the weaker complexes (which is not too surprising).

Without further data it would be pointless to speculate about the intensity trend for the b_2 modes. Table 3.12 shows that the ν_{26} band is drastically narrowed and reduced in intensity. One can at least say that vibrational relaxation seems to be making a strong contribution to the band shape, because of the more Gaussian profile.

E. Suggestions for Further Work.

In spite of the experimental difficulties, measurements on the $\nu_{(C-H)}$ stretching bands may give the most information on the extent of electron

---

* The pyridine-Br_2 value was measured in benzene, the others in carbon tetrachloride which may account for the difference.

interaction in the donor molecule. The pyridine-ICN $\nu_{(C-H)}$ stretching bands, are definitely much stronger than the corresponding pyridine-IBr bands although a full study and Beer's Law plots would be needed to establish the exact intensities.

It would be very interesting to repeat the work of Ferguson et al.[117,118] on the halo-substituted benzenes, and also carry out measurements on the methyl halo-substituted benzenes. Ferguson did not make measurements on the $\nu_{(C-H)}$ stretching bands. Furthermore, in the methyl halo-benzenes one would expect differences between the alkyl C-H band intensities and the ring C-H band intensities. In fact, studies on the changes of $\nu_{(C-H)}$ band intensities may be worthwhile on systems where it is impossible to use the n.m.r. spectrum because it is too complex.

For the weaker complexes intensity studies are not possible without accurate equilibrium constants. These are not available at present, or were determined from the ultra-violet region and the concentrations are much lower. It would be very interesting to measure the equilibrium constant of the pyridine-ICN complex using all the infrared bands of the donor and acceptor. From a series of measurements a series of K_c values could be determined.

Strictly speaking the equilibrium constant for the interaction of a donor, D, with an acceptor A to form a complex, C, is

$$K_a = \frac{a_C}{a_D a_A} = K_c K_\gamma \qquad \ldots\ldots \quad [3.4.]$$

where

$$K_c = \frac{C_C}{C_D C_A} \qquad \ldots\ldots \quad [3.5.]$$

and

$$K_\gamma = \frac{\gamma_C}{\gamma_D \gamma_A} \qquad \ldots\ldots \quad [3.6.]$$

The symbols a, C and γ represent activity, concentration and activity coefficient, respectively.

It is generally assumed that K_γ is unity.[79] However, the above experiment would determine how far K_γ deviated from this. It is also possible that 2:1 complexes are present, e.g. the aromatic hydrocarbon-tetracyanoethylene complexes contain 2:1 species[119c] as well as 1:1. There is also evidence[119d] of a 2:1 benzene-I_2 complex at high benzene concentrations. Chapter 7 also confirms the existence of (pyridine)$_2$-ICl and (pyridine)$_2$-IBr complexes in the solid state. The u.v. determinations of K_c should discover whether these complexes exist in solution.

Chapter 5 shows that the life-time of the 'complex' is crucial in determining the band shape in the far-infrared. Since the equilibrium constant is a crude measure of the life-time, it would be interesting to compare the equilibrium constant measured in the u.v. region and the far-infrared region at the same concentrations. Further consideration of these results would give information on the solvent effects on a particular band. Table 3.15. shows that this is considerable for the ν_{10} band of the pyridine-I_2 complex.

The 'solvent effect' on the pyridine-IBr complex in dioxan is quite dramatic. It would appear that K_c has fallen considerably from 10^4 mole/litre^{-1} in carbon tetrachloride. Work continues in this laboratory to determine the exact value of K_c, both from infrared and u.v. measurements for the pyridine-IBr and pyridine-ICl complexes in dioxan.

It would also be worthwhile to try and determine the equilibrium constants and other physical parameters for the donor-solvent and acceptor-solvent interactions. It should then be possible to correct for base line errors, which are a major source of error in intensity measurements.

Finally, it would be of value to carry out Raman studies on the pyridine-ICl vibrations to separate the rotational and vibrational contributions. This would be especially helpful to establish the mechanism for the b_2 modes which seem to have a large gaussian component. This is, of course, linked to the

Table 3.15.

Comparison of the Pyridine-I_2 Complex Intensities with those of the Pyridine-Br_2 and Pyridine-IC1

Mode	Band posn./ $cm.^{-1}$	[Pyridine] moles $litre^{-1}$	[Iodine] moles $litre^{-1}$	C1 x 10^6/ (mole $cm.^{-2}$)	Area/ $cm.^{-1}$	Intensity/ Darks	$\Delta\bar{\nu}_{\frac{1}{2}}$/ $cm.^{-1}$	Pyridine-IC1 Intensity Darks	Pyridine-IC1 $\Delta\bar{\nu}_{\frac{1}{2}}$/ $cm.^{-1}$	Pyridine-Br_2 Intensity Darks	Pyridine-Br_2 $\Delta\bar{\nu}_{\frac{1}{2}}$/ $cm.^{-1}$
	3100-3000	Considerable fall in intensity		on complexation							
ν_4	1596			5·488	12·8	2330		2950	4·2		
ν_{14}	1448	0·5976	$4·99 \times 10^{-2}$	2·50	7·48	2992	4·0	4300	4·2		4·5
ν_{14}	1448			5·488	14·32	2609					
ν_{15}	1356	0·5976	$10·933 \times 10^{-2}$	5·488	0·63715	120	Too weak	250	Not quoted		
ν_6	1216			2·50	4·607	1840	4·0	1800	3·5	1300	4·0
ν_6	1213			5·488	11·28	2055	3·0				
ν_{17}				5·488	2·16	393	3·0	450	5·0		
ν_{18}	1071			2·5	6·1	2440	4·0	3350	2·5		
ν_{18}	1070			5·488	13·68	2490					
ν_8	1030	Slightly reduced in intensity.		Half band width about same						Reduced and broadened	
ν_9	1007			2·5	4·19	1676	3·5	3430	3·5	2200	6·0
ν_{10}	622	0·5976		2·5	5·234	2100	5·0			1400	6·0
	621	0·5976		5·488	12·186	2620	5·0				
	623			1·319	3·1454	2500*	6·0	1940	4·0		
	623			1·057	2·249	2120†	6·0				

* In $CHC1_3$

† In C_6H_6

standard techniques of band shape analysis, i.e. (a) band fitting, (b) curve resolving where applicable, (c) calculation of correlation curves, (d) moment analysis. A brief discussion of these techniques has been given in Chapter 2.

CHAPTER 4

II. Studies on the Acceptor Vibrations and External Modes

A. Introduction.

Studies of the changes in the vibrational spectra of the donor (D) and acceptor (A) molecules, when they combine to form a complex, have been a powerful aid in determining the nature of the interaction.[122]

With the development of efficient interferometers, it is possible to make measurements more-or-less routinely in the far-infrared region of the spectrum. This has resulted in it being comparatively easy to measure the vibrations of the donor against the acceptor. There are now a large number of papers[123] in the literature dealing with the spectra of the pyridine bases with the halogens.

The aim of this work is to extend the knowledge available on frequency changes of the acceptor spectra on complexation, to include information on intensities and band shapes. The correlation function (see Chapter 2) of an infrared band consists of an orientational part and a vibrational part. Whilst it is impossible to separate these in the infrared, quite different effects on the correlation function occur if either the orientational or vibrational part predominates.

A study of the temperature and concentration dependence on the band shape, coupled if possible with a comparison of the 1st overtone band of the same vibration, should establish which mechanism predominates. Furthermore, the vibrational part depends on the vibration/rotation interaction, and is independent of the direction of the transition moment, whilst the reverse is true for the orientational part. Therefore absorption modes which belong to the same symmetry class, having a predominantly orientational contribution, should have very similar correlation functions. The reverse is not necessarily true for bands controlled by a vibrational mechanism.

It should therefore be possible to gain more understanding of the mechanism, or mechanisms, which give rise to absorption in the far-infrared region. Absorptions at higher energy (infrared region), and lower energy (microwave) have mechanisms which are now well understood. The microwave absorptions are well interpreted in terms of pseudo pure rotation and translation of the overall dipole moment of the molecule. Near infrared absorptions are explained as being due to molecular vibrations.

Systems such as dioxan-I_2 and benzene-I_2 were originally considered as well-defined charge transfer complexes in view of moderately severe, and quite specific, perturbations of the benzene and iodine vibrational spectra.[125] However, Hanna[126] considers that benzene and iodine interact only by means of classical electrostatic forces[126] giving a collisional complex with a much shorter life-time. This is supported by the observation of a low frequency absorption, which is far better explained by a collision induced mechanism, than as a normal vibrational mode (see Chapter 5).

Experimental.

The complex solutions were prepared as described in Chapter 3. The more deeply coloured crystalline impurity described by Yarwood and Person[124] (found in crystals of the complex) was separated from the complex by washing with the chloroform and identified (see Chapter 7). The yield of the impurity was 1% from the pyridine-ICl complex and about 10% for the pyridine-IBr complex.

The cell used was a demountable solution cell with polythene plates. Usually it was possible to measure the path length of thin spacers interferometrically. For thicker spacers, where compression of the Teflon is less important, a micrometer was used to measure the path length.

For measurements on the I-C and C-N stretching vibrations of iodine cyanide KBr plates were used with the P.E. 577 and G.S.2A spectrometers. Caesium iodide plates must not be used as reaction takes place with the plates

to produce ionic species. With dilute solutions reaction is much slower with the KBr plates, and the bands were reproducible over the two or three hours taken to scan the spectra. Apart from the need to polish the plates frequently reaction was not a problem. The instrument and plates used will be indicated in the tables following.

B. Frequency and Intensity Studies.

It is possible to explain the intensity perturbation of the donor spectrum in terms of the strength of the charge-transfer interaction. This is reflected by the electron affinity of the acceptor, where the latter are available. The complex 'strength' is also reflected in the size of the equilibrium constant. As seen in Chapter 3 the size of the intensity perturbation followed the order of the equilibrium constants, i.e. pyridine-ICl > pyridine-IBr > pyridine-I_2 > pyridine-Br_2 > pyridine-ICN.

The aim of the frequency and intensity studies is to see if this trend is reflected in the acceptor spectra.

1. The Pyridine-ICl complex.

Yarwood and Person[124] have carried out measurements on the complexes of ICl with pyridine, 3-picoline, and 2,6-lutidine in benzene. It was felt to be worthwhile to carry out a number of measurements on pyridine-ICl in benzene, and a few other solvents, to ensure that the results are reproducible. It is also worth checking, that solvent effects are not the predominant factor in determining intensities.

Table 4.1. shows the results for pyridine-ICl. Band shape analysis data where available is included in all tables. The discussion on the band shape data will be found in the section following.

Spectrum 4.1. shows pyridine-ICl in benzene. It is apparent that the $\nu_{(I-Cl)}$ and $\nu_{(N-I)}$ bands both have very similar shapes.

Table 4.1.

Studies on the Pyridine-ICl Complex

Mode	Solvent	Band Position/ $cm.^{-1}$	$\Delta\bar{\nu}_{\frac{1}{2}}$/ $cm.^{-1}$	Area/ $cm.^{-1}$	Cl/mol. $cm.^{-2}$	Intensity[b]/ Darks	α/$ps.^{-1}$	$\tau_{1/e}$/ps.	Temperature/°C
$\nu_{(N-I)}$	Benzene	142	23	24·15	$6·664 \times 10^{-3}$	3623	-0·92	0·64	
	Benzene	142	24	20·70	$6·278 \times 10^{-3}$	3300			
	Benzene	142	25	14·11	$4·25 \times 10^{-3}$	3320			
	[a]T.H.F.	147	20	12·39	$3·73 \times 10^{-3}$	3750			
	Dioxan	150		5·83	$1·9 \times 10^{-3}$	3070	-1·0	0·93	
	Chloroform	149	22	13·78	$4·696 \times 10^{-3}$	4300			
	Benzene	142	Average 3,400 ± 200						
$\nu_{(I-Cl)}$	Benzene	291		75·77	$6·664 \times 10^{-3}$	11370			
	Benzene	291		64·30	$6·278 \times 10^{-3}$	10240			
	Benzene	292	22	46·53	$4·25 \times 10^{-3}$	10948	-0·98	0·82	
			Average 11,000 ± 800						
	T.H.F.	288	21	45·77	$3·73 \times 10^{-3}$	12870	-1·22	0·83	
	Chloroform	283	26	47·32	$4·696 \times 10^{-3}$	12400			
	Chloroform	286	26					0·88	50
	"	283	24					0·72	21
	"	280	21						0
	"	278	24					0·76	-25
	"	275	22					0·84	-50
$\nu_{(N-I)}$	Chloroform	145	24					0·77	50
		151	26					0·83	21
		152	32						0
		153	32					0·76	-25
		159	30						-50

[a] T.H.F. = Tetrahydrofuran.

[b] 1 Dark is 10^{-3} 1 $mol.^{-1}$ $cm.^{-2}$.

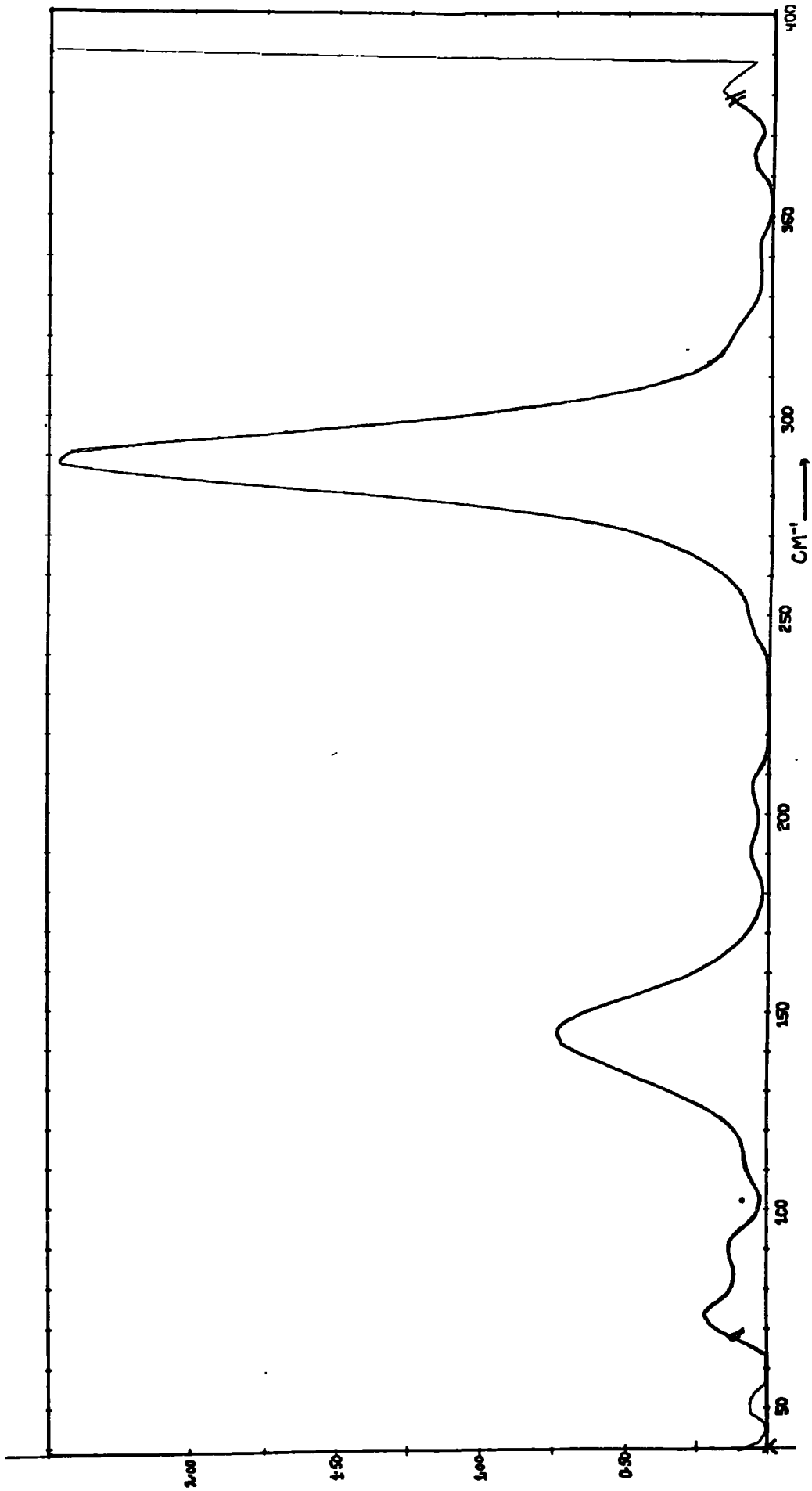

Spectrum 4.1. Pyridine-ICl in benzene at a concentration of 0·05M. The pathlength is 0·1 mm.

The results are within the error quoted by Yarwood and Person. They are slightly lower, perhaps, because they used a grating instrument with a low signal-noise ratio, and a certain amount of noise was amplified and included in the integration.

Solvents affect the intensity but only by about 10% of the integrated value. More polar solvents appear to favour more polar species (i.e. more delocalisation of charge). This results in a higher C.ds term in the the expression for $d\mu$ and hence a greater intensity. (For a discussion of this theory see equation 3.2. of Chapter 3).

Somewhat surprisingly the bands are broader in chloroform than tetrahydrofuran (especially the $\nu_{(I-Cl)}$ band). This broadening may be explained by the different nature of the solvent interaction with the complex dipole. Chloroform interacts by hydrogen bonding favouring the negative end of the complex dipole (i.e. the chlorine atom). Whilst tetrahydrofuran favours the positive end, i.e. the ring and iodine atom. The broadening, in general, is explained by vibrational relaxation due to collision with the surrounding solvent molecules. It would appear from the N.Q.R. data[31] that chloroform will solvate the chlorine atom because of the large negative charge localised on the chlorine atom.

This, of course, affects the $\nu_{(I-Cl)}$ vibration more than the $\nu_{(N-I)}$ explaining why the $\nu_{(I-Cl)}$ band is broader than the $\nu_{(N-I)}$ in chloroform. However, more data in a range of hydrogen-bonding solvents, and studies in a range of other solvents with varying donor (i.e. ionisation potentials) powers, will be needed to prove or disprove this suggestion.

Solvent absorption prevented measurements on the $\nu_{(I-Cl)}$ stretching vibration in dioxan. However, it appears that the more polar the solvent the more structures of the type 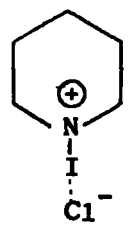 are favoured. This indicates that,

as the polarity of the solvent increases the $\nu_{(N-I)}$ frequency rises and the $\nu_{(I-Cl)}$ frequency falls. The Table 4.2. shows the dipole moments of the molecules used in this work.

The pyridine-ICl results in benzene, tetrahydrofuran and chloroform agree with this trend. The value of the $\nu_{(N-I)}$ frequency in dioxan is anomalous ($\bar{\nu}_{(N-I)}$ = 150 cm.$^{-1}$).

Dioxan has zero dipole moment in the chair form, as the two lone pair moments cancel each other out. However, the molecule probably has a large instantaneous dipole on collision. This is the reason, why even in pure dioxan, the collisional mode can be observed at 70 cm.$^{-1}$ in the far-infrared spectrum. So the effective 'local' dipole moment is probably quite large.

The intensity of the $\nu_{(N-I)}$ band in dioxan may be low due to dissociation of the complex into pyridine and ICl. This dissociation is quite significant in the pyridine-IBr complex (see Chapter 3). It is not clear at present why the intensity is not greatly increased in chloroform in line with the larger frequency perturbation, as compared to say benzene. It is worth noting that solvent bands appear weakly on the ratioed spectrum. In particular a chloroform band at 261 cm.$^{-1}$ and a benzene band at 300 cm.$^{-1}$ This must be due to the solvent bands being increased in intensity due to interaction with the complex. These bands appear to increase in intensity as the concentration of complex is increased. They appear to be stronger for the pyridine-IBr than the pyridine-ICl complex - presumably because of the greater dipole moment of the former complex. No quantitative studies were made on these bands.

2. <u>The Pyridine-IBr and 2,6-Dimethylpyridine-IBr Complexes.</u>

Yarwood[30] observed for the methyl pyridine substituted complexes, that even one α-methyl group, causes a significant decrease in the 'overlap' between the two molecules, as measured by the intensity and frequency perturbations of the $\nu_{(N-I)}$ bands. Even though the equilibrium constant

Table 4.2.

Donor	Dipole Moment[b]	Acceptor	Dipole Moment	Complex	Dipole Moment
Pyridine	2•1D	I_2	0	Pyridine-I_2	4•5D
2,5-Me_2 pyridine	2•1D	Br_2	0	Pyridine-Br_2[a]	6•37D
Trioxane	2•08D	Cl_2	0		
Acetonitrile	3•2D	ICl	2•0D		
Diethyl Sulphide	1•5D	IBr	4•32D		
Diethyl Ether	1•2D	ICN	3•72D		
Chloroform	1•05D				
p-Dioxan	0•02D				
Tetrahydrofuran	1•8D				
Carbon Disulphide	0				
Benzene	0				
Dimethyl Sulphoxide	3•8D				
Ethylacetate	1•78D				

[a] (in benzene). J. D'Hondt, T.H. Zeegers-Huyskens, Journal of Molecular Structure, 1971, 10, 135.

[b] From Landolt Börnstein, Auflage 6, Band 1, Teil 3 (Springer-Verlag, 1951).

changes dramatically only for the 2,6-dimethyl pyridine complex.[136] Indeed the studies on the ICl, IBr and I_2 complexes of the methyl pyridines show, that K_c increases from the value for pyridine complexes when one α-methyl group is introduced.[134] Thus if the intensity of the $\nu_{(N-I)}$ band is determined primarily by the degree of 'overlap' between the complexing molecules, it seems that the K_c values are increased by the electrical contribution more than they are depressed by the steric or entropy contribution. In the case where two α-methyl groups are present the entropy contribution to K_c is predominant.

The frequency maximum and intensity for the $\nu_{(N-I)}$ band are a very sensitive measure of base-halogen interaction. The changes in the $\nu_{(N-I)}$ frequency, show that the interaction is weakened by inserting two methyl groups, whilst in terms of free energy of interaction there is a much smaller change.[136]

It was decided to carry out a brief intensity and band shape study on the 2,6-dimethyl pyridine-IBr to see if the same pattern is followed as for the 2,6-dimethyl pyridine-ICl complex.

Table 4.3. shows the intensity and band shape data for the pyridine-IBr and 2,6-dimethyl pyridine-IBr complexes. The $\nu_{(N-I)}$ band in the 2,6-dimethyl pyridine-IBr complex, showed the same fall in frequency and intensity compared to the pyridine-IBr complex. In view of the similarity with the study by Yarwood[30] on the analogous ICl complexes, it was decided not to pursue this topic any further.

The solvent effects on the frequency and intensity follow no definitive pattern. The $\nu_{(N-I)}$ band position is at a lower frequency in dioxan than in benzene. This is the reverse of the situation in the pyridine-ICl complex. I have no explanation for this at present.

In the absence of a full N.Q.R. study one would expect that less negative charge would be localised on the bromine atom, than the chlorine atom. On the Pauling

Table 4.3.

Studies on the Pyridine-IBr and 2,6-Dimethyl Pyridine-IBr Complexes.

Mode	Solvent	Band Position/ $cm.^{-1}$	$\Delta\bar{\nu}_{\frac{1}{2}}$/ $cm.^{-1}$	Intensity Darks	$\alpha/ps.^{-1}$	$\tau_{1/e}$/ps.	Temperature/°C	Complex
$\nu_{(I-Br)}$	Benzene	206	16	6250		1·17		Pyridine-IBr
	"			7100		1·29		"
	"			6675		1·13		"
	"			6198		1·26		"
	"			6250				"
	"			6800				"
	"			7300				"
	"			7000				"
			Average	6700 ± 500	0·7	1·2 ± 0·1		"
	Carbon Disulphide	209	13	6357	0·5	1·3		2,6-Dimethyl Pyridine-IBr
	Polythene Disc	194						"
	T.H.F.	203	14	7000				Pyridine-IBr
	Chloroform	208	18	6400		1·28		"
	Benzene	205	16		0·64	1·1		Pyridine-d_5-IBr
$\nu_{(N-I)}$	Benzene	135	24	2832		0·71		"
	"			3300		0·72		"
	"			2600		0·6		"
	"			3200				"
	"			3100				"
	"			3000				"
	"			3000				"
	"			2940				"
	"			2840				"
	"		Average	2800 ± 300	1·3	0·7 ± 0·1		"
$\nu_{(N-I)}$	T.H.F.	135	17					"
	Chloroform	136	21	2733				"
	Benzene	127	22		1·14	0·65		Pyridine-d_5-IBr
	Carbon Disulphide	110	17	1605	1·0	0·7		2,6-Dimethyl Pyridine-IBr
	Polythene Disc	126						"
$\nu_{(N-I-Br)}$ Bend	Polythene Disc	61						"

scale the electronegativities are bromine, 2·8; chlorine, 3·0. This would indicate a smaller solvent effect on the bromine atom if the previous argument holds. The pyridine-IBr complex decomposes into pyridine and IBr in dioxan (see Chapter 3). For this reason an intensity was not quoted. The effect of a small amount of pyridine on the frequency and intensity of the complex has not been investigated at the time of writing. There was no evidence in the spectrum of the presence of a band due to IBr_2^- (178 $cm.^{-1}$) - the most likely product of decomposition.

$$PyIBr + PyIBr \rightleftharpoons Py_2I^+ + IBr_2^-$$

Spectrum 4.2. shows pyridine-IBr in benzene which illustrates how the $\nu_{(N-I)}$ band is significantly broader than the $\nu_{(I-Br)}$ band.

3. Effects of Altering the Concentration of Donor and Temperature on the Frequency and Intensity.

During the course of this work it became apparent that the results obtained in the study on the pyridine-I_2 halogen complex in cyclohexane differed very significantly from those obtained by Lake and Thompson.[134] This was because Lake and Thompson assumed that if the pyridine was in excess over the iodine concentration, all the iodine would be complexed. They then expected the far-infrared 'complex' bands to arise from the $\nu_{(N-I)}$ and $\nu_{(I-I)}$ stretching modes.

It was decided to carry out a systematic investigation on the two experimental factors which could account for the discrepancies. These are changes of temperature, and donor concentration. In the case of the pyridine-ICl and pyridine-IBr complexes only temperature studies were carried out. It is inherent in the nature of the 1:1 complex that the donor:acceptor concentration ratio will be 1:1.

The results of the temperature variation studies are shown in Table 4.4. for the pyridine-I_2, pyridine-ICl and pyridine-IBr complexes. Spectrum 4.3.

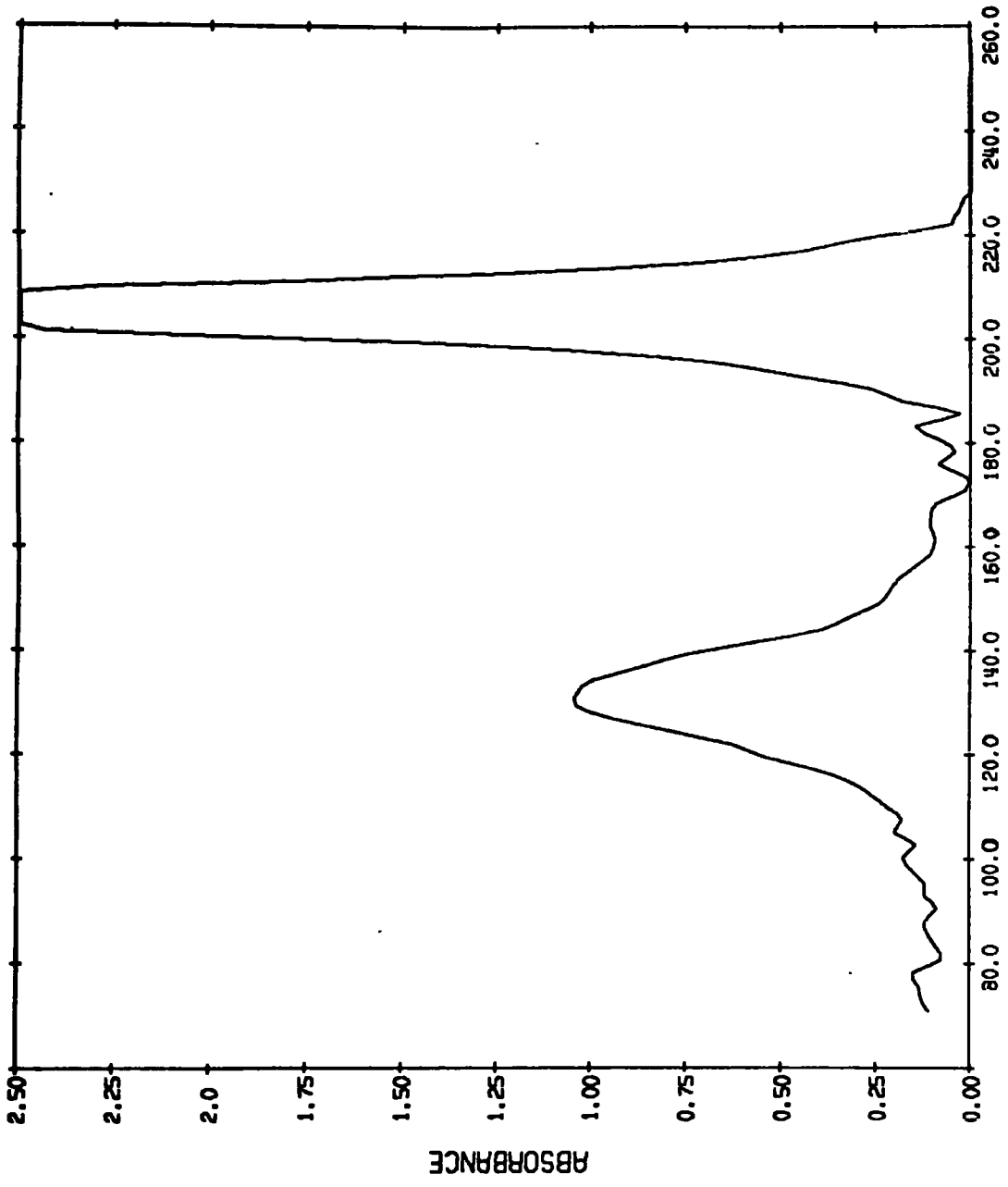

Spectrum 4.2. Pyridine-IBr in benzene showing the different shapes of the two low frequency bands.

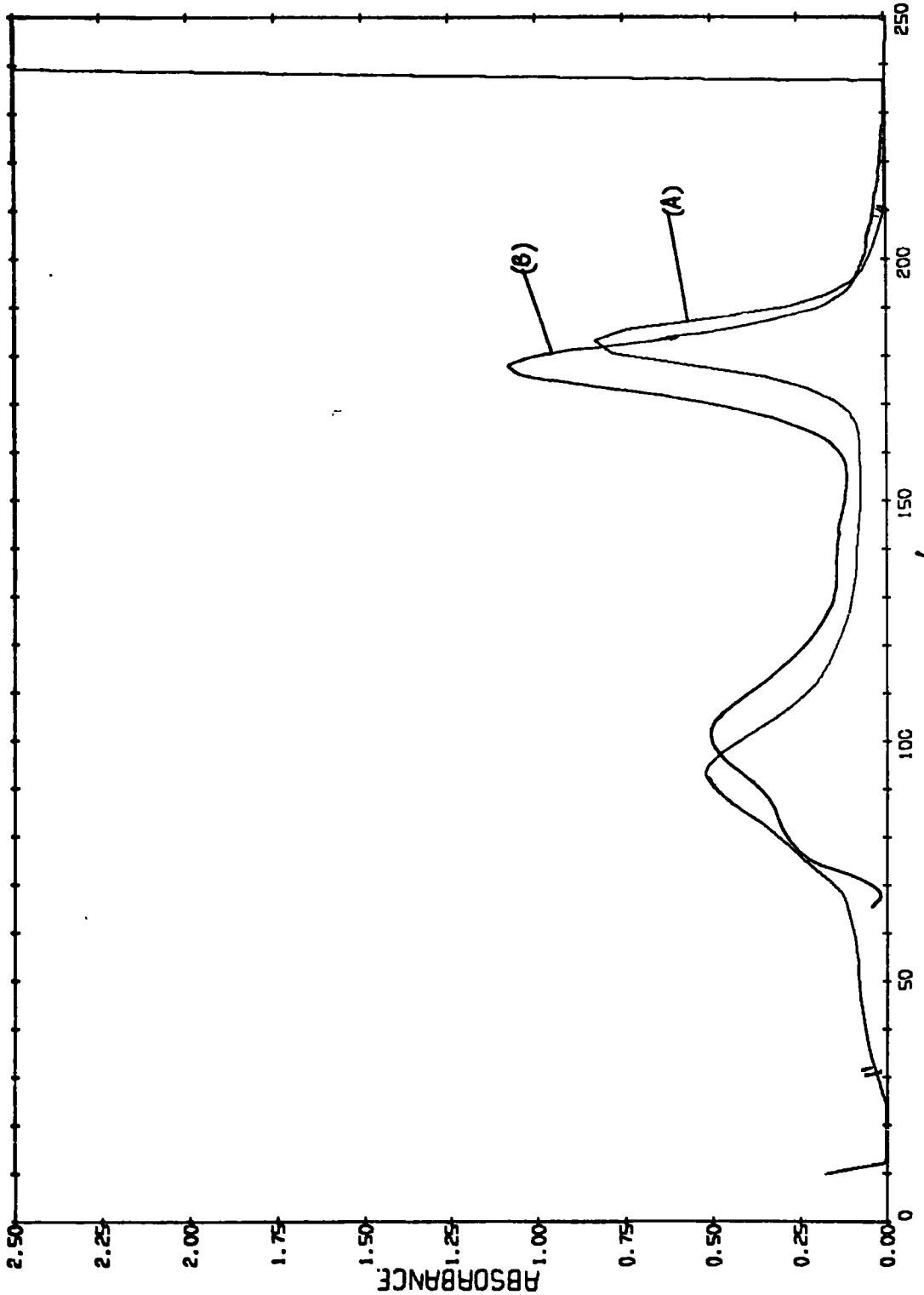

Spectrum 4.3. Pyridine-I_2 complex in cyclohexane (A). Pyridine/I_2 ratio of 3:1. (B) Pyridine/I_2 ratio of 80:1.

Table 4.4.

Effect of Temperature on the Far-Infrared Bands

T/°C	Pyridine-ICl*				Pyridine-IBr*				Pyridine-I_2†			
	$\bar{\nu}_{(I-Cl)}$/ $cm.^{-1}$	$\Delta\bar{\nu}_{\frac{1}{2}}$/ $cm.^{-1}$	$\bar{\nu}_{(D-I)}$/ $cm.^{-1}$	$\Delta\bar{\nu}_{\frac{1}{2}}$/ $cm.^{-1}$	$\bar{\nu}_{(I-Br)}$/ $cm.^{-1}$	$\Delta\bar{\nu}_{\frac{1}{2}}$/ $cm.^{-1}$	$\bar{\nu}_{(D-I)}$/ $cm.^{-1}$	$\Delta\bar{\nu}_{\frac{1}{2}}$/ $cm.^{-1}$	$\bar{\nu}_{(I-I)}$/ $cm.^{-1}$	$\Delta\bar{\nu}_{\frac{1}{2}}$/ $cm.^{-1}$	$\bar{\nu}_{(D-I)}$/ $cm.^{-1}$	$\Delta\bar{\nu}_{\frac{1}{2}}$/ $cm.^{-1}$
75									183	-	86	
60									183	8	88	25
50	283	26	145	24	203	-	134					
45									183	8	89	20
30									183	8	92	20
21	283	24	151	26	200	17	139	30				
10									183	8	93	20
0	280	21	152	32	200	17	142	30				
-10									183		97	
-25	278	24	153	32	200	17	142	30				
-50	275	22	159	30	198	15	146	36				
Fall/ °Rise of T			0·14				0·12				0·09	
Rise/ °Rise of T	·08				·05				-			

* In chloroform

† In cyclohexane

shows the effect of excess pyridine concentration on the pyridine-I_2 spectrum in cyclohexane.

It can be seen from Table 4.4. that for the three complexes the low frequency band shows a shift to higher wave number as the temperature is lowered. This is consistent with the work of Pardoe[128] who found for polar molecules that as the temperature is lowered the frequency increases. He found for dichloromethane a fall of 0·19 $cm.^{-1}/^{o}C$. The value for the $\nu_{(D-I)}$ vibration in the pyridine-ICl complex of 0·14 $cm.^{-1}/^{o}C$ is consistent with a polar rigid complex, the iodine complex value is the least consistent and the IBr is intermediate.

For non-polar liquids Pardoe found a very small shift to lower frequencies (a rise of 0·033 $cm.^{-1}/^{o}C$). The $\nu_{(D-I)}$ band for pyridine-ICl is not behaving as though it arose from a collisional mechanism. Rather, the behaviour is more consistent with what is expected from the Poley Hill[129] absorption mechanism (which considers the absorption as due to the damped rotation of the complex dipole in a cage of solvent molecules). However, for both polar and non-polar molecules Pardoe observed a drop in half-band width of the low frequency band on cooling. The reverse is observed in the pyridine-ICl and IBr cases, whilst $\nu_{(D-I)}$ absorption for pyridine-I_2 follows the same trend.

In the pyridine-ICl and pyridine-IBr cases a small decrease of the acceptor frequency occurs on lowering the temperature. The corresponding increase in the donor-I frequency in these cases indicates, a strengthening of the complex as the temperature is lowered with more electron donation. The $\nu_{(I-I)}$ absorption is remarkably resistant to frequency change with both strong and weak donors. This possibly implies that most of the temperature effect is influencing the librational motion of the complex.

The above results indicate that no one mechanism can describe the properties of the low frequency bands. At least three effects are suspected to be present:-

(a) the change of dipole moment of the complex due to the continuous change in the molecular environment during vibration,

(b) a charge-transfer delocalisation moment due to changing molecular overlap during vibration,

(c) absorption caused by the 'complex' dipole librating in a cage of solvent molecules.

The effect of viscosity changes on the frequency is not clear. As the temperature is lowered the viscosity increases. According to Moelwyn-Hughes,[133a] the vibrational-collisional frequency for molecules in the liquid phase is thought to increase as the viscosity increases. No studies were made on viscosity changes in this work. However, the values listed below taken from the 'Handbook of Chemistry and Physics' published by the Chemical Rubber Co. 1966, shows that the viscosity of chloroform does change quite significantly within the temperature range studied.

Temperature/ ^{o}C	Viscosity/ Centipoise
-13	0·855
0	0·700
8·1	0·643
15	0·596
20	0·58
25	0·542
30	0·514
39	0·500

The hindered rattling of the permanent dipole in a cage of solvent molecules (or Poley Hill[129] absorption) can theoretically be derived from the Gordon formula,[130]

$$A = \frac{\pi}{3c^2}\vec{\mu}_z^{\,2}\left(\frac{1}{I_x} + \frac{1}{I_y}\right) \qquad \ldots\ldots \quad [4.1.]$$

$\vec{\mu}_z$ is the dipole moment along the molecular axis.

I_x and I_y are the moments of inertia perpendicular to this axis. This gives about 140 1 $mole^{-1}$ $cm.^{-2}$ for the low frequency band in the pyridine-I_2 complex. There would appear to be a very small contribution to the band intensity, but the formula probably does not apply since a rigid 'complex' is not present.

The pyridine-I_2 complex acceptor and far-infrared $\nu_{(D-I)}$ bands are known to be quite sensitive to the solvent used.[132] The results are summarised in Table 4.5. If the increase of frequency of the $\nu_{(D-I)}$ vibration and reduction of the $\nu_{(I-I)}$ vibrational frequency, with increase of pyridine concentration, was due to increased complex stabilisation, one would expect a parallel increase of intensity as the amount of pyridine is increased.

Whilst the intensity of the $\nu_{(I-I)}$ band increases slightly the low frequency band is practically constant in intensity. This is consistent with Pardoe's results. Both bands broaden as the medium becomes more polar.

It is interesting to note that the addition of excess pyridine or the use of benzene produces the same solvation effect, i.e. both bands broaden and the frequencies approach each other. This would imply that the solvation of the complex is due to the pyridine molecules; however, the exact mechanism is not clear.

It must be noted that the concentrations of pyridine used would favour a 2:1 complex. One would expect the equilibrium constant of a 2:1 complex, to be much smaller than that of the 1:1 complex. If the equilibrium constant was of the order of 1 litre $mole^{-1}$, there would be a considerable concentration of the 2-pyridine-I_2 complex, at a ratio of pyridine to iodine of 250:1. However, it should be possible to test for this by seeing if the infrared inactive band at 374 $cm.^{-1}$ in pyridine appears on complexation. If the 2:1 complex was of the form,

$$C_5H_5N\cdots I^{\delta+}\cdots NC_5H_5$$
$$\qquad\qquad\quad |$$
$$\qquad\qquad\quad I^{\delta-}$$

Table 4.5.

Concentration Dependence of the Two Low Frequency Bands of the Pyridine-I_2 Complex

Ratio Pyridine:I_2	Pyridine conc. (mole litre^{-1})	Iodine conc. (mole litre^{-1})	$\nu_{(I-I)}$ Band			Band Composite			Solvent
			$\bar{\nu}$/cm.$^{-1}$	$\Delta\bar{\nu}_{\frac{1}{2}}$/cm.$^{-1}$	B_i/Darks	$\bar{\nu}$/cm.$^{-1}$	$\Delta\bar{\nu}_{\frac{1}{2}}$/cm.$^{-1}$	B_i/Darks	
23:1	2·167	0·0934	176	12	3375	104	28	1901	Cyclohexane
87:1	1·980	0·0227	178	12	2680	104	28	2170	"
73:1	1·630	0·0224	178	11	2468	101	28	2036	"
25:1	0·583	0·0229	181	10	2430	98	23	1980	"
14:1	0·320	0·0227	182	9	2292	93	22	1890	"
7:1	0·159	0·0228	182	9	2362	90	21	1431	"
		Effect of Varying I_2 Concentration and Solvent							
21:1	0·159	0·0077	183	8	1946	92	20	1460	Cyclohexane
7:1	0·159	0·0228	182	9	2292	93	22	1890	"
26:1	3·738	0·1409	172	12	3556				Benzene
14:1	2·370	0·1711	170	13	2219				Chloroform

this would explain the large intensity of $\nu_{(I-I)}$ band with excess pyridine. However, without further data the discussion must end here.

It may be noted in passing that equilibrium constants measured in the ultra-violet region, would favour the 1:1 complex as the solutions used were very dilute. The n:m interactions may result in frequency shifts sufficient only to produce band-broadening effects.

There is plenty of evidence (see Chapter 7) of 2:1 and 1:2 complexes of pyridine with the halogens in the solid state. However, these solid complexes are ionic in nature and decompose in solution. For the concentrations studied there was no evidence of the polyhalogen anions that these complexes give in solution, in the far-infrared spectra. It would appear therefore that if there is a n:m interaction the species present is not ionic. It is very difficult to distinguish between bulk solvent effects, and specific solute-solvent effects with the techniques available at present.

One final point is that the intensity of the bands appears to be dependent upon the iodine concentration as well as the pyridine. This follows the same pattern at for dioxan-I_2 (see Chapter 5). However, further data is needed to establish this conclusively as the deviation in Table 4.5. may just be experimental error. This has probably not been observed previously because (i) the solubility of iodine is low, this has resulted in measurements being made at effectively about one concentration of iodine ($0{\cdot}02 \pm 0{\cdot}02M$); (ii) the high solubility of pyridine in cyclohexane, which allows a large range of concentrations masking charges due to different iodine concentrations; (iii) the difficulties of avoiding the formation of ionic solids at high iodine concentrations.

4. Studies on the Pyridine-ICN Complex.

Measurements in the 100 - 500 $cm.^{-1}$ region were carried out using the FS720 interferometer. Measurements on the $\nu_{(C-N)}$ band in the 2200 - 2300 $cm.^{-1}$

region were carried on the modified GS2A as described in Chapter 1.

ICN is a linear triatomic molecule with symmetry $C_{\infty v}$. Table 4.5A. shows the fundamental frequencies,

$\nu_{(I-C)}$ Σ^+ I → ←C←N

$\nu_{(C-N)}$ I → C → ←N

ν_b I—C—N (I ↓, C ↑, N ↓)

Table 4.5A

Frequency Data for the ICN Complex

State	$\bar{\nu}_{(I-C)}$/ cm^{-1}	$\bar{\nu}_b/cm^{-1}$	$\bar{\nu}_{C-N}$/ $cm.^{-1}$
[a] Liquid	470	321	2158
[b] Solid (-180°C)	452	329	2176
Benzene soln.		320	2167
Pyridine/$CHCl_3$	426	338	2156
Pyridine/n.heptane	440	346	2166
Dioxan soln.	466	329	2165
Cyclohexane soln.	-	310	-
Et_2S/cyclohexane soln.	-	321	-
Acetone/cyclohexane	466	-	-
Chloroform soln.	473	321	2171

[a] N. West and M. Farnsworth, Journal Chemical Physics, 1933, 1, 402.

[b] W. Freitag and E.R. Nixon, Journal Chemical Physics, 1956, 24, 109.

Iodine cyanide appears, at first inspection, to be a very interesting subject for band shape analysis and intensity studies. The free acceptor has three vibrations, all infrared and Raman active. The normal co-ordinate calculation in Chapter 6 shows that the perturbation of the donor frequencies, at least for the IBr and ICl complexes, can be explained in terms of the G

matrix (mass effect) and L matrix (vibrational mixing) variations. Pyridine is considered to complex at the iodine atom which explains the fall of the $\nu_{(I-C)}$ frequency on complexation. However, the $\nu_{(C-N)}$ band is known[140] to show drastic intensity perturbations on complexation. The $\nu_{(C-N)}$ frequencies do not change much with different donors (see Chapter 5) but the C-N bond stretching force constant is high[141] and so the vibration is localised within the bond to a considerable extent. However, at the time of writing there appears to be no information on the band shape in the literature. This is possibly because of the great experimental difficulties of making accurate measurements on the band shape in this system.

The intensity and band shape results for the pyridine-ICN complex are shown in Table 4.6.

The $\nu_{(C-N)}$ band intensity shows a dramatic fall on complexation with pyridine in chloroform and the band appears to broaden. However, careful inspection of the band shows that it may be a 'doublet' (spectrum 4.4.) since there is asymmetry on the low energy side. This is presumably because there is interaction between chloroform and ICN. This $CHCl_3$-ICN 'complex' causes a very significant increase in the C-H intensity in chloroform. It was found that when a 10% solution (by weight) of chloroform in carbon tetrachloride was saturated with ICN, a considerable increase in the $\nu_{(C-H)}$ band intensity was observed. The band also became broader.

According to Thomas and Orville Thomas[142] the following hydrogen bonded structures are important.

$$I\text{-}C{\equiv}N\cdots\cdots H\text{-}CCl_3$$

$$I\text{-}\overset{+}{C}{=}\overset{-}{N}\cdots H\text{-}CCl_3$$

$$I\text{-}\overset{+}{C}{=}N\text{-}H\cdots\overset{-}{C}Cl_3$$

Table 4.6.

Studies on the Pyridine-ICN Complex

Mode	Solvent	Band posn./ $cm.^{-1}$	$\Delta\bar{\nu}_{\frac{1}{2}}/cm.^{-1}$	[Donor] moles/litre	[Acceptor] moles/litre	Intensity/ Darks	$\alpha/ps.^{-1}$	$\tau_{1/e}$ /ps.
$\nu_{(C-N)}$	Chloroform	2156	14	0·3825	0·1317	150		
$\nu_{(I-C)}$	Chloroform	433	23	0·4987	0·2162	3800	-1·18	
				0·3987	0·226	3680		
ν_{bend}	Chloroform	338	12·5	0·366	0·237	260	-0·47	1·02
	Heptane	327	7	0·3825	0·03516	327		
$\nu_{(D-I)}$	Chloroform	105	48	0·366	0·237	1100		0·35

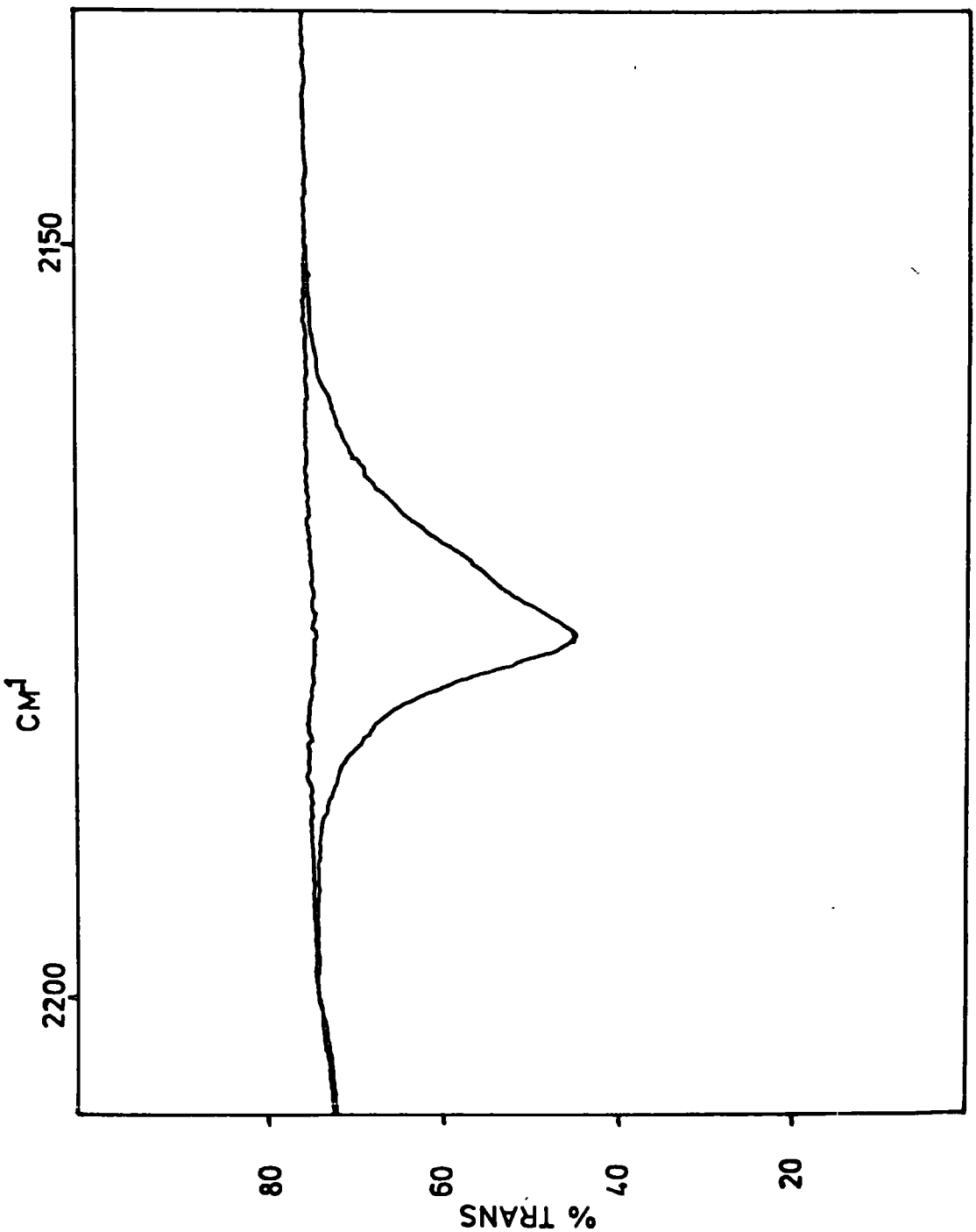

Spectrum 4.4. The $\nu_{(CN)}$ band of ICN in a pyridine/chloroform mixture showing asymmetry to low frequency and possible 'doublet' structure.

As the CN bond is stretched due to the hydrogen bond the increased electronic charge on the nitrogen is stabilised by increased delocalisation energy. The intensity increase must then be partly due to the increased importance of the ionic form and partly due to the fact that the length of the dipole in the ionic form is increased as a result of the delocalisation of the electrons.

An attempt was then made to study the $\nu_{(C-N)}$ band of the pyridine-ICN complex in carbon tetrachloride. The band was still asymmetric. It would appear that 'free' ICN is still present with a 10:1 excess of pyridine to ICN or that the asymmetry is due to environmental (or other) effects. The problem is made worse by the fact that the $\nu_{(C-N)}$ band belonging to the complex with pyridine is dramatically reduced in intensity. The $\nu_{(C-N)}$ band corresponding to the ICN 'solvated' in carbon tetrachloride (or 'complexed' in chloroform) is effectively increased in intensity, compared to the 'complexed' band. This causes base-line problems to be very severe. A possible way of avoiding this problem is discussed in 'suggestions for further work'.

Even more powerful electronic influences may be present. According to Townes and Dailey[143] in BrCN and ICN there is a significant contribution from the resonance structure[54] $\overset{+}{I}{=}C{=}\overset{-}{N}$. ICN will thus have a dipole moment $\overrightarrow{ICN}$. However, in the complex, contributions from structures of the type (A) will be more important as the negative charge will tend to be localised on

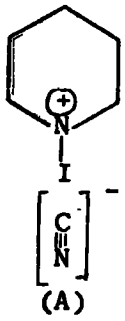

(A)

the carbon. The transition moment of the $\nu_{(C-N)}$ vibration will be reduced or even reversed in direction. This accounts for the

fall in intensity. However, there seems no satisfactory explanation of the lack of intensity perturbation of the bending (ν_b) band on going from strong donors to weak donors.

N.Q.R. measurements[141] on the free acceptor support the hypothesis that pyridine $\overset{+}{-}I\cdots\cdots[CN]^-$ contributes significantly to the pyridine-ICN complex. The following canonical forms contribute to the mesomeric state.

$I-C\equiv N$	$\overset{+}{I}=C=\bar{N}$	$\overset{+}{I}\overset{\ominus}{C}\equiv N$
I	II	III
95%	1%	4%

In view of the significant contribution of structure III to the free acceptor, one would expect an even greater contribution in the complex.

Whether the broadening of the ν_b band in the pyridine-ICN complex on going from heptane to chloroform is a general solvent effect or a more specific interaction is not clear. The structural anisotropy of the solvent molecules could be a factor in broadening the complex vibrational bands, the complex molecule being in different environments according to which 'sides' or 'ends' of the solvent molecules are turned towards it.

The $\nu_{(I-C)}$ band shows the normal large increase in intensity on complexation. The external $\nu_{(N-I)}$ mode is included for the sake of completeness. It is worth commenting at this point what a sensitive measure the $\nu_{(N-I)}$ intensity is of the complex strength in the series pyridine-ICl, pyridine-IBr, pyridine-I_2 and pyridine-ICN, i.e. 3,700, 2,800, 2,000, 1,100 darks.

5. Studies on the Pyridine-Bromine Complex.

Studies on the pyridine bromine complex were limited to confirming that the intermolecular N····Br stretching vibration occurred at a higher frequency than the N···I stretching vibration. This piece of information was important in comparing the frequency perturbation of bands in the donor spectrum of the pyridine-Br_2 and pyridine-I_2 complexes.

The Br-Br and N-Br stretching bands occurred at 230 and 124 $cm.^{-1}$ respectively for the pyridine-Br_2 complex in benzene. This is in good agreement with the values obtained by D'Hondt and Zeegers-Huyskens.[137] A weak absorption was also observed at 189 $cm.^{-1}$ corresponding to anti-symmetric stretching of the Br_3^- ion. According to Ginn et al.[138] the formation of Br_3^- is due to the following equilibrium.

$$2Pyr\text{-}Br_2 \rightleftharpoons Pyr_2Br^+ + Br_3^-$$

D'Hondt and Zeegers-Huyskens also observed absorptions at 168 and 140 $cm.^{-1}$ involving anti symmetric and symmetric stretching of the N-Br-N portion of the Pyr_2Br^+ cation. However, at the concentrations used in this work, they were too weak to be observed. Spectrum 4.5. shows the pyridine-Br_2 complex in benzene measured using the FS720 with a 50 gauge beam splitter.

The intensity of the benzene-Br_2 'complex' has been measured and a value[139] of 420 $dm.^3$ $mole^{-1}$ $cm.^{-2}$ quoted for the $\nu_{(Br\text{-}Br)}$ band at 305 $cm.^{-1}$ This is considerably higher than for the benzene-iodine complex. Whilst a number of workers[134,137] have looked at the frequencies of the pyridine-Br_2 complexes, no one seems to have quoted intensities. The intensities measured are quoted in Table 4.7. They are greater than the pyridine-I_2 values as was observed in the benzene-Br_2 and benzene-I_2 complexes. The intensities also seem to be dependent on the donor concentration.

Why the intensity should be larger is not immediately obvious. The dipole moment is larger in the pyridine-Br_2 complex than for pyridine-I_2 (see Table 4.2.). However, if Person's[120] values are correct the electron affinity of bromine is lower than iodine. Hanna[119] also considers the polarisability of bromine to be less than iodine. The available polarisabilities are quoted in Table 4.8.

Table 4.7.

Studies on the Pyridine-Bromine Complex

Mode	Solvent	Band posn./ $cm.^{-1}$	$\Delta\bar{\nu}_{\frac{1}{2}}$/ $cm.^{-1}$	mole-litre [pyridine]	mole-litre [Bromine]	Intensity/ 'Darks'
$\nu_{(N-Br)}$	Benzene	120	34	0·2513	0·1002	3652
	Chloro-form	124	34	0·3396	0·07312	4536
$\nu_{(Br-Br)}$	Carbon Tetra-chloride	246	24	0·4721	0·09725	6669
	Benzene	230	21	0·2513	0·1002	5720

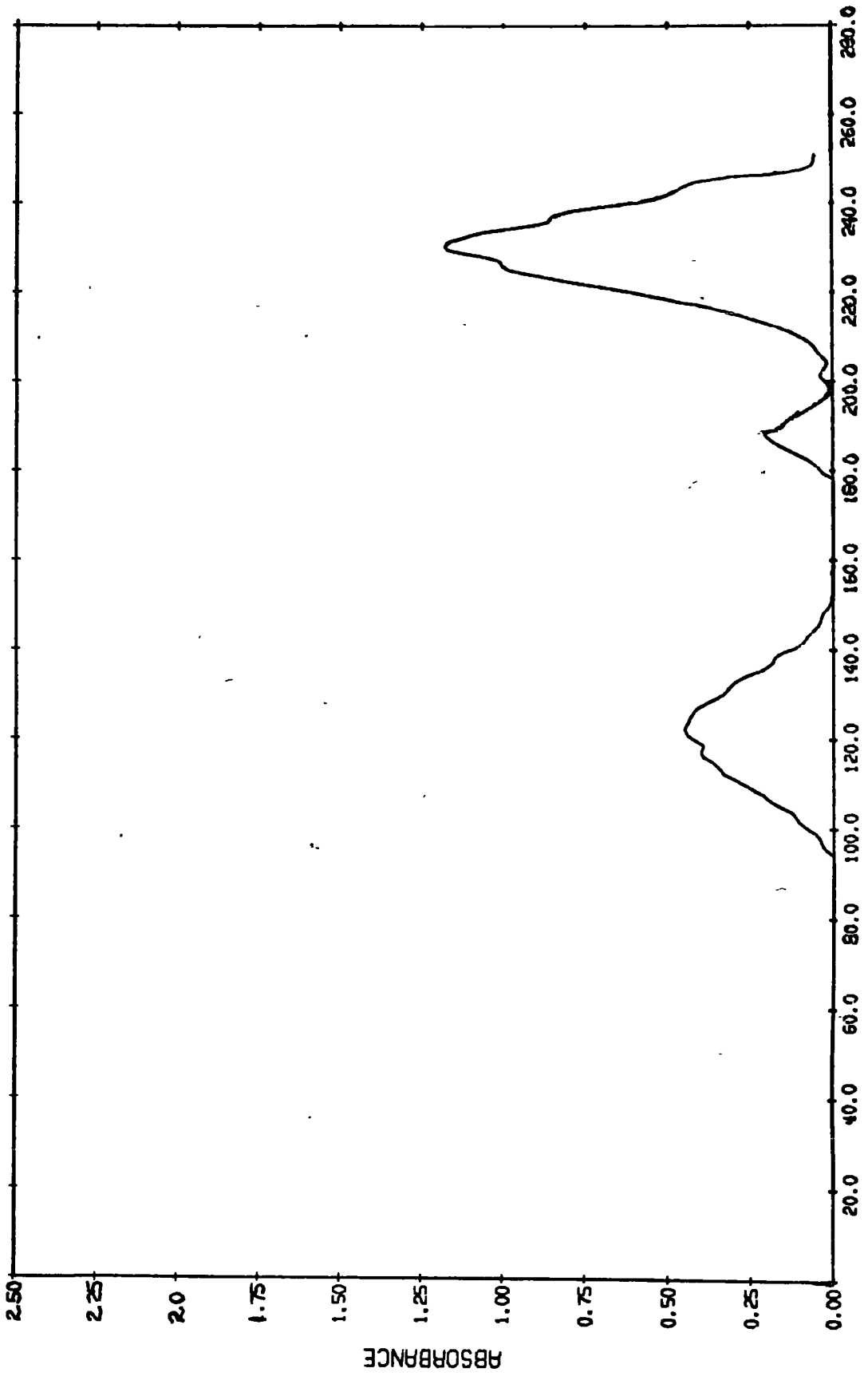

Spectrum 4.5. Pyridine-Br_2 complex in benzene solution. The band at 190 $cm.^{-1}$ is due to a small amount of Br_3^-.

Table 4.8.

Molecule	Polarisability $cm.^3 \times 10^{25}$
I_2	175
ICl	136
Br_2	99•5
Cl_2	66

C. Band Shape Studies.

The Fourier transform of an observed absorption band gives the time dependent correlation function Ø(t) (see Chapter 2). Spectroscopists normally obtain two parameters from the correlation function to characterise it, and to compare it with the correlation functions determined from other bands. These parameters are:-

(i) The $\tau_{1/e}$ Values.

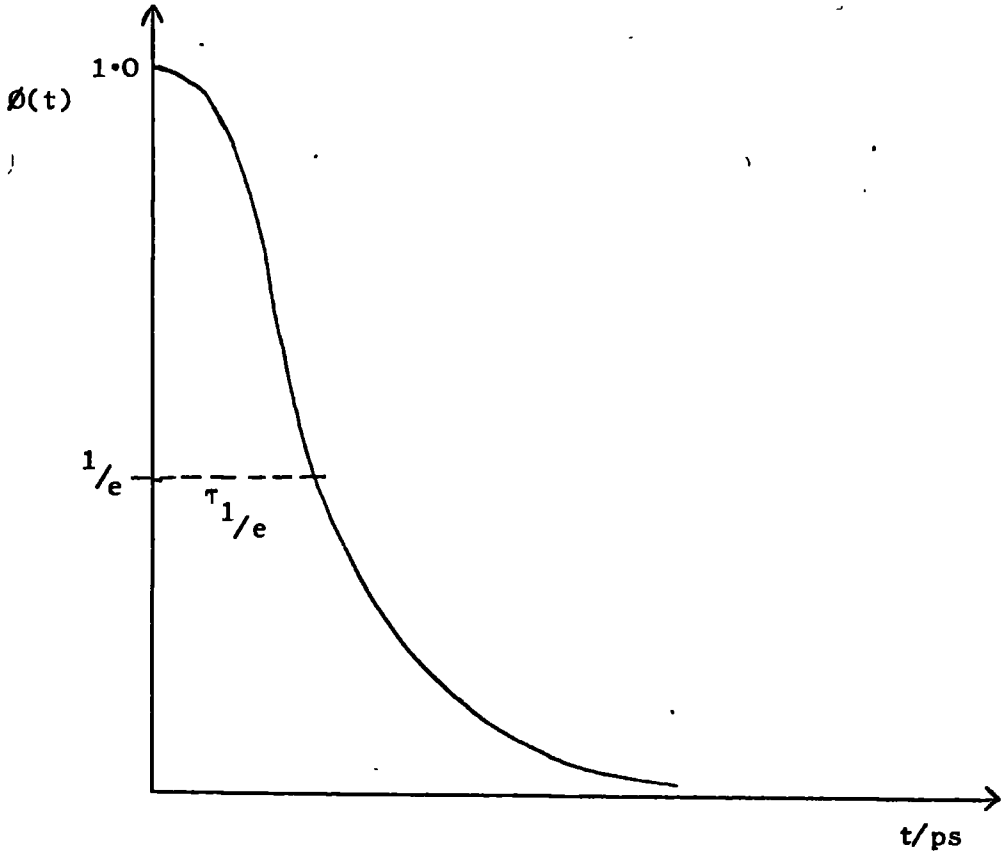

Fig. 4.1.

The Figure 4.1. shows how the correlation function decays with time. The Gaussian component, which affects the correlation function for all values of t, has the greatest contribution at short times. The vibrational relaxation mechanism gives a large Gaussian contribution to the band profile, so if a large real Gaussian component is present then vibrational effects must be important. However, the absence of a Gaussian component does not indicate a total lack of vibrational effects.

This is because, whilst the 'Bratos Dephasing Mechanism'[73] gives a distorted Gaussian component to the band profile, there are at least two other vibrational relaxation mechanisms[146f] which need not give a Gaussian component to the band profile. These are vibrational energy dissipation with the cage of solvent molecules and resonance energy transfer.

Vibrational energy dissipation is due to permanent dipole-transition dipole interactions between the molecules considered and the molecules (like or unlike) in the surrounding environment. This process should therefore be dependent upon the 'polarity' of the surrounding medium and the broadening caused by such effects are expected to be removed on dilution with a non-polar solvent. This effect is quite likely to be present for some of the complexes studied here.

Resonance energy transfer is a kind of transition dipole-transition dipole interaction between the absorbing molecules. There is a 'chain excitement effect' from one molecule to another in the dynamically surrounding environment which leads to energy relaxation between the molecules and an associated broadening.

The $\tau_{1/e}$ value of the autocorrelation curve is the time it takes $\phi(t)$ to fall to $\frac{1}{e}$ of its original values. Since the function is normalised (i.e. at t = 0, $\phi(0) = 1$) $\tau_{1/e}$ is the time taken for $\phi(t)$ to fall from 1 to 0·378.

For very accurate data it is better to use the absolute correlation time, i.e.

$$\tau = \int_{-\infty}^{+\infty} \phi(t)dt$$

this is the time for $\phi(t)$ to fall from 1 to 0.

(ii) The slope (α) of the Log $\phi(t)$ v. t plot is equal to ($\alpha_R + \alpha_v$) (see Chapter 2). If α_R (rotational diffusion coefficient) is much larger than α_v one may approximate the slope α to α_R. This approximation is true for light molecules such as acetonitrile.[145]

Where rotational effects predominate expressions of the type:

$$(\Delta\bar{\nu}_{\frac{1}{2}}) \text{ observed} \approx \delta_o + A\exp(-U_{OR}/kT) \quad \ldots\ldots \quad [4.2.]$$

(where δ_o is the residual width)

have been used to calculate[131] the mean re-orientation potential barrier, U_{OR}. The above equation predicts that the band width should fall as the temperature is lowered.

Where the data was accurate enough α values are quoted as they may be of use to other workers in the infrared group at Durham. With the exception of the ICN complex discussion will be limited to the $\tau_{1/e}$ values.

If rotational motion is predominant in the ICN molecule the following discussion relates the α values to the diffusion coefficients. The diffusion coefficient is a measure of the rate of rotational damping about a particular axis. One would expect that the α value obtained for the $\nu_{(C-N)}$ band would be the same as that derived for the $\nu_{(I-C)}$ band.

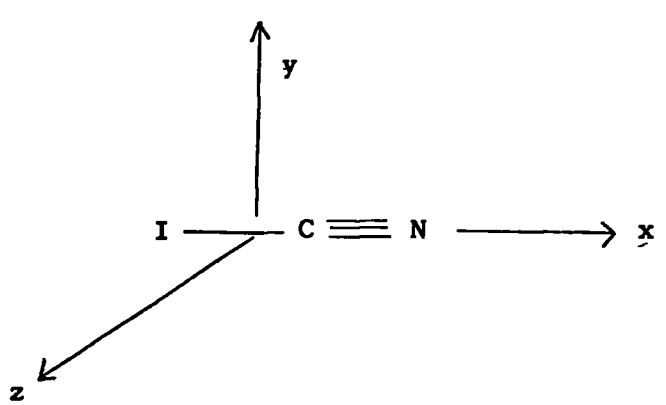

This is because rotational motion observed is the same for the two vibrations. For the stretching modes the diffusion coefficients obtained ($D_y = D_z$) are the same, i.e.

$$D_y = D_z = \alpha_R[\nu_{(I-C)} \text{ or } \nu_{(C-N)}]/2 \quad \ldots\ldots [4.3.]$$

Because of its high moment of inertia about the I_y and I_z axes the molecule will spin preferentially about the x axis.

The observed α_R(bend) will thus lead to a value of D_x via,

$$D_x = \alpha_R(\nu_b) - D_z \quad \ldots\ldots [4.4.]$$

1. On the Pyridine-ICl Complex.

Temperature studies on the $\nu_{(N-I)}$ and $\nu_{(I-Cl)}$ showed that the band width did not obey equation 4.2. It was decided to try and establish whether the absorptions at 140 $cm.^{-1}$ and 290 $cm.^{-1}$ were correctly assigned to 'vibrations'.

Chapter 5 shows the existence of a benzene-ICl complex in cyclohexane and that the life-time is > 1·6 ps. This information is provided by the observation of both 'free' and complexed $\nu_{(I-Cl)}$ bands in the mixed solvent. Thus the $\nu_{(I-Cl)}$ band is definitely due to a vibrational mode.

The logarithmic correlation curves for the pyridine-ICl complex were slightly curved probably due to the isotopic splitting of the two low frequency bands. The two bands have approximately the same width ($\Delta\bar{\nu}_{\frac{1}{2}}$ = 22 $cm.^{-1}$). The α values of -0·92 ps^{-1} and -0·98 ps^{-1} and $\tau_{1/e}$ values of 0·64 and 0·82 ps are consistent with this (see Table 4.1. and Fig. 4.2.).

The great similarity in shape of the two bands suggests that they arose from the same mechanism, i.e. the absorption at 140 $cm.^{-1}$ is due to the $\nu_{(N-I)}$ vibration.

2. Studies on Pyridine-IBr and 2,6-Dimethyl Pyridine-IBr.

For pyridine-IBr the correlation curves are not coincident. The α values are 0·7 and 1·3 ps^{-1} with $\tau_{1/e}$ values of 1·2 and 0·7 ps. This implies that the $\nu_{(N-I)}$ band in the pyridine-IBr complex is composite or the band shape

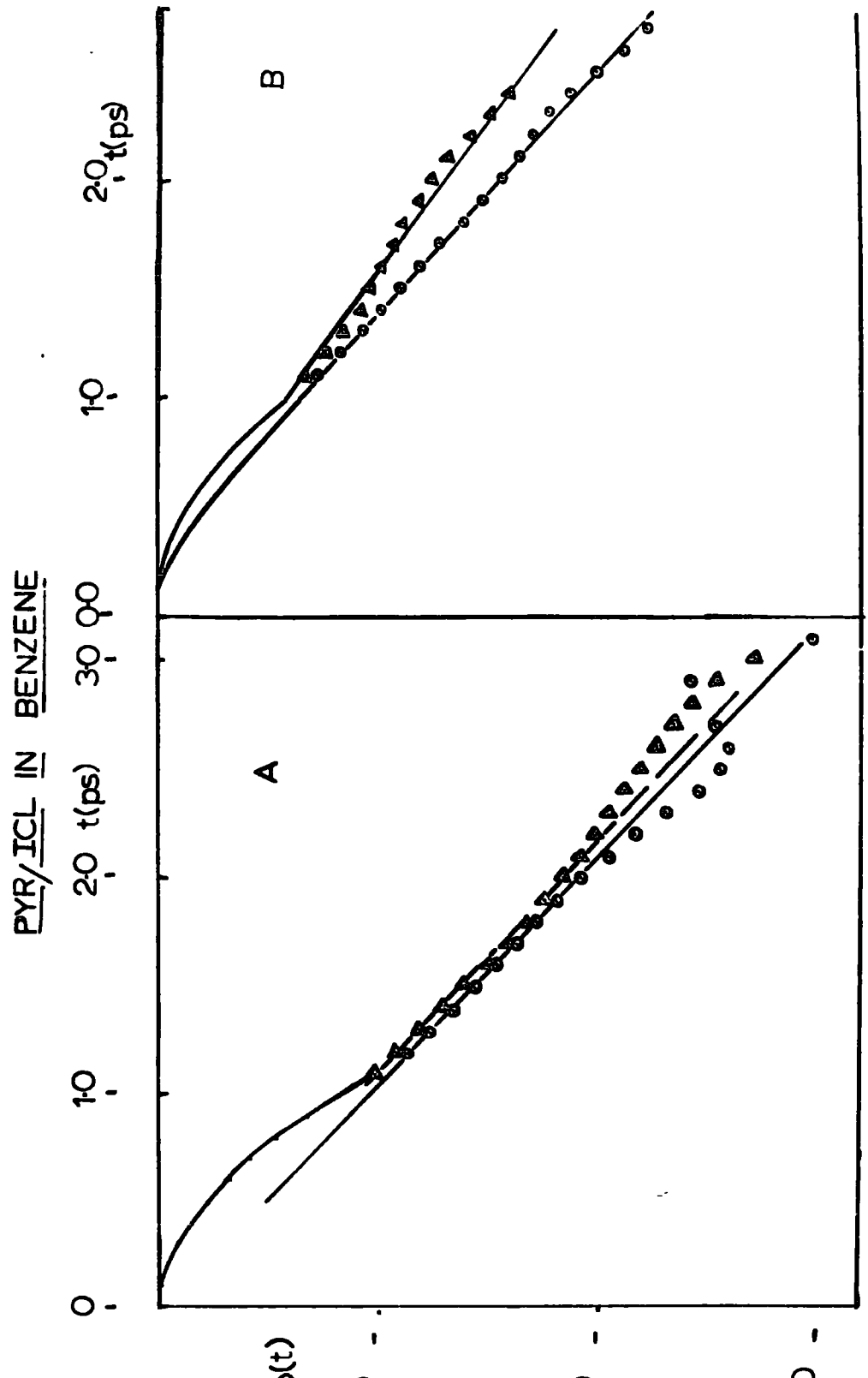

Fig. 4.2. TIME AUTOCORRELATION CURVES FOR PYRIDINE-ICL IN BENZENE,
A. BAND AT 150CM^{-1} B. BAND AT 290CM^{-1}

is controlled by vibrational relaxation which is independent of the direction of the transition moment.

The probable answer is that the increased mass of the bromine suppresses the rotation slightly more than in the ICl complex since the bands are slightly narrowed but that vibrational relaxation has the main contribution to the band shape in both cases.

The pyridine d_5-IBr and the 2,6-dimethyl pyridine-IBr far-infrared bands had very similar shapes to the pyridine-IBr complex. The increased moment of inertia of the 2,6-dimethyl pyridine showed no effect on the band shape compared to the pyridine-IBr complex.

One must conclude, therefore, that rotation about the axes perpendicular to the C_2 axis are completely suppressed in pyridine-IBr. The α-values are likely to be mainly vibrational damping constants, and are not a measure of the rate of diffusion. Since α_v is independent of the transition moment, this accounts for the difference in shape of the two bands.

It is worth noting that if the far-infrared spectra of the pyridine-ICl and pyridine-IBr complexes, are controlled by vibrational relaxation, the fact that the $\tau_{1/e}$ values are the same for the $\nu_{(N-I)}$ and $\nu_{(I-Cl)}$ bands in the pyridine-ICl complex may be coincidental. This is because the Bratos mechanism shows that $(\tau_{1/e})$ vibrational is independent of the direction of the transition moment. Thus, it is not too surprising that the $\tau_{1/e}$ is significantly different for the two vibrations in the pyridine-IBr complex. The fact that $\tau_{1/e}$ for the $\nu_{(N-I)}$ vibration is higher for the pyridine-ICl complex, than for pyridine-IBr, may be due to the longer life-time of the former complex. This is reflected by the higher equilibrium constant of the pyridine-ICl complex.

3. Studies on the Pyridine-I_2 Complex.

As can be seen from Table 4.5. both bands have increasing total half-band widths, as the medium becomes more polar. This is reflected by the auto-

correlation curves for the $\nu_{(I-I)}$ bands (see Figures 4.3 and 4.4). The slope α, is related to the damping constant α_v of the vibration, since one would expect that the heavy iodine molecule would be rotating only slowly at room temperature. The strong concentration dependence of α_v is consistent with a vibrational relaxation mechanism.

The size of the translational contribution to α is not clear. Yarwood[65] has calculated very approximately that the IBr molecule should suffer a 50% drop in velocity on collision with a benzene molecule, during the first picosecond. This indicates that the translational correlation function changes quite rapidly, over the period under consideration (0-5 ps).

As can be seen from Table 4.9., $\tau_{1/e}$ increases as the pyridine concentration increases. This vibrational relaxation is slowed down as the pyridine concentration is increased. This must be due to the environment becoming more isotropic, due to specific 1:1 interactions. This is the same argument used by Rothschild,[146e] to explain the increasing τ_v value for quinoline, on going from gas to liquid, to carbon disulphide solution, to crystalline solid. This suggests that the increasing pyridine concentration causes an increase in $\tau_{1/e}$ because iodine collides more frequently with pyridine molecules. One very interesting phenomena that occurs is that the same frequency shift occurs using a less inert solvent with a smaller pyridine concentration, e.g. 0·24M pyridine solution in benzene gives a very similar correlation curve to a 1·21M pyridine solution in cyclohexane with the same iodine concentration in both cases (see Figure 4.4.). The exact mechanism for this process has yet to be established.

D. Suggestions for Future Work.

It would seem that vibrational relaxation processes are predominant in the pyridine-halogen complexes. However, one further test can still be applied to throw more light on this. Bratos[61] has clearly shown that in the case of rapid vibrational modulation, the $\tau_{1/e}$ value ought to depend critically on

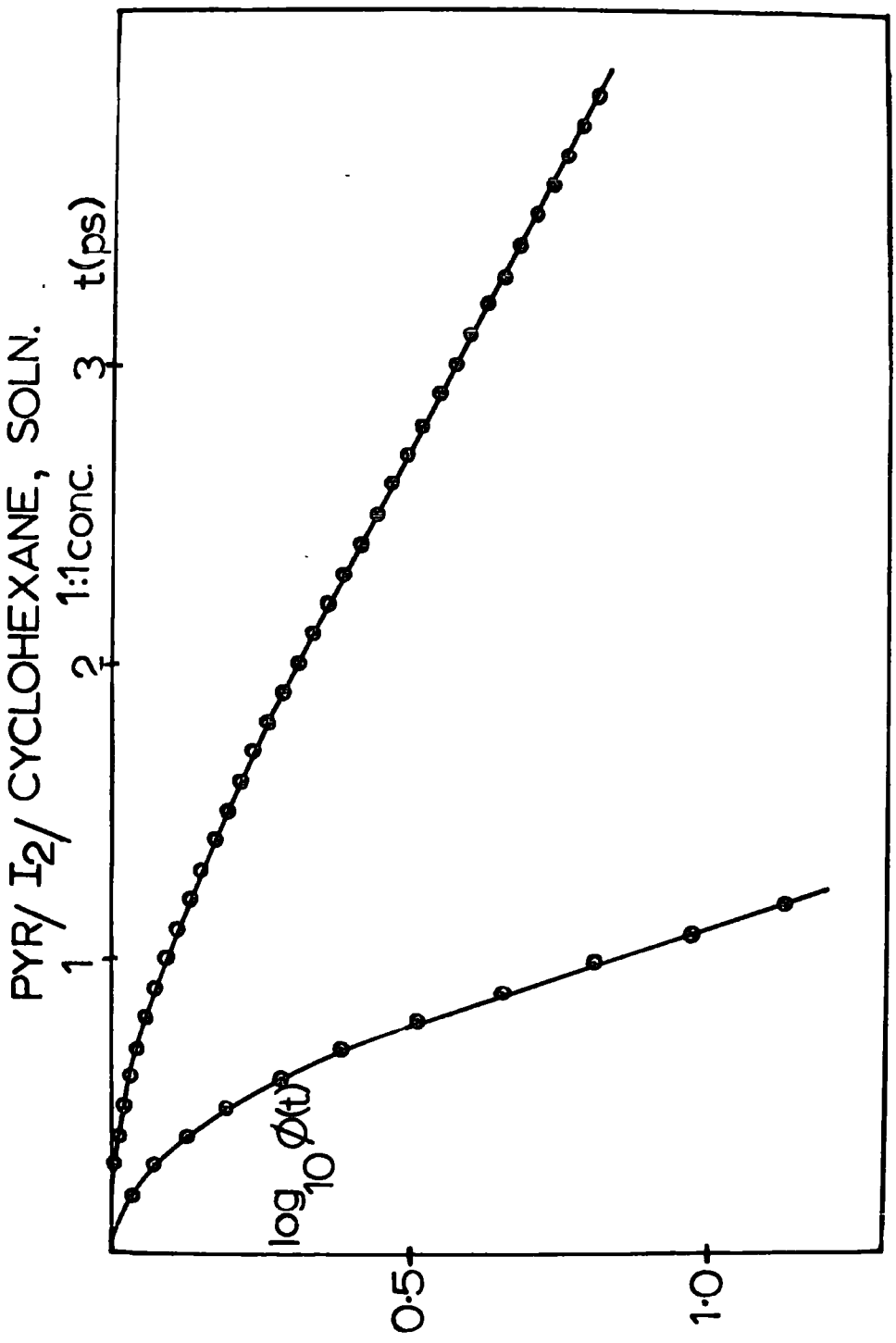

Fig. 4.3. PYRIDINE - I_2/CYCLOHEXANE, AUTOCORRELATION CURVES FOR TWO LOW FREQUENCY BANDS, 1:1 CONC. RATIO.

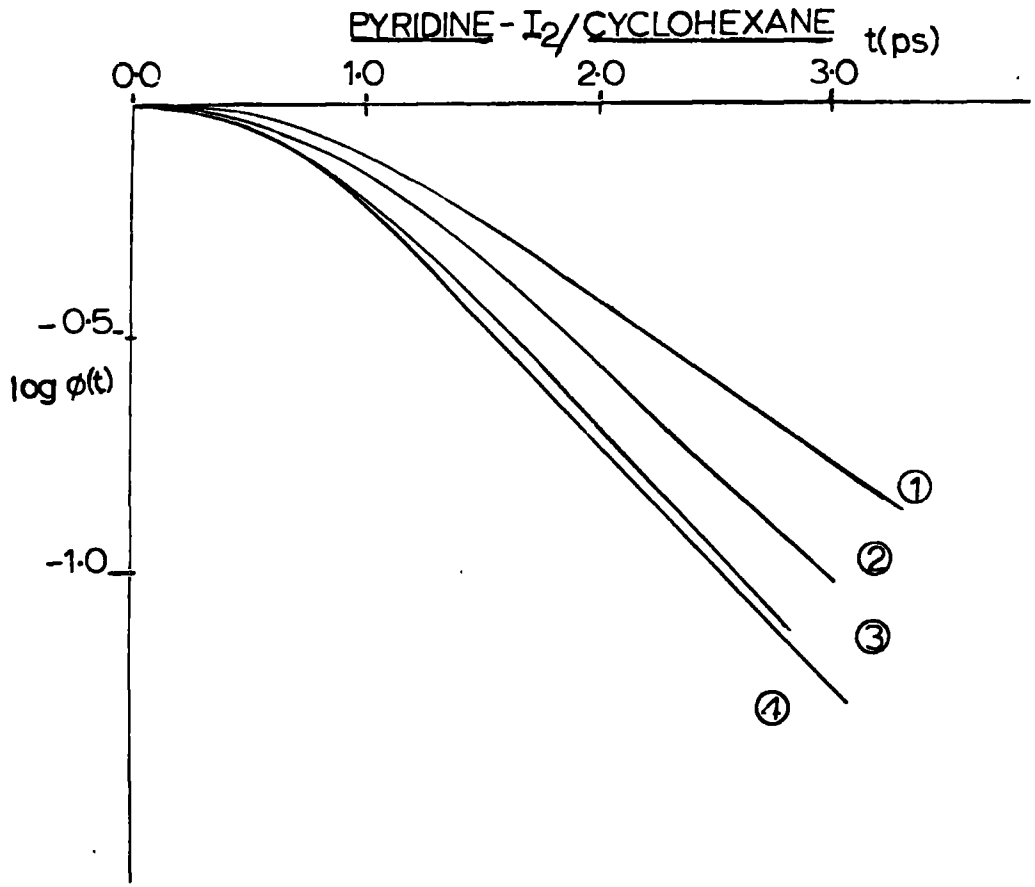

Fig. 4.4. AUTOCORRELATION CURVES FOR PYRIDINE - I_2/ CYCLOHEXANE AT VARYING PYRIDINE CONC. ν(I-I) BAND IODINE CONCENTRATION 0·02M, PYRIDINE(1)0·17M(2)0·62M (3) 1·21M (4)0·24M (SOLUTION 4 IN BENZENE).

Table 4.9.

Pyridine-Iodine Band Shapes

Mode	Solvent	Band Position/ $cm.^{-1}$	α/ $ps.^{-1}$	$\tau_{1/e}$/ ps.	
$\nu_{(I-I)}$	Cyclohexane	183		0·39	increasing pyridine concentration ↓
		182		0·43	
		172		0·65	
		171		0·66	
$\nu_{(N-I)}$	Cyclohexane	90	1·08	0·59	increasing pyridine concentration ↓
		103	1·3	0·76	

the excited state quantum number. Thus by comparison of $\tau_{1/e}$ for the fundamental band and first overtone the dependence on v' may be determined. Since the frequency is doubled, a naive picture suggests the time scale, and hence $\tau_{1/e}$, also to be doubled, on comparing the first overtone with the fundamental. However, whilst some dependence on v' was observed $\tau_{1/e}$ was not doubled for IBr in benzene.

Another valuable reason for looking at overtone bands is that it would give more information on that very difficult problem, of a full assignment of the pyridine bands, since the assignment of the overtones has not been firmly established, and overtones in simpler molecules are used to assign the fundamentals. The above discussion also explains why the overtones are sometimes broader than the fundamentals.

No work appears to have been done on the band shape of sum and difference bands. It would seem to be very worthwhile to gain more information on these bands, in order that a theoretical model could be built up.

It would be very interesting to see if the band shape, and intensity, of the low frequency bands of the pyridine-I_2 spectrum depend on the iodine concentration. The analogous dioxan-I_2 'complex' intensities do depend on the iodine concentration (see Chapter 5). Also does the low frequency band in the pyridine-I_2 complex reach some limiting width before reaction takes place? This occurs in pure pyridine, i.e.

$$2Pyr + 2I_2 \rightleftharpoons PyrI_2 + PyrI_2 \rightleftharpoons Pyr_2I^+ + I_3^-$$

It is still not clear if the frequency increase of the low frequency band, in the pyridine-I_2 complex, is due to chemical or solvent polarity effects. It may be possible to test for this by comparing two solutions of equal conductance. One consisting of pyridine/I_2 in cyclohexane, the other pyridine/I_2/cyclohexane, plus a polar solvent added, to bring the conductances equal to original solution.

For the pyridine-ICN complex, the problem is to ensure that all the ICN molecules are complexed. This should eliminate doublets in the acceptor spectrum.

Since intensities found by Thomas and Orville Thomas [142] in CCl_4 are always greater than those in C_2Cl_4, perhaps C_2Cl_4 solvates the ICN molecules less than CCl_4. Presumably the difference is due to the C-Cl bonds having different polarities in the two molecules, owing to the different valence states of the carbons causing different interactions with the ICN. Hopefully, if measurements were carried out in C_2Cl_4 as solvent, the vibrational bands of ICN would be singlets.

If the experimental problems could be overcome it should be very interesting to compare the vibrational spectra of the series of acceptors, ClCN, BrCN, and ICN. In explaining the observed nuclear quadrupole coupling constants of the halogen atoms in XCN molecules, reasonable agreement was obtained by making the assumption that some degree of s-p hybridization was present both for the halogen and nitrogen atoms. The following canonical forms were the major contributors to the mesomeric state:

X-C≡N	X=C=N	$\bar{X}\overset{+}{C}\equiv N$	$\overset{+}{X}\bar{C}\equiv N$
I	II	III	IV

The relative importance[143] of these forms was then determined.

	I	II	III	IV
ClCN	85	8	7	0
BrCN	97	3	0	0
ICN	95	1	0	4

It would be very interesting to compare the intensities and other spectral properties in view of the different hybridization of the central carbon atom. The importance of form IV in ICN, gives support to the strong contribution of

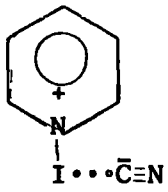

in the complex structure. However, this may not be the case for the pyridine-BrCN and pyridine-ClCN complexes.

In conclusion it can be seen that intensity studies, linked to band shape analysis, can give valuable information on the mechanisms of interaction in solution. The half band width is too crude an estimate of band shape.

The technique gives information on charge transfer, dipole-dipole interactions and solvent effects. Some estimate can be made of which resonance form predominates.

Finally systematic use of the above methods may be the only way to obtain a complete assignment of the vibrational spectrum of a large molecule.

CHAPTER 5

Studies on the Vibrations of the Acceptor and External Modes with Weak Donors

A. Introduction.

The scope of this work falls into two parts. In the first part a large range of donors were complexed with halogen and interhalogen acceptors. The far-infrared spectra were compared, to see if there were any drastic variation of acceptor spectrum on varying the donor.

Where solvent absorption did not prevent it, a search was made to see if the low energy absorption corresponded to a vibrational band or a collisional band. In most cases the lack of similarity in band shape of the '$\nu_{(D-X)}$' and $\nu_{(X-Y)}$ bands indicated that the '$\nu_{(D-X)}$' band was much broader than the $\nu_{(X-Y)}$ band, and did not obey the Beer-Lambert Law. (The effect of a temperature variation was also anomalous.) It can be seen from spectrum 5.1. that even as weak a 'donor' as cyclohexane gives rise to a 'collisional' band at about 110 $cm.^{-1}$ with cyclohexane.

Measurements on the intensity of $\nu_{(D-X)}$ band on varying the donor concentration suffer from the problem that most donors are polar in nature. A non-polar molecule (e.g. n-heptane) does not form a strong enough complex with a non-polar acceptor (e.g. iodine) to give bands of appreciable intensity. However, in the case of dioxan, the collisional band was strong enough to be observed, both for the 'free' donor, and for the iodine complex.

This leads to the second part of this work. An intensive investigation of the low energy band for the dioxan-I_2 complex to try and find out what laws controlled its 'vibrational' spectroscopic properties. This system also has the advantage that, since dioxan is non-polar, the 'polar solvent effects' (which may be operative for, say, tetrahydrofuran) are unlikely to be important.

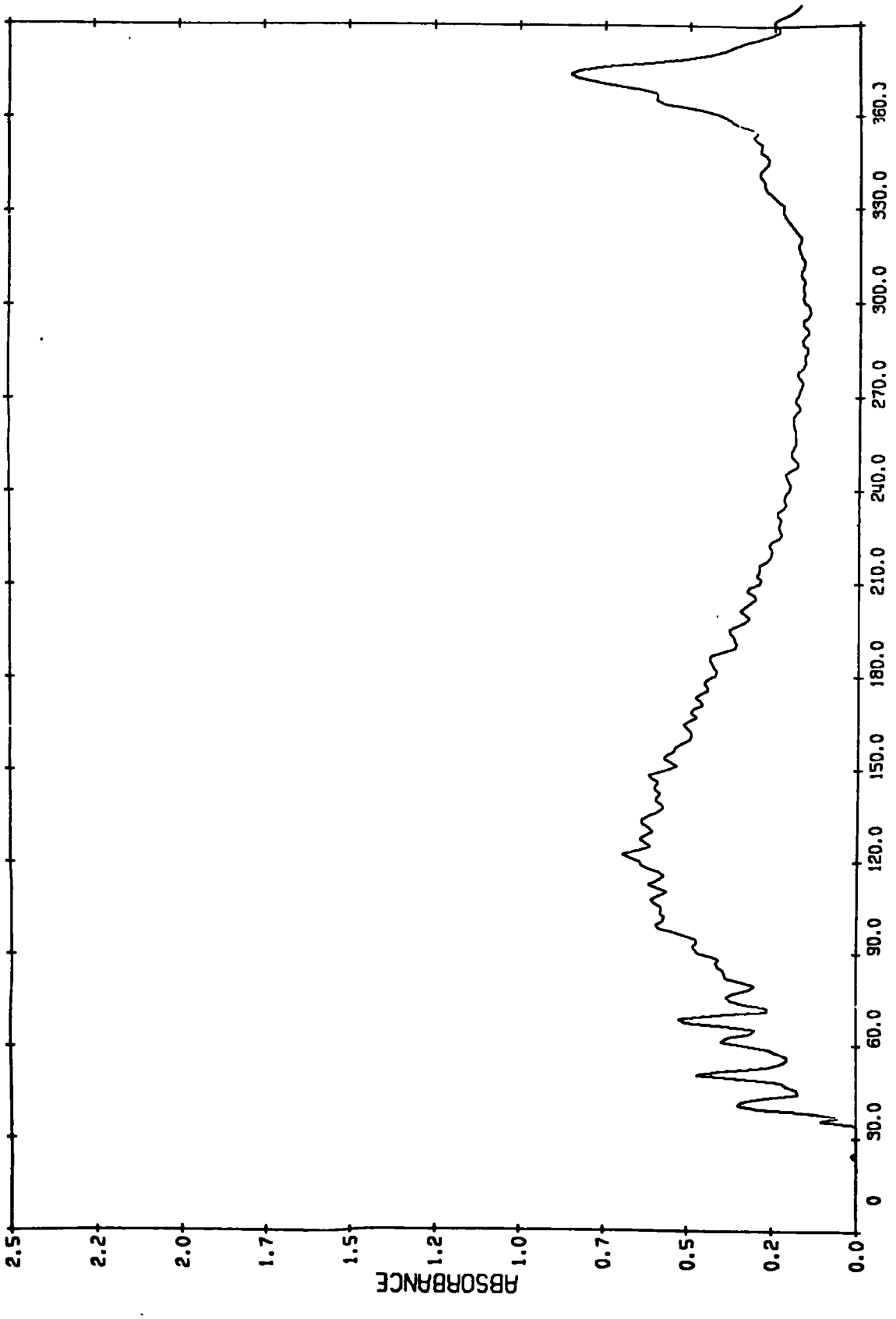

Spectrum 5.1. illustrating the low frequency 'collisional' absorption observed for a cyclohexane-IC1 mixture at $\approx$ 110 $cm.^{-1}$

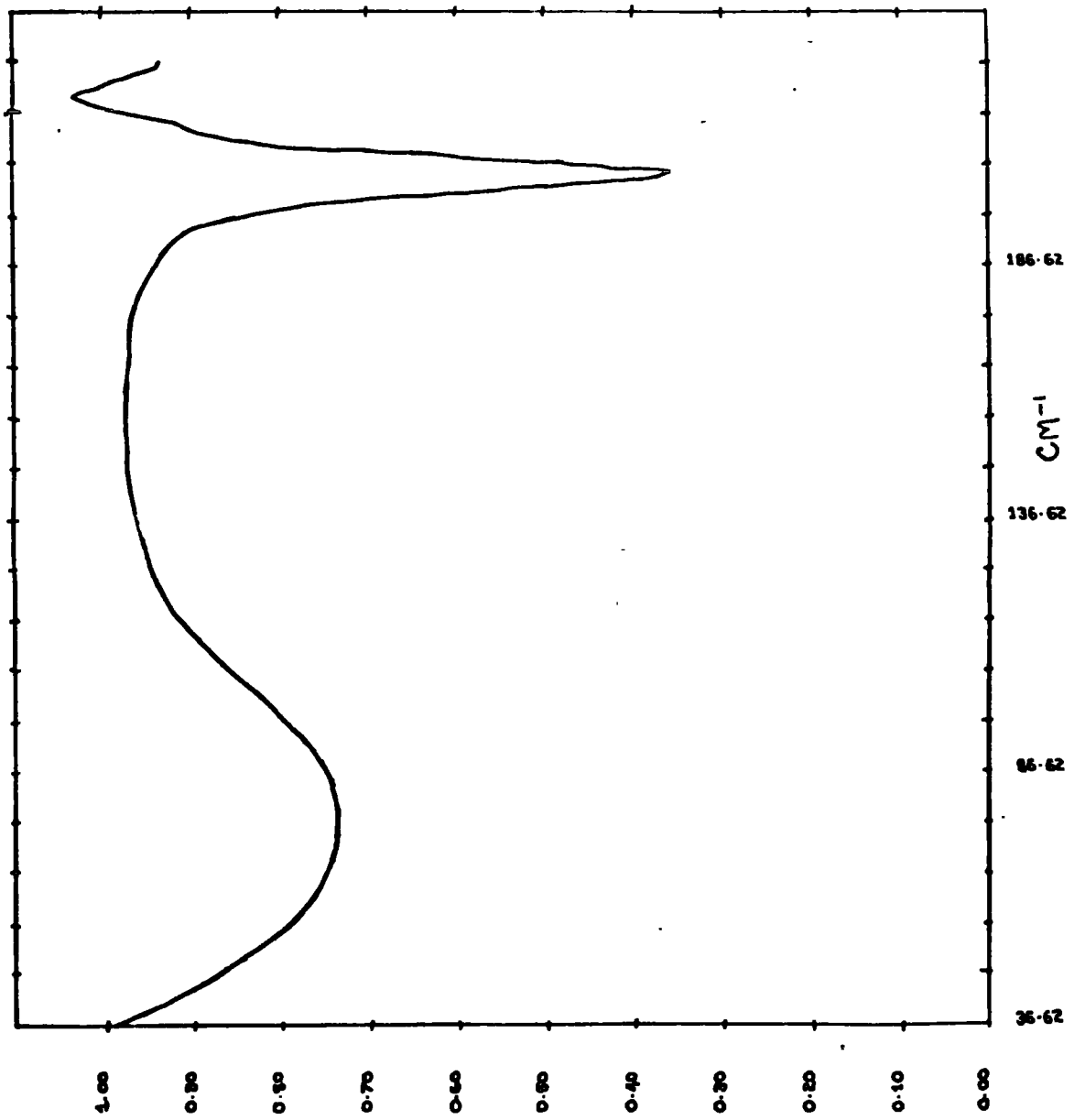

Spectrum 5.2. Far-infrared spectrum of a dioxan/I_2/cyclohexane mixture showing the $\nu_{(I-I)}$ band at 205 $cm.^{-1}$ and the $\nu_{(D-I)}$ band at 80 $cm.^{-1}$

Spectrum 5.2. shows the two low frequency bands for a dioxan/I_2/ cyclohexane mixture.

B. The Acceptor Spectra.

1. Iodine Chloride Complexes with Weak Donors.

Since ICl is highly reactive most of this work was concentrated on the less reactive acceptors, i.e. I_2, IBr and ICN. However, the intensity of 'free' ICl in cyclohexane was measured, as this is important in the discussion of the normal co-ordinate calculation (Section 6B). It was also important to try and establish that the ICl band in the benzene complex was a vibrational, and not a collisional, absorption.

If a collisional mechanism is predominant one would not expect to see 'free' and 'complexed' halogen in a mixture, since any 'complex' present must have a very short life-time (i.e. only 'sticky' collisions). If one approximates the rate of forward reaction to the collision frequency, the equilibrium constant is a rough measure of the complex life-time. This assumes of course, that the complex life-time (τ_c) is greater than the collision frequency converted to seconds (τ_{col}). Varying the concentration of donor or acceptor should just act as a solvent effect, in a collisional complex. However, high resolution Raman studies[85] showed no trace of 'free' iodine expected from an equilibrium mixture of free and complexed components. On the other hand, a free iodine band is observed for somewhat stronger interactions[85] (e.g. between mesitylene and I_2).

As explained in Chapter 2, the complex life-times from dipole moment studies are of the order of one p.s. Hence, the 'stability' of the complex depends upon the time scale one is considering. In the ultraviolet region (at, for example, 40,000 $cm.^{-1}$) the observation time for one transition is 8×10^{-4} p.s. Hence, the complex may appear to be very stable when examined

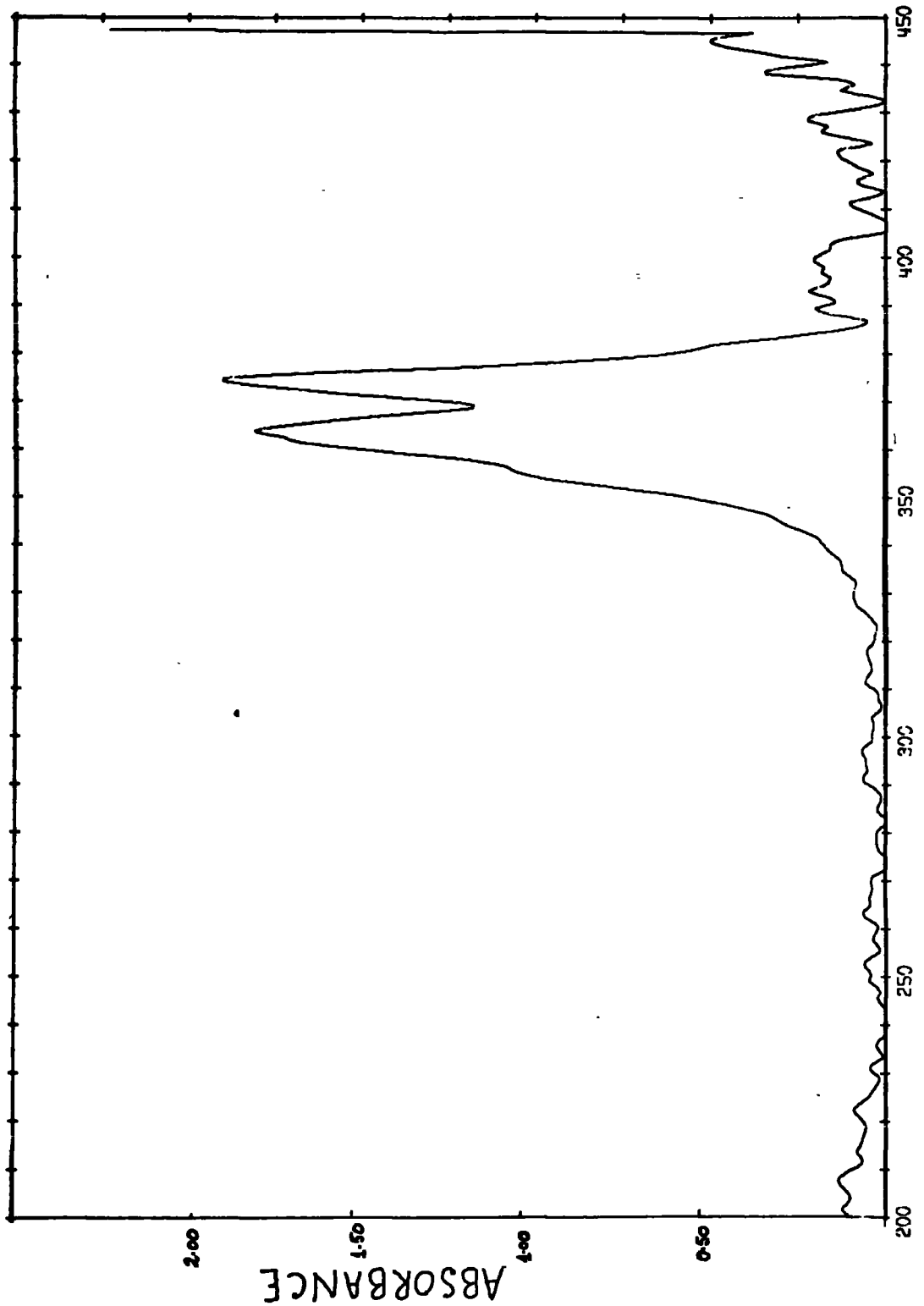

Spectrum 5.3. Far-infrared spectrum of a mixture of benzene and ICl in cyclohexane showing both free (375 $cm.^{-1}$) and complexed 355 $cm.^{-1}$ $\nu_{(I-Cl)}$ bands. The concentrations are, benzene, O·23M; ICl, O·09M. The path length is O·65 cm.

Table 5.1.
Studies on IC1 with Different Donors

Donor	Solvent	$\bar{\nu}_{(I-Cl)}$/ $cm.^{-1}$	$\Delta\bar{\nu}_{\frac{1}{2}}$/ $cm.^{-1}$	[Donor] moles/ litre	[Acceptor] moles/litre	Intensity/ Darks	τ_1/e/ ps.	Comments	I.P Donor/ eV
Benzene	Benzene	352	19	13·3M	$9·876 \times 10^{-2}$	1850			9·24
Benzene	Cyclo-hexane			0·2843M	$9·249 \times 10^{-2}$	1773			
Benzene	Cyclo-hexane			0·621	$12·48 \times 10^{-2}$	1942			
Benzene	Cyclo-hexane			0·4843	$14·74 \times 10^{-2}$	1950			
				AVERAGE	=	1878 ± 200			
Cyclo-hexane	Cyclo-hexane	370	18	10·4	$7·14 \times 10^{-2}$	875			9·88
n-Heptane	Heptane	372	17	6·83	$4·27 \times 10^{-2}$	720			10·08
Acetonitrile	Dichloro-ethane	348	16	2·89	$5·316 \times 10^{-2}$	2836	1·21		12·22
Dioxan	Heptane	354	14	1·04M	$2·486 \times 10^{-2}$	3091	1·3		9·13
Diethyl Sulphide	Cyclo-hexane	297	14					$IC1_2^-$ decomposition prevented intensity measurements	
Dimethyl-sulphoxide	Cyclo-hexane	313						"	

in the ultraviolet region. In the far-infrared, however, (at say 40 $cm.^{-1}$) the time for one transition is 0·8 p.s. i.e. greater or as great as the complex life-time. Thus, the complex could not 'vibrate' with a frequency equivalent to 40 $cm.^{-1}$ if its life-time is of the same order of magnitude.

The far-infrared spectrum of a mixture of benzene/ICl/cyclohexane showed both 'free' (375 $cm.^{-1}$) and 'complexed' (355 $cm.^{-1}$) $\nu_{(I-Cl)}$ bands. This means that the complex life-time is greater than the resolution (20 $cm.^{-1}$) required to separate them, i.e. greater than 0·16 p.s. The fact that one could resolve a band at 355 $cm.^{-1}$ supported the assignment of this band to a $\nu_{(I-Cl)}$ vibration (see Spectrum 5.3.).

The Table 5.1. summarises the data obtained on the ICl complexes studied. The values obtained are in reasonable agreement with Person et al.[144] In view of the dependence of the complex bands on both the donor and acceptor concentrations (see Chapters 3 and 4), it is probable that intensities are only exactly reproducible if the same concentration of donor and acceptor are used.

At first glance, one would expect acetonitrile with its larger dipole moment to form a stronger complex than pyridine (on purely electrostatic' grounds), giving a $\nu_{(I-Cl)}$ frequency < 291 $cm.^{-1}$ (the pyridine value). In fact the reverse is the case (see Table 5.1.). This can be understood by considering the structure of the cyanide ion. The CN^- is isoelectronic with nitrogen. The triple bond in the CN^- ion is weaker than the N-N triple bond, because both the σ and π bands are unsymmetrical, and are polarized towards the more electronegative nitrogen. The 2 σ_c orbital is a 2s2p hybrid localized on the carbon atom. This is of the highest energy and its electrons can thus be donated in σ-bond formation.

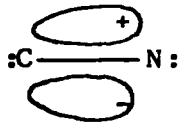

FREE ION

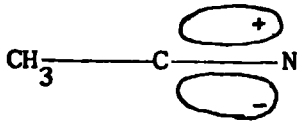

Polarisation to the nitrogen

A

B

Bonding of another group through the carbon (as in acetonitrile) favours structure A causing the nitrogen lone pair to be partially withdrawn, hence the nitrogen is a poor electron donor, and acetonitrile-ICl a weak complex.

The intensities follow the ionization potential of the donor, as the charge transfer model predicts. Acetonitrile is the exception, but here dipole moment forces will also contribute to the intensity.

2. Iodine Bromide Complexes with Weak Donors.

The intensity and band shape data is summarised in Table 5.2. It can be seen that the intensities follow the ionisation potential of the donor. The lower the ionisation potential the greater the electronic interaction, and hence the larger the intensity. The one exception is diethyl ether with a slightly higher ionisation potential, and higher intensity than benzene. However, this molecule possesses a dipole moment, unlike benzene, and so dipole-dipole interactions will also contribute to the intensity, accounting for the slightly higher intensity in ether.

IBr is such a large heavy molecule that the value of τ_R (or $\tau_{R_{1/e}}$) is expected to be large, and the spectrum should be predominantly controlled by vibrational and translational effects,[65] both of which will be affected by intermolecular interactions with the solvent.

As explained in Chapter 2 vibrational relaxation is induced by variation of the intermolecular potential V on a dynamically surrounded solute molecule. The extent of relaxation, is proportional to $\frac{\partial V}{\partial Q}$ where Q is the particular normal co-ordinate considered, and thus this contribution to the band profile is expected to be different for each mode considered. (Since Q changes from one mode to another.) A shift to higher or lower frequency for the $\nu_{(I-Br)}$ band profile is caused by a change of force constant, and hence normal co-ordinate Q. Since ∂V is unknown, however, it is difficult to estimate what change is expected.

Table 5.2.

Studies on IBr with Different Donors

Donor	Solvent	$\bar{\nu}_{(I-Br)}$/ $cm.^{-1}$	$\Delta\bar{\nu}_{\frac{1}{2}}$/ $cm.^{-1}$	[Donor] mole/litre	[Acceptor]$_{-1}$ mole/litre^{-1}	Intensity/ Darks	$\alpha_{(t)}$/ $picosec^{-1}$	$\tau_{1/e}$/ picosec	I.P. Donor/ eV
Diethyl-sulphide		207	8·0	0·1816	$1·591 \times 10^{-2}$	2943	-0·45	1·78	8·45
		207					-0·38		
Ether		248	7·0	0·5037	$8·46 \times 10^{-3}$	750	-0·28	2·14	9·53
Dioxan	Cyclo-hexane	250	10·0	3·1	$4·23 \times 10^{-2}$	1500	-0·35	1·32	9·13
Dioxan	Cyclo-hexane	250	10·0	1·18	$4·461 \times 10^{-2}$	1400	-0·42	1·28	
Benzene	Benzene	249	8[a]		$13·266 \times 10^{-2}$	650			9·24
Cyclo-hexane	Cyclo-hexane	262	12	9·27	$10·166 \times 10^{-2}$	240			9·88
Heptane	Heptane	262	12	6·83	$8·266 \times 10^{-2}$	125			10·08

[a] $\Delta\bar{\nu}_{\frac{1}{2}}$ taken from reference 65.

Table 5.2. shows that the band width decreases (and $\tau_{1/e}$ increases) on going from cyclohexane to solvents with better donor properties. It would appear that vibrational relaxation is considerably slowed down in diethyl ether and diethyl sulphide. This must be due to the environment becoming more isotropic, due to the specific 1:1 interactions. This is not too surprising, since diethyl sulphide seems to form strongest complex as judged by the intensity and frequency perturbations.

However, it is not clear how much broadening occurs due to weak interactions in solution with a statistical distribution of complexes of differing stoichiometry. These would, in general have n:m stoichiometry according to

$$nA + mB \rightleftharpoons AnBm$$

and would be relatively short-lived. Such a situation would give rise to overlapping of a number of individual bands, which differ only slightly in frequency leading to band broadening.

A recent paper on band shape studies[65] of the ICl and IBr complexes in benzene has shown that translational effects are also very important. In the first picosecond of interaction with a benzene molecule, the IBr molecular velocity is reduced by about 50%. The experimental data shows a 40% decrease in correlation time on going from cyclohexane to benzene. A similar sort of interaction is expected for ICl. However, orientational diffusion probably also contributes to the band profile.

3. Iodine Cyanide Complexes with Weak Donors.

The results for the three different fundamental vibrations of iodine cyanide are presented in Table 5.3. The values are in reasonable agreement with Person et al.[149] The weak band observed in the dioxan-ICN spectrum by Person at 442 $cm.^{-1}$ was also observed in this work at the same frequency. The band was again observed in the spectra of dioxan with I_2 and IBr.

Table 5.3.

Studies on ICN with Different Donors

Mode	Solvent	Donor	Band position/ $cm.^{-1}$	$\Delta\bar{\nu}_{\frac{1}{2}}$ / $cm.^{-1}$	[Donor] $mole/litre^{-1}$	[ICN] $mole/litre^{-1}$	Intensity/ Darks	$\tau_{1/e}$ ps.	$\alpha/ps.^{-1}$	$-2{\cdot}303\ \alpha^{-1}/ps.$
$\nu_{(C-N)}$	Chloroform	Chloroform	2163	12	12·5	0·2247	790	1·49	-0·62	1·427
					12·5	0·237	807			
					12·5	0·1031	780	1·34		
					12·5	0·1637	860			
	Dioxan	Dioxan	2165	10	11·73	0·3955	342	1·70	-0·42	0·967
	Benzene	Benzene	2165	9	13·3	0·0812	360			
	Chloroform	Pyridine	2165	13	0·682	0·1987	170	1·1	-0·61	1·4
	Carbon Tetra-chloride	Pyridine	2165	14	0·971	0·0936	190	0·98	-0·69	1·6
$\nu_{(I-C)}$	Chloroform	Chloroform	485	14	12·5	0·2371	700			
	Chloroform	Diethyl-Sulphide	437	19	0·324	0·2747	1300	0·95	-1·1	2·53
	Benzene	Benzene	475	14	13·3	0·1904	960		-0·36	0·82
	Chloroform	Pyridine	428	24	0·725	0·1032	3730	0·68	-1·4	3·22
ν_{bend}	Cyclohexane	Diethyl-Sulphide	320	8	0·601	0·579	280	1·98	-0·35	0·806
	Chloroform	Chloroform	321	12	12·5	0·574	270	1·2	-0·58	1·335
	Chloroform	Chloroform	320	11	12·5	0·2371	240			
	Chloroform	Pyridine	338	10	0·725	0·1032	200	1·08	-0·47	1·08
	Benzene	Benzene	320	8	13·3	0·1436	397	1·75	-0·30	0·6909
	Benzene	Benzene	320	8	13·3	0·2001	332		-0·34	0·783
	Polythene Disc		338							
lattice Mode	Polythene Disc		140							

Vibrational spectral studies[150] on dioxan shows that dioxan has a centre of symmetry in the vapour phase and in the liquid, since there is mutual exclusion between infrared and Raman bands. Thus, the spectra are interpreted in terms of C_{2h} symmetry. The band arising at 440 $cm.^{-1}$ in the complex is probably the infrared inactive a_g mode, observed by Ellestad et al.[150] at 435 $cm.^{-1}$ in the Raman spectrum.

The $\nu_{(I-C)}$ band shows the characteristic fall in frequency, and increase in intensity as the strength of the complex increases.

The ν_b band does not show any systematic change on complex formation. Most surprisingly this band has an intensity, and frequency, which is remarkably independent of donor. Furthermore, one would expect the degeneracy of the band to split in the complex. One would expect at least a broadening on complexation with pyridine. In fact, the band if anything narrows in chloroform solution. The fall in intensity of $\nu_{(C-N)}$ band and dramatic rise of the $\nu_{(I-C)}$ band must indicate a large change of the bond moments on complexation.

The only explanation at present available for the lack of perturbation of the bending mode appears to be as follows. The large amount of charge situated on the three atoms causes the bending mode to be heavily damped by intermolecular forces. One would expect the stretching modes to be less affected by intermolecular forces. The high solubility in chloroform, benzene and dioxan indicates that strong forces are present. In other words the increased intensity expected from the larger moments in the complex, are cancelled out by a reduction in bending motion due to stronger forces, i.e. a larger C but smaller ds term in equation 3.2.. Vibrational mixing with the donor is not as great as in the pyridine-ICl case, since the 405 $cm.^{-1}$ band in pyridine is only shifted to 415 $cm.^{-1}$ in the ICN complex. It is increased to 420 $cm.^{-1}$ for the pyridine-ICl complex in chloroform. This is in spite of the extra ICN bending mode which gives rise to band relatively nearby at 330 $cm.^{-1}$ Therefore, contributions from vibrational mixing can be ignored to a first approximation.

It is worth commenting at this stage how valuable a whole complex molecular orbital calculation would be. Here the electron densities on the ring, and the halogen atoms can be assigned in an unambiguous way. However, the actual computation is at present too complex. In the absence of this, n.q.r. measurements would be of value.

For the pyridine-IC1 complex Hanna[31] (from n.q.r. measurements) strictly defines the no bond state as I, where the electric field of the pyridine

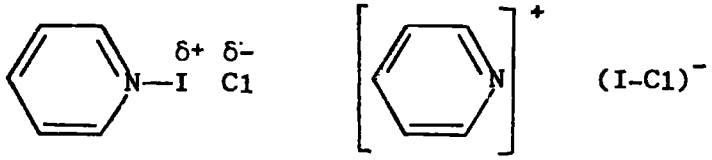

I II

lone pair has induced an additional dipole in IC1. The charge transfer complex is strictly defined as II. An n.q.r. study of pyridine-ICN complex would be most valuable to give some idea of the charge distribution in the acceptor.

It can be seen that the $\nu_{(C-N)}$ band intensity is quite sensitive to the solvent used. Both π-donor and n-donor solvents produce a decrease in intensity, whilst the hydrogen bonding solvent chloroform produces an increase in intensity. The situation is reversed for the ν_b and $\nu_{(I-C)}$ bands.

This appears to indicate that b_π or n → ICN interaction occurs at the iodine end of the ICN molecule while hydrogen bonding occurs at the N-atom (however, see Chapter 4 for further discussion of this interaction). Donor action by the CN group leads, of course, to an increase in intensity of the $\nu_{(C-N)}$ band.

Work in this laboratory shows that the band shape of the $\nu_{(C-N)}$ band in benzene is only weakly temperature dependent.[54] This indicates that the band shape is controlled by vibrational rather than orientational effects.

As explained in Chapter 4 the diffusion coefficients about the three axes of ICN are as follows:

$$D_y = D_z = \alpha_R \ (\nu_{(I-C)} \text{ or } \nu_{(C-N)})/2$$

$$\therefore \quad D_x = \alpha_R(\nu_b) - D_z \text{ (for rotation about the symmetry axis x)}$$

(assuming $\emptyset(t) = \exp[-(\alpha_R + \beta_v)t]$) at long t; $\alpha_R \gg \beta_v$ (where the symmetry axis is designated by x).

The diffusion coefficients measured in this work are shown in Table 5.4. The apparent diffusion coefficients indicate that, unlike acetonitrile, for weak donors, motion of ICN about the x axis is about the same 'tumbling' motion about the y and z axes. This is not what is expected for ICN from considerations of moment of inertia alone (which would obviously favour motion about the x axis).

The diffusion coefficients are larger in chloroform than in benzene. This implies that the ICN molecule is rotating faster in chloroform than in benzene. However, the re-orientational effects are probably small since the value for D_y is higher for pyridine than benzene (calculated from $\nu_{(C-N)}$ bands). The negative values obtained for the strong complexes (calculated from $\nu_{(I-C)}$ bands) are physical impossibilities. This shows that vibrational/translation effects are important with possibly some vibrational/(residual) rotational interaction.

In conclusion it can be seen that ICN with its large dipole moment (3·72D), and high moment of inertia has vibrational band properties which are very susceptible to intermolecular forces. One of the reasons why the complexed pyridine bands had lower intensities (see Chapter 3) for the pyridine-ICN complex in carbon tetrachloride than in chloroform may be due to the chloroform interacting with the ICN, and reducing its effective further complexing ability. Thus, it may only be possible to consider complexing

Table 5.4.

Summary of Apparent Diffusion Coefficients for ICN

Solvent	Interacting Molecule	$D_y = D_z/ps^{-1}$ from $\nu_{(I-C)}$	$D_y = D_z/ps^{-1}$ from $\nu_{(C-N)}$	D_x/ps^{-1} from $\nu_{(I-C)}$	$D_x\ ps^{-1}$ using $\nu_{(C-N)}$	Period of 'free' rotation/ ps. from Log Ø(t)of $\nu_{(C-N)}$ bands
Benzene	Benzene		0·46		0·32 ± 0·08	
Chloro-form	Chloroform	0·75	0·71	0·58	0·62	1·2
Dioxan	Dioxan		0·48			1·2
Chloro-form	Pyridine	1·61	0·70		-0·53	
Cyclo-hexane	Diethylsulphide	1·27		-0·47		
Carbon Tetra-chloride	Pyridine		0·8			
Comparison with other rotational diffusion coefficients taken from J. Yarwood, Spectroscopy Letters, 1972, 5(6+7), 193.						
			From α_{11}		From $\alpha_{\perp}$	
	Acetonitrile		0·37		1·29	1·0
	Methyl Iodide		0·34		1·97	0·2

Table 5.5.

Studies on Iodine Complexes with Weak Donors

Mode	Solvent	Donor	Donor Conc. moles/litre^{-1}	Acceptor conc. moles/litre^{-1}	Band posn./ cm.$^{-1}$	$\Delta\bar{\nu}_{\frac{1}{2}}$/ cm.$^{-1}$	Intensity/ Darks	α/ ps.$^{-1}$	τ_1/e ps.	Ionisation potential/ eV	K_c/litre mole^{-1}
$\nu_{(D-I)}$	Cyclohexane	Diethylsulphide	0·3276	0·03531	147	30	3704	-1·94	0·58	8·45	180
	"	Pyridine	See Chapter 4		90	34	1800		0·6	9·27	146
$\nu_{(I-I)}$	Cyclohexane	Diethylsulphide	0·3276	0·03531	171	10	2600	-0·35	1·71	8·45	180
	"	"	1·08	0·03318			2200	-0·335	1·51		
	"	"	0·1245	0·01149	172	9	2030				
	"	Dithiane	0·0561	0·042	166	13·5	2557	-0·76	1·26		77
	Carbon Disulphide	Carbon Disulphide	15·93	0·703	202	11·5	40	-0·51	1·23	10·07	
	Benzene	Benzene	13·3	0·219	204	12	287			9·24	0·15
	Cyclohexane	Dioxan	2·3	0·05	205	6	700	-0·275		9·13	0·89
	Cyclohexane	Ethyl acetate	1·37	0·293	205	9·5		-0·38	1·36	10·10	0·49
	Cyclohexane	T.H.F.	2·65		202	8	550	-0·32	1·62	9·54	
	Cyclohexane	Ether	2·23	0·0712	204	8	203				
	Benzene	Thiourea	Saturated	Saturated	194						8500
	Cyclohexane	D.M.S.O.	2·145	0·0947	194	12	1092	-0·65	1·07	8·71	11·2
	Cyclohexane	Pyridine	See Chapter 4		183	7	2000	-0·31	1·37	9·27	146

properties in a particular solvent. It is clear, at least for ICN, that intermolecular forces and vibrational relaxation are predominant in controlling the band shape. The relatively long period of 'free rotation' (before the $\log \emptyset(t)$ vs t plot becomes linear) of 1·2 ps. supports the conclusions of Rothschild;[146d] that the formation of 'clusters' in the liquid phase is unlikely to have a significant effect on the initial part of the autocorrelation curve.

4. Studies on Iodine Complexes with Weak Donors.

The original aim of this work was to extend the study of Yarwood and Person[150] on iodine complexes, in order to obtain more information on the spectral properties of the $\nu_{(D-I)}$ stretching modes.

However, it was found that both low frequency bands in the diethyl sulphide-I_2 and dioxan-I_2 complexes do not obey the Beer-Lambert Law. It is worth commenting that Yarwood and Person obtained their most consistent results for the benzene-I_2 complex. This was probably because, as benzene was used as solvent, the donor concentration was kept constant at 13·3M.

In a similar fashion to the pyridine-I_2 complex in Chapter 4, the $\nu_{(I-I)}$ band intensity changed by over a 100% depending on the donor concentration. This was especially true of donors with a dipole moment. In the absence of a full concentration study it is only valid to discuss one band as being more intense than another, if the ratio of the two intensities is greater than 2:1. Fortunately for the intensities found in Table 5.5. this is usually true.

For the non-polar donors; benzene, dioxan and carbon disulphide, the intensities follow the expected dependence on ionisation potential. The bands tend to narrow as the ionisation potential increases, which is what is expected for a strong complexation. However, the frequency perturbation is in the reverse direction.

There seems little correlation between any well-known physical parameter and the frequency shift. Drago[151] has attempted to predict the enthalpies of

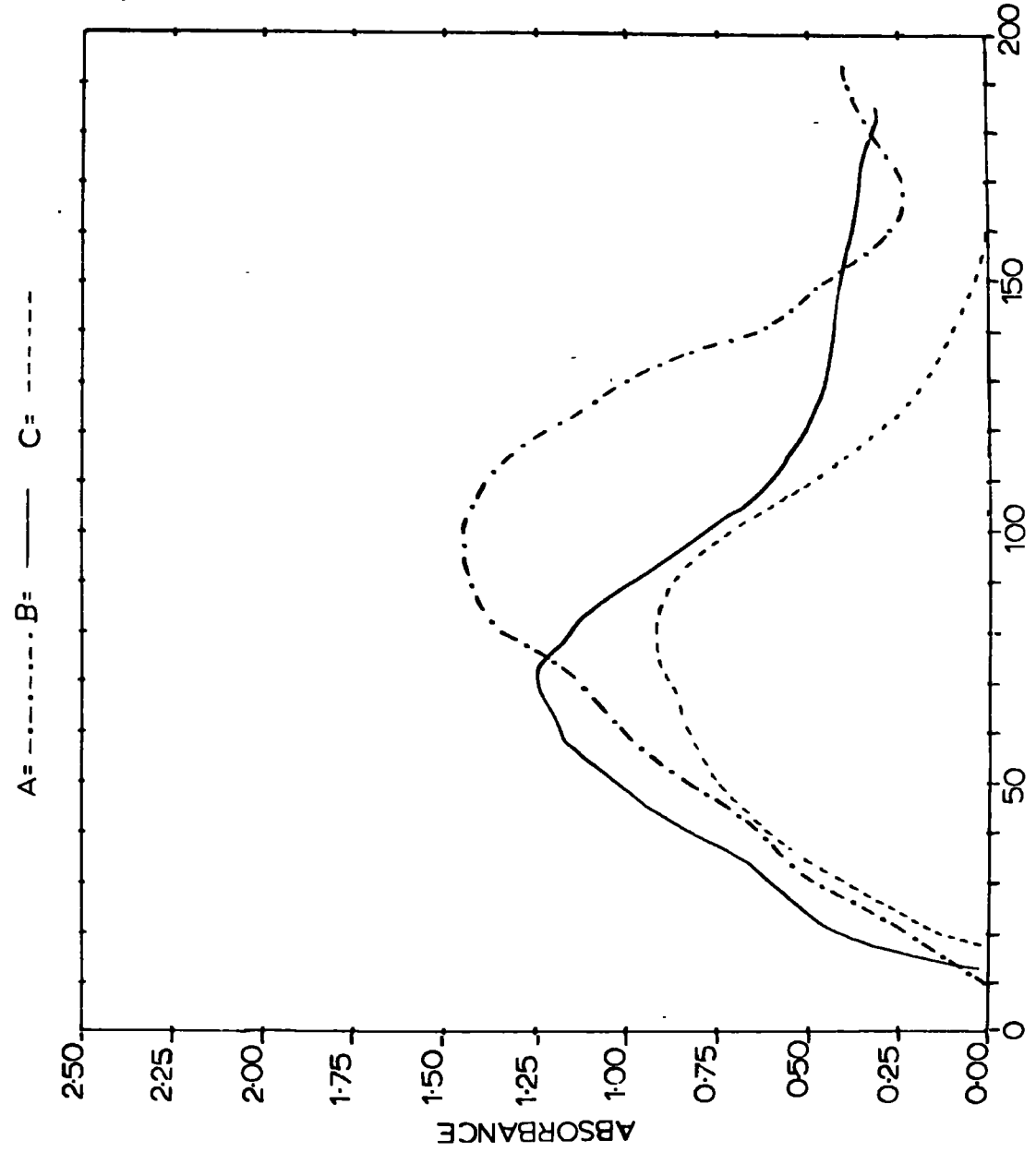

Spectrum 5.4. Very low frequency infrared spectra of iodine in (A) benzene at 0·05M, (B) carbon disulphide at 0·5M, (C) p-dioxan at 0·2M. (The path length is 0·35 cm. and temperature 20°C.)

adduct formation in the gas-phase and in poorly solvating media by,

$$-\Delta H = E_A E_B + C_A C_B \quad \ldots\ldots \quad [5.1.]$$

The subscripts A and B indicate acceptor and donor, respectively, while E and C are two empirically derived parameters assigned to each donor and acceptor.

Drago then considers the possibility that C is related to 'softness' and E to 'hardness' originally developed on the 'hard' acid 'soft' base model.[152] The Drago E and C model predicts that the larger the E and C values of the donor, the more strongly the interaction with the acid. For the weak (soft acid) I_2, since 'soft' prefers 'soft' and 'hard' prefers 'hard', the C term should be the more important.

Table 5.7.

Complex	Band Position/cm.$^{-1}$	C_B	E_B
Diethyl Sulphide-I_2	171	7·4	0·339
Pyridine-I_2	183	6·4	1·17
Dimethyl Sulfoxide-I_2	194	2·85	1·34
Tetrahydrofuran-I_2	202	4·27	0·978
Benzene-I_2	204	0·681	0·525
Diethyl Ether-I_2	204	3·25	0·963
Dioxan-I_2	205	1·74	0·975

Table 5.7. shows the correlation with the Drago parameters. The correlation seems reasonable except for benzene and D.M.S.O. However the table predicts the benzene frequency to be > 206 cm.$^{-1}$ Since the equation 5.1. is for a dilute solution, and a 13·3M solution was used, this does not seem unreasonable. The table predicts a D.M.S.O. frequency of 205 cm.$^{-1}$, which again seems reasonable for a more dilute solution.

This method does at least show one thing. The frequency shift must be interpreted by two or more parameters. However, much more data in dilute solutions is required to determine if the correlation is fortuitous.

The intensities follow the ionisation potentials expected for benzene and D.M.S.O., which are lower than would be expected from this approach. The low value in benzene is almost certainly due to the fact that benzene is non-polar, and has a much smaller electrostatic contribution to the intensity.

The donor-acceptor bonding molecular orbital is described[151] as a linear function of covalent (charge-transfer) and electrovalent wave functions.

$$\psi = a\psi_{cov} + b\psi_{el} \qquad \ldots\ldots \quad [5.2.]$$

Therefore, a molecule with an appreciable dipole moment, and no low energy acceptor orbitals, will interact best with donors which have the largest lone pair dipole moment (i.e., $b \gg a$, in equation 5.2.).

Iodine interacts best with those donors that have low ionisation potentials, i.e. $a \gg b$. This is because iodine has zero dipole moment, and has an essentially covalent interaction. For this reason the best correlation was obtained between intensity and ionization potential for those molecules which have zero dipole moment (i.e. causing smaller induced dipoles in the iodine).

Finally, let us consider the band observed at 147 $cm.^{-1}$ for the diethyl sulphide-I_2 complex. Yarwood and Person[150] were reluctant to assign this band to the $\nu_{(D-I)}$, because of the possibility of reaction to give I_3^-. However, it is not now considered that this is the case because:

(a) the correlation functions from the $\nu_{(D-I)}$ band for pyridine-I_2 and diethyl sulphide-I_2 are coincident. This is reflected in similar half band widths and $\tau_{1/e}$ values. This implies that both absorptions arise from the same relaxation mechanisms.

(b) the $\nu_{(S-I)}$ and $\nu_{(I-I)}$ bands which were separated manually, have intensities which can be explained in terms of the charge-transfer theory, i.e. they have high intensities, and because of the small frequency separation 'intensity borrowing' by the $\nu_{(S-I)}$ band has occurred, or possibly I_3^- impurity is also present.

(c) The half-band width of the absorption arising from antisymmetric stretching of the I_3^- ion is 10·5 cm.$^{-1}$, obtained from a spectrum of I_3^- in pure acetone. One would not expect solvent broadening to increase this to 30 cm.$^{-1}$ (Table 5.5).

(d) Yamada et al.,[153] have assigned the bands at 149, and 195 cm.$^{-1}$ to the $\nu_{(S-I)}$ mode for the diethyl sulphide-IBr and ICl complexes respectively. Using a range of donors they assigned bands between 95 and 205 cm.$^{-1}$ to the $\nu_{(S-I)}$ mode.

The final question is why the $\nu_{(S-I)}$ frequency is so high. Possible roles for d-orbitals in chemical bonds were discussed at length in 1954 by Craig, Marcol, Nyholm, Orgel and Sutton.[154] They concluded that the d-orbitals contract as a result of perturbation by the ligands. Craig and Magnusson[155] showed how diffuse d-orbitals would contract, and their energies would drop, in the field of a set of positive charges surrounding the sulphur atom.

Craig and Zauli[156] published key work on SF_6. They considered the effect on the sulphur 3s,3p and 3d orbitals of the field of six neutral fluorine atoms, sited in the octahedral positions, at an S-F distance of 3·0 a.u. (1·59Å). Their calculation was purely electrostatic, and no account was taken of possible overlap densities in bonds or exchange terms. They found that the mean radius of the d-orbital contracts from 3·0Å to 1·5Å.

One must conclude for the diethyl sulphide-halogen complexes, that the more electronegative the substituents the more the d-orbitals are involved in bonding. This accounts for the increase in frequency of the $\nu_{(S-I)}$ band in the I_2, IBr and ICl complexes. Finally the possibility of mixing of modes (reference 36, p.34) cannot be ruled out.

C. Studies on the External Modes of the Dioxan-Halogen Complexes.

1. Introduction.

In view of the dependence of the $\nu_{(I-I)}$ band intensity on solvent, concentration of donor, and concentration of acceptor (see also Chapter 4),

it was decided to investigate the spectral properties of the $\nu_{(D-I)}$ mode in a weak donor. This absorption is expected to occur below 100 $cm.^{-1}$

Dioxan was chosen as donor, because it is non-polar and a good solvent for the halogens. Dioxan, in the absence of an acceptor, shows an absorption at about 70 $cm.^{-1}$ This absorption is thought[157] to be caused by classical quadrupole-induced dipole interactions (in general multipole-induced dipole interactions). The mechanism giving rise to this absorption is regarded as collisional for non-polar molecules such as dioxan.

On the other hand, in polar molecules the molecular dipole 'librates' in a 'cage' of surrounding molecules (either the same species or solvent). This Poley-Hill model[129] is similar to the idea[157,158] of a residual rotation of the molecular dipole in the liquid phase. There is little difference between a Poley-Hill liquid phase absorption and a pressure broadened gas-phase spectrum. For the system p-dioxan XY/cyclohexane (X = Y = I, Br, Cl; X = I, Cl, Br, CN) a low frequency absorption is observed which is similar to that observed for pyridine-I_2 in the same solvent. (See Spectra 5.4. and 5.5.). Whilst, the pyridine-halogen complexes are thermodynamically quite stable,[134] the corresponding dioxan complexes are very much weaker, and the bands observed should probably not be assigned to the motion of a 'rigid' complex. These bands are even observed with as weak a donor as carbon disulphide. (See Spectrum 5.4.).

2. Discussion.

It is questionable if a well-defined $\nu_{(D-A)}$ band exists for these 'complexes'. The complex life-time is of the order of 1 ps, and there may be no more than a few vibrational periods during the complex life-time. Kettle and Price[84] have shown that the dipole moments measured for mixtures of non-polar donors with non-polar halogens, can be entirely accounted for by the mutual classical van der Waals interaction of the components. It can be seen

from Table 5.6. that the iodine complex has the largest intensity. Since I_2 has the largest polarisability, this again supports the induced dipole theory.

Table 5.6. shows that the non-polar dioxan and I_2 give rise to a dipole moment of 1D in the complex. Gordon[130] has deduced a formula for the intensity of a condensed phase 'rotational' band of a rigid complex.

$$A = \frac{N\pi}{3c^2} \vec{\mu}_z^2 \left(\frac{1}{I_x} + \frac{1}{I_y}\right) \qquad \ldots\ldots [5.3.]$$

Equation 5.3. only depends on the dipole moments $\vec{\mu}_z$ and moments of inertia I_x and I_y. The estimated intensities are shown in Table 5.6. The very much larger intensities observed appear to arise from a collision induced mechanism - the dioxan having large <u>local</u> dipoles despite having only a very small overall permanent moment.

One would expect that ν_{max} would be proportional to the collision frequency. For unlike molecules, A and B, ν_{max} is proportional to $\left(\frac{1}{M_A} + \frac{1}{M_B}\right)^{\frac{1}{2}}$. The constant of proportionality for the dioxan-X_2 systems is shown in Table 5.6. Reasonably good agreement is obtained, the value of ν_{max} for dioxan-Cl_2 could be increased by a chloroform solvent effect.

The situation is more complicated for systems containing IX molecules, since dipole-induced dipole forces lead to a stronger interaction, and the complex becomes more 'rigid'. (There may even be a Poley-Hill contribution to the intensity.) The frequencies and intensities of the observed bands tend to decrease as the dipole moment of the 'complex' increases. From equation 5.3. one would expect a large increase of intensity, so presumably induced dipole fluctuations have a considerable impact on the intensity.

The intensity of the $\nu_{(D-I)}$ mode depends upon the concentration of donor and acceptor. It was decided to make a rigorous study of the $\nu_{(D-I)}$ band in the dioxan-I_2 complex. This complex was chosen because (a) it has the most intense band of the dioxan-halogen series (see Spectrum 5.5.); (b) since

Table 5.6.

The Far-Infrared Data for the External Modes for p-Dioxan-XY Complexes in Cyclohexane

[Donor] mole/litre^{-1}	Halogen	[Halogen] mole/litre^{-1}	Band posn./ cm.$^{-1}$	$\Delta\bar{\nu}_{\frac{1}{2}}$ / cm.$^{-1}$	Intensity[a] (1 mole^{-1} cm.$^{-2}$)	Intensity[b] (Gordon formula) (1 mole^{-1} cm.$^{-2}$)	Complex[c] Dipole Moment	α_{11}[d] (X 10^{25}cm.^{3})	$\bar{\nu}_{max}/\left(\frac{1}{M_A}+\frac{1}{M_B}\right)^{\frac{1}{2}}$
1·3M	I_2	0·054	80 ± 4	55 ± 5	1250	3·9	1·0D	175	610
	Br_2	0·145	85	50	800	10	1·3D	99·5	640
	Cl_2	e	140					66	870
	ICl	0·132	102	51	1020	106	4·0D	136	
	IBr	0·082	97	49	700	63	3·6D		
	ICN	0·084	78	54	940	129	4·4D		

[a] Intensities calculated assuming all the halogen complexed.

[b] Intensity calculated from equation 5.

[c] From Reference 84.

[d] Polarisabilities from Reference 119a

[e] Dried chlorine bubbled into dioxan/chloroform solution, concentration unknown.

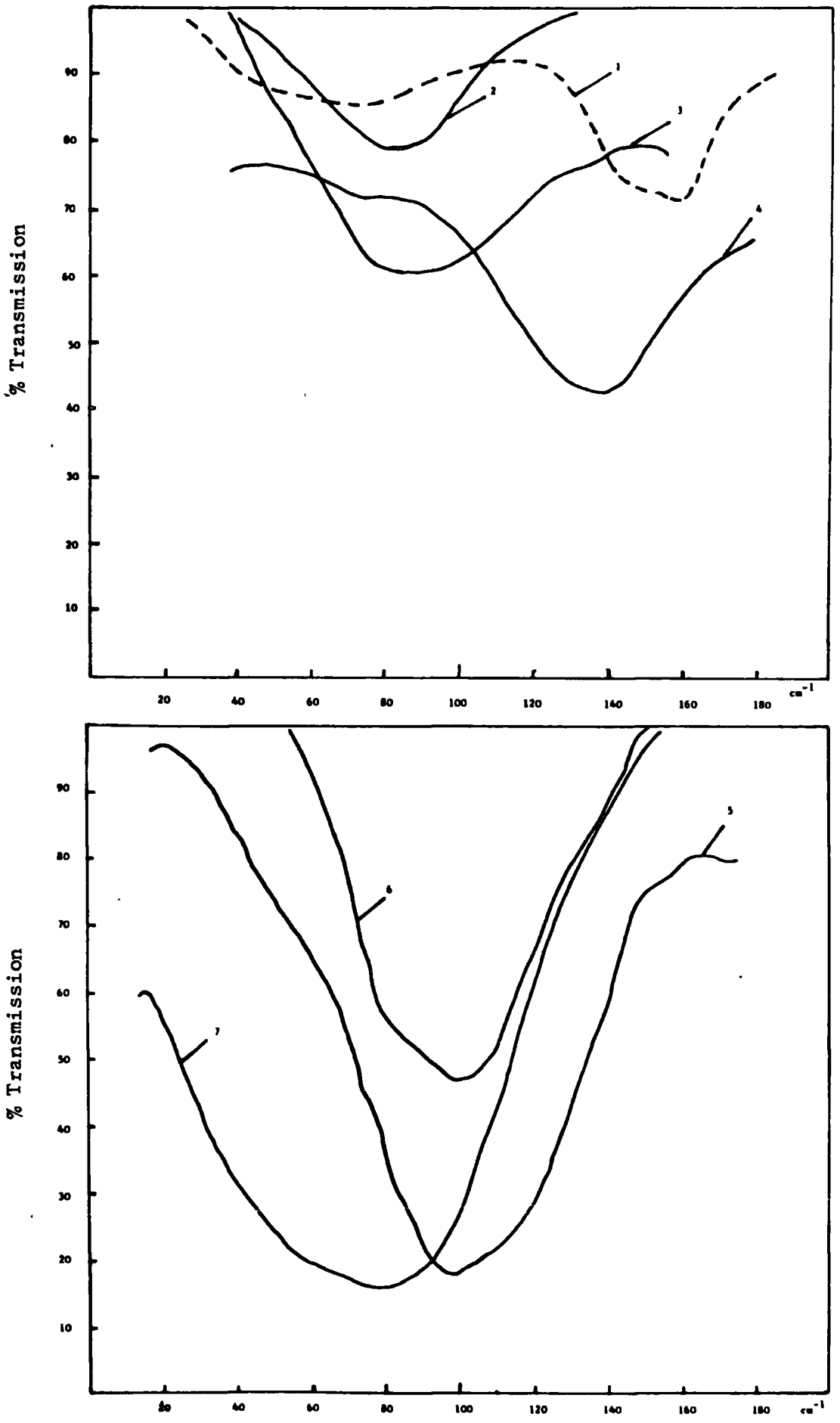

Spectrum 5.5. Far-infrared spectra of 1·3M dioxan in cyclohexane with added halogen. Concentrations of halogen are (1) zero; (2) I_2, O·054M; (3) Br_2, O·145M; (4) Cl_2, conc. not known; (5) ICl, O·132M; (6) IBr, O·082M; (7) ICN, O·084M.
(N.B. In cases 2-7 the spectrum of 1·3M dioxan has been subtracted off).

Table 5.8.

Effects of Changing p-Dioxan and Iodine Concentrations on the Far-Infrared Band Area

[Dioxan]/ mole/litre^{-1}	[Iodine]/ mole/litre^{-1}	$\bar{\nu}_{max}$/cm.$^{-1}$	$\Delta\bar{\nu}_{\frac{1}{2}}$/ cm.$^{-1}$	Band Area/ cm.$^{-1}$
0·23	0·058	88	54	7·0
0·38	0·056	-	-	8·8
0·68	0·055	83	52	12·0
1·28	0·054	80	-	11·7
2·81	0·054	78	44	28·0
11·38	0·054	76	-	70·0
3·44	0·032	78	54	13·9
3·44	0·067	75	52	30·0
3·44	0·123	77	56	56·0
3·44	0·136	84	50	78·0
3·44	0·169	78	55	78·0
3·44	0·209	78	-	118·0

both dioxan and iodine are non-polar dipole-induced dipole forces should be less.

3. A Systematic Study of the Dependence of the Intensity of '$\nu_{(D-I)}$' Mode in the Dioxan-I_2 Complex on Concentration of Donor and Acceptor.

The intensities in Table 5.6. depend upon what one considers to be the concentration of the complex. Since dioxan is present in a 25:1 excess, one would expect most of the halogen to be complexed (K_c = 0·89 mole litre^{-1}). However, the band does not obey the Beer-Lambert Law.

The absorption thus appears to be due to sticky collisions (i.e. contacts) rather than a 'well-defined' complex. If the band were due to a $\nu_{(D-A)}$ mode of a 'well defined' complex, one would expect an intensity dependent only on the iodine concentration (as long as [Dioxan] ≫ [Iodine]). For a collision induced band one would expect.[64]

$$\text{Total Area} = K_1[\text{donor}][\text{halogen}] + K_2[\text{donor}][\text{donor}] + K_3[\text{Halogen}][\text{Halogen}] + \text{terms from a 'sticky' collision ...} \quad [5.4.]$$

Table 5.8. shows the effect of changing p-dioxan and iodine concentrations on the far-infrared band area.

Spectrum 5.5. shows dioxan solutions containing a halogen molecule. The spectra have been obtained in the double beam mode by ratioing the solution spectrum against a 'blank' containing the same concentration of dioxan. Areas measured from bands obtained in this fashion should have eliminated most of $K_2[\text{donor}][\text{donor}]$ term in equation 5.4. At small halogen concentrations the third term can be neglected. One would therefore expect the area to be a function of $[\text{dioxan}]^x[I_2]^y$. To test this we kept the concentration of I_2 and dioxan constant in turn. In each case the area was measured over a range of either dioxan or iodine concentration (see Table 5.8.). Graphs of the Log_{10}(Area) v $[I_2]$ and Log_{10}(Area) v [Dioxan] were then plotted. Graphs 5.1. and 5.2. show that x = 0·55; y = 1·2.

GRAPH 5.1 LOG[AREA] v $[I_2]$ PLOT FOR LOW FREQUENCY BAND DIOXAN - I_2 COMPLEX

CONSTANT [DIOXAN] = 3.4 M

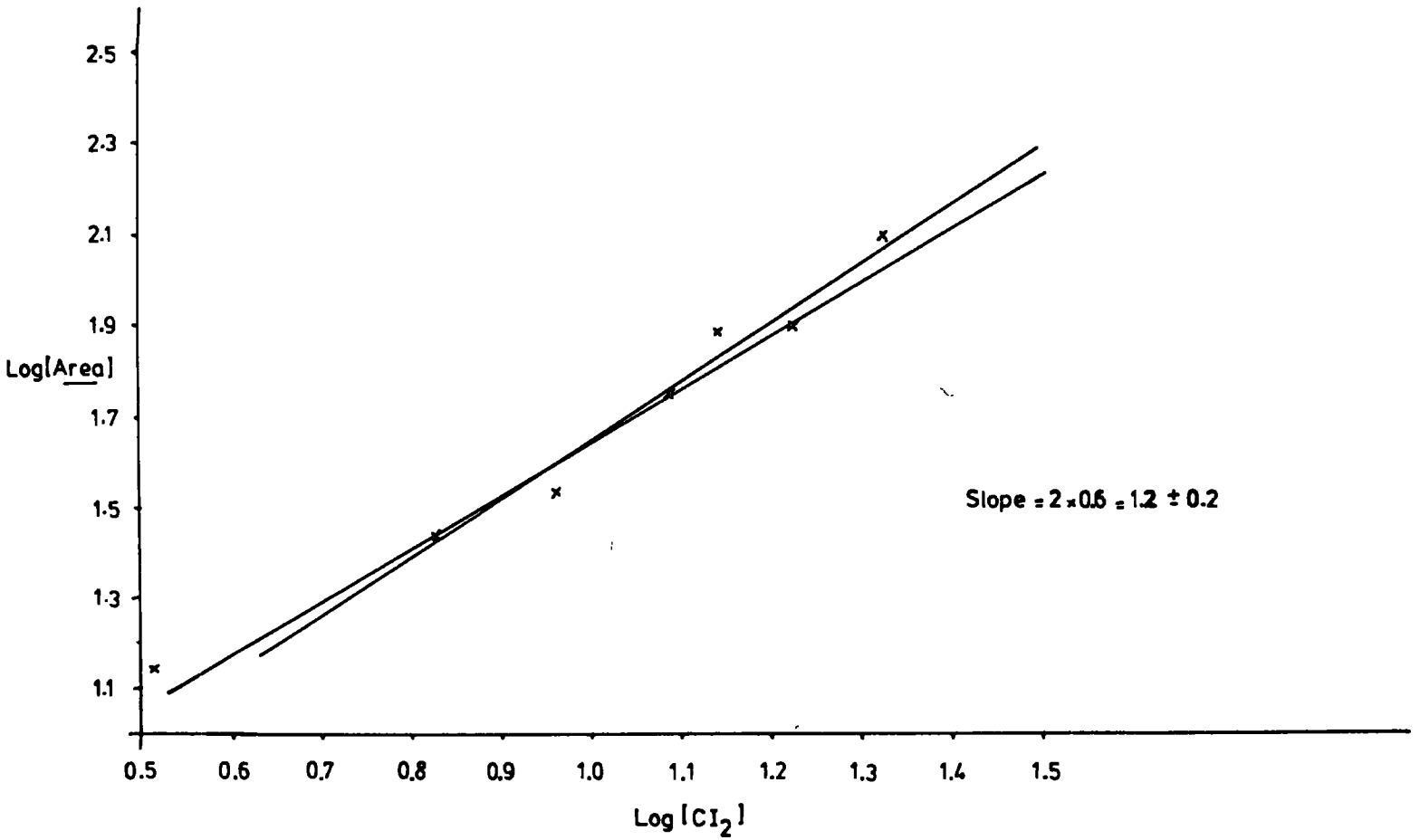

GRAPH 5.2 LOG (AREA) v [DIOXAN] PLOT FOR LOW FREQUENCY BAND DIOXAN - I_2 COMPLEX

CONSTANT [I_2] = 0.055 M

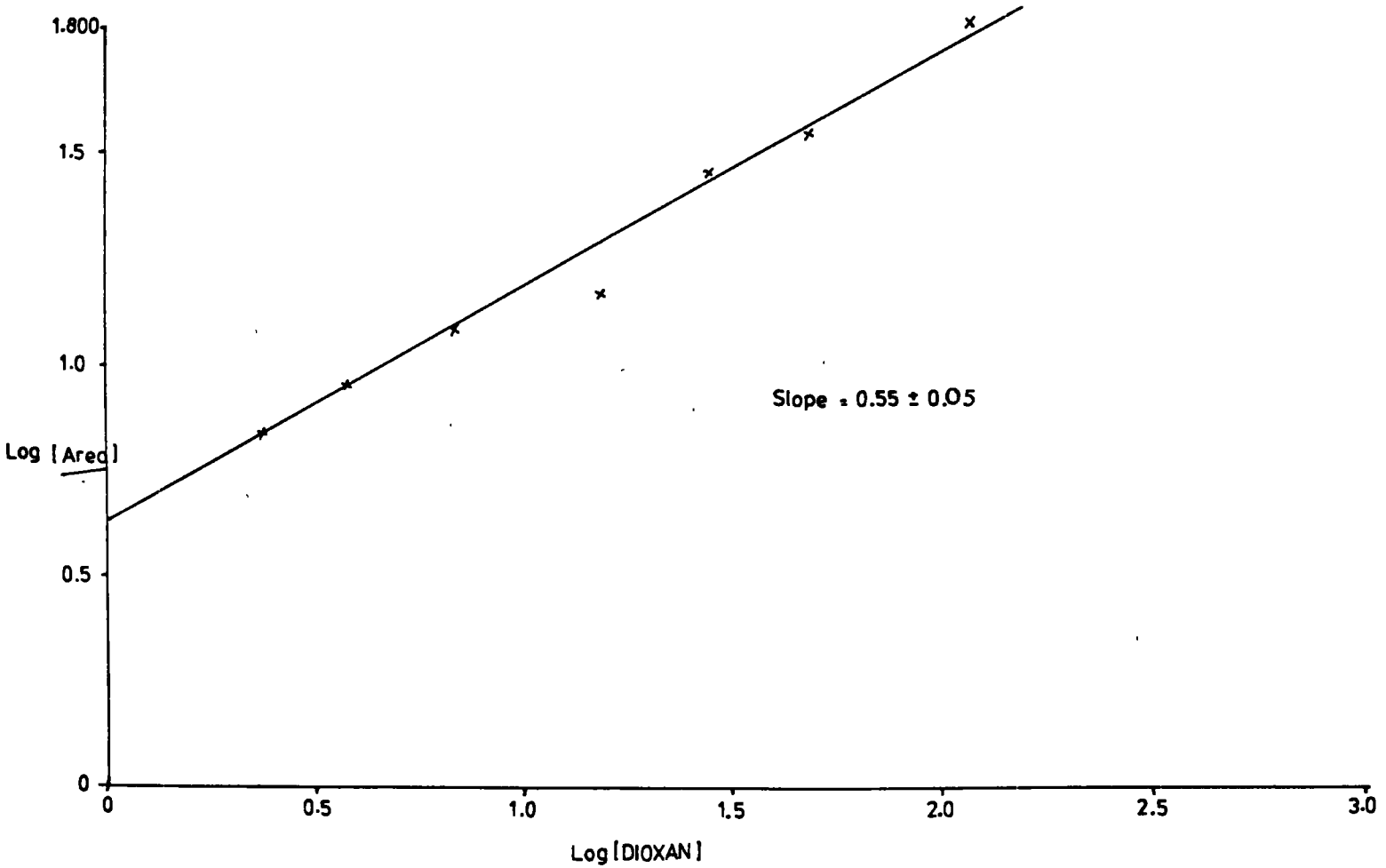

Equation 5.4. assumes the path length 1 is constant. Strictly we should write

$$\frac{AREA}{1} = K[Dioxan]^x[I_2]^y$$

or $$AREA = 1K[Dioxan]^x[I_2]^y$$

Since 1 was kept constant at 6·5 mm.

$$AREA = K_1[Dioxan]^x[I_2]^y$$

or at constant $[I_2]$.

$$Log(Area) = x\ Log\ [Dioxan] + K_2$$

at constant [Dioxan]

$$Log(Area) = y\ Log\ [I_2] + K_3$$

where K, K_1, K_2 and K_3 are all constants. This does show conclusively that the band does not obey the Beer Lambert Law. However, this experiment would have to be made with a range of iodine complexes before a complete interpretation of the data could be made.

D. Suggestions for Future Work.

It is clear that an intensity study must be carried out at constant donor and constant acceptor concentrations. A temperature variation study is desirable for the weak complexes, as a collision induced band is likely[64] to be more sensitive to temperature than an internal vibration.

The extreme width of the low frequency band has not been explained quantitatively. Far infrared band widths have been attributed to

(a) coupling of intermolecular motion with internal vibrational modes,[160]

(b) anharmonic nature of the resonances involved,[161]

(c) overlapping of a series of damped resonances of similar energy, the range of energies being caused by Brownian diffusion of the interacting molecule,[162]

(d) collisional broadening.

If the life-times for weak complexes are about 1 ps then the uncertainty broadening could be of the order of 5 $cm.^{-1}$

The frequency variation may be of little significance, because the band width is of the same order as the frequency.[163] The broadness of the bands is reflected in the $\tau_{1/e}$ values. For the dioxan halogen complexes the value was 0·3 - 0·4 p.s.

It is clear that more data is required on range of donors (strong and weak) coupled with temperature studies, before the exact nature of the collisional mechanism can be elucidated. The great similarity of the band shape of the low frequency mode, with a range of weak donors and acceptors, does at least show that it arises from the same mechanism, and is not an internal vibration.

In conclusion the frequency shift and increase in intensity on complexation is fairly well explained by the charge transfer mechanism for strong donors. For weak donors where the dipole-dipole, induced-dipole etc. forces are relatively more important the situation is much less well understood.

CHAPTER 6

Normal Co-ordinate Studies on Pyridine-Halogen Complexes

A. Introduction.

The aim of the work described in this chapter was to extend the pyridine force field to produce one suitable for the pyridine-halogen complexes. In this way it was hoped to account for the changes in frequency of the pyridine molecule on complexation, and to evaluate $\partial\mu/\partial Sj$, the change of transition moment with symmetry co-ordinate. The $\partial\mu/\partial Sj$ values give some idea of the electronic re-distribution during vibration, and the nature and extent of vibrational mixing.

The force field arises from changes in the potential energy of the molecule during vibration and, in principle, it can be calculated by solving the electronic wave equation, and hence determining this energy as a function of molecular configuration. However, at present, the mathematical difficulties are too great, and we attempt to deduce the force field by calculation from the observed vibrational frequencies, and thus obtain empirical information on the electronic binding in the molecule.

Most infrared spectroscopic analyses used by organic chemists are based on the premise that assignments for stretching frequencies can be approximated by the application of Hooke's law.[164] Equation 6.1. shows the relationship between frequency of oscillation, atomic masses, and the force constant of the bond (strictly) only true for a diatomic molecule.

$$\bar{\nu} = \frac{1}{2\pi c}\left(\frac{f}{\mu}\right)^{\frac{1}{2}} \qquad \ldots\ldots \quad [6.1.]$$

where $\bar{\nu}$ = the vibrational 'frequency' ($cm.^{-1}$)

c = velocity of light (cm./sec.)

f = force constant of bond (dynes/cm.)

μ = the reduced mass $(\frac{M_x M_y}{M_x + M_y})$ where M_x and M_y are the atomic masses.

The value of f is approximately 5 x 10^5 dynes/cm. for single bonds and approximately two and three times this value for double bonds and triple bonds, respectively.

However, when two bond oscillators share a common atom they seldom behave as individual oscillators, unless the individual oscillation frequencies are widely different. This is because there is mechanical coupling or interaction between the oscillators.

The requirements for effective interaction are:

(a) The vibrations usually belong to the same symmetry species.

(b) Strong coupling between stretching vibrations requires a common atom between the groups.

(c) Interaction is greatest when the coupled groups absorb, individually, near the same frequency.

(d) Coupling between stretching and bending vibrations can occur if the stretching bond forms one side of the changing angle.

(e) A common bond is required for coupling of bending vibrations.

Usually, little or no interaction occurs between groups separated by two or more bonds.

The full normal co-ordinate calculation for the pyridine-XY complexes will determine how much the frequency shifts of the donor and acceptor on complexation are due to mass effects, and how much to changes in the force constants (chemical bonding effects). A normal co-ordinate calculation is also of value in the assignment of vibrational bands. This should be particularly useful in the pyridine case where some vibrations are doubly assigned (Chapter 3). Unfortunately, force field calculations are still not accurate enough to give a definite assignment for all the molecular vibrations.

The vibrational frequencies of a molecule depend upon two terms. The first term is the atomic masses and geometry of the equilibrium configuration. The second term is the force field which restores the molecule to its equilibrium configuration. This represents the interaction between nuclear and electronic motion. The main problem in determining force constants from observed frequencies is that, a N-atomic molecule has 3N-6 fundamental vibrational frequencies, but there are $\frac{(3N-6)(3N-5)}{2}$ independent force constants. Whilst molecular symmetry reduces the number of independent force constants, the number still usually exceeds the number of observed frequencies.

The problem of calculating force constants from observed data for the complexes studied here is not soluble, unless certain simplifying assumptions are made. Since the $\nu_{(N-I)}$ band frequency in pyridine-IX complexes (X = Cl, Br; see Chapter 4), and methyl pyridine-ICl complexes (where steric effects are not important[30]) are very similar (130 ± 10 cm.$^{-1}$, see Chapter 4) the interaction terms (between the N-I-X part and the pyridine ring) affecting this vibration are expected to be small. It was therefore decided, in the first instance, to approximate the pyridine-IX complexes (X = Cl, Br) to linear triatomic molecules.

B. General Outline of the Theory.

The Wilson GF matrix theory[165,166,167,168] is applicable to any molecule. However, calculations for large molecules are exceedingly complex, and a computer is essential to determine the vibrational frequencies. The principle equations used in the theory will be quoted in this thesis without proof. In order to explain the general method, the theory will then be used to derive the equations for the linear triatomic molecule. We shall then go on to determine the force constants of the triatomic molecule model.

The problem is solved in a set of symmetry co-ordinates, S, given by,

$$S = UR \qquad \ldots\ldots [6.2.]$$

These symmetry co-ordinates, which transform according to the molecular point group under consideration, are linear combinations of the atomic displacement co-ordinates (R). U, of course, is the matrix which relates S and R. Having written down or calculated (see below) the potential energy (f) and kinetic energy (g) matrices in terms of the co-ordinates R one can then calculate,

$$F = UfU^T \qquad \ldots\ldots [6.3.]$$

and,

$$G = UgU^T \qquad \ldots\ldots [6.4.]$$

The F and G matrices are the ones used to determine the potential (V) and kinetic energies (T) of the molecule in terms of the symmetry co-ordinates,

$$2V = S^T FS \qquad \ldots\ldots [6.5.]$$

$$2T = S^T G^{-1} S \qquad \ldots\ldots [6.6.]$$

The potential and kinetic energies are related to the vibrational frequencies, λ, by a set of normal co-ordinates, Q, in terms of which the V and T matrices are diagonal.

So we write $2V = Q^T \Lambda Q \qquad \ldots\ldots [6.7.]$

and $2T = \dot{Q}^T E \dot{Q} \qquad \ldots\ldots [6.8.]$

where $\dot{Q} = \frac{dQ}{dT}$ and Λ is a diagonal matrix of vibrational eigenvalues.

The normal co-ordinates, Q, are related to the symmetry co-ordinates S, by the 'mixing' matrix, L by,

$$S = LQ \qquad \ldots\ldots [6.9.]$$

It can be shown that these matrices are then related by

$$L\Lambda = GFL \qquad \ldots\ldots [6.10.]$$

or $$|GF - E\Lambda|L = 0 \qquad \ldots\ldots [6.11.]$$

and this is the secular determinantal equation must be solved.

It is often convenient to calculate the g matrix from a B matrix where B represents the transformation from Cartesian displacement co-ordinates, x, to internal co-ordinates R, i.e.

$$R = Bx \qquad \ldots\ldots \quad [6.12]$$

g is then calculated from,

$$g = BM^{-1}B^{T} \qquad \ldots\ldots \quad [6.13]$$

where M^{-1} is a diagonal matrix of the reciprocal masses.

The g matrix can be calculated from general formulae given in such works as ref. 68 (p.206) or ref. 168. The g matrix elements will only be non-zero if it couples two internal co-ordinates which have one or more common nuclei.

Taking as an example the linear triatomic molecule XYZ

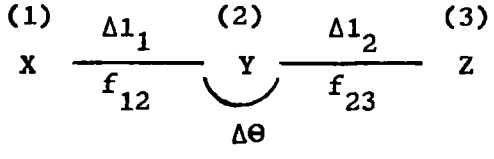

Fig. 6.1.

The g matrix is written as shown in Table 6.1.

Table 6.1.

Displacement co-ordinates	Δl_1	Δl_2	$\Delta\theta$
Δl_1	$\mu_x + \mu_y$	$-\mu_y$	0
Δl_2	$-\mu_y$	$\mu_y + \mu_z$	0
$\Delta\theta$	0	0	$g(\Delta\theta\cdot\Delta\theta)$

Ref. 68 shows, from standard formulae, that,

$$g(\Delta\theta.\Delta\theta) = \rho_{12}^2 \quad \mu_x + \rho_{23}^2\mu_z + \mu_y(\rho_{12}^2 + \rho_{23}^2 - 2\rho_{12}\rho_{23}C\theta)$$

(where $C\theta = \text{Cos}\theta$).

$\rho_{ij} = \frac{1}{l_{ij}}$ since $\theta = 180^o$, $\text{Cos}\theta = -1$ and $\text{Sin}\theta = 0$.

$$g(\Delta\theta.\Delta\theta) = \frac{\mu_x}{l_1^2} + \frac{\mu_z}{l_2^2} + (l_1^{-2} + l_2^{-2} + 2l_1^{-1}l_2^{-1})\mu_y$$

$$g(\Delta l_1\Delta l_2) = \mu_y\text{Cos}\theta = -\mu_y$$

$$g(\Delta l_1\Delta\theta) = -\frac{1}{l_2}\text{Sin}\theta\mu_y = 0$$

Therefore, it can be seen in principle how the g matrix can be evaluated for any molecule. Having calculated the G and F matrices the equation 6.11. can be solved for λ the frequencies of vibration. The calculation for molecules with a small number of atoms can be done manually. For larger molecules a computer is essential.

C. Calculation for the Linear Triatomic Model.

The linear triatomic molecule XYZ has two stretching frequencies $\nu_{(X-Y)}$ and $\nu_{(Y-Z)}$ and three force constants; $k_{(X-Y)}$ (or f_{12}), $k_{(Y-Z)}$ (or f_{23}) and the interaction force constant k_{13}. Isotopic substitution should only affect the G matrix. Therefore, one has two extra stretching frequencies for X(deuterated) YZ, and XYZ molecules, and it should be possible to evaluate k_{13}. The triatomic molecule calculation for pyridine-h_5-IBr and pyridine-d_5-IBr has been published in the Journal of Molecular Structure, 1971, 10, 147-153, and the paper is included in Appendix B.

An outline of the method and the main findings is all that will be included in this chapter.

The total potential energy of the molecule may be written as,

$$2V = f_{12}\Delta l_1^2 + f_{23}\Delta l_2^2 + k_{13}\Delta l_1\Delta l_2 + f_\theta.\Delta\theta^2 \quad \ldots\ldots [6.14.]$$

There are two frequencies and three force constants so isotopic substitution or other information is necessary to calculate k_{13}. A suitable set of symmetry co-ordinates which transform as the point group $C_{\infty v}$ are,

$$S_1 \equiv R_1 = \Delta l_1$$
$$S_2 \equiv R_2 = \Delta l_2$$
$$S_3 \equiv R_3 = (l_1 l_2)^{\frac{1}{2}}\Delta\theta$$

writing this in matrix form.

	Δl_1	Δl_2	$(l_1 l_2)^{\frac{1}{2}}\Delta\theta$
S_1	1	0	0
S_2	0	1	0
S_3	0	0	1

Thus we have, U = E (unit matrix).

$$G = U^T g U = E^T g E = g$$
$$F = E f E^T = f$$

The f matrix is,

	Δl_1	Δl_2	$(l_1 l_2)^{\frac{1}{2}}\Delta\theta$
Δl_1	f_{12}	k_{13}	0
Δl_2	k_{13}	f_{23}	0
$(l_1 l_2)^{\frac{1}{2}}\Delta\theta$	0	0	f_θ

The g matrix is as in Table 6.1. Expanding equation 6.11. for $\nu_{(X-Y)}$ and $\nu_{(Y-Z)}$ vibrations.

$$\begin{vmatrix} G_{11} & G_{12} \\ G_{21} & G_{22} \end{vmatrix} \begin{vmatrix} F_{11} & F_{12} \\ F_{21} & F_{22} \end{vmatrix} - \begin{vmatrix} 1 & 0 \\ 0 & 1 \end{vmatrix} \begin{vmatrix} \lambda_1 & 0 \\ 0 & \lambda_2 \end{vmatrix}$$

i.e.
$$\begin{vmatrix} (G_{11}F_{11} + G_{12}F_{21}) & (G_{11}F_{12} + G_{12}F_{22}) \\ (G_{21}F_{11} + G_{22}F_{21}) & (G_{21}F_{12} + G_{22}F_{22}) \end{vmatrix} - \begin{vmatrix} \lambda_1 & 0 \\ 0 & \lambda_2 \end{vmatrix} = 0$$

$$(-\lambda)^2 + (-\lambda)(G_{11}F_{11} + 2F_{12}G_{12} + F_{22}G_{22}) + (F_{11}F_{22} - F_{12}^2)(G_{11}G_{22} - G_{12}^2) = 0$$

$\lambda = 4\pi^2C^2\omega^2$ where ω is the frequency in $cm.^{-1}$

On substituting with our g and f matrices we obtain,

$$0{\cdot}058893(\omega_1^2 + \omega_2^2) = (f_{12}+f_{23} + 2k_{13})\mu_y + f_{12}\mu_z + f_{23}\mu_x \quad \text{.....} \quad [6.15]$$

f = md/Å μ = a.m.u.

and $$(0{\cdot}058893\omega_1\omega_2)^2 = (f_{12}f_{23} - k_{13}^2)(\mu_x\mu_y + \mu_x\mu_z + \mu_y\mu_z) \quad \text{.....} \quad [6.16]$$

Our computer program calculates f_{12} and f_{23} over a range of k_{13}.

Equation 6.16 is the equation of an ellipse and the force constant ellipses for the series pyridine-IX (X = I, Br, Cl) were plotted out with the ellipses for the corresponding pyridine-d_5 complexes. The largest frequency change was observed for the $\nu_{(N-I)}$ band in the pyridine-IBr complex. The ICl and I_2 complexes showed changes of 4 and 3·5 $cm.^{-1}$ (see Appendix B) respectively, which was not enough to give distinct crossing points. The two crossing points correspond to k_{13} = 0·1 - 0·2 md/Å and k_{13} = 0·5 - 0·6 md/Å so it is necessary to choose the correct solution before calculating the transition moment $\partial\vec{\mu}/\partial S_j$. Gayles[170] found, for similar trimethylamine complexes, that k_{13} was negative. This is not possible for the pyridine complexes since as the D-I bond is stretched the I-X bond is strengthened (the halogen becoming more similar to the free molecule) and we would expect k_{13} to be positive if the charge-transfer model is valid.

The values obtained if k_{13} = 0·6 md/Å are,

$$\text{(a)} \quad \frac{\partial\mu}{\partial R_{I-X}} > \frac{\partial\mu}{\partial R_{D-I}}$$

which is expected if vibrational mixing is not predominant in determining the intensities. This is in line with previous estimates[169] of $k_{13} \approx$ 0·4 md/Å.

(b) The $\frac{\partial\mu}{\partial R_{I-X}}$ data are in the order ICl ≈ IBr > I_2

(c) The $\frac{\partial\mu}{\partial R_{D-I}}$ data are in the order ICl > I_2 > IBr

The values obtained if k_{13} = 0·1 md/Å are

(i) The $\frac{\partial\mu}{\partial R_{D-I}}$ data are in the order IBr > ICl > I_2

(ii) The $\frac{\partial\mu}{\partial R_{I-X}}$ data are in the order

ICl > IBr > I_2 which is expected on thermodynamic grounds.

(iii) $(\frac{\partial\mu}{\partial R_{D-I}}) \approx (\frac{\partial\mu}{\partial R_{I-X}})$ for pyridine-ICl

$\frac{\partial\mu}{\partial R_{D-I}} > \frac{\partial\mu}{\partial R_{I-X}}$ for pyridine-IBr

$\frac{\partial\mu}{\partial R_{D-I}} > \frac{\partial\mu}{\partial R_{I-X}}$ for pyridine-I_2

It can be seen that neither value of k_{13} gives

$$(\frac{\partial\vec{\mu}}{\partial R})_{I-X} > (\frac{\partial\vec{\mu}}{\partial R})_{D-I}$$

and the values of $(\frac{\partial\vec{\mu}}{\partial R})_{I-X}$ and $(\frac{\partial\vec{\mu}}{\partial R})_{D-I}$ respectively

following the series ICl > IBr > I_2, which is what is expected on thermodynamic, intensity and frequency perturbation grounds. From the data one cannot say conclusively whether k_{13} = 0·1, or 0·6 md/Å. A value of 0·1 - 0·2 md/Å fits better with a value of 0·22 md/Å obtained using Badger's rule.[123b] However, Badger's rule can often be greatly in error.

Watari[123b] has also estimated the following force constants for the pyridine-ICl complex: k_{ICl} = 1·18 md/Å; k_{N-I} = 0·91 md/Å; k_{13} = 0·22 md/Å. He calculated k_{I-Cl} from Badger's rule and solved for k_{13} using the observed $\nu_{(I-Cl)}$ and $\nu_{(N-I)}$ band positions at 265 and 170 $cm.^{-1}$ in a paraffin mull.

In conclusion, it can be seen that the value of k_{13} is either 0·1 or 0·6 md/Å in the pyridine-IBr complex. Person (ref. 78, p.41) favours the value of 0·6 md/Å for k_{13} reasoning from the change of k_{D-I} and k_{I-X} with other strong donors. One of the aims of the whole molecule's normal co-ordinate calculation was to determine which value of k_{13} is the correct one.

D. Whole Molecule Calculation.

1. Force Field Calculations on Pyridine.

Before attempting to carry out a force field calculation on pyridine-XY complexes it is necessary to repeat the force field calculation for pyridine. This is because force field calculations involve a large number of terms and great care must be taken to avoid errors. However, there are a number of checks which can be made if the pyridine calculation is successfully repeated.

Firstly, the U matrix will transform the f and g matrices into two smaller sub-matrices for the class A_1 and B_1 vibrations. Secondly, if the calculated frequencies from the force field agree with the published values this ensures that the correct force field is being used.

There are at least two force fields for pyridine in the literature. Long et al.[104] have calculated the vibrational frequencies for pyridine and pyridine-d_5. They transferred Whiffen's[165] internal force constants directly from benzene to pyridine. Duinker[113] has used a different force field to Long and Thomas. In particular, the diagonal C-C stretching force constant for the Duinker force field is 7·015 md/Å, whereas Whiffen calculates 5·553 md/Å. Duinker argued that the value of 7·015 md/Å for the f_{C-C} in benzene, was in better agreement with the values for the corresponding force constants in ethane (5 md/Å), ethylene (10 md/Å), and acetylene (15 md/Å). However, the supplementation of either force field by the extra terms included for the pyridine-XY complex should indicate which donor frequencies are 'sensitive' to complexation, and whether they increase or decrease.

Long et al.[104] have quoted the G and F matrices for pyridine and pyridine-d_5. In spite of a great deal of work checking our arithmetic, we were unable to reproduce the published pyridine frequencies from these matrices. Duinker has discussed some of the inconsistencies (reference 113, p.125). Furthermore, Long and Thomas used the benzene (D_{6h}) symmetry co-ordinates. Whilst the point group for pyridine (C_{2v}) is a sub-group of benzene (D_{6h}), and hence the symmetry co-ordinates appropriate to the pyridine molecule may be correlated with those of benzene. We felt it to be best, from the interpretive point of view, to use the simplest symmetry co-ordinates possible.

These are the Nielsen-Berryman[171] symmetry co-ordinates which do not mix internal co-ordinates from different equivalent sets. These are shown in Table 6.2. Two A_1 and one B_1 redundant co-ordinates are implicitly contained in these co-ordinates. The existence of a redundancy implies that at least two of the deformation co-ordinates are dependent on one another. However, as Steele emphasizes (ref. 68, p.69) the extra co-ordinates results in zero roots which the program outputs as zero frequencies. The redundancy was not eliminated as it was neither necessary nor worthwhile.

The geometry of pyridine and the force constants (shown in Table 6.3.) were supplied to the program 'LINDA' (supplied by courtesy of Dr. D. Steele of Royal Holloway College, University of London). The frequencies obtained are shown in Table 6.4. For reasons which will become apparent in the subsequent section, the G matrix was also evaluated by using a program originally written by J.H. Schachtschneider.[174] The G matrix was then fed into 'LINDA' which had been modified to accept it. The frequencies obtained were identical (see Table 6.4). The slight deviation of the Long and Thomas values are probably because part of their calculation was 'manual', and 'rounding errors' resulted. From this one can conclude that:

Table 6.2.

Normalised Nielson and Berryman Symmetry Co-ordinates for Pyridine

A_1	A_1	
	S_1	$\frac{1}{\sqrt{2}}(\Delta R_1 + \Delta R_6)$
	S_2	$\frac{1}{\sqrt{2}}(\Delta R_2 + \Delta R_5)$
	S_3	$\frac{1}{\sqrt{2}}(\Delta R_3 + \Delta R_4)$
	S_4	Δr_4
	S_5	$\frac{1}{\sqrt{2}}(\Delta r_2 + \Delta r_6)$
	S_6	$\frac{1}{\sqrt{2}}(\Delta r_3 + \Delta r_5)$
	S_7	$R_o \Delta \alpha_1$
	S_8	$R_o \Delta \alpha_4$
	S_9	$\frac{1}{\sqrt{2}}(\Delta \alpha_2 + \Delta \alpha_6)$
	S_{10}	$\frac{1}{\sqrt{2}}(\Delta \alpha_3 + \Delta \alpha_5)$
	S_{11}	$\frac{1}{\sqrt{2}}(\Delta \beta_2 - \Delta \beta_6)$
	S_{12}	$\frac{1}{\sqrt{2}}(\Delta \beta_3 - \Delta \beta_5)$
B_1	S_{13}	$\frac{1}{\sqrt{2}}(\Delta R_1 - \Delta R_6)$
	S_{14}	$\frac{1}{\sqrt{2}}(\Delta R_2 - \Delta R_5)$
	S_{15}	$\frac{1}{\sqrt{2}}(\Delta R_3 - \Delta R_4)$
	S_{16}	$\frac{1}{\sqrt{2}}(\Delta r_2 - \Delta r_6)$
	S_{17}	$\frac{1}{\sqrt{2}}(\Delta r_3 - \Delta r_5)$
	S_{18}	$\frac{1}{\sqrt{2}}(\Delta \alpha_2 - \Delta \alpha_6)$
	S_{19}	$\frac{1}{\sqrt{2}}(\Delta \alpha_3 - \Delta \alpha_5)$
	S_{20}	$\Delta \beta_4$
	S_{21}	$\frac{1}{\sqrt{2}}(\Delta \beta_2 + \Delta \beta_6)$
	S_{22}	$\frac{1}{\sqrt{2}}(\Delta \beta_3 + \Delta \beta_5)$

Table 6.3.

Individual Force Constants for Pyridine and Pyridine-XY

In-plane Constants	
f_R	5·553
$f_{R\,oR}$	0·633
f_{RmR}	0·113
f_{RpR}	0·573
f_r	5·093
f_{ror}	0·025
f_{rmr}	0·008
f_{rpr}	-0·040
f_β	0·864
$f_{\beta o\beta}$	0·012
$f_{\beta m\beta}$	-0·018
$f_{\beta p\beta}$	-0·019
f_α	1·031
$f_{\alpha o\alpha}$	0·185
$f_{Ro\alpha}$	-0·180
$f_{Ro\beta}$	0·043
$f_{Rm\beta}$	-0·063
$f_{Rp\beta}$	0·043
$f_{\alpha o\beta}$	-0·127

UNITS: $x10^5$ dynes/cm.

ALL OTHER CONSTANTS ASSUMED ZERO

Table 6.4.

Pyridine Frequencies (all given in $cm.^{-1}$)

Mode	Observed	Calculated using 'LINDA' program	Using Schachtschneider G matrix program,	Long and Thomas (ref. 104)
A_1 vibrations				
ν_1	3054	3076	3076	3075
ν_2	3054	3053	3053	3052
ν_3	3036	3069	3069	3069
ν_4	1580	1600	1600	1597
ν_5	1482	1487	1487	1486
ν_6	1218	1175	1175	1178
ν_7	1069	1031	1031	1030
ν_8	1030	1007	1007	1007
ν_9	990	985	985	981
ν_{10}	603	605	605	605
B_1 vibrations				
ν_{11}	3083	3078	3078	3078
ν_{12}	3054	3045	3045	3044
ν_{13}	1572	1576	1576	1575
ν_{14}	1436	1426	1426	1420
ν_{15}	1375	1313	1313	1311
ν_{16}	1217	1251	1251	1249
ν_{17}	1148	1155	1155	1154
ν_{18}	1068	1052	1052	1056
ν_{19}	652	615	615	615

(a) the Schachtschneider program gives the correct G matrix,

(b) the correct f matrix is being used (see table 6.3).

In view of the similarity of the pyridine and pyridine-IX complexes the numbering of atoms, co-ordinates, group theory, and the calculation of the g matrix, will be left to the next section.

2. Calculation for Pyridine-IX Complexes.

(i) Group Theory.

Both pyridine and pyridine-IX belong to the point group C_{2v}, and possess the following elements of symmetry: E, C_{2v} and $2\sigma_v$.

Pyridine.

The vibrational representation reduces as,

$$\Gamma_{vib} = 10A_1 + 3A_2 + 9B_1 + 5B_2 \quad (27 \text{ vibrations})$$

The A_2 vibrations are infrared inactive but all vibrations should be Raman active.

Pyridine-IX Complexes.

The vibrational representation reduces as,

$$\Gamma_{vib} = 12A_1 + 11B_1 + 3A_2 + 7B_2 \quad (33 \text{ vibrations})$$

The extra vibrations on complexation are,

$$2A_1 + 2B_1 + 2B_2$$

Pyridine-XYZ Complexes.

$$\Gamma_{vib} = 13A_1 + 3A_2 + 12B_1 + 8B_2 \quad (36 \text{ vibrations})$$

The extra vibrations on complexation are $3A_1 + 3B_1 + 3B_2$

(ii) Numbering of Atoms and Co-ordinates.

The geometry of the pyridine molecule has been determined from microwave spectroscopy.[172] It was found that there was a significant deviation from the structure of a regular hexagon. The C-N and C-C distances are 1·340 and 1·394Å respectively (see Figure 6.2.). The numbering system is also shown in Figure 6.2.

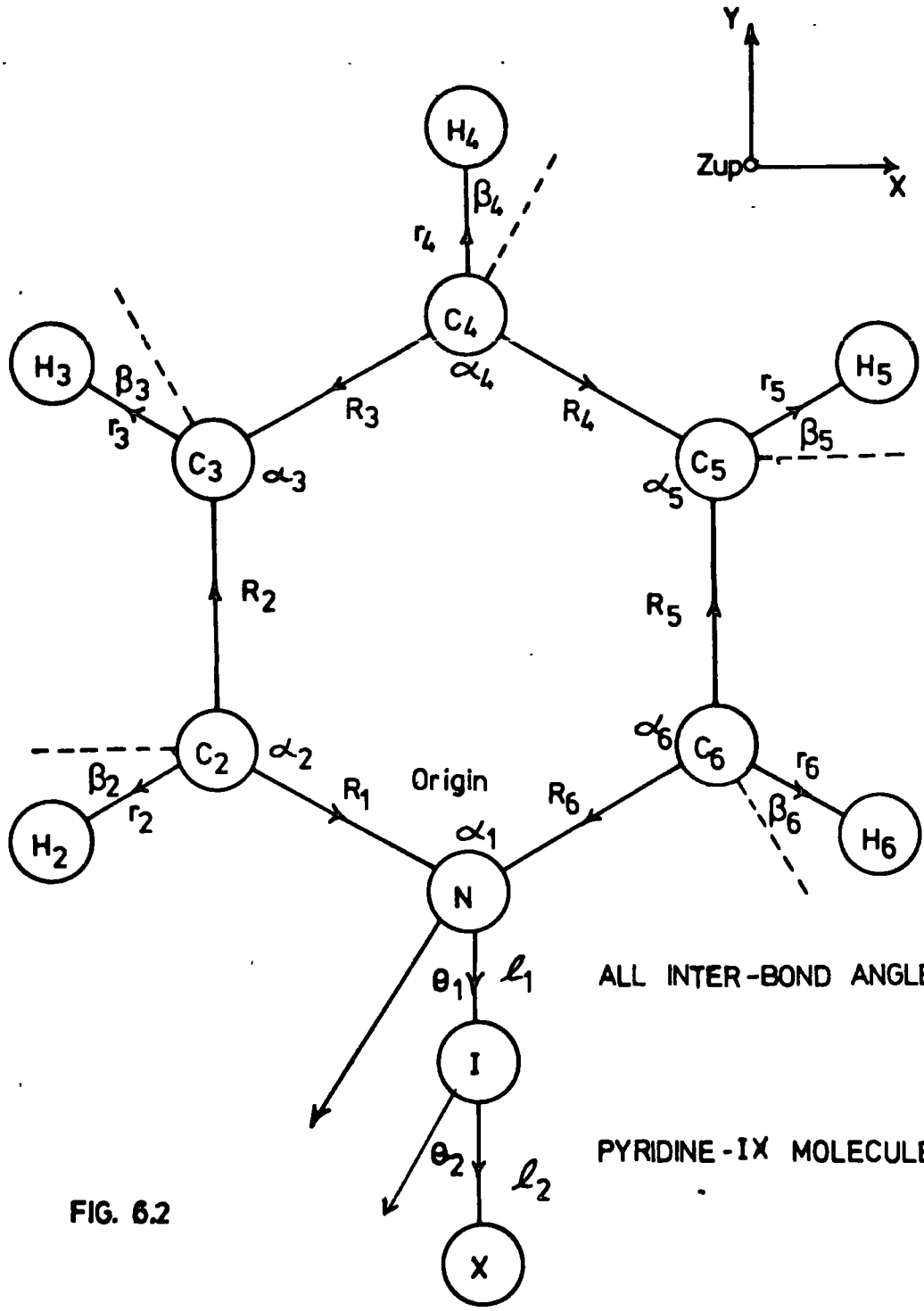

ALL INTER-BOND ANGLES 120°

PYRIDINE-IX MOLECULE (C_{2v})

FIG. 6.2

The full set of geometric parameters is as follows,

$$\alpha_1 = 116^{\circ}50'$$

$$\alpha_4 = 118^{\circ}20'$$

$$\alpha_5 = 118^{\circ}32'$$

$$\alpha_6 = 123^{\circ}53'$$

$$\beta_5 = 121^{\circ}18'$$

$$\beta_6 = 115^{\circ}53'$$

$R_4 = 1{\cdot}3944\text{Å}$ $\quad$ $r_4 = 1{\cdot}0773\text{Å}$

$R_5 = 1{\cdot}3945\text{Å}$ $\quad$ $r_5 = 1{\cdot}0805\text{Å}$

$R_6 = 1{\cdot}3402\text{Å}$ $\quad$ $r_6 = 1{\cdot}0843\text{Å}$

In view of the approximations made in the force field it was decided to assume a regular hexagonal shape for the ring. In order to be consistent with the work of Crawford and Miller[173] C-C and C-H bond lengths of 1·39Å and 1·08Å respectively were used. Furthermore, the geometry of the complex in chloroform solution (where the free donor and free acceptor frequencies were compared with the complex frequencies) is unknown. In the absence of any further information, the 'regular hexagon approximation' seems a reasonable approximation.

(iii) Symmetry Co-ordinates Used.

The symmetry co-ordinates used for pyridine are shown in Table 6.2. and have been discussed above. In the pyridine-IX complex four extra symmetry co-ordinates are required, for the $2a_1 + 2b_1$ extra planar vibrations. The extra co-ordinates used were as shown in Table 6.5.

(iv) Outline of the Calculation of the g Matrix.

In order to read the geometry of the molecule into the program a system of axes and an origin must be chosen. The choice is arbitrary. In order to be consistent with Long and Thomas[104] we have used the same numbering system. Our choice of origin was the crossing point of the bisector of the

line joining atom C_2 with atom C_6 (see Figure 6.2.). From Figure 6.2. it can be seen that the Cartesian co-ordinates of the atoms are as given in Table 6.6.

Table 6.5.

Extra Nielson-Berryman Co-ordinates for the Pyridine-IX Complex

Mode	
$\underline{A_1}$	
S_{23}	$\Delta 1_1$
S_{24}	$\Delta 1_2$
$\underline{B_1}$	
S_{25}	$\frac{1}{\sqrt{2}}(\Delta\theta_1 + \Delta\theta_2)$
S_{26}	$\frac{1}{\sqrt{2}}(\Delta\theta_1 - \Delta\theta_2)$

Table 6.6.

Cartesian Co-ordinates for Pyridine and Pyridine-IC1

Atom	No.	X/Å	Y/Å	Z/Å
N	1	0	-0•695	All zero since molecule is planar
C_2	2	-1•205	0	
C_3	3	-1•205	1•39	
C_4	4	0	2•085	
C_5	5	1•205	1•39	
C_6	6	1•205	0	
H_2	7	-2•141	-0•504	
H_3	8	-2•141	1•894	
H_4	9	0	3•165	
H_5	10	2•141	1•894	
H_6	11	2•141	-0•504	
I	12	0	-2•955	
C1	13	0	-5•465	

(v) Evaluation of the g Matrix.

The program 'LINDA' supplied by courtesy of Dr. Steele had sub-routines to describe the ΔR, Δr, $\Delta\alpha$, and $\Delta\beta$ co-ordinates. These sub-routines are used in the calculation of the vibrational frequencies. The calculated frequencies of pyridine have been discussed previously and are listed in Table 6.4.

Unfortunately 'LINDA' did not possess a sub-routine to describe the $\Delta\theta_2$ co-ordinate. This is the linear inplane bending of the N-I-X part of the molecule.

For this reason we had to resort to the calculation of the G matrix using the program originally written by J.H. Schachtschneider. The program evaluates B and G matrix elements for six types of internal co-ordinates for configurations of up to 29 atoms, and for an arbitrary number of isotopically modified molecules. The input data are: the masses and Cartesian co-ordinates of the atoms, a control card describing each internal co-ordinate, and a U matrix.

The control card describing the internal co-ordinate is practically identical to the analogous one used in 'LINDA'. There are 8 parameters on the card i.e. NI, NCOD, N1, N2, N3, N4, N5 and N6. NI gives the number assigned to the internal co-ordinate, NCOD is a code number identifying the type of internal co-ordinate, and N1, N2, N3, N4, N5 and N6 give the numbers of the atoms defining the internal co-ordinates.

The B matrix is evaluated by the s vector method. Unit vectors along the bonds are expressed in Cartesian co-ordinates.

$$e_{ij} = [(x_j - x_i)\vec{i} + (y_j - y_i)\vec{j} + (z_j - z_i)\vec{k}]/r_{ij}$$

The g matrix is related to the s vectors by,

$$g_{ij} = \sum_{k=1}^{3N} s_{ik} \cdot s_{jk} \mu_k \qquad \ldots\ldots \quad [6.17]$$

In view of the problems caused by the linear valence angle bending co-ordinate a very brief description of the s vectors referring to this co-ordinate follows.[174]

Linear Valence Angle Bending, $r_{ixjx}\Delta\theta$,

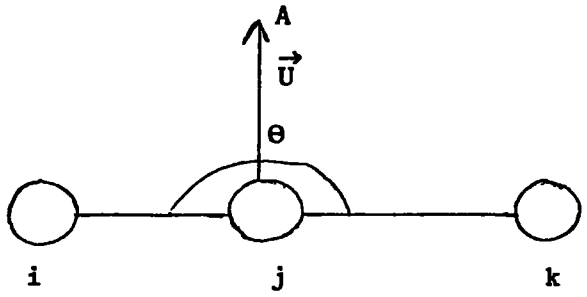

Fig. 6.3.

Let $\vec{U}$ be a unit vector to point A perpendicular to i-j-k, and $\vec{UP}$ a unit vector perpendicular to the plane of A-j-k (see Figure 6.3.)

then,

$$\vec{UP} = e_{jk} \times \vec{U}$$

The s vectors for the in plane perpendicular bending co-ordinates are

$$\vec{s}_i(\theta) = -r_{ixjx}\vec{U}/r_{ji}$$

$$\vec{s}_k(\theta) = -r_{ixjx}\vec{U}/r_{jk}$$

$$\vec{s}_j = -(\vec{s}_i(\theta) + \vec{s}_k(\theta))$$

The G matrices for pyridine, pyridine-IBr and pyridine-IC1 obtained using the Schachtschneider program were used with the programme 'LINDA' as explained previously. Exactly the same geometry as for the pyridine molecule was used in both the pyridine, and complexed pyridine calculations. The IX acceptor was assumed to lie along the C_2 axis as indicated by the crystal structure.[109] The extra information required on the N-I and I-X distances are shown in Table 6.7.

(vi) The f Matrix Used.

The first 22 rows and columns of the f matrix in Table 6.8. represent the f matrix used for pyridine. Rows 23, 24, 25, 26 contain the additional force constants relating to the pyridine-IX complex. The force constants for the D-I and I-X bonds were calculated as described in Appendix B (using

Table 6.7.

Complex	N-I Distance/ Å	I-X Distance/ Å	Reference
Pyridine-ICl	2·26	2·51	109b
'Free' ICl		2·32	109b
Pyridine-IBr	2·26	2·66	109a
Free-IBr		2·47	109a

the triatomic molecule approximation). The interaction force constant k_{13} was also evaluated although a completely unambiguous result for k_{13} was not obtained. It was not found necessary to alter the pyridine force field to get a good frequency fit. It was however, necessary to introduce a few small cross terms in columns 23 - 26 (see discussion below).

(vii) The Program Used to Calculate the Vibrational Frequencies from the Force Field

Modern computing routines and programs for deriving eigenvalues and eigenvectors lend themselves to the solution of symmetric matrices. It is therefore necessary to convert the problem into an alternative form in which the matrices are symmetric. This also has the advantage that any redundant co-ordinates need not be eliminated. Gussoni and Zerbi[175] have outlined a method of eliminating the redundancies. This is necessary where the secular equation is set up in the form $|F-G^{-1}\Lambda| L = 0$ because problems with the zero roots occur.

The flow diagram reproduced by kind permission from 'Theory of Vibrational Spectroscopy' by D. Steele[68] indicates the stages in the program (Fig. 6.3.).

(a) The Cartesian co-ordinate system, as described previously for pyridine, is read in on cards. The computer is thus informed of the relative positions in space of the atoms.

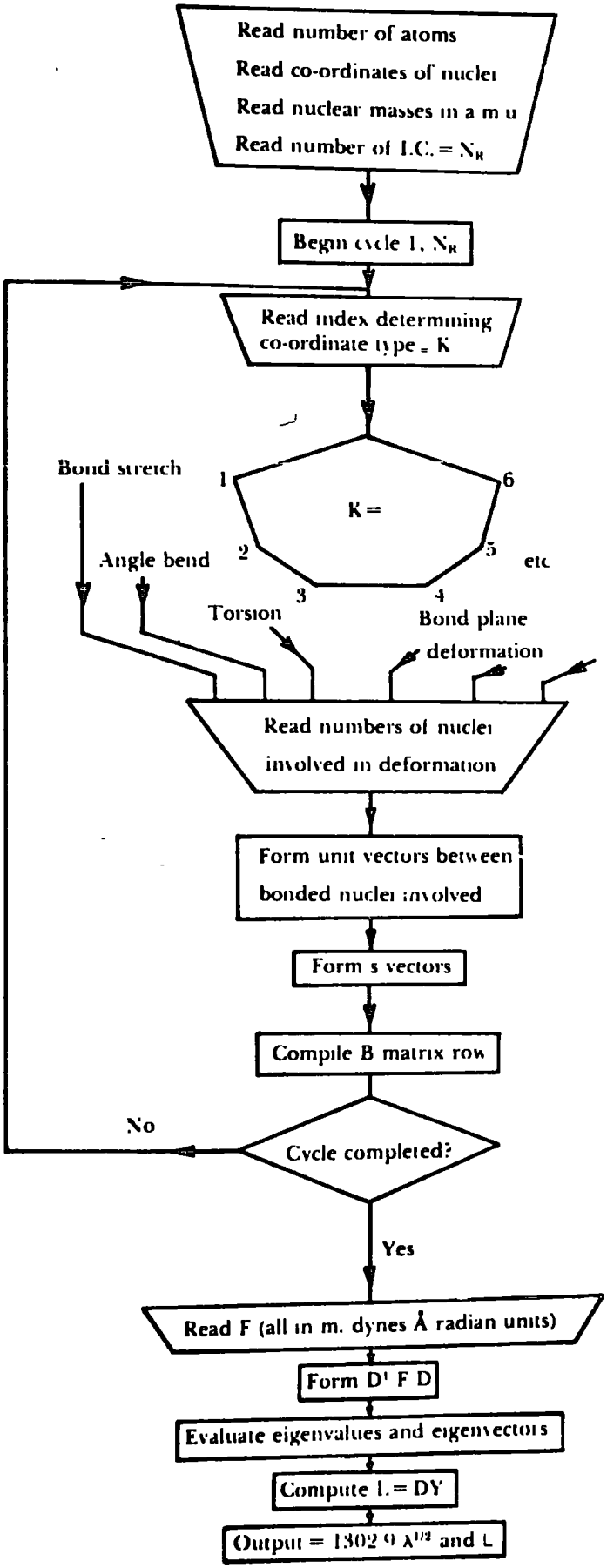

Fig. 6.3.

Reproduced by permission from Ref. 68.

(b) The appropriate s vectors for each co-ordinate are calculated and the B matrix is then calculated for the molecule and printed out. Hence the G matrix is evaluated and printed for examination.

(c) The eigenvalues and eigenvectors are then evaluated using the method described by Steele (ref. 68, pp. 26-28 and pp. 100-102). The method[176,177] involves diagonalising the matrix G giving a set of eigenvalues, Λ', and eigenvectors, A

$$GA = A\Lambda'$$

The secular determinant then takes the form

$$W^{T}FWY = Y\Lambda'$$

where $W = A\Lambda'^{\frac{1}{2}}$ ($WW^{T} = G$). The matrix $W^{T}FW$ is symmetric and has the same eigenvalues as GF and eigenvectors (Y) given by $L = WY$.

(d) Finally, the potential energy matrix is calculated from the matrix $L^{\dagger}FL$ (- this is also normalised) and this is printed in a way which shows the contribution from each symmetry co-ordinate to a given normal mode.

(viii) Results and Discussion.

The results of the calculations made on the whole complex molecule are shown in Tables 6.9 - 6.12 (on the following pages). The different force field employed in attempts to get better fits to the observed frequencies are indicated below and are referred to by a 'set No.' in Table 6.11 and 6.12. The basic initial force field of Long and Thomas for pyridine (force constants given in Table 6.3) was employed throughout with the exception of the change in f_R described below.

Table 6.8.

	1	2	3	4	5	6	7	8	9	10	11	12	13	14	15	16	17	18	19	20	21	22	23	24	25	26
	ΔR_1	ΔR_2	ΔR_3	ΔR_4	ΔR_5	ΔR_6	Δr_2	Δr_3	Δr_4	Δr_5	Δr_6	$\Delta\alpha_1$	$\Delta\alpha_2$	$\Delta\alpha_3$	$\Delta\alpha_4$	$\Delta\alpha_5$	$\Delta\alpha_6$	$\Delta\beta_2$	$\Delta\beta_3$	$\Delta\beta_4$	$\Delta\beta_5$	$\Delta\beta_6$	Δl_1	Δl_2	$\Delta\theta_1$	$\Delta\theta_2$
1 ΔR_1	5·553	0·633	0·113	0·573	0·113	0·633						−0·180	−0·180					−0·043	+0·063	−0·043	0·043	−0·063	0·1	0·05	0·1	–
2 ΔR_2	0·633	5·553	0·633	0·113	0·573	0·113							−0·180	−0·180				0·043	−0·043	+0·063	−0·043	0·043				
3 ΔR_3	0·113	0·633	5·553	0·633	0·113	0·573								−0·180	−0·180			−0·063	0·043	−0·043	+0·063	−0·043				
4 ΔR_4	0·573	0·113	0·633	5·553	0·633	0·113									−0·180	−0·180		0·043	−0·063	0·043	−0·043	+0·063				
5 ΔR_5	0·113	0·573	0·113	0·633	5·553	0·633										−0·180	−0·180	−0·043	0·043	−0·063	0·043	−0·043				
6 ΔR_6	0·633	0·113	0·573	0·113	0·633	5·553						−0·180					−0·180	+0·063	−0·043	0·043	−0·063	0·043	0·1	0·05	0·1	–
7 Δr_2							5·093	0·025	0·008	−0·040	0·008															
8 Δr_3							0·025	5·093	0·025	0·008	−0·040															
9 Δr_4							0·008	0·025	5·093	0·025	0·008															
10 Δr_5							−0·040	0·008	0·025	5·093	0·025															
11 Δr_6							0·008	−0·040	0·008	0·025	5·093															
12 $\Delta\alpha_1$	−0·180					−0·180						1·031	0·185				0·185	+0·127				−0·127	0·100		0·10	0·10
13 $\Delta\alpha_2$	−0·180	−0·180										0·185	1·031	0·185					+0·127							
14 $\Delta\alpha_3$		−0·180	−0·180										0·185	1·031	0·185			−0·127		+0·127						
15 $\Delta\alpha_4$			−0·180	−0·180										0·185	1·031	0·185			−0·127		+0·127					
16 $\Delta\alpha_5$				−0·180	−0·180										0·185	1·031	0·185			−0·127		+0·127				
17 $\Delta\alpha_6$					−0·180	−0·180						0·185				0·185	1·031				−0·127					
18 $\Delta\beta_2$	−0·043	0·043	−0·063	0·043	−0·043	+0·063						+0·127		−0·127				0·864	0·012	−0·018	−0·019	−0·018				
19 $\Delta\beta_3$	+0·063	−0·043	0·043	−0·063	0·043	−0·043							+0·127		−0·127			0·012	0·864	+0·012	−0·018	−0·019				
20 $\Delta\beta_4$	−0·043	+0·063	−0·043	0·043	−0·063	0·043								+0·127		−0·127		−0·018	0·012	0·864	0·012	−0·018				
21 $\Delta\beta_5$	0·043	−0·043	+0·063	−0·043	0·043	−0·063									+0·127		−0·127	−0·019	−0·018	0·012	0·864	0·012				
22 $\Delta\beta_6$	−0·063	0·043	−0·043	+0·063	−0·043	0·043						−0·127				+0·127		−0·018	−0·019	−0·018	0·012	0·864				
23 Δl_1																							0·6	0·1		
24 Δl_2																							0·1	1·41		
25 $\Delta\theta_1$																									0·10	0·05
26 $\Delta\theta_2$																									0·05	0·10

Table 6.9A.

Potential Energy Matrix for the a_1 Vibrations of Pyridine (Force Field of Long and Thomas)

$\bar{\nu}_{obs}/cm.^{-1}$	3054	3054	3036	1580	1482	1218	1069	1030	990	603
$\bar{\nu}_{calc}/cm.^{-1}$	3076	3069	3053	1600	1487	1175	1031	1007	985	605
mode	ν_1	ν_2	ν_3	ν_4	ν_5	ν_6	ν_7	ν_8	ν_9	ν_{10}
S_1 C-C MOTION	0·0	0·2	0·0	9·8	14·4	1·5	23·7	0·1	38·3	3·2
S_2 C-C MOTION	0·1	0·1	0·3	42·3	0·0	6·3	0·2	1·7	26·2	14·7
S_3 C-C MOTION	0·7	0·0	0·1	10·8	13·8	1·8	30·0	4·4	21·6	3·6
S_4 C-H MOTION	38·6	14·0	46·0	0·3	0·2	0·1	0·1	0·3	0·1	0·1
S_5 C-H MOTION	1·3	81·6	15·7	0·1	0·1	0·0	0·1	0·3	0·2	0·0
S_6 C-H MOTION	59·1	2·9	36·8	0·1	0·1	0·0	0·2	0·1	0·6	0·0
S_7 α-DEFORMATION	0·0	0·2	0·0	5·0	1·6	3·0	0·2	17·8	2·6	24·0
S_8 α-DEFORMATION	0·0	0·1	0·6	5·4	1·5	3·7	0·2	17·9	3·1	22·6
S_9 α-DEFORMATION	0·1	0·5	0·0	2·6	0·7	1·4	9·1	28·2	3·3	12·1
S_{10} α-DEFORMATION	0·1	0·4	0·4	2·6	0·8	1·9	9·0	28·3	3·6	11·2
S_{11} β-DEFORMATION	0·0	0·0	0·0	10·0	34·3	39·0	14·1	0·6	0·2	4·2
S_{12} β-DEFORMATION	0·0	0·0	0·0	11·0	32·4	41·2	13·1	0·3	0·2	4·3

Table 6.9B

Potential Energy Matrix for the b_1 Vibrations of Pyridine (Force Field of Long and Thomas)

$\bar{\nu}_{obs}/cm.^{-1}$		3083	3054	1572	1439	1375	1217	1148	1068	652
$\bar{\nu}_{calc}/cm.^{-1}$		3078	3045	1576	1426	1313	1251	1155	1052	615
mode		ν_{11}	ν_{12}	ν_{13}	ν_{14}	ν_{15}	ν_{16}	ν_{17}	ν_{18}	ν_{19}
S_{13}	C-C MOTION	0·1	0·2	18·1	5·1	11·1	35·6	7·0	5·3	10·7
S_{14}		0·4	0·0	0·8	22·5	18·3	5·0	7·1	37·7	-
S_{15}		0·1	0·2	36·6	0·8	14·8	7·6	17·0	8·6	9·1
S_{16}	C-H MOTION	49·5	49·3	0·2	0·4	0·0	0·2	0·0	0·2	0·1
S_{17}		49·7	49·1	0·7	0·1	0·0	0·0	0·0	0·3	0·1
S_{18}	α-DEFORMATION	0·1	0·6	6·2	6·2	0·2	4·9	0·6	3·2	36·8
S_{19}		0·1	0·6	11·8	0·1	0·0	1·2	1·3	8·0	37·0
S_{20}	β-DEFORMATION	0·0	0·0	15·7	23·0	13·0	3·6	31·3	13·7	3·0
S_{21}		0·0	0·0	8·3	2·3	42·1	18·0	7·2	14·5	1·4
S_{22}		0·0	0·0	1·6	39·6	0·5	23·9	28·4	8·5	1·8

Table 6.10A.

Comparison of Calculated Frequencies for Pyridine and Pyridine-IX Complexes (a_1 Modes)

Mode	Pyridine $\nu_{obs}/cm.^{-1}$	Pyridine $\nu_{calc}/cm.^{-1}$	Pyridine-ICl $\nu_{obs}/cm.^{-1}$	Pyridine-ICl $\nu_{calc}/cm.^{-1}$ Set 1	Pyridine-ICl $\nu_{calc}/cm.^{-1}$ Set 2	Pyridine-ICl $\nu_{calc}/cm.^{-1}$ Set 3	Pyridine-IBr $\nu_{obs}/cm.^{-1}$	Pyridine-IBr $\nu_{calc}/cm.^{-1}$ Set 1	Pyridine-IBr $\nu_{calc}/cm.^{-1}$ Set 2	Pyridine-IBr $\nu_{calc}/cm.^{-1}$ Set 3	Pyridine-IBr $\nu_{calc}/cm.^{-1}$ Set 4
ν_1	3054	3075	-	3075	3076	3076	-	3076	3076	3076	3076
ν_2	3054	3069	-	3069	3069	3069	-	3069	3069	3069	3070
ν_3	3036	3036	-	3053	3053	3053	-	3053	3053	3053	3053
ν_4	1580	1600	1601	1602	1602	1616	1602	1602	1602	1602	1617
ν_5	1482	1487	-	1489	1488	1494	1478	1489	1488	1488	1493
ν_6	1218	1175	1212	1177	1178	1178	1212	1177	1177	1178	1179
ν_7	1068	1031	1067	1035	1033	1039	1068	1034	1033	1033	1039
ν_8	1029	1007	1034	1016	1013	1013	1033	1015	1013	1022	1023
ν_9	992	985	1011	995	993	1002	1010	994	993	990	999
ν_{10}	605	605	631	625	619	622	628	624	620	635	637
ν_{11}	-	-	290	289	294	294	202	201	204	201	201
ν_{12}	-	-	140	135	133	133	135	128	127	125	125

Table 6.10B

Comparison of Calculated Frequencies for Pyridine and Pyridine-IX Complexes (b_1 Modes)

Mode	Pyridine $\nu_{obs}/cm.^{-1}$	Pyridine $\nu_{calc}/cm.^{-1}$	Pyridine-IC1 $\nu_{obs}/cm.^{-1}$	Pyridine-IC1 $\nu_{calc}/cm.^{-1}$ Set 1	Pyridine-IC1 $\nu_{calc}/cm.^{-1}$ Set 3	Pyridine-IBr $\nu_{obs}/cm.^{-1}$ Set 4	Pyridine-IBr $\nu_{calc}/cm.^{-1}$ Set 1	Pyridine-IBr $\nu_{calc}/cm.^{-1}$ Set 3	Pyridine-IBr $\nu_{calc}/cm.^{-1}$ Set 4
ν_{13}	3083	3078		3078	3078		3078	3078	3078
ν_{14}	3054	3045		3045	3045		3045	3045	3045
ν_{15}	1572	1576		1578	1590	1578	1579	1579	1593
ν_{16}	1439	1426	1451	1430	1434	1450	1433	1433	1439
ν_{17}	1375	1313	1353	1313	1325	1355	1313	1313	1325
ν_{18}	1217	1251	1212	1259	1264	1212	1265	1265	1273
ν_{19}	1148	1155	1155	1155	1159	1155	1155	1155	1160
ν_{20}	1068	1052	1067	1057	1061	1068	1060	1060	1066
ν_{21}	652	615		617	618	652	616	616	618
ν_{22}	-	-	-	169	125	-	219	219	220
ν_{23}	-	-	-	70	46·5	-	-	-	-

Table 6.11A.

Potential Energy Matrix for the a_1 Vibrations of Pyridine-ICl

Mode	ν_1				ν_2				ν_3				ν_4				ν_5				ν_6				ν_7				ν_8				ν_9				ν_{10}				ν_{11}				ν_{12}			
ν_{obs}/cm.$^{-1}$	-				-				-				1601				1478[a]				1212				1067				1034				1010				631				140				290			
ν_{calc}/cm.$^{-1}$	3075	3076	3076	3076	3069	3069	3070	3070	3053	3053	3053	3053	1602	1616	1614	1616	1489	1494	1492	1493	1177	1178	1177	1178	1035	1039	1037	1038	1016	1013	1013	1021	995	1002	998	998	625	622	625	634	135	133	133	129	289	294	294	294
Set No.	1	3	4	5	1	3	4	5	1	3	4	5	1	3	4	5	1	3	4	5	1	3	4	5	1	3	4	5	1	3	4	5	1	3	4	5	1	3	4	5	1	3	4	5	1	3	4	5
S_1	0·0	0·0	0·0	0·0	0·2	0·2	0·2	0·2	0·0	0·0	0·0	0·0	10·3	10·4	9·9	10·3	14·3	14·9	15·0	14·7	1·9	1·7	1·6	1·7	31·9	29·2	24·2	25·9	0·1	0·3	0·0	0·1	26·2	30·2	38·4	35·0	5·1	4·5	3·9	4·7	0·4	0·8	0·1	0·1	0·2	0·0	0·0	0·0
S_2 ΔR_{CC}	0·1	0·1	0·1	0·1	0·1	0·1	0·1	0·1	0·3	0·3	0·3	0·3	41·9	42·7	42·9	42·7	0·0	0·0	0·0	0·0	5·6	5·4	5·7	5·3	0·2	0·0	0·2	0·1	0·5	0·1	0·2	0·3	31·5	32·2	30·5	31·6	13·1	13·3	13·3	13·5	0·7	1·3	1·5	1·5	0·6	0·0	0·0	0·0
S_3	0·7	0·7	0·7	0·7	0·0	0·0	0·0	0·0	0·1	0·1	0·1	0·1	10·4	10·7	11·0	10·7	14·2	14·7	14·3	14·7	1·8	1·7	1·7	1·7	25·9	28·0	32·0	31·0	0·6	0·0	1·1	0·2	34·8	33·5	26·1	28·4	3·7	3·7	3·6	3·6	0·1	0·1	0·1	0·3	0·1	0·0	0·0	0·0
S_4	38·6	39·1	39·1	39·1	14·1	13·3	13·3	13·3	46·0	46·1	46·2	46·2	0·2	0·3	0·3	0·3	0·2	0·2	0·2	0·2	0·1	0·1	0·1	0·1	0·1	0·1	0·1	0·2	0·1	0·1	0·2	0·1	0·3	0·3	0·1	0·2	0·1	0·1	0·1	0·1	0·0	0·0	0·0	0·0	0·0	0·0	0·0	0·0
S_5 ΔR_{CH}	1·3	1·1	1·1	1·1	81·3	82·1	82·1	82·1	15·8	15·4	15·4	15·4	0·1	0·1	0·1	0·1	0·1	0·1	0·1	0·1	0·0	0·0	0·0	0·0	0·1	0·1	0·1	0·1	0·2	0·2	0·3	0·2	0·6	0·5	0·4	0·6	0·0	0·0	0·0	0·0	0·0	0·0	0·0	0·0	0·0	0·0	0·0	0·0
S_6	59·1	58·8	58·8	58·8	2·9	3·1	3·1	3·1	36·8	37·0	37·0	37·0	0·1	0·1	0·1	0·1	0·1	0·1	0·1	0·1	0·0	0·0	0·0	0·0	0·1	0·1	0·2	0·1	0·3	0·3	0·2	0·3	0·3	0·4	0·5	0·3	0·0	0·0	0·0	0·0	0·0	0·0	0·0	0·0	0·0	0·0	0·0	0·0
S_7	0·0	0·0	0·0	0·0	0·2	0·2	0·2	0·2	0·0	0·0	0·0	0·0	5·3	5·1	5·0	5·2	1·7	1·7	1·7	1·7	3·5	3·2	3·1	3·5	3·6	2·1	1·0	3·4	15·6	16·8	17·9	16·2	1·1	0·4	0·5	0·3	19·7	21·0	21·2	19·1	2·6	4·8	4·5	8·1	2·0	0·0	0·0	0·1
S_8 $\Delta\alpha$	0·0	0·0	0·0	0·0	0·1	0·1	0·1	0·1	0·6	0·6	0·6	0·6	5·3	5·2	5·3	5·2	1·7	1·7	1·5	1·7	3·3	3·2	3·3	3·0	3·6	2·1	0·9	3·3	15·5	16·8	17·5	15·7	1·1	0·3	0·5	0·3	23·9	23·7	23·7	25·0	0·3	0·5	0·7	0·6	0·3	0·0	0·0	0·0
S_9	0·1	0·1	0·1	0·1	0·5	0·5	0·5	0·5	0·0	0·0	0·0	0·0	2·6	2·6	2·6	2·6	0·7	0·7	0·7	0·7	1·8	1·6	1·6	1·9	1·3	2·9	5·4	1·3	32·9	32·1	31·0	33·1	1·4	0·5	0·4	1·0	9·6	10·3	10·2	8·8	1·5	2·7	3·0	5·7	1·1	0·0	0·0	0·0
S_{10}	0·1	0·1	0·1	0·1	0·4	0·4	0·4	0·4	0·4	0·4	0·4	0·4	2·6	2·6	2·6	2·6	0·7	0·7	0·8	0·7	1·6	1·6	1·7	1·4	1·3	2·9	5·5	1·4	32·8	32·1	30·6	32·6	1·3	0·5	0·4	0·9	12·2	12·0	12·3	13·4	0·1	0·2	0·1	0·1	0·1	0·0	0·0	0·0
S_{11} $\Delta\beta$	0·0	0·0	0·0	0·0	0·0	0·0	0·0	0·0	0·0	0·0	0·0	0·0	10·4	9·9	9·5	9·8	33·1	32·8	33·7	32·9	40·4	40·5	39·6	40·6	14·8	15·8	15·4	15·6	0·0	0·0	0·2	0·0	0·2	0·1	0·1	0·0	4·4	4·4	4·4	4·5	0·1	0·1	0·1	0·2	0·1	0·0	0·0	0·0
S_{12} $\Delta\beta$	0·0	0·0	0·0	0·0	0·0	0·0	0·0	0·0	0·0	0·0	0·0	0·0	10·4	10·1	10·6	10·2	33·0	32·2	31·7	32·3	39·8	40·7	41·3	40·6	15·9	16·0	14·6	16·0	0·0	0·1	0·2	0·0	0·0	0·0	0·2	0·1	4·1	4·2	4·2	4·2	0·1	0·3	0·3	0·4	0·1	0·0	0·0	0·0
S_{13} Δr(H-I)	0·0	0·0	0·0	0·0	0·0	0·0	0·0	0·0	0·0	0·0	0·0	0·0	0·2	0·1	0·1	0·2	0·2	0·2	0·2	0·2	0·3	0·2	0·2	0·3	1·4	0·7	0·4	0·8	1·3	1·0	0·8	1·0	1·3	1·2	2·0	1·3	3·9	3·1	3·2	3·1	73·1	89·1	89·4	82·7	0·6	2·1	2·0	1·6
S_{14} Δr(I-Cl)	0·0	0·0	0·0	0·0	0·0	0·0	0·0	0·0	0·0	0·0	0·0	0·0	0·0	0·0	0·0	0·0	0·0	0·0	0·0	0·0	0·0	0·0	0·0	0·0	0·0	0·0	0·0	0·0	0·0	0·0	0·0	0·0	0·0	0·0	0·0	0·0	0·1	0·0	0·0	0·0	21·0	0·2	0·1	0·1	94·8	97·6	97·6	98·0

[a] Very weak band - this is value for pyridine-IBr.

Table 6,11B

Potential Energy Matrix for the b_1 Vibrations of Pyridine-ICl

Mode		ν_{13}			ν_{14}			ν_{15}			ν_{16}			ν_{17}			ν_{18}			ν_{19}			ν_{20}			ν_{21}			ν_{22}			ν_{23}		
$\bar{\nu}_{obs}/cm.^{-1}$		-			-			-			1451			1353			1212			1155			1067			-			-			-		
$\bar{\nu}_{calc}/cm.^{-1}$		3078	3078	3078	3045	3045	3045	1578	1590	1590	1430	1434	1434	1313	1325	1325	1259	1264	1264	1155	1159	1159	1057	1061	1061	617	618	618	169	125	126	70	47	47
Set		1	3	6	1	3	6	1	3	6	1	3	6	1	3	6	1	3	6	1	3	6	1	3	6	1	3	6	1	3	6	1	3	6
S_{15}	ΔR_{CC}	0·1	0·1	0·1	0·2	0·2	0·2	19·0	19·2	19·2	5·6	4·6	4·6	10·8	17·4	17·4	34·5	30·4	30·4	6·4	4·5	4·5	3·6	4·3	4·3	10·5	10·3	10·3	2·0	1·1	1·1	0·0	0·0	0·0
S_{16}		0·4	0·4	0·4	0·0	0·0	0·0	0·7	0·7	0·7	22·6	25·1	25·1	17·9	19·6	19·6	5·5	2·8	2·8	6·6	5·0	5·0	37·6	36·7	36·7	0·0	0·0	0·0	0·3	0·1	0·1	0·3	0·1	0·1
S_{17}		0·1	0·1	0·1	0·2	0·2	0·2	36·2	37·4	37·4	0·4	0·6	0·6	14·5	17·8	17·8	9·2	6·4	6·4	17·0	14·1	14·1	7·9	8·1	8·1	9·1	8·9	8·9	0·3	0·1	0·0	0·1	0·0	0·0
S_{18}	ΔR_{CH}	49·9	49·9	49·7	48·9	48·9	49·1	0·3	0·3	0·3	0·5	0·4	0·4	0·0	0·0	0·0	0·2	0·2	0·2	0·0	0·0	0·0	0·2	0·2	0·2	0·1	0·1	0·1	0·3	0·1	0·0	0·0	0·0	0·0
S_{19}		49·3	49·3	49·5	49·6	49·6	49·3	0·7	0·7	0·7	0·1	0·1	0·1	0·0	0·0	0·0	0·0	0·0	0·0	0·0	0·0	0·0	0·3	0·3	0·3	0·1	0·1	0·1	0·3	0·1	0·0	0·0	0·0	0·0
S_{20}	$\Delta\alpha$	0·1	0·1	0·1	0·6	0·6	0·6	6·5	6·4	6·4	6·4	6·1	6·1	0·2	0·0	0·0	4·3	4·7	4·7	0·7	0·7	0·7	2·6	2·6	2·6	36·8	37·0	37·0	0·2	0·1	0·1	0·5	0·2	0·2
S_{21}		0·1	0·1	0·1	0·6	0·6	0·6	11·8	11·6	11·6	0·2	0·2	0·2	0·0	0·0	0·0	0·9	0·9	0·9	1·5	1·5	1·5	8·2	7·8	7·8	36·9	37·2	37·2	0·1	0·1	0·0	0·1	0·1	0·1
S_{22}	$\Delta\beta$	0·0	0·0	0·0	0·0	0·0	0·0	15·0	14·4	14·4	23·6	22·5	22·5	13·2	13·3	13·3	2·6	0·8	0·8	32·3	35·0	35·0	13·7	14·2	14·2	3·0	3·0	3·0	3·0	3·0	0·0	0·0	0·0	0·0
S_{23}		0·0	0·0	0·0	0·0	0·0	0·0	7·9	7·5	7·5	3·0	3·3	3·3	42·8	31·6	31·6	16·0	28·7	28·7	6·6	7·2	7·2	16·4	16·4	16·4	1·4	1·4	1·4	0·1	0·1	0·0	0·0	0·0	0·0
S_{24}		0·0	0·0	0·0	0·0	0·0	0·0	1·7	1·7	1·7	37·1	36·6	36·6	0·6	0·2	0·2	25·6	24·5	24·5	28·8	31·9	31·9	8·3	8·7	8·7	1·8	1·8	1·8	0·1	0·1	0·0	0·0	0·0	0·0
S_{25}	$\Delta\Theta$	0·0	0·0	0·0	0·0	0·0	0·0	0·2	0·1	0·1	0·6	0·3	0·3	0·0	0·0	0·0	1·2	0·7	0·7	0·1	0·0	0·0	1·0	0·5	0·5	0·1	0·0	0·0	97·3	98·5	98·5	0·0	0·0	0·0
S_{26}		0·0	0·0	0·0	0·0	0·0	0·0	0·0	0·0	0·0	0·1	0·1	0·1	0·0	0·0	0·0	0·1	0·1	0·1	0·0	0·0	0·0	0·2	0·1	0·1	0·3	0·1	0·1	0·0	0·0	0·0	99·1	99·6	99·6

Table 6.12B.

Potential Energy Matrix for the b_1 Vibrations of Pyridine-IB-

Mode		ν_{13}			ν_{14}			ν_{15}			ν_{16}			ν_{17}			ν_{18}			ν_{19}			ν_{20}			ν_{21}			ν_{22}		
$\bar{\nu}_{obs}$/cm.$^{-1}$								1578			1450			1355			1212			1155			1068			652					
$\bar{\nu}_{calc}$/cm.$^{-1}$		3078	3078	3078	3045	3045	3045	1579	1579	1593	1433	1433	1439	1313	1313	1325	1265	1265	1273	1155	1155	1160	1060	1060	1066	616	616	618	219	219	220
Set		1	3	5	1	3	5	1	3	5	1	3	5	1	3	5	1	3	5	1	3	5	1	3	5	1	3	5	1	3	5
S_{15}	ΔR_{CC}	0·1	0·1	0·1	0·2	0·2	0·2	19·7	19·7	20·3	5·9	11	5·3	10·7	10·7	18·1	33·3	33·5	27·5	5·9	5·9	4·1	2·8	2·8	2·8	10·2	10·2	9·9	3·7	4·9	4·7
S_{16}		0·4	0·4	0·4	0·0	0·0	0·0	0·6	0·6	0·5	22·4	22·5	24·8	18·0	18·0	20·1	5·7	5·7	2·6	6·3	6·3	4·7	38·1	38·3	37·0	0·0	0·0	0·0	0·5	0·6	0·7
S_{17}		0·1	0·1	0·1	0·2	0·2	0·2	35·8	35·8	36·8	0·2	0·2	0·2	14·5	14·5	18·4	10·1	10·2	7·0	17·0	17·0	14·1	7·3	7·3	7·3	9·2	9·2	9·0	0·1	0·1	0·1
S_{18}	ΔR_{CH}	50·0	50·0	50·0	48·8	48·8	48·8	0·3	0·3	0·3	0·5	0·5	0·5	0·0	0·0	0·0	0·2	0·2	0·2	0·0	0·0	0·0	0·1	0·1	0·1	0·1	0·1	0·1	0·0	0·0	0·0
S_{19}		49·2	49·2	49·2	49·6	49·6	49·6	0·7	0·7	0·7	0·1	0·1	0·1	0·0	0·0	0·0	0·0	0·0	0·0	0·0	0·0	0·0	0·3	0·3	0·3	0·1	0·1	0·1	0·0	0·0	0·0
S_{20}	$\Delta\alpha$	0·1	0·1	0·1	0·6	0·6	0·6	6·8	6·8	6·8	6·3	6·4	6·2	0·2	0·2	0·0	3·8	3·9	4·0	0·7	0·7	0·8	2·2	2·2	2·1	37·3	37·3	37·5	0·4	0·5	0·5
S_{21}		0·1	0·1	0·1	0·6	0·6	0·6	11·7	11·7	11·5	0·2	0·2	0·3	0·0	0·0	0·0	0·7	0·7	0·6	1·6	1·6	1·6	8·4	8·4	8·1	36·8	36·9	37·1	0·1	0·2	0·1
S_{22}	$\Delta\beta$	0·0	0·0	0·0	0·0	0·0	0·0	14·6	14·6	13·7	24·3	24·3	23·6	13·1	13·1	13·0	2·0	2·0	0·2	33·2	33·2	36·1	13·5	13·6	14·1	3·0	3·0	3·0	0·0	0·0	0·0
S_{23}		0·0	0·0	0·0	0·0	0·0	0·0	7·6	7·6	7·1	3·4	3·4	4·0	42·9	42·9	30·3	15·4	15·5	29·1	6·0	6·0	6·4	17·3	17·4	18·3	1·4	1·4	1·4	0·1	0·2	0·2
S_{24}		0·0	0·0	0·0	0·0	0·0	0·0	1·8	1·8	1·9	35·6	35·7	34·2	0·6	0·6	0·1	26·7	26·8	27·2	29·1	29·1	32·2	8·3	8·3	8·7	1·7	1·7	1·7	0·1	0·1	0·1
S_{25}	$\Delta\theta$	0·0	0·0	0·0	0·0	0·0	0·0	0·3	0·3	0·2	0·6	0·5	0·5	0·0	0·0	0·0	1·2	0·9	1·0	0·1	0·1	0·0	0·9	0·7	0·7	0·1	0·1	0·1	52·2	52·9	53·0
S_{26}		0·0	0·0	0·0	0·0	0·0	0·0	0·2	0·2	0·2	0·5	0·4	0·4	0·0	0·0	0·0	1·0	0·7	0·7	0·1	0·0	0·0	0·8	0·4	0·5	0·1	0·0	0·0	42·7	40·5	40·5

Table 6.12A.

Potential Energy Matrix for the a_1 Vibrations of Pyridine-1Br

Mode	ν_1				ν_2				ν_3				ν_4				ν_5				ν_6				ν_7				ν_8				ν_9				ν_{10}				ν_{11}				ν_{12}			
$\tilde{\nu}_{obs}/cm^{-1}$	-				-				-				1602				1478				1212				1068				1033				1010				628				202				133			
$\tilde{\nu}_{calc}/cm.^{-1}$	3076	3076	3076	3076	3060	3060	3070	3070	3053	3053	3053	3053	1602	1602	1617	1616	1480	1488	1493	1494	1177	1177	1179	1178	1034	1033	1039	1040	1015	1013	1023	1015	994	993	999	1004	624	620	637	626	201	204	201	201	128	127	125	128
Set No.	1	2	4	5	1	2	4	5	1	2	4	5	1	2	4	5	1	2	4	5	1	2	4	5	1	2	4	5	1	2	4	5	1	2	4	5	1	2	4	5	1	2	4	5	1	2	4	5
S_1	0·0	0·0	0·0	0·0	0·2	0·2	0·2	0·2	0·0	0·0	0·0	0·0	10·3	10·2	10·4	10·3	14·3	14·3	14·7	14·8	1·8	1·8	1·7	1·8	31·4	29·8	27·2	31·0	0·1	0·2	0·0	6·6	27·2	30·2	31·8	25·6	5·0	4·6	5·1	4·8	0·3	0·0	0·1	0·3	0·3	0·8	0·1	0·3
S_2 ΔR_{CC}	0·1	0·1	0·1	0·1	0·1	0·1	0·1	0·1	0·3	0·3	0·3	0·3	42·0	42·0	42·7	42·7	0·0	0·1	0·0	0·0	5·6	5·7	5·2	5·3	0·1	0·0	0·0	0·1	0·3	0·1	0·8	1·0	31·9	32·5	30·6	29·8	13·4	13·6	13·2	13·0	0·6	0·1	0·5	0·6	0·6	1·4	0·7	0·6
S_3	0·7	0·7	0·7	0·7	0·0	0·0	0·0	0·0	0·1	0·1	0·1	0·1	10·4	10·5	10·6	10·6	14·2	14·1	14·8	14·8	1·8	1·8	1·7	1·7	26·6	28·2	29·1	26·1	0·3	0·0	1·3	1·0	34·7	33·9	28·8	32·6	3·7	3·7	3·6	3·6	0·1	0·0	0·0	0·0	0·1	0·1	0·2	0·0
S_4	38·6	38·6	38·1	38·1	14·0	14·1	13·3	13·3	46·0	46·0	46·2	46·2	0·2	0·3	0·3	0·3	0·2	0·2	0·2	0·2	0·1	0·1	0·1	0·1	0·1	0·1	0·2	0·1	0·1	0·1	0·1	0·1	0·3	0·3	0·3	0·3	0·1	0·1	0·1	0·1	0·0	0·0	0·0	0·0	0·0	0·0	0·0	0·0
S_5 ΔR_{CH}	1·3	1·3	1·1	1·0	81·5	81·5	82·1	82·1	15·8	15·8	15·4	15·4	0·1	0·1	0·1	0·1	0·1	0·1	0·1	0·1	0·0	0·0	0·0	0·0	0·1	0·1	0·0	0·1	0·2	0·2	0·2	0·1	0·5	0·5	0·6	0·6	0·0	0·0	0·0	0·0	0·0	0·0	0·0	0·0	0·0	0·0	0·0	0·0
S_6	39·1	39·1	38·8	38·8	2·9	2·9	3·1	3·1	36·8	36·8	37·0	37·0	0·1	0·1	0·1	0·1	0·1	0·1	0·1	0·1	0·0	0·0	0·0	0·0	0·1	0·1	0·0	0·1	0·3	0·3	0·4	0·4	0·3	0·4	0·3	0·3	0·0	0·0	0·0	0·0	0·0	0·0	0·0	0·0	0·0	0·0	0·0	0·0
S_7	0·0	0·0	0·0	0·0	0·2	0·2	0·2	0·2	0·0	0·0	0·0	0·0	5·3	5·2	5·2	5·2	1·7	1·7	1·7	1·7	3·4	3·4	3·6	3·3	3·1	2·1	3·1	2·9	16·0	17·0	14·9	15·7	0·8	0·2	1·0	1·9	20·0	20·7	18·4	20·2	1·9	0·3	1·6	1·9	2·1	4·8	4·2	2·1
S_8	0·0	0·0	0·0	0·0	0·1	0·1	0·1	0·1	0·6	0·6	0·6	0·6	5·3	5·3	5·2	5·2	1·7	1·6	1·7	1·7	3·3	3·4	2·9	3·2	3·1	2·1	4·9	2·9	15·9	16·9	14·4	15·6	0·7	0·2	1·0	1·9	23·7	23·5	23·2	23·9	0·2	0·0	0·2	0·2	0·2	0·3	0·4	0·2
S_9 $\Delta\alpha$	0·1	0·1	0·1	0·1	0·5	0·5	0·5	0·5	0·0	0·0	0·0	0·0	2·6	2·6	2·7	2·6	0·7	0·7	0·7	0·7	1·7	1·7	1·9	1·7	1·7	3·2	0·3	1·7	32·7	32·1	33·5	32·1	1·0	0·2	2·2	3·0	9·8	10·2	8·4	9·9	1·1	0·2	1·0	1·1	1·2	2·7	2·9	1·2
S_{10}	0·1	0·1	0·1	0·1	0·4	0·4	0·4	0·4	0·4	0·4	0·4	0·4	2·6	2·6	2·6	2·6	0·7	0·7	0·7	0·7	1·6	1·7	1·3	1·6	1·7	3·2	0·3	1·7	32·6	32·1	32·9	32·0	1·0	0·2	2·2	2·9	12·1	11·9	13·6	12·2	0·1	0·0	0·1	0·1	0·1	0·2	0·0	0·1
S_{11}	0·0	0·0	0·0	0·0	0·0	0·0	0·0	0·0	0·0	0·0	0·0	0·0	10·4	10·3	9·9	9·9	33·2	33·4	32·7	32·5	40·3	40·0	40·9	40·8	14·9	15·0	15·0	15·6	0·0	0·0	0·2	0·0	0·2	0·1	0·0	0·2	4·4	4·3	4·6	4·4	0·1	0·0	0·0	0·1	0·1	0·1	0·1	0·1
S_{12} $\Delta\beta$	0·0	0·0	0·0	0·0	0·0	0·0	0·0	0·0	0·0	0·0	0·0	0·0	10·5	10·6	10·1	10·0	33·0	32·9	32·4	32·4	39·9	40·2	40·3	40·4	15·8	15·3	16·3	16·4	0·0	0·1	0·0	0·0	0·0	0·0	0·0	0·0	4·1	4·1	4·2	4·1	0·1	0·0	0·1	0·1	0·1	0·3	0·2	0·1
S_{13} $\Delta r(N-X)$	0·0	0·0	0·0	0·0	0·0	0·0	0·0	0·0	0·0	0·0	0·0	0·0	0·2	0·2	0·2	0·2	0·2	0·2	0·2	0·2	0·3	0·2	0·3	0·3	1·2	0·8	1·3	1·2	1·3	1·0	1·2	1·5	1·3	1·4	1·3	0·9	3·8	3·2	3·7	3·8	0·3	11·9	0·3	0·3	71·1	82·2	68·5	71·1
S_{14} $\Delta r(X-Br)$	0·0	0·0	0·0	0·0	0·0	0·0	0·0	0·0	0·0	0·0	0·0	0·0	0·0	0·0	0·0	0·0	0·0	0·0	0·0	0·0	0·0	0·0	0·0	0·0	0·0	0·0	0·0	0·0	0·0	0·0	0·0	0·0	0·0	0·0	0·0	0·0	0·0	0·0	0·0	0·0	93·3	87·3	93·9	95·4	24·1	7·0	22·7	24·1

Pyridine-ICl (all values in md/Å).

SET 1, $k_{13} = 0{\cdot}6$ $f_R = 5{\cdot}55$

SET 2, $k_{13} = 0{\cdot}1$ $f_R = 5{\cdot}55$

SET 3, $k_{13} = 0{\cdot}1$ $f_R = 5{\cdot}70$

SET 4, $k_{13} = 0{\cdot}1$ $f_R = 5{\cdot}70$ and $f_{R1_1} = 0{\cdot}1$, $f_{R1_2} = 0{\cdot}05$

SET 5, same as Set 4 with $f_{\alpha 1_1} = 0{\cdot}1$

SET 6, same as Set 5 with $f_{\alpha\theta_1} = 0{\cdot}1m$, $f_{\alpha\theta_2} = 0{\cdot}1$

Pyridine-IBr (all values in md/Å)

SET 1, $k_{13} = 0{\cdot}6$ $f_R = 5{\cdot}55$

SET 2, $k_{13} = 0{\cdot}1$ $f_R = 5{\cdot}55$

SET 3, $k_{13} = 0{\cdot}6$ $f_R = 5{\cdot}55$, $f_{R1_1} = 0{\cdot}1$, $f_{R1_2} = 0{\cdot}5$

SET 4, $k_{13} = 0{\cdot}6$ $f_R = 5{\cdot}70$, $f_{R1_1} = 0{\cdot}1$, $f_{R1_2} = 0{\cdot}05$, $f_{\alpha 1_1} = 0{\cdot}1$

SET 5, same as Set 4 with $f_{R\theta_1} = 0{\cdot}1$, $f_{\alpha\theta_1} = 0{\cdot}1$

(a) Explanation of the Frequency Changes.

It can be seen from Tables 6.9. and 6.10. that shifts in frequency on going from pyridine to the complex can mainly be accounted for by changes in the G matrix. With the exception of the ν_7 mode for the pyridine-ICl complex (which is practically unaltered) all the a_1 class frequency shifts are either reproduced quantitatively or are partially reproduced in the correct direction. It is worth noting that the agreement is best for those frequencies where the agreement between calculated and observed values was best in the Long and Thomas calculation on pyridine, i.e. the ν_9 and ν_{10} vibrations. The difference between calculated and observed values is probably due to errors in the Long and Thomas force field.

It is interesting to note that two of the three vibrations with the largest C-C stretching contributions (ν_4 and ν_9) are increased in frequency on complexation. This could be due to an increase in the C-C bond force

constant (i.e. f_R). However, this would imply stronger bonding in the pyridine ring, and the charge transfer model implies that the opposite may occur, i.e. electrons are removed to some extent from the ring. In the absence of a molecular orbital calculation it is pointless to speculate further. Duinker[113] considers the f_R force constant should be $\approx$ 7 md/Å i.e. much higher than the Long and Thomas value. Increasing f_R from 5·55 md/Å to 5·7 md/Å leads (for pyridine-ICl) to a small increase in the $\bar{\nu}_7$ and $\bar{\nu}_9$ values in the correct direction. The $\bar{\nu}_4$ value is explained very well without an increase in f_R and the increase of this constant to 5·7 md/Å leads to a $\bar{\nu}_4$ value which is too large. However, the C-N and C-C force constants have been assumed to be equal, and this is probably not entirely realistic. If one assumes that most of the positive charge in the pyridine ring is localised on the nitrogen in the pyridine-IX complexes then one would expect the C-N bond force constant to be reduced. The resonance structure:

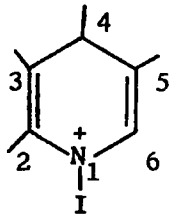

Cl^-

would then tend to give an increase of the force constants between positions 2 and 3 and 5 and 6. One would then expect that the vibrational contribution of the S_1 symmetry co-ordinate (see Tables 6.9. and 6.11.) would reduce the frequency whilst a contribution from the S_2 symmetry co-ordinate would increase the frequency. This is probably the reason why the ν_7 band is unaltered in frequency, since it has the largest S_1 contribution (30%) and the smallest S_2 (0%) (see Table 6.11A.) and neither of these contributions alters very much on going to the complex. The ν_4, ν_9, ν_{10} vibrations with

large S_2 contributions, show large frequency increases. Of these normal modes only ν_9 shows very large changes of normal co-ordinate on going to the complex and in that instance the contribution from S_2 decreases while that from S_1 increases. It is not clear therefore that such an argument can always account for frequency shifts observed.

b. Effect of Altering k_{13}.

The effect of increasing k_{13} from 0·1 to 0·6 md/Å, without allowing any force constant cross terms between internal co-ordinates of the N-I-X part and the pyridine ring (Sets 1 and 2) is to increase the mixing between these modes and ν_7, ν_8, ν_{10} vibrations of pyridine. The mixing is, however, only of the order of 3% for the most sensitive (ν_{10}) donor mode (see Tables 6.11. and 6.12.). In general, the frequency shifts calculated with the two different interaction constants are unchanged. It is therefore not possible to say from this data which value of k_{13} is preferred.

c. Change of Normal Co-ordinates in the Complex.

As expected only small changes occur in vibrational mixing on going from pyridine to the complex. (This can be seen by referring to Tables 6.9. and 6.10. - 6.12). The changes in mixing between vibrations of donor molecule are also fairly small on going to the complex. The main changes for pyridine-ICl on complexation are as follows:

(i) The ν_7 vibration shows a decrease in ring bending ($\Delta\alpha$) character.

(ii) The ν_8 vibration shows a decrease in the carbon-carbon stretching character and a small increase in the $\Delta\alpha$ bending character. (See for example, Tables 6.9. and 6.11.).

It is interesting to note in passing that the two a_1 modes which show the least frequency change on complexation (ν_7 and ν_8), should show the largest normal co-ordinate change. The effects of normal co-ordinate may cancel each other out in these cases because the increase of $\Delta\alpha$ bending

character would reduce the frequency, whilst increase of the C-C stretching character would increase the frequency (assuming, that is, that a pure ring bending mode have a lower frequency than a C-C stretching mode).

d. Effect of Introducing Cross Terms in the f Matrix.

The Long and Thomas force field has quite large cross terms for the pyridine molecule, i.e. $f_{ROR} = 0{\cdot}633$ md/Å
$f_{RpR} = 0{\cdot}573$ md/Å
$f_{R\alpha} = -0{\cdot}18$ md/Å
$f_{\alpha\beta} = -0{\cdot}127$ md/Å

(see Table 6.3.).

One would therefore imagine that for the pyridine-ICl complex there would be significant cross terms with the acceptor co-ordinates. One would expect that f_{R1}, ($f_{101} = k_{13}$) and $f_{\theta\beta}$, at least, might be quite significant. The cross terms described in this section do not represent the final set, but rather the state of knowledge on the force field at the time of writing.

Introduction of small cross terms f_{R1_1} and f_{R1_2} (representing interaction constants between the internal co-ordinates ΔR_1 or ΔR_6 and $\Delta 1_1$ or $\Delta 1_2$) at 0·1 and 0·05 md/Å gives rise to small frequency changes and small changes in normal co-ordinate. Table 6.13 shows some of the effects of introducing cross terms.

Table 6.13.

Effect of Introducing Cross Terms in f Maxtrix (Pyridine-ICl)

Mode	Set 3 $k_{13} = 0{\cdot}1$ No cross terms	Set 5 $k_{13} = 0{\cdot}1$ With cross terms
ν_7	1039	1037
ν_{10}	622	625
ν_9	1002	998
ν_4	1616	1614
ν_8	1013	1013
ν_5	1494	1492
$\nu_{(N-I)}$	133	133
$\nu_{(I-Cl)}$	294	294

As can be seen from Table 6.11A, apart from the ν_{10} mode at 625 cm.$^{-1}$, the calculated frequencies tend to make the agreement worse.

The changes of normal co-ordinate can be summarised as follows. The $\nu_{(N-I)}$ component becomes more mixed with the normal co-ordinates corresponding to Q_9 and Q_{10}. There is also a small decrease in the $\nu_{(N-I)}$ character for the normal co-ordinates Q_7 and Q_8. This correlates with the observed data to the extent that the ν_7 and ν_8 vibrations are relatively unperturbed in frequency, whilst the ν_9 and ν_{10} bands show large perturbations, i.e. the ν_7 and ν_8, and ν_9 and ν_{10} vibrations are affected in the same way. The normal co-ordinate for the $\nu_{(N-I)}$ and $\nu_{(I-Cl)}$ vibrations are unchanged except for a difference in the $C\hat{C}C$ bending character of the $\nu_{(N-I)}$ vibration. However, $\nu_{(N-I)}$ and $\nu_{(I-Cl)}$ are significantly mixed with Q_7, Q_8 and Q_9 without any cross terms (i.e. through the kinetic energy matrix).

In view of the closeness of the ν_{10} frequency to the $\nu_{(N-I)}$ frequency it was decided to introduce a small (0·1 md/Å) cross term for the $C\hat{C}C$ and 1_1 stretch interaction. This resulted (Set 5) in a large frequency increase (of 7 cm.$^{-1}$) for the Q_{10} mode. However, the Q_8 mode at 1034 cm.$^{-1}$ is also increased in frequency. On complexation the observed Q_8 mode shows only a small frequency increase (observed 3 cm.$^{-1}$, calculated 8 cm.$^{-1}$) so the value of 0·1 md/Å is probably too high. There is also a frequency decrease in the $\nu_{(N-I)}$ mode with a large increase of the S_7 contribution.

The ν_8 and ν_{10} move in the correct direction, but the $\nu_{(N-I)}$ frequency moves away from the 140 cm.$^{-1}$ observed value. The available data is summarised in Table 6.14.

It was found that the frequencies and normal co-ordinates of the b_1 modes are relatively insensitive to the interaction constants introduced in order to obtain a better frequency fit for the a_1 modes. When the appropriate $f_{R\theta_1}$ or $f_{\alpha\theta_1}$ cross terms were introduced, the a_1 modes suffered

a greater perturbation than the b_1 modes. The effect was strongest on the low frequency ν_8 - ν_{12} modes.

Table 6.14.

Effect of $f_{\alpha 1}{}_1$ Cross Term on Normal Co-ordinates of Pyridine-IC1

Mode	Freq. Set 4/ $cm.^{-1}$	Freq. Set 5/ $cm.^{-1}$	Contribution from S_7	S_8	S_{13}
ν_8	1013		17•9	17•5	0•8
		1021	16•2	15•7	1•0
ν_{10}	625		21•2	23•7	3•2
		634	19•1	25•0	3•1
$\nu_{(N-I)}$	133•2		4•5	0•7	89•4
		129•1	8•1	0•9	82•7
ν_4	1614		5•0	5•3	0•1
		1616	5•2	5•2	0•2

In conclusion it can be seen that the frequency shifts on complexation are adequately accounted for by the mass effect and by the introduction of the force constants, $k_{(D-I)}$, $k_{(I-X)}$ and k_{13}. It is not necessary to change the internal pyridine force field, although some 'cross terms' of the type f_{R1} and $f_{R\theta}$ may be needed. The vibrational mixing is what would be expected, i.e. the acceptor (low frequency modes) mix most with the low frequency modes of the donor of the same symmetry class. This is illustrated by the fact that the $\nu_{(N-I)}$ mode (band at 135 $cm.^{-1}$) is much more mixed with the $\nu_{(I-X)}$ mode at 200 $cm.^{-1}$ for the pyridine-IBr complex, than for the pyridine-IC1 complex (Table 6.12A) even though the two $\nu_{(N-I)}$ calculated frequencies are similar. It is interesting to note that the b_1 mode calculated at 1251 $cm.^{-1}$ for pyridine moves to 1264 $\pm$ 4 in the complex. This mode shows the largest frequency perturbation of the b_1 modes. Therefore this is good evidence for the assignment of the band at 1247 $cm.^{-1}$ to the ν_{16}, b_1 mode. This conclusion was suggested by the intensity studies (see Chapter 3).

E. Suggestions for Future Work.

It is clear that a better fit can be obtained from more studies on the cross terms in the f matrix. Work continues on this topic in the laboratory. Having solved the 'G matrix problem' it is now possible to carry out a normal co-ordinate calculation on any pyridine-XY molecule. The frequency data are given in this thesis for pyridine-I_2, pyridine-Br_2, and pyridine-Cl_2 complexes. It would also be very easy to extend this calculation to any pyridine complex with a linear acceptor. This suggests calculations on complexes such as pyridine-ICN, pyridine-INC, pyridine-ICNO. Chapter 3 also contains information on the pyridine-ICN complex which could be used in this work.

Finally in Chapter 5 it was shown that the $\nu_{(S-I)}$ frequency for the complexes, diethyl-sulphide-I_2, diethyl-sulphide-IBr, and diethyl-sulphide-ICl is exceedingly high. This must be mirrored in the $\nu_{(S-I)}$ force constant which will, in turn, affect the donor frequencies. It would therefore be extremely interesting to study the donor vibrations of the diethyl-sulphide molecule to see if the perturbation on complexation is greater than for the pyridine complex.

It would then be interesting to carry out a normal co-ordinate calculation on diethyl-sulphide-halogen complexes. The triatomic molecule approximation should be well worth carrying out with $(C_2H_5)_2S$-ICl and $(C_2D_5)_2S$-ICl as outlined at the beginning of this chapter. The ICl complex is chosen as it would be expected to be the most 'rigid'. One would expect, because the mass difference is 10 units, a more definitive 'crossing point' for the force constant ellipses. [Care must be taken to keep the donor and acceptor concentrations identical when the $\nu_{(S-I)}$ frequencies for the $(C_2H_5)_2S$-ICl and $(C_2D_5)_2S$-ICl complexes are measured. This is to avoid 'solvent' effects].

The force field for diethyl-sulphide has been determined by Geiseler and Hanschmann.[178] Tranquille et al.[179] have calculated the force field for the very similar molecule dimethyl-sulphide. Thus it can be seen that this calculation only requires the extra terms in the force field due to the acceptor molecule. This assumes, of course, that the donor force field is relatively unchanged as in the pyridine-ICl and pyridine-IBr complexes.

CHAPTER 7

Studies on Solid Complexes of ICl and IBr

A. Introduction.

Whilst not being part of the main project discussed in this thesis, the inorganic chemistry of donor-acceptor complexes is a fascinating field in its own right. It became apparent during the preparation of the pyridine-IBr and pyridine-ICl complexes that more than one product was present. It was felt to be worthwhile to investigate this further. Pyridine seems capable of forming 1:1, 1:2, 2:1 complexes with acceptors. Whittaker[180] has, for example, prepared the following series of complexes with ICl_3.

Complex	Melting Point/^{o}C
Pyridine-2ICl_3	140
Pyridine-ICl_3	69
2Pyridine-ICl_3	168

The analogous complexes were also made using pyridine and IBr.

B. The Pyridine-2IBr Complex.

This was prepared by adding pyridine in carbon tetrachloride to an excess of IBr (also in carbon tetrachloride). The analytical data is given in Table 7.1. along with that for the other complexes prepared.

The complex (in the form of a brown powder) was analysed by using the 'Schoniger oxygen flask' technique as described in 'Organic Elemental Analysis' by G. Ingram (Chapman Hall, 1963). The total halogen was estimated potentiometrically using Ag/AgCl electrodes in an aqueous acetone medium. It can be seen that the compound is almost certainly pyridine-2IBr. The melting point (52^{o}C) is in good agreement with the value obtained (53^{o}C) by Whittaker[181] from freezing point curves. In solution the compound behaved

Table 7.1.

Complex	%C Theor.	%C Obs.	%N Theor.	%N Obs.	%H Theor.	%H Obs.	%I Theor.	%I Obs.	%Br Theor.	%Br Obs.
Pyridine-2IBr	12·17	12·02	2·83	2·81	1·01	1·05	51·5	52	32·4	33
Pyridine-IBr	20·9	21·0	4·89	4·6	1·748	1·5	44·4	44	27·97	28
2Pyridine-IBr	32·7	33·1	7·65	7·3	2·732	2·4	34·6	35·7	21·8	-
Pyridine-Br_2	25·1	25·2	5·85	5·7	2·09	2·41	-	-	66·9	-
Pyridine-ICl	24·8	25·1	5·79	5·6	2·07	2·5	52·5	-		
2Pyridine-ICl	37·4	37·1	8·73	8·4	3·12	3·1	39·6			

Thanks are due to Mr. R. Coult for the iodine and bromine analyses.

exactly like a mixture of pyridine-IBr and IBr. The Raman spectrum was kindly obtained by Dr. P.L. Goggin of Bristol University and is shown in Spectrum 7.1. It was not possible at room temperature to obtain a spectrum because the sample absorbed too strongly. However, on cooling to liquid nitrogen temperatures bands were observed at 180, 194, 211, 219, 231, 236 (sh), 384, 389, 392, 395, 402, 408, 426, 432, 439, 444 and 450 $cm.^{-1}$ The spectrum is obviously very complex. It can be seen from Spectrum 7.2. that, whilst the infrared spectra of pyridine-IBr and pyridine-ICl are practically the same, the relative intensities are very different for the pyridine-2IBr complex. The bands in the far-infrared (Spectrum 7.3.) follow the same pattern as those in the Raman spectrum and comparison with the spectrum of the 1:1 complex (in Spectrum 7.4.) shows clearly that a quite different compound has been made.

If the compound follows the reaction path of pyridine and iodine then we expect:

$$2Pyr + 4IBr \longrightarrow Pyr_2I^+ + I_3Br_4^-$$

analogous to $2Pyr + 4I_2 \longrightarrow Pyr_2I^+ + I_7^-$

and one would expect the anion to have a complex far-infrared spectrum. Furthermore, the $(Pyr_2I)^+$ cation is expected[93,183] to absorb at 636 and 435 $cm.^{-1}$ Absorptions are in fact observed at these frequencies (Spectrum 7.2.). At the time of writing Professor J. Smith of London University is attempting to obtain a bromine n.q.r. spectrum of this compound in an attempt to get more information on the nature of the anion.

If the anion is $I_3Br_4^-$ it was hoped that by pumping on the compound over a few days and weighing regularly one could obtain the series of anions:

$$I_3Br_4^- \longrightarrow IBr + I_2Br_3^-$$

$$I_2Br_3^- \longrightarrow IBr + IBr_2^-$$

However, the spectrum obtained by this method could be only interpreted

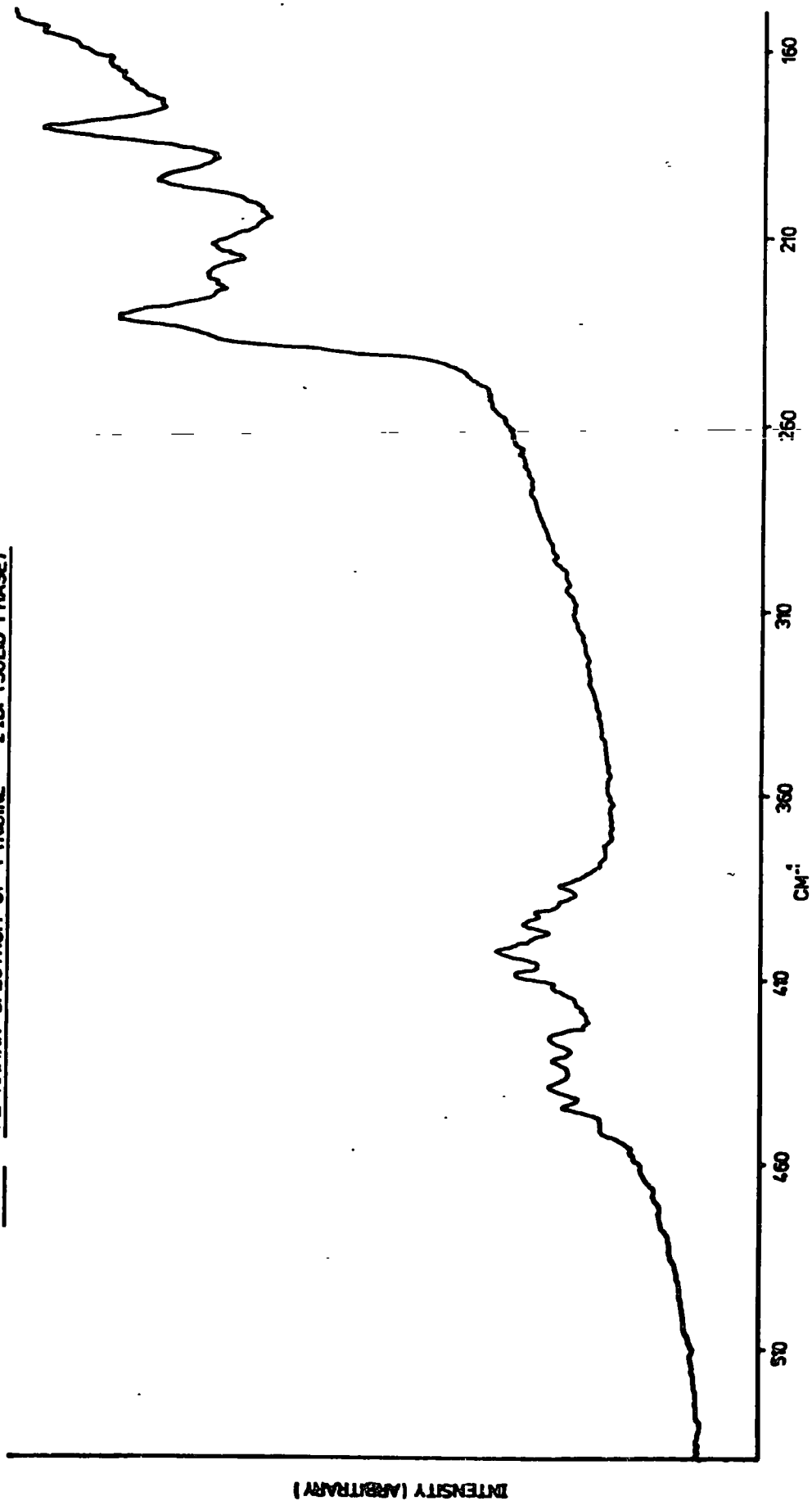

FIG. 71 THE RAMAN SPECTRUM OF PYRIDINE - 2 IBr (SOLID PHASE)

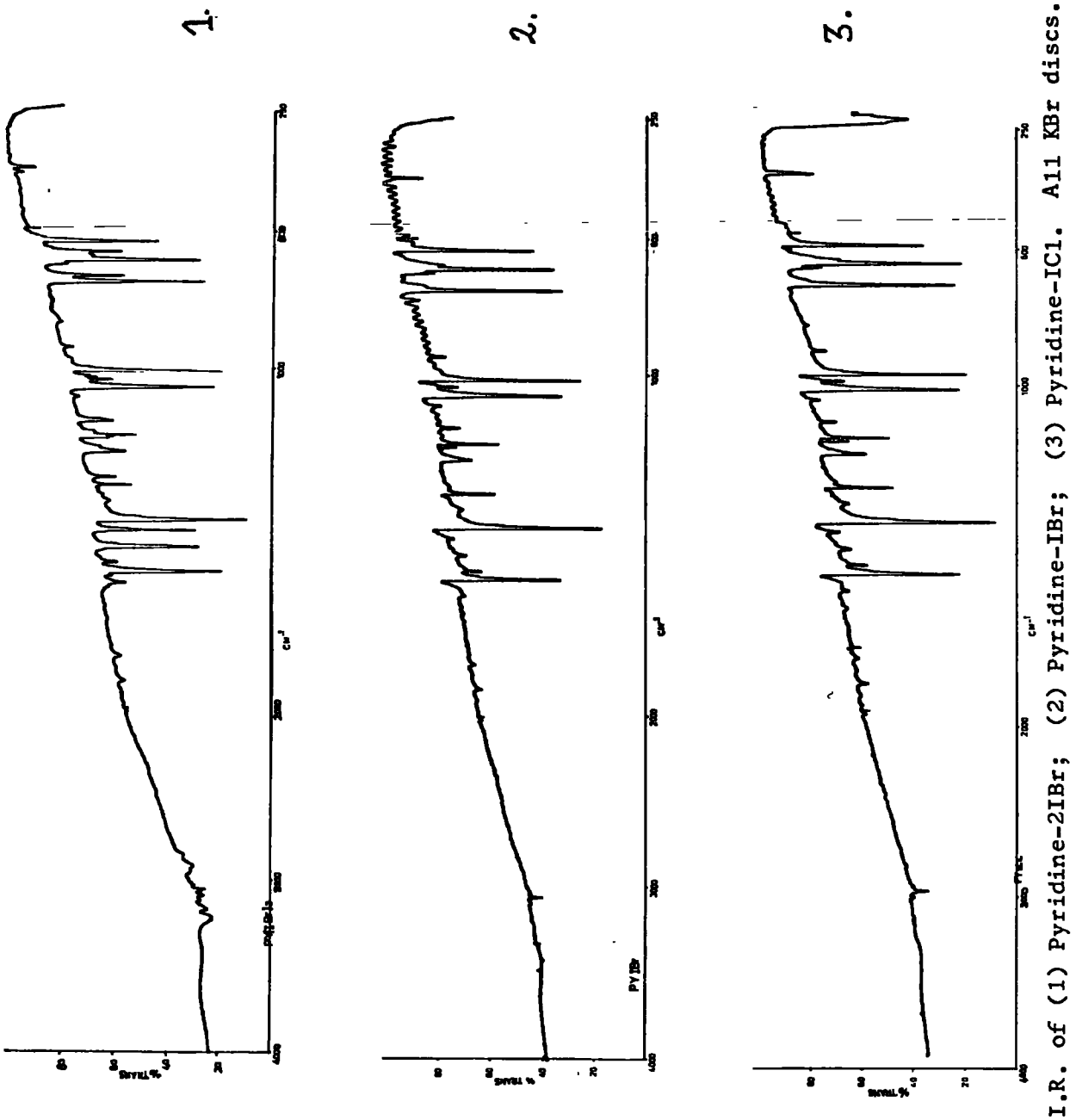

Spectrum 7.2. Near I.R. of (1) Pyridine-2IBr; (2) Pyridine-IBr; (3) Pyridine-ICl. All KBr discs.

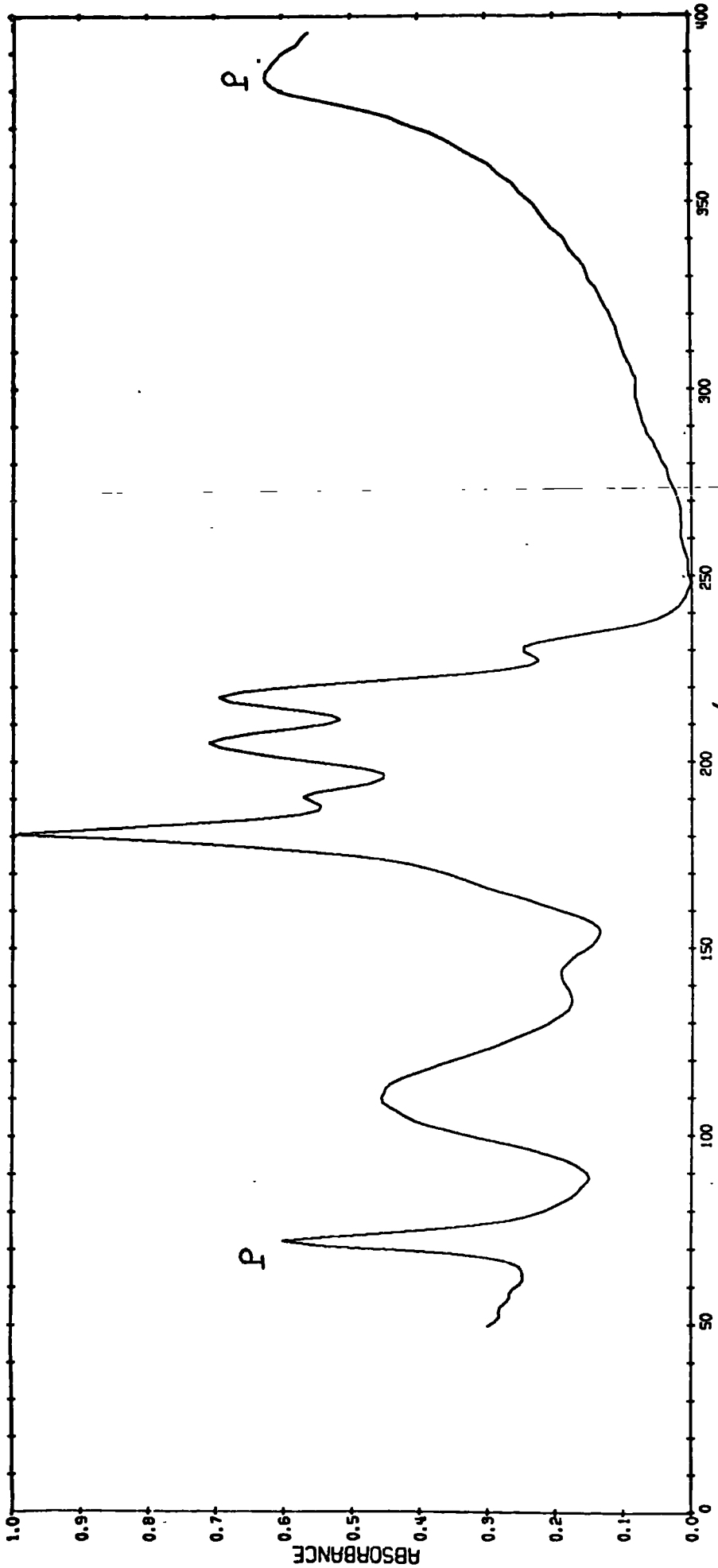

Spectrum 7.3. Far-infrared of pyridine-2IBr nujol mull. (Band marked P are due to polyethylene cell windows).

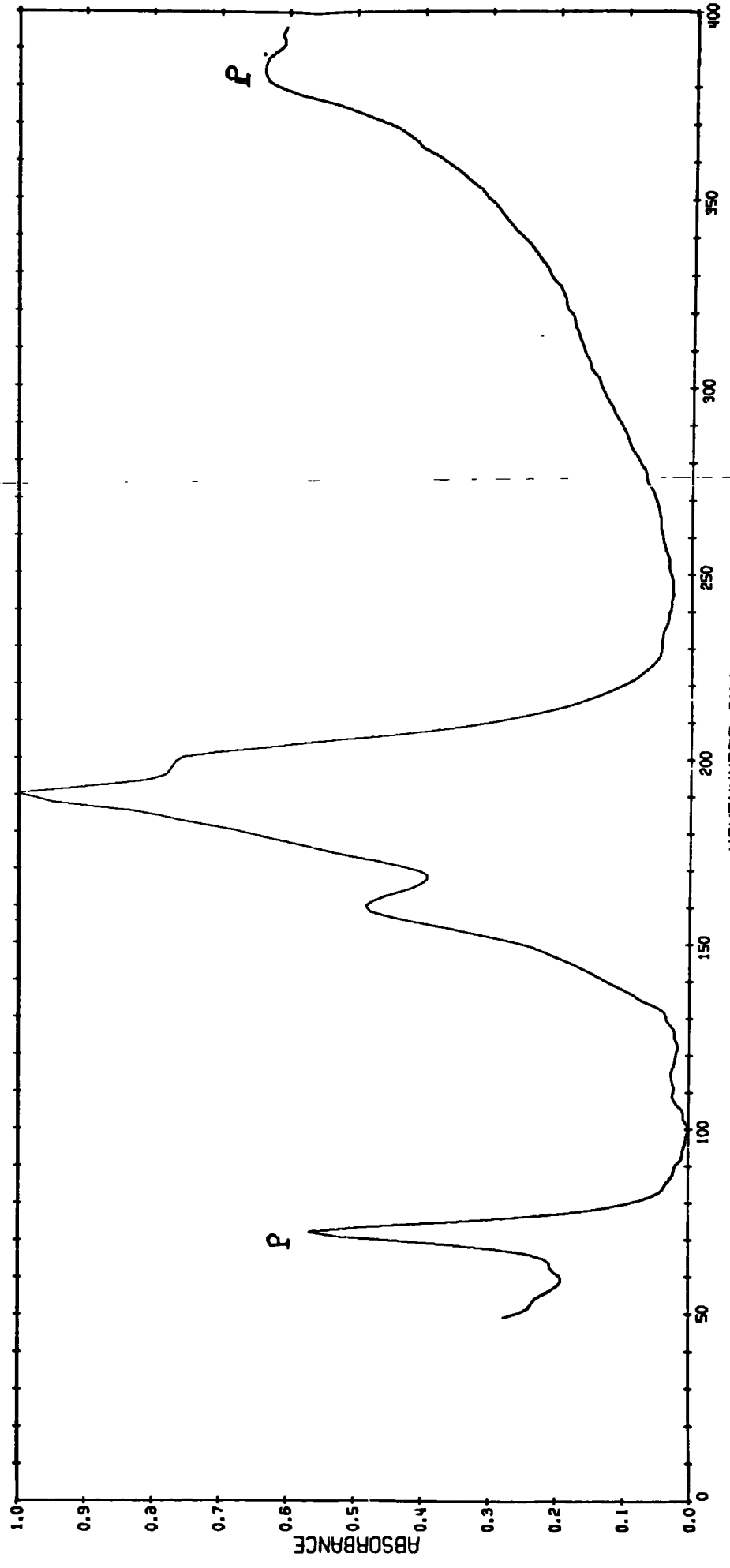

Spectrum 7.4. Far-infrared spectrum of pyridine-IBr (nujol mull). (The bands marked P are due to polyethylene cell windows).

in terms of a mixture of pyridine-IBr and pyridine-2IBr.

C. The Pyridine-2ICl Complex.

When the preparation described above was repeated with ICl instead of IBr, a red oil was obtained (m.p. $\approx 7^{o}C$). This experiment was repeated in a cold room at -5^{o} and a brown powder was then obtained. However, attempts to obtain an infrared spectrum at room temperature failed due to the loss of ICl.

D. The 2Pyridine-ICl and 2Pyridine-IBr Complexes.

These compounds were extracted from freshly prepared pyridine-ICl and pyridine-IBr by washing with chloroform. The 1:1 complex dissolved much more readily in the chloroform. The analysis is shown in Table 7.1. The 2:1 2Pyr-ICl complex was a white powder and the 2Pyr-IBr was an orange powder. One would assume the structures are $Pyr_2I^+Cl^-$ and $Pyr_2I^+Br^-$ on the basis of the lack of absorption in the far-infrared region (apart from ν_{22} (a_2) band at 375 $cm.^{-1}$) which is consistent with presence of only a X^- anion (see Spectrum 7.5.). Whilst the near-infrared spectra of the cations are identical, the 'characteristic' frequencies of Pyr_2I^+ at 636 and 435 $cm.^{-1}$ were <u>not</u> observed. The nearest band was at 662 $cm.^{-1}$ (see Spectrum 7.6.).

E. Solid Complexes of Iodine.

From a solution of iodine dissolved in dioxan, red crystals were obtained. However, these rapidly decomposed in the solid state to give a black powder. This analysed as dioxan/I_3. In the pyridine case, golden crystals were obtained from a solution of pyridine/cyclohexane/iodine. These crystals rapidly lost pyridine to give the pyridine-$2I_2$. The far-infrared spectrum of the I_7^- ion is shown in Spectrum 7.7. Spectrum 7.8. shows that the characteristic frequencies at 636 and 435 $cm.^{-1}$ are present. This compound is known to contain $Pyr_2I^+I_7^-$ units.[182]

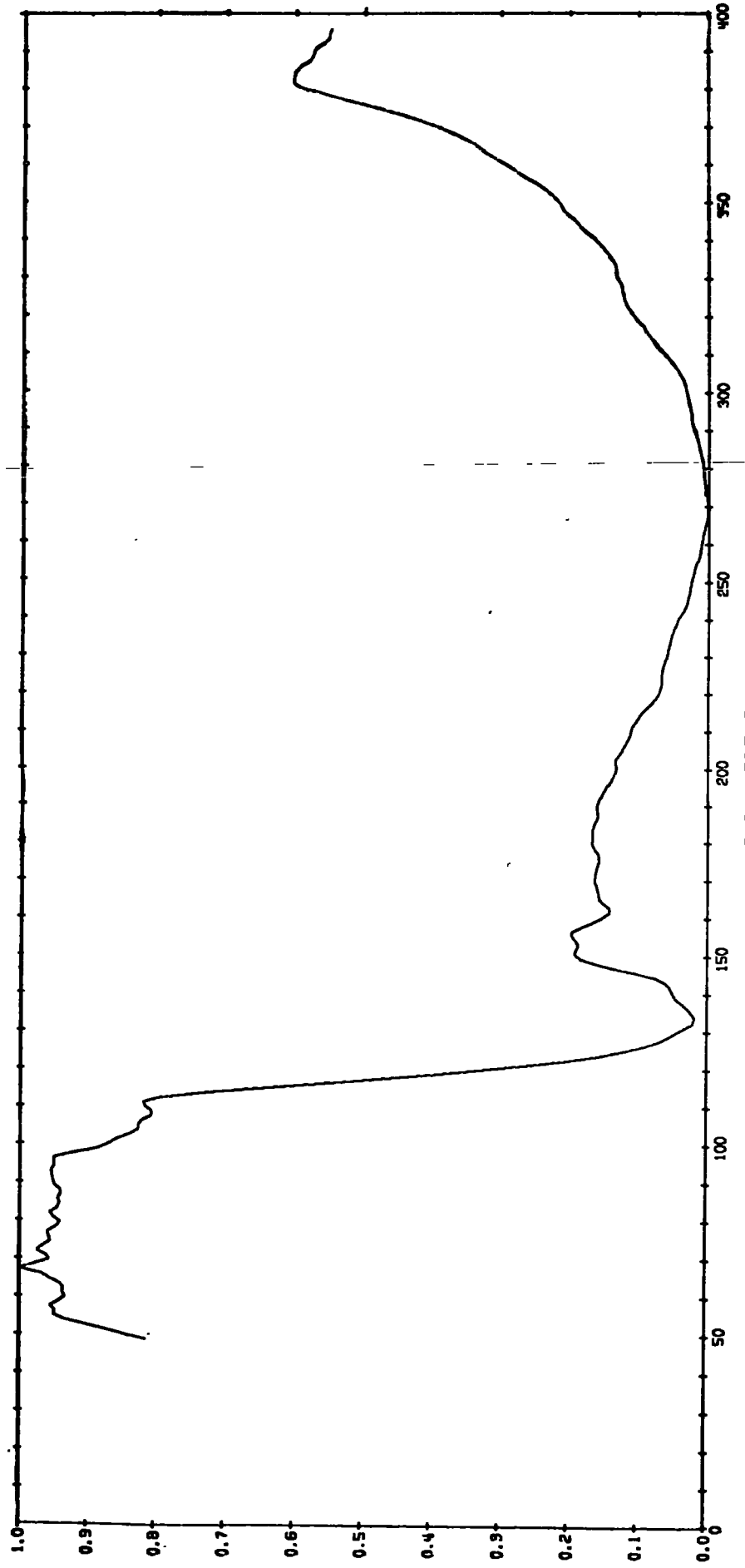

Spectrum 7.5. Far-infrared spectrum of 2-pyridine-IBr (CsI disc).

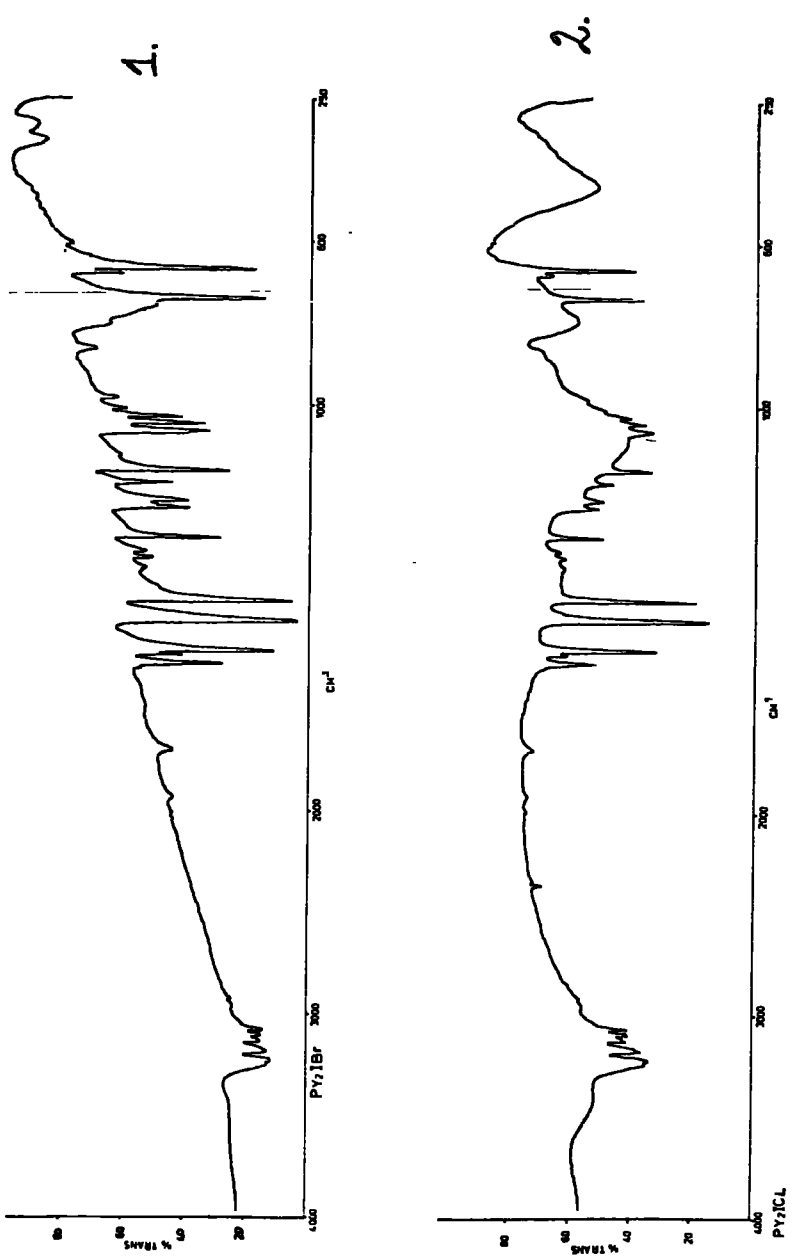

Spectrum 7.6. Near infrared spectrum of (1) 2-pyridine-IBr; (2) 2-pyridine-ICl; (3) pyridine-d-ICl (all in KBr discs).

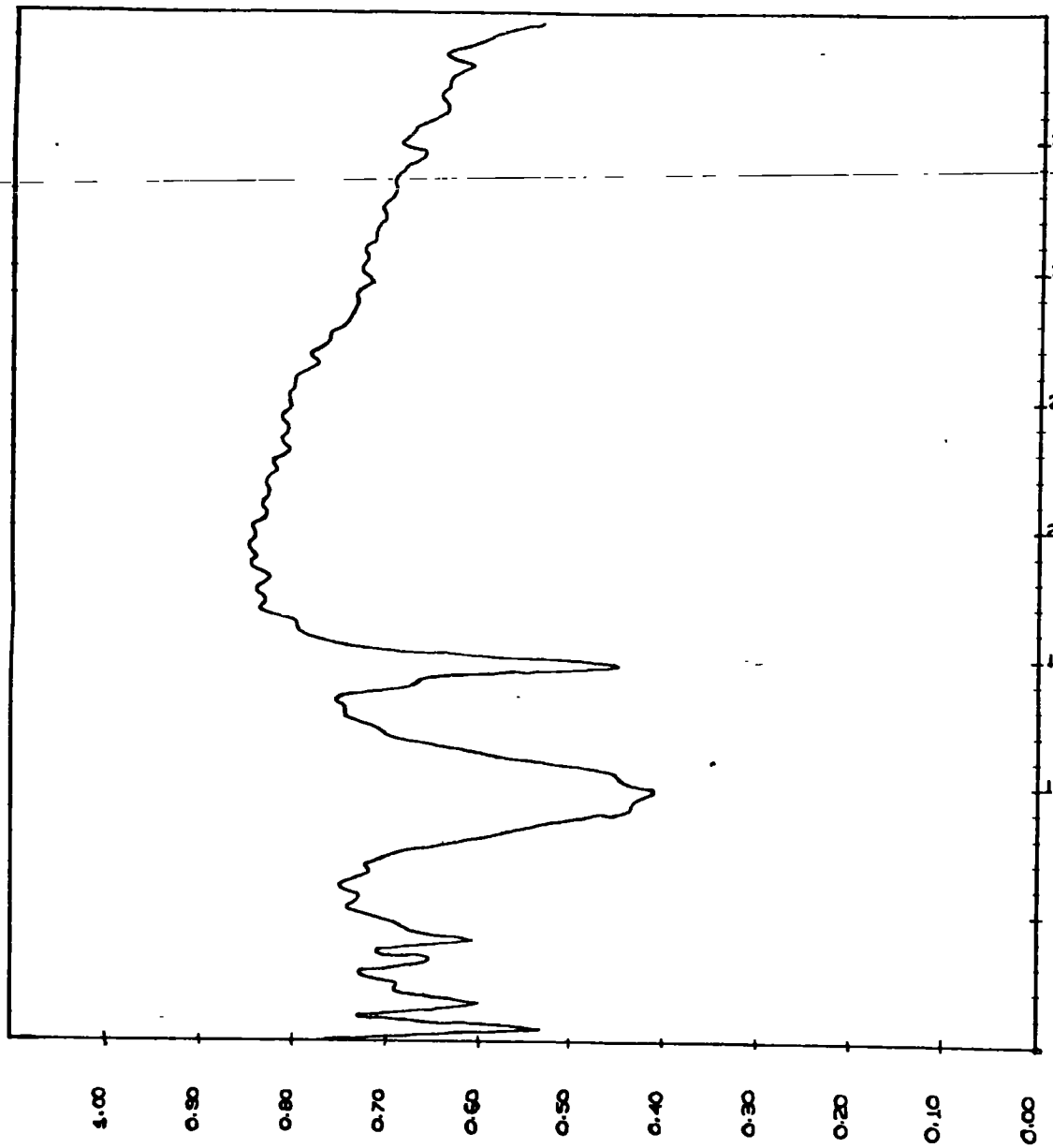

Spectrum 7.7. Far infrared spectrum of pyridine-$2I_2$ i.e. $Pyr_2I^+I_7^-$ (ratioed polythene disc).

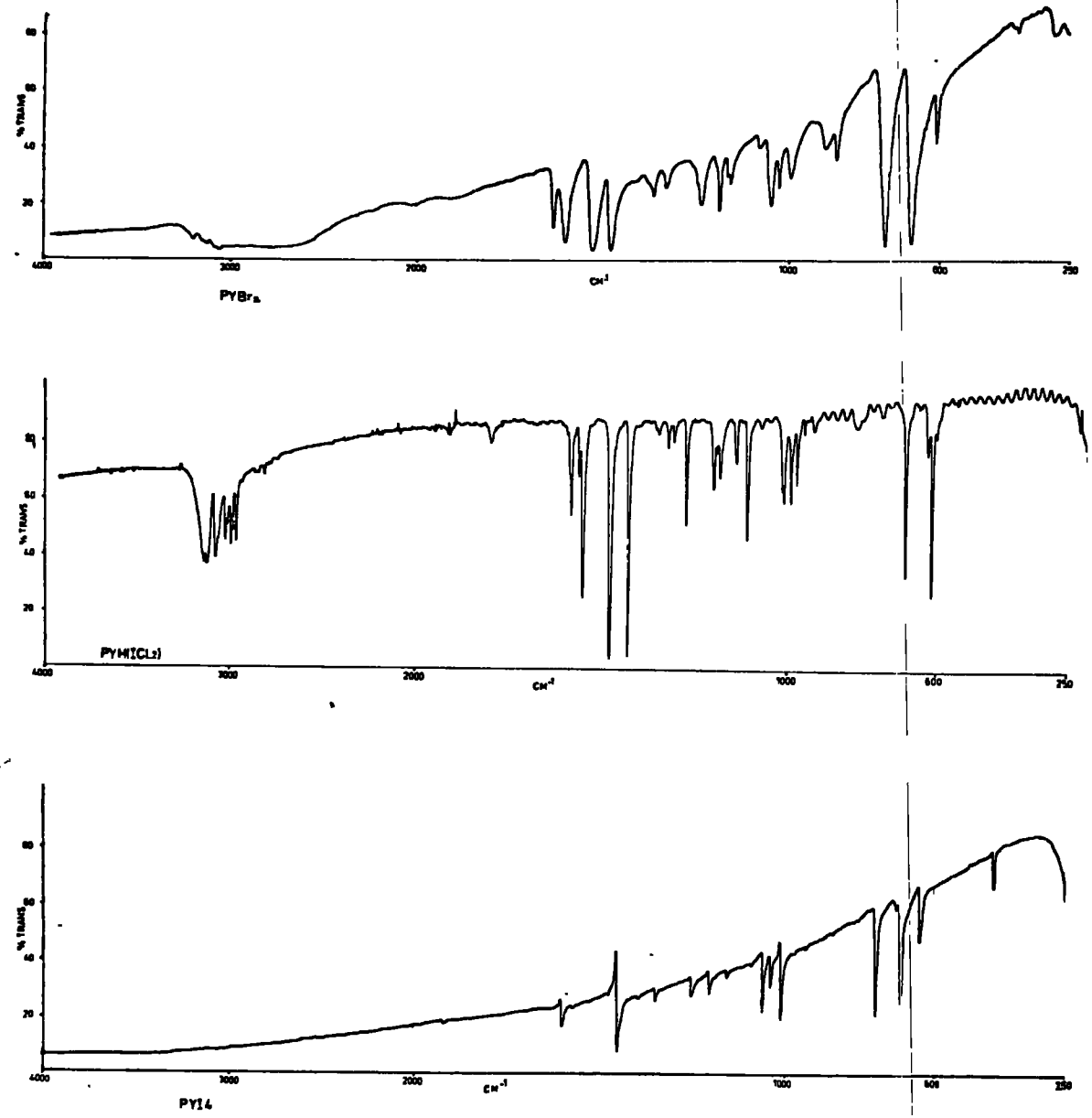

Spectrum 7.8. Near infrared spectra of (a) pyridine-Br_2; (b) $[pyridine\text{-}H]^+IC1_2^-$; (c) $[pyridine_2I]^+I_7^-$ (KBr discs).

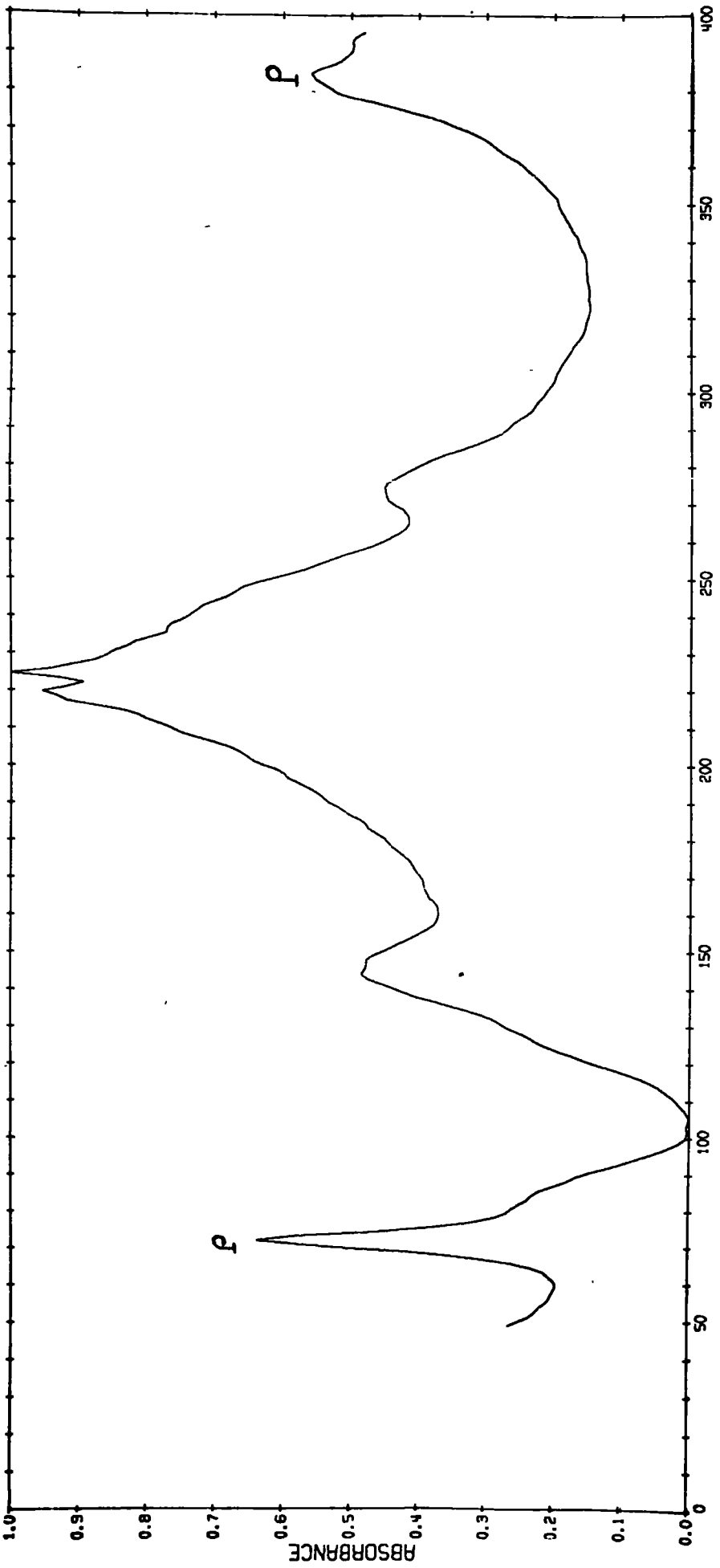

Spectrum 7.9. Far-infrared of $PyrH^{+}IC1_{2}^{-}$ in a nujol mull.

F. The Pyridine$H^+IC1_2^-$ Complex.

Although the $IC1_2^-$ anion is known to have very strong bands it was decided to determine the intensity from a known compound. This was to ensure that the weak $IC1_2^-$ impurity bands observed in some donor/IC1 solutions were responsible for only a small amount of decomposition. The compound was prepared using:

$$Pyr\text{-}IC1 + HC1 \longrightarrow Pyr^+H + IC1_2^-$$

in chloroform solution. The ionic compound was dissolved in tetrahydrofuran. The bands at 224 and 260 had intensities of 20,400 and 2,370 darks respectively. The first $IC1_2^-$ band is thus the strongest one studied in this work. (See Figure 7.9.).

The near-infrared spectrum of the donor was very similar to that of benzene. This is not surprising since C_6H_6 and $C_5H_5NH^+$ are isoelectronic.

APPENDIX A

Program DCHO5277

MAIN

```
      C SPECTRAL CALC FROM FS720 DCH0527 COMPLETE AUTOCORRELATION METHOD DUPLICATE DECK
      C COOLEY-TUKEY TRANSFORMATION ROUTINE
0001        IMPLICIT REAL*4(A-H,O,V-Z),INTEGER*4(J-N,P-U)
0002        DIMENSION A(4096),C(4096),B(2048),D(2048),F(1),G(1),H(50)
0003        DIMENSION O(2048),V(11),I(15),ZX(20)
0004        COMMON A,C,B,D
0005      102 FORMAT(4F6.3)
0006      140 FORMAT(20A4)
0007      101 FORMAT(3I2,3XA4,1XA4)
0008      103 FORMAT(I3)
0009      100 FORMAT(I4,2XF5.2,2XF7.2,2XF7.2,2XI1,2XI1,2XI1,2XI1,2XI1)
      C SET COUNTERS
0010        READ(8,103) NSETS
0011       11 IF(NSETS)13,13,12
0012       12 I(7)=0
0013          I(9)=0
0014        READ(8,100) N,FSINT,FREQL,FREQH,IOPUT,NSIG, NABS,NOUT,NCARD
      C N=NO OF POINTS TO BE TRANSFORMED,SINTV=SAMPLING INTERVAL IN MICRONS,FREQL=LOWER
      C FREQ LIMIT IN RECCM,FREQH=UPPER   FREQ LIMIT IN REC CM,IOPUT=NO OF OUTPUT
      C POINTS PER RESOLUTION=1,2,3,4 OR 5 ONLY
      C READS IN DATE (I11 TO I13) AND TAPE REF NOS, ALSO GAIN CONTROL SETTINGS(V3 TO V6)
      C V3 AND V4 FOR SAMPLE AND V5 AND V6 FOR BACKGROUND
      C ZX IS THE TITLE FOR EACH SPECTRUM
0015        READ(8,101)I(11),I(12),I(13),I(14),I(15)
0016        READ(8,102)(V(J),J=3,6)
0017        READ(8,140) ZX
0018        WRITE(6,200) N,FSINT,FREQL,FREQH,IOPUT,NSIG,NABS,NOUT,NCARD
0019      200 FORMAT(1H I4,2XF5.2,2XF7.2,2XF7.2,5(2X,I1))
0020       28 I(7)=I(7)+1
0021          Z=FLOAT(N)
0022          HI=3.14159265
      C CALLS SUBROUTINE WHICH READS IN BINARY DATA FROMTAPE OR SIMULATES IN-PUT FOR
      C TESTING PURPOSES

0023        CALL TPREAD(M,NOUT)
0024        CALL SUBDH(N,Z,M,NOUT)
0025        J=N/2
0026        L=J
0027        K=N/4
0028        Z=Z/2.0
      C J IS 1/2N TO START WITH,LIS HALVED AT EACH SUCCESSIVE STAGE IN THE TRANS-
      C FORMATION.MAX VALUE OF J IS 1024
0029        CALL SUBTM(N,NOUT)
0030        CALL SUBPT(I(9),I(7),Z,FSINT,FREQL,FREQH,IOPUT,I(14),I(15),V(3),
           IV(4),V(5),V(6),I(11),I(12),I(13),ZX,NABS,NOUT,NCARD)
0031        IF(NSIG.EQ.1) GO TO 31
0032        GO TO 113
0033       31 IF(I(7).1).GT.1)GO TO 29
0034        GO TO 30
0035       30 DO 3 M=1,N
0036        O(M)=A(M)
0037        3 CONTINUE
      C STORES BACKGROUND SPECTRAL ARRAY AFTER PLOTTED OUT
0038        GO TO 28
      C GOES BACK TO PICK UP SAMPLE      TAPE AND LIKE-WISE TRANSFORMS AND PLOTS
0039       29 DO 4 M=1,N
0040        4 A(M)=A(M)/O(M)
0041        CALL SUBPT(I(9),I(7),Z,FSINT,FREQL,FREQH,IOPUT,I(14),I(15),V(3),
           IV(4),V(5),V(6),I(11),I(12),I(13),ZX,NABS,NOUT,NCARD)
      C RATIOS SAMPLE TO BACKGROUND AFTER 2ND TRANSFORM AND PLOT BACK-GROUND IN
      C THE ARRAY O AND SAMPLE IS IN ARRAY A
0042      113 NSETS=NSETS-1
0043        GO TO 11
0044       13 CALL EXIT
0045        END
```

SUBTM

```
      C SUBROUTINE FOR TRANSFORMATION OF DATA TO GIVE SPECTRAL OUTPUT
      C     THIS PROGRAM MAKES USE OF A TECHNIQUE DUE TO J.W. COOLEY AND J.W.
      C     TUKEY (MATH. OF COMPUTATION,VOL 19,PG.295,1965). MODIFICATIONS TO
      C     THIS TECHNIQUE HAVE BEEN MADE SO THAT FOURIER ELEMENTS COME OUT
      C     IN A NORMAL ORDER. THE APPROPRIATE SINES AND COSINES MAKE USE OF
      C     INTERNAL MACHINE SUBROUTINES. FOR REDUCTION OF 8192 INPUT POINTS
      C     TO 8192 OUTPUT POINTS, THE TIME IS ABOUT 1 MINUTE.
      C     IF THIS DIMENSION IS USED, THERE IS LITTLE ROOM FOR OTHER
      C     CALCULATION, HOWEVER IT CAN OPERATE ON TAPES WHERE ORIGINAL DATA
      C     HAS BEEN PRETREATED AND OUTPUT MAY ALSO BE A SEPARATE PROGRAM.
0001          SUBROUTINE SUBTM(NMAX,NOUT)
0002          DIMENSION TR1(4096),TI1(4096),TR2(2048),TI2(2048)
0003          COMMON TR1,TI1,TR2,TI2
      C     SETTING OF CONSTANTS THAT DO NOT CHANGE DURING PROGRAM
      C     NMAX=NUMBER OF POINTS TO BE PROCESSED = 2
      C     IHALF USED TO KEEP TRACK OF N
      C     KHALF USED TO DETERMINE WHERE PARTIAL SUMS ARE TO BE STORED
      C     DURING EACH PASS
0004          JHALF=NMAX/2
0005          IHALF=NMAX/2
0006          KHALF=NMAX/4
0007          PI=3.14159265
      C CLEARS ARRAY TI1 READY FOR COMPUTATION
0008          DO 10 I=1,NMAX
0009       10 TI1(I)=0.0
      C     CHECK TO SEE IF N PASSES HAVE BEEN MADE
0010       34 IF(IHALF)999,65,37
      C     SETTING OF CONSTANTS FOR EACH PASS
      C     WR,WI ARE THE REAL AND IMAGINARY PARTS OF EXP(2*PI*J*K/NMAX)
      C     RESPECTIVELY AND = 1,0 AT THE START OF EACH PASS
0011       37 JP=0
0012          WR=1.0
0013          WI=0.0
      C     I AND L ARE THE REAL INDICES OF THE LOCATIONS TO WHICH THE PARTIAL
      C     SUMS WOULD BE TRANSFERRED IF TR1,TI1,TR2,TI2 WERE OF
      C     EQUAL LENGTH. TR2,TI2 NEEDED FOR AUXILIARY STORAGE
0014          DO 81 I=1,JHALF
0015          L=I+JHALF
      C     JK=J*K AND DETERMINES PROPER FREQUENCIES DURING PASS
0016          IF(IHALF-1)38,38,39
0017       38 JK=I-1
0018          ANG=   PI*FLOAT(JK)/FLOAT(JHALF)
0019          WR=COS(ANG)
0020          WI=SIN(ANG)
0021          GO TO 48
0022       39 IMOD=I-(I/IHALF)*IHALF
0023          IF(IMOD)999,48,41
0024       41 JK=I-IMOD
0025          IF(JK-JP)999,48,43
0026       43 ANG=   PI*FLOAT(JK)/FLOAT(JHALF)
0027          JP=JK
0028          WR=COS(ANG)
0029          WI=SIN(ANG)
      C     IP AND IQ ARE THE LOCATIONS OF PREVIOUSLY CALCULATED PARTIAL SUMS
      C     STORED IN TR1,TI2 WHICH ARE TO BE USED IN PRESENT PARTIAL
      C     SUM. THE RESULTS ARE TEMPORARILY STORED IN TR1,TI1,TR2,TI2
      C     DEPENDING IN RELATION OF I to KHALF
0030       48 IP=JK+I
```

SUBTM

```
0031                IQ=IP+IHALF
                C   I AND IU ARE INDICES OF TR2,TI2 WHERE RESULTS OF PARTIAL SUMS ARE
                C   STORED AND CORRESPOND TO I AND L RESPECTIVELY FOR
                C   I LESS THAN OR EQUAL TO KHALF
0032                IF(I-KHALF)51,51,53
0033              51 IU=I+KHALF
0034                AR=TR1(IP)
0035                AI=TI1(IP)
0036                BR=TR1(IQ)*WR-TI1(IQ)*WI
0037                BI=TR1(IQ)*WI+TI1(IQ)*WR
0038                TR2(I)=AR+BR
0039                TI2(I)=AI+BI
0040                TR2(IU)=AR-BR
0041                TI2(IU)=AI-BI
0042                GO TO 81
                C   FURTHER CALCULATIONS DURING THIS PASS AND HENCE MAY BE USED
                C   FOR TEMPORARY STORAGE OF RESULTS CORRESPONDING TO I AND L
                C   RESPECTIVELY FOR I GREATER THAN KHALF
0043              53 IL=I-KHALF
0044                IU=IL+JHALF
0045                AR=TR1(IP)
0046                AI=TI1(IP)
0047                BR=TR1(IQ)*WR-TI1(IQ)*WI
0048                BI=TR1(IQ)*WI+TI1(IQ)*WR
0049                TR1(IL)=AR+BR
0050                TI1(IL)=AI+BI
0051                TR1(IU)=AR-BR
0052                TI1(IU)=AI-BI
0053              81 CONTINUE
                C   STORES PARTIAL SUMS JUST CALCULATED (TR1,TI1,TR2,TI2) IN TR1,TI1
                C   IN THE PROPER ORDER PRIOR TO NEXT PASS
0054                JJJ=KHALF+1
0055                DO 83 IK=JJJ,JHALF
0056                JJMK=IK-KHALF
0057                JJPK=IK+KHALF
0058                JJPJ=IK+JHALF
0059                TR1(IK)=TR1(JJMK)
0060                TI1(IK)=TI1(JJMK)
0061                TR1(JJPJ)=TR1(JJPK)
0062                TI1(JJPJ)=TI1(JJPK)
0063                TR1(JJMK)=TR2(JJMK)
0064                TI1(JJMK)=TI2(JJMK)
0065                TR1(JJPK)=TR2(IK)
0066              83 TI1(JJPK)=TI2(IK)
                C   RESETS IHALF AS A COUNTER FOR N
0067                IHALF=IHALF/2
0068                WRITE(6,110) IHALF
0069             110 FORMAT(7H IHALF=,I3)
0070                GO TO 34
0071              65 CONTINUE
0072                IF(NOUT.EQ.1) GO TO 107
0073                GO TO 108
0074             107 WRITE (6,100)
0075                GO TO 50
0076             108 WRITE(6,104)
0077             104 FORMAT (22H TRANSFORMED ELEMENTS)
0078                WRITE(6,102)(TR1(J),J=1,JHALF)
0079             102 FORMAT(/10F12.4)
0080                WRITE(6,100)
0081             100 FORMAT(26H TRANSFORMATION COMPLETED)
0082                GO TO 50
0083             999 WRITE(6,101)
0084             101 FORMAT(42H ERROR CAUSED BY INVALID CONTROL PARAMETER)
0085              50 RETURN
0086                END
```

SUBDH

```
0001          SUBROUTINE SUBDH(N,Z,M,NOUT)
0002          IMPLICIT REAL*4(A-H,O,V-Z),INTEGER*4(I-N,P-U)
0003          COMMON A(4096),C(4096),B(2048),D(2048)
0004        111 FORMAT(1X,10F12.6)
0005        101 FORMAT(1X,10F12.3)
0006          MM=1
0007          CALL AMX(MM,M,J,AMAX,AVE)
0008          T=N/2
0009          IF(M-N) 12,13,14
0010         12 DO 9 K=M,N
0011          A(K)=A(M)
0012          9 CONTINUE
0013          GO TO 13
0014         14 L=J-T
0015          IF(L.LE.0) L=1
0016          LL=L+N
0017          IF(M.LT.LL) GO TO 16
0018          GO TO 18
0019         16 DO 17 K=M,LL
0020         17 A(K)=A(M)
0021         18 DO 15 K=1,N
0022          A(K)=A(L+K-1)
0023         15 CONTINUE
0024          WRITE(6,106)
0025        106 FORMAT(/54H    COPIED INTERFEROGRAM                    )
0026          WRITE(6,101) (A(K),K=1,N)
0027         13 DO 3 K=1,N
0028          C(K)=A(K)-AVE
0029          3 CONTINUE
0030          WRITE(6,102)
0031        102 FORMAT(/54H  REDUCED INTERFEROGRAM                      )
0032          WRITE(6,101)(C(K),K=1,N)
0033          DO 4 K=1,N
0034          ASUM=0.0
0035          DO 5 KK=1,N
0036          K1=KK+K-1
0037          IF(K1-N) 6,6,7
0038          7 K1=K1-N
0039          6 ASUM=ASUM+C(KK)*C(K1)
0040          5 CONTINUE
0041          A(K)=ASUM
0042          4 CONTINUE
0043          WRITE(6,103)
0044        103 FORMAT(/54H  AUTOCORRELATED INTERFEROGRAM               )
0045          WRITE(6,101)(A(K),K=1,N)
0046          CALL AMX(MM,M,J,AMAX,AVE)
0047          DO 8 K=1,N
0048          A(K)=A(K)/AMAX
0049          8 CONTINUE
0050          WRITE(6,105)
0051        105 FORMAT(/54H NORMALISED INTERFEROGRAM                    )
0052          WRITE(6,111)(A(K),K=1,N)
0053          DO 10 K=1,T
0054          APOD=COS(3.141593*(K-1)/(N-2))**2
0055          A(K)=A(K)*APOD
0056          A(N-K+2)=A(N-K+2)*APOD
0057         10 CONTINUE
0058          A(1+T)=0.0
0059          DO 11 K=1,N
0060          C(K)=0.0
0061         11 CONTINUE
0062          WRITE(6,104)
0063        104 FORMAT(/54H FINAL DATA SET LENGTH = N AFTER ADPOD ISATION
0064          WRITE(6,101)(A(K),K=1,N)
0065          RETURN
0066          END
```

AMX

```
0001          SUBROUTINE AMX(MM,M,J,AMAX,AVE)
0002          COMMON A(4096),C(4096),B(2048),D(2048)
0003          AMAX=0
0004          AVE=0
0005          DO 1 K=1,M
0006          AVE=AVE+A(K)
0007          IF(A(K)-AMAX) 1,1,2
0008          2 AMAX=A(K)
0009          J=K
0010          1 CONTINUE
0011          WRITE(6,200) J
0012        200 FORMAT(3H J=,I4)
0013          L=-3
0014          DO 3 IQ=1,7
0015          KK=J+L
0016          C(IQ)=A(KK)
0017          L=L+1
0018          3 CONTINUE
0019          WRITE(6,1000) (C(IQ),IQ=1,7)
0020       1000 FORMAT(//7E10.4)
0021          AVE=AVE/(M-MM+1)
0022          WRITE(6,201) AVE
0023        201 FORMAT(/1H,8HAVERAGE=F6.0)
0024          RETURN
0025          END
```

SUBPT

```
      C  SUBROUTINE FOR PLOTTING OUT SPECTRAL DATA OBTAINED BY TRANSFORMATION IN A FORM
      C  WHICH CAN BE RECOGNISED AS A SPECTRUM
0001        SUBROUTINE SUBPT(I9,I7,Z,FSINT,FREQL,FREQH,IOPUT,I14,I15,V3,V4,
           1V5,V6,I11,I12,I13,ZX,NABS,NOUT,NCARD)
0002        IMPLICIT  REAL*4(A-H,O,V-Z), INTEGER*4(J-N,P-U)
0003        DIMENSION AA(4000),BB(4000)
0004        DIMENSION H(50),I(15),G(1),F(1),V(11),ZX(20)
0005        COMMON A(4096),C(4096)
0006      3 I9=1+I9
0007        WRITE(6,200) I9
0008      200 FORMAT(/6H I9 = ,I3)
0009        V(7)=1
0010        IF(I9.EQ.4) GO TO 26
0011        DATA H/1.0,2*9.0,1.0,5.0,60.0,30.0,2*4.0,30.0,60.0,5.0,7.0,105.0,
           135.0,5.0,1.0,2*9.0,1.0,5.0,35.0,105.0,7.0,6.0,108.0,27.0,4.0,8.0,
           184.0,56.0,2*7.0,56.0,84.0,8.0,4.0,27.0,108.0,6.0,16.0,2*81.0,
           1128.0,16.0,128.0,4*125.0/
0012        K=41
0013        L=1
0014        DO 120 Q=2,5
0015        DO 121 IX=2,Q
0016        C(10*Q+IX)=-H(L)/H(K)
0017        C(10*Q-IX)=H(1+L)/H(K)
0018        C(30*Q+IX)=H(2+L)/H(K)
0019        C(30*Q-IX)=-H(3+L)/H(K)
0020        L=4+L
0021        K=1+K
0022      121 CONTINUE
0023      120 CONTINUE
0024        DATA I/1,2,3,5,4,0/
0025        GI=Z*FSINT
0026        GI=5000.0/GI
0027        WRITE(6,201) GI
0028      201 FORMAT(/18H FREQ INCREMENT = ,F8.4)
      C GI GIVES THE INCREMENT IN FREQ FOR THE BASIC ARRAY OF SIZE Z.G IS IN REC CM
0029        FI=5000.0/FSINT
      C FIIS  THE ALIAS FREQUENCY WHICH IS 1/2*FSINT,FI IS IN REC CM

0030        X=FREQL/GI
0031        X=X-0.5
0032        K=INT(X)
0033        Y=FREQH/GI
0034        Y=Y-0.5
0035        Q=INT(Y)
      C THIS HAS PRODUCED AN ARRAY OF SIZE Q-K WHICH IS REQUIRED FOR INTERPOLATION OF
      C SPECTRAL DATA
0036        Y=0
0037        IK=K-1
0038        L=Q+1
0039        DO 10 M=IK,L
0040        IF(A(M).LT.Y) GO TO 10
0041        Y=A(M)
0042       10 CONTINUE
0043        WRITE(6,400)Y
0044      400 FORMAT(16H LARGEST VALUE=,F10.6)
       C THIS CALCULATES LARGEST A(M) IN ARRAY FROM I TO L READY FOR NORMALISATION
0045        Y = 1/Y
0046       40 MI=19+7
0047        V(MI)=Y
```

S(SPT

```
C THIS STORES THE NORMALISATION FACTORS V(8)-V(11)
0048          DO 11 M=IK,L
0049          A(M)=A(M)*Y
0050       55 IF(I9.EQ.3) GO TO 51
0051          GO TO 11
0052       51 IF (A(M))53,53,54
0053       53 A(M)=0.0
0054          GO TO 11
0055       54 A(M)=SQRT(A(M))
0056       11 CONTINUE
C CARRIES OUT NORMALISATION PROCEDURE ON A(M) SPECTRAL ELEMENTS BY DIVIDING BY
C THE MAXIMUM VALUE OF A(M) WHERE M RUNS FROM IKTO L
0057          IF(I9.NE.1) GO TO 2o
C WRITES OUT CURRENT DATE WHEN I(9)=1
0058       12 WRITE(6,107) I11,I12,I13
0059      107 FORMAT(//8HIDATE = ,I2,1XI2,1XI2)
0060          WRITE(6,140) ZX
0061      140 FORMAT(30A4)
0062       2o GO TO(4,2,3,6),I9
0063        2 WRITE(6,112)
0064      112 FORMAT(55H  NORMALISED SAMPLE SPECTRUM                          )
0065          GO TO 300
0066        4 WRITE(6,113)
0067      113 FORMAT(55H  NORMALISED BACKGROUND SPECTRUM                      )
0068          GO TO 300
0069        3 WRITE(6,114)
0070      114 FORMAT(55H  ABSOLUTE TRANSMITTANCE RATIO OF SAMPLE/BACKGROUND   )
0071          GO TO 300
0072        6 WRITE(6,115)
0073      115 FORMAT(55H  I(9)=4,AN ERROR HAS OCCURRED                        )
0074      300 GO TO (9,8),I9
0075          GO TO 48
0076        8 WRITE(6,116) I14
0077      116 FORMAT(22H SAMPLE TAPE REF NO = A5)
0078          GO TO 48

0079        9 WRITE(6,117) I15
0080      117 FORMAT(26H BACKGROUND TAPE REF NO = A5)
0081       48 WRITE(6,118) Y
0082      118 FORMAT(21H NORMALISING FACTOR =, F10.6)
0083          IF(I9.NE.3) GO TO 43
0084          CALL SUBCOR(V(8),V(9),V(10),V3,V4,V5,V6,V(7))
0085          IF(NABS.EQ.1) GO TO 63
0086          WRITE(6,124)
0087      124 FORMAT(20H FREQ TRANSMITTANCE)
0088          GO TO 50
0089       63 WRITE(6,127)
0090      127 FORMAT(17H FREQ  ABSORBANCE)
0091          CALL SUBLPL
0092          GO TO 34
0093       43 WRITE(6,122)
0094      122 FORMAT(17H FREQ AMPLITUDE )
0095       50 CALL SUBLP
0096       34 P=10*IOPUT
0097          R=30*IOPUT
0098          G(1)=FLOAT(IOPUT)
0099          G(1)=GI/G(1)
C GI IS THE FREQ INCREMENT WHICH RESULTS IF IOPUT >1
0100          JJ=0
0101          DO 61 MI=K,Q
0102          DO 62 IK=1,IOPUT
0103          JJ=JJ+1
0104          X=FLOAT(MI)
0105          X=X*GI
0106          IF(X.GT.F1) GO TO 35
C FI IS THE ALIAS FREQUENCY
0107          IF(IK.GT.1) GO TO 27
0108          F(1)=A(1+MI)
0109          F(1)=F(1)*V(7)
0110          GO TO 29
0111       27 Y=FLOAT(IK)
0112          Y=Y-1
0113          Y=Y*G(1)
0114          X=X+Y
0115          IF(MI.EQ.Q) GO TO 350
C CHECKS FOR END OF ARRAY K-Q
0116          Y=A(MI)*C(P+IK)
0117          E=A(1+MI)*C(P-IK)
0118          Y=Y+E
0119          E=A(2+MI)*C(R+IK)
0120          Y=Y+E
0121          E=A(3+MI)*C(R-IK)
0122          F(1)=Y+E
0123          F(1)=F(1)*V(7)
0124       29 AA(JJ)=X
0125          BB(JJ)=F(1)
C USES INTERPOLATING COEFFICIENTS C TO GIVE CORRECTED AMPLITUDES F(1) AT THE
C NEW FREQ INTERVAL G(1). THE FREQ CORRESPONDING TO AMPL F(1) IS X
0126          IF(I9.EQ.3) GO TO 28
0127          GO TO 25
0128       28 IF(NABS.EQ.1) GO TO 64
0129          GO TO 25
0130       64 CALL SUBGPL(V(7),X,F(1),I9,NCARD,NOUT)
0131          GO TO 62
0132       25 CALL SUBGP(V(7),X,F(1),I9,NCARD,NOUT)
C 24 IS BEGINNING OF PLOT ROUTINE
0133       62 CONTINUE
0134       61 CONTINUE
0135      350 QQ=Q-K
0136          QQ=QQ*IOPUT
0137          WRITE(6,190) Q,K,QQ,IOPUT
0138      190 FORMAT(5I5)
0139          IF(NCARD.EQ.0) GO TO 35
0140          GO TO (301,302),NCARD
0141      301 IF(I9.EQ.3) GO TO 302
0142          GO TO 35
0143      302 WRITE(7,189)(AA(JJ),BB(JJ),JJ=1,QQ)
0144          WRITE(6,191)
0145      191 FORMAT(1X 'HAS PUNCHED CARD OUTPUT')
0146      189 FORMAT(5(F7.2,F7.4,1X))
0147       35 RETURN
0148          END
```

TPREAD

```
0001            SUBROUTINE TPREAD(M,NOUT)
0002            DIMENSION A(4096)
0003            COMMON A
0004            I=1
0005         10 K=I+19
0006            READ(5,100)(A(J),J=I,K)
0007            DO 50 J=I,K
0008            IF(A(J)) 20,50,50
0009         50 CONTINUE
0010            I=I+20
0011            GO TO 10
0012         20 M=J-1
0013            IF(NOUT.EQ.1) GO TO 21
0014            WRITE(6,101)(A(J),J=1,M)
0015         21 WRITE(6,102) M
0016        100 FORMAT(20F4.0)
0017        101 FORMAT(/10F6.0)
0018        102 FORMAT(19H NO OF DATA POINTS=,I4)
0019            RETURN
0020            END
```

SUBLP

```
      C SUBROUTINE USED TO SET UP LINE PRINTER SO THAT DATA CAN BE OBTAINED IN
      C SPECTRAL FORM
0001            SUBROUTINE SUBLP
0002            DIMENSION CHAR(101),XNUM(11)
0003            DATA DOT,DIV/1H.,1H+/
0004            DATA XNUM/0.0,0.1,0.2,0.3,0.4,0.5,0.6,0.7,0.8,0.9,1.0/
0005            WRITE(6,101) XNUM
0006        101 FORMAT(17X,F3.1,10(7X,F3.1))
0007            DO 90 K=1,101
0008         90 CHAR(K)=DOT
0009            DO 91 IZ=1,21
0010            IK=1
0011            IK=IK+5*(IZ-1)
0012         91 CHAR(IK)=DIV
0013            WRITE(6,100) CHAR
0014        100 FORMAT(1H,17X,101A1)
0015            RETURN
0016            END
```

```
0001            SUBROUTINE SUBGP(V7,X,F1,I9,NCARD,NOUT)
0002            DIMENSION CHAR(101)
0003            DATA BLANK,PLOT,PLUS/1H,1H*,1H+/
0004            Y=F1
0005            IF(NOUT.EQ.1) GO TO 105
          C THIS HAS MULTIPLIED AMPLITUDE BY V(7) TO CORRECT FOR GAIN SETTINGS.V(7)=1
          C EXCEPT WHEN I(9)=3 IN WHICH CASE V(7) IS COMPUTED IN SUBPT
0006            DO 92 K=2,101
0007         92 CHAR(K)=BLANK
0008            CHAR(1)=PLUS
0009            I=(Y*100)+0.5
0010            IF(I.GT.100) GO TO 3
0011            IF(I.LT.1) GO TO 5
0012            GO TO 4
0013          3 I=101
0014            GO TO 4
0015          5 I=2
0016          4 CHAR(I)=PLOT
0017            WRITE(6,103) X,Y, CHAR
0018        103 FORMAT(1X,F6.2,3X,F6.4,3X,101A1)
0019        105 CONTINUE
0020            END
```

SUBCOR

```
0001            SUBROUTINE SUBCOR(V8,V9,V10,V3,V4,V5,V6,V7)
0002            XNC=V8/(V9*V10)
0003            XNC=SQRT(XNC)
0004            WRITE(6,100) XNC
0005          100 FORMAT(1H,26H NORMALISATION CORRECTION=,F10.4)
0006            GSAM=V3+V4*10.0
0007            GBKG=V5+V6*10.0
0008            DGAIN=GSAM-GBKG
0009            IF(DGAIN)5,7,7
0010            5 DGAIN=-DGAIN
0011            7 VP=DGAIN/20.0
0012              VP=VP*2.3025851
0013              VP=EXP(VP)
0014              VX=1.0/VP
0015              V7=XNC*VX
0016              WRITE(6,101) VP,VX,V7
0017          101 FORMAT(1H ,3HVP=,F12.4,3HVX=,F12.4,3HV7=,F12.4)
0018            RETURN
0019            END
```

SUBLPL

```
0001          SUBROUTINE SUBLPL
0002          DIMENSION CHAR(101),XNUM(11)
0003          DATA DOT,DIV/1H.,1H+/
0004          DATA XNUM/0.00,0.25,0.50,0.75,1.00,1.25,1.50,1.75,2.00,2.25,2.50/
0005          WRITE(6,101) XNUM
0006      101 FORMAT(16X,F4.2,10(6X,F4.2))
0007          DO 90 K=1,101
0008       90 CHAR(K)=DOT
0009          DO 91 IZ=1,21
0010          IK=1
0011          IK=IK+5*(IZ-1)
0012       91 CHAR(IK)=DIV
0013          WRITE(6,100) CHAR
0014      100 FORMAT(1H,17X,101A1)
0015          RETURN
0016          END
```

SUBGPL

```
0001          SUBROUTINE SUBGPL(V7,X,F1,I9,NCARD,NOUT)
0002          DIMENSION CHAR(101)
0003          DATA BLANK,PLOT,PLUS/1H,1H.,1H+/
0004          Y=F1
0005          Y=1.0/Y
0006          Y=ALOG(Y)
0007          IF(NOUT.EQ.1) GO TO 105
0008          DO 92 K=2,101
0009       92 CHAR(K)=BLANK
0010          CHAR(1)=PLUS
0011          I=(Y*40)+0.5
0012          IF(I.GT.100) GO TO 3
0013          IF(I.LT.1) GO TO 5
0014          GO TO 4
0015        3 I=101
0016          GO TO 4
0017        5 I=2
0018        4 CHAR(I)=PLOT
0019          WRITE(6,103) X,Y,CHAR
0020      103 FORMAT(1X,F6.2,3X,F6.4,3X,101A1)
0021      105 CONTINUE
0022       11 RETURN
0023          END
```

APPENDIX B

Normal Coordinate Studies on Pyridine-Halogen Complexes

FAR-INFRARED INTENSITY AND NORMAL COORDINATE STUDIES ON PYRIDINE–HALOGEN COMPLEXES

G. W. BROWNSON AND J. YARWOOD
Chemistry Department, University of Durham, Durham City (England)
(Received July 13th, 1971)

ABSTRACT

Absolute integrated intensity data have been determined for the two low frequency bands due to ν(D–I) and ν(I–X) in pyridine–IX (X = I,Cl,Br) complexes. Along with the normal coordinates, calculated using a linear triatomic model, these data have been used to calculate dipole derivatives $\partial\vec{\mu}/\partial R_j$ values. Pyridine-d_5–IBr spectra have been used to estimate possible values of the interaction force constant k_{13}. The dipole moment change $\partial\vec{\mu}/\partial R_{D-I}$ calculated for the pyridine–I_2 complex using a simple model is considerably lower than that observed, implying that "charge-transfer" effects contribute significantly to the band intensities.

Numerous attempts have been made in the past to compare the acceptor strengths of the halogens and interhalogens with strong donors such as pyridine. From thermodynamic (K_c) measurements[1,2], for example, the acceptor strength decreases in the order ICl > IBr > I_2. The same conclusion was drawn from studies on the frequencies of the bands[3-5] arising from ν(I–X) and ν(D–I) stretching modes of the molecule pyridine–I–X, which occur in the far-infrared region. Complications arise, as already pointed out[6-8], using K_c measurements because the equilibrium constant includes entropy contributions, introduced, for example, by steric effects (reliable $\Delta H°$ values being unavailable to date). The dangers of using relative frequency shifts have also been discussed[6-8] and it is clear that changes in *force constant* must be compared if one is to take account of vibrational mixing, especially of the two low frequency stretching modes (of species A_1, if the complex molecule has C_{2v} symmetry). Such mixing may cause both frequency and intensity changes of differing amounts in going from one complex to another and it is desirable to compare transition moments, $\partial\vec{\mu}/\partial R$ if possible.

Hitherto a linear triatomic model has been used[6-8] to estimate the normal coordinates and transition moments relating to the two low frequency modes ν(I–X) and ν(D–I). This approximation should be a reasonable one in view of the

TABLE 1

FREQUENCY, INTENSITY, NORMAL COORDINATE AND TRANSITION MOMENT DATA FOR PYRIDINE–IX COMPLEXES

Complex	$\nu(I\text{–}X)^a$ (cm^{-1})	$\nu(D\text{–}I)^a$ (cm^{-1})	$B(I\text{–}X)^b$	$B(D\text{–}I)^b$	k_{13} ($mdyn\,Å^{-1}$)	k_{I-X} ($mdyn\,Å^{-1}$)
Pyridine–ICl (benzene)	292	140	11900±200	3700±200	0.0	1.36
					0.1	1.41
					0.2	1.45
					0.3	1.48
					0.4	1.51
					0.5	1.52
					0.6	1.52
					0.1	
					0.6	
Pyridine–IBr (benzene)	206 (205)[f]	133–35 (127)[f]	6500±100	2800±100	0.0	1.00
					0.1	1.18
					0.2	1.28
					0.3	1.36
					0.4	1.40
					0.5	1.43
					0.6	1.43
					0.1	
					0.6	
Pyridine–I_2 (cyclohexane)	183	93	2500± 40	1950± 60	0.0	1.13
					0.1	1.27
					0.2	1.37
					0.3	1.45
					0.4	1.50
					0.5	1.54
					0.6	1.55
Pyridine (cyclohexane)	183[g]	94[g]	2930[g]	2790[g]	0.1	1.27
					0.2	1.37
					0.5	1.54
					0.6	1.55

[a] All values are ±1 cm^{-1}.
[b] Intensities in "darks" (cm^{-1} cm^2 $mmole^{-1}$). Errors are standard errors from a least squares fit of the Beer–Lambert law plots.
[c] Units are 10^{-12} gł.
[d] Units are D $Å^{-1}$.
[e] "Corrected" values (see text).
[f] Values for C_5D_5N–IBr.
[g] Data of Lake and Thompson (ref. 10).

k_{D-I} (mdyn Å^{-1})	L_{11}^{-1}[c]	L_{12}^{-1}[c]	L_{21}^{-1}[c]	L_{22}^{-1}[c]	$\partial\vec{\mu}/\partial R_{I-X}$[d]	$\partial\vec{\mu}/\partial R_{D-I}$[d]
0.63	6.57	−0.88	2.68	9.36	6.61	−7.93
0.62	6.74	−0.22	2.22	9.40	7.27	−6.93
0.62	6.87	+0.41	1.76	9.39	7.67	−6.28
0.64	6.97	1.02	1.31	9.34	8.12	−5.45
0.68	7.04	1.62	0.85	9.25	8.62	−4.64
0.73	7.08	2.21	0.40	9.13	8.92	−3.75
0.80	7.10	2.82	−0.08	8.96	9.30	−2.73
					4.80[e]	−6.80[e]
					(4.7)[e]	
					6.62[e]	−3.97[e]
					(6.8)[e]	
0.73	6.75	−3.92	7.08	8.93	2.02	−9.40
0.62	8.16	−1.84	5.40	9.57	4.44	−7.80
0.60	8.87	−0.39	4.13	9.74	5.92	−6.52
0.62	9.31	+0.79	3.03	9.72	7.04	−5.37
0.63	9.61	2.03	1.80	9.53	8.12	−4.07
0.68	9.76	3.17	0.62	9.21	9.05	−2.76
0.76	9.75	4.35	−0.66	8.72	9.80	−1.31
					3.83[e]	−7.60
					(3.8)[e]	
					9.17[e]	−1.65
					(9.10)[e]	
0.34	9.12	−1.91	6.87	9.82	1.83	−6.31
0.31	9.99	−0.61	5.62	9.94	3.00	−5.60
0.31	10.51	+0.50	4.49	9.99	3.91	−4.97
0.33	10.90	1.52	3.38	9.89	4.72	−4.31
0.36	11.19	2.51	2.26	9.69	5.49	−3.60
0.41	11.37	3.45	1.15	9.39	6.18	−2.89
0.48	11.41	4.43	−0.07	8.98	6.84	−2.09
0.32	9.92	−0.66	5.67	9.98	2.84	−6.70
0.32	10.49	+0.47	4.52	10.00	3.93	−6.00
0.42	11.36	3.46	1.14	9.41	6.63	−3.71
0.48	11.42	4.43	−0.07	8.96	7.41	−2.79

relatively high frequencies of the pyridine, A_1, vibrations which are changed very little[6] on going to the complex. There has, however, been a major problem in the past in that *assumed* values of the interaction constant k_{13}[6–8] have had to be used. This problem has now been avoided by the use of pyridine-d_5 to obtain extra frequency data without changing the donor properties. We have calculated the force constants f_{12} and f_{23} for a range of interaction constants and plotted the usual ellipses[8] to find the mathematical solution for these two constants. Fig. 1 shows these ellipses for pyridine–IBr and pyridine-d_5–IBr in the region where they

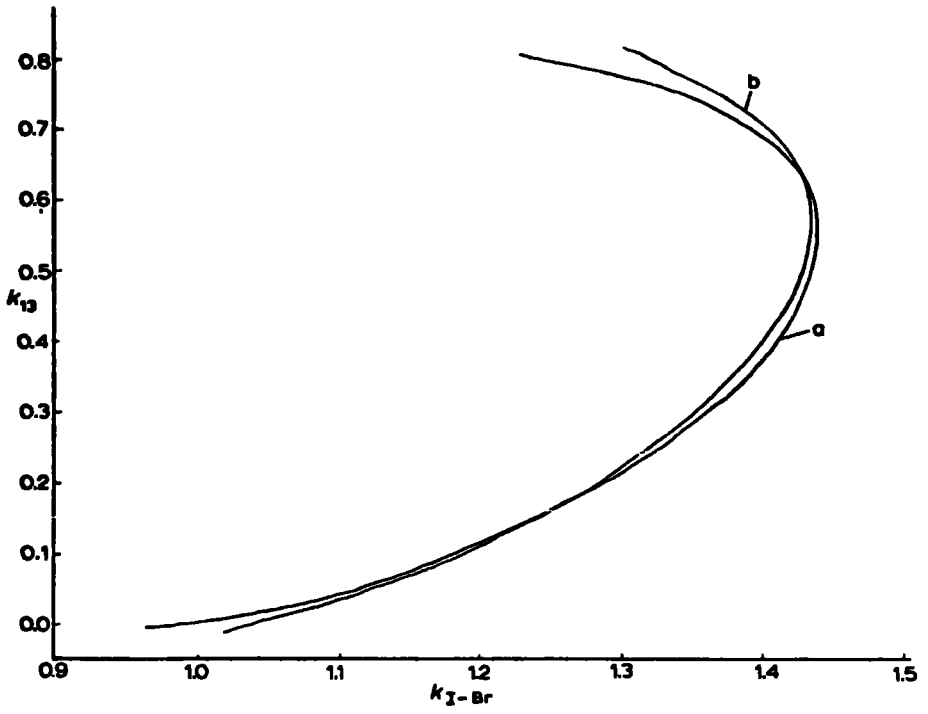

Fig. 1. Force constant ellipses for pyridine–IBr (a) and pyridine-d_5–IBr (b) using a linear triatomic model.

cross. The two crossing points correspond to k_{13} = 0.1–0.2 mdyn Å^{-1}* and k_{13} = 0.5–0.6 mdyn Å^{-1}, so it is necessary to choose the correct solution before proceeding to calculate the transition moment data. In view of previous estimates of this interaction constant (i.e. about 0.4 mdyn Å^{-1})[8,9] we would expect the 0.6 mdyn Å^{-1} value to be more acceptable but we have obtained the normal coordinate matrix (L^{-1}) and the transition moments for the whole range of k_{13} values to see how they vary. The results are shown for the three complexes in Table 1. It should be noted that we have not observed sufficient frequency shift on going to the pyridine-d_5 complexes of iodine and iodine monochloride for a unique solution to be obtained so we have assumed the same values of k_{13} for these complexes. There is, of course, another set of solutions of f_{12} and f_{23} not shown in Table 1. We have chosen the solutions for which the force constants ellipses cross. It should be emphasised that the choice of force constants made (a large f_{I-X} with a small f_{D-I}, for example) depends on the assignment of the original frequencies to the normal vibrations of the pyridine–I–X system. It has been usual in the past[3-11] to assign the band at higher wave number to the ν(I–X) vibration and the other band to the intermolecular stretching mode, ν(D–I). Since it is the lower frequency band which shows a frequency shift on isotopic substitution it seems likely that this band corresponds to the mode which is mostly D–I stretching. This is the opposite from the situation found by Gayles[12] for trimethylamine–halogen complexes. The two

* 1 mdyn Å^{-1} = 10^{-2} N m^{-1} in S.I. units.

vibrations are, of course, expected to be "mixed" and the L^{-1} matrix elements in Table 1 show that this is the case. These normal coordinates also show that, as expected, the closer the two frequencies the more severe is such mixing. The fact that a significant frequency shift is observed only for the iodine monobromide complex can be rationalised in this way since the vibrational coupling is greatest for this complex (the two frequencies are closest in this case). Gayles[12] concluded that, for the trimethylamine complexes, k_{13} was negative. This is not the case for pyridine complexes and, since as the D–I bond is stretched the I–X bond is strengthened (the halogen becoming closer to the "free" molecule), we would expect k_{13} to be positive[13].

Intensity data for both vibrations have now been obtained for all three complexes. Since there was a discrepancy between our intensity data[8] for pyridine–I_2 and those of Lake and Thompson[10] we have remeasured the intensities of the two far-infrared bands in cyclohexane over a range of pyridine concentrations. The intensity of the low frequency band is again significantly different from the previous value[10]. No major variations in band intensity are apparent although we are further investigating the effect[11] of solvent polarity. The data shown in Table 1 are average values using $K_c = 140$ l mole^{-1} (ref. 2). It should be noted that, although the indeterminant signs of the dipole derivatives $(\partial\vec{\mu}/\partial Q_i)_0$ lead to two values of $\partial\vec{\mu}/\partial R_j$ in each case, we have chosen the sign combination of the $(\partial\vec{\mu}/\partial Q_i)_0$ parameters which leads to the two transition moments having *opposite* signs[8].

In order to compare directly the values of $\partial\vec{\mu}/\partial R_{I-X}$ for the three complexes it is necessary to subtract the contributions made by the "free" halogen in an "inert" solvent. We have recently remeasured the intensities of the ν(I–Cl) and ν(I–Br) bands for these interhalogens in carbon tetrachloride and heptane. The "*diatomic*" contributions[8] $\partial\vec{\mu}/\partial r$ are 2.5 D Å^{-1} and 0.7 D Å^{-1} respectively*. On subtracting these values from the computed $\partial\mu/\partial R_{I-X}$ values we get the "corrected" values shown in Table 1. The alternative is to subtract the values of $(\partial\vec{\mu}/\partial Q_i)_0$ for the "free" halogen *before* computing $\partial\vec{\mu}/\partial R_{I-X}$ and $\partial\vec{\mu}/\partial R_{D-I}$ for the complex. The two calculations should be roughly equivalent and do indeed lead to similar values corrected of $\partial\vec{\mu}/\partial R_{I-X}$ for both complexes.

It may be seen from Table 1 that in all three cases the relative absolute value of the two transition moments is reversed on going from $k_{13} = 0.1$ to 0.6 mdyn Å^{-1}. At $k_{13} = 0.6$ the $\partial\vec{\mu}/\partial R_{I-X}$ value is the greatest but at $k_{13} = 0.1$ the $\partial\vec{\mu}/\partial R_{D-I}$ value is now the larger. Although, at first sight, we may except $\partial\vec{\mu}/\partial R_{I-X} > \partial\vec{\mu}/\partial R_{D-I}$ it is clear that if we accept the values for $k_{13} = 0.6$ then the $\partial\vec{\mu}/\partial R_{I-X}$ data are in the order IBr > I_2 > ICl while the $\partial\vec{\mu}/\partial R_{D-I}$ data are in the order ICl > IBr > I_2. There will, of course, be errors in these parameters, due to the use of a simplified model, but the data show that the ICl complex is the "strongest" complex using one transition moment and the "weakest" using the other. On the other hand, if

* 1 D Å^{-1} = 3.335×10^{-20} Coulomb in S.I. units.

we examine the data for $k_{13} = 0.1$ we find that the order of transition moments is now ICl > IBr > I_2 using $\partial\vec{\mu}/\partial R_{D-I}$ and IBr > ICl > I_2 using $\partial\vec{\mu}/\partial R_{I-X}$. Since thermodynamically[1,2] the iodine complex is very much weaker than the other two this would appear to be the most reasonable choice of the two. Further, a value of k_{13} in the region of 0.1–0.2 mdyn $Å^{-1}$ fits better with the value of 0.22 mdyn $Å^{-1}$ obtained using Badgers rule[14].

Assuming this choice to be correct the question arises whether it is reasonable to have $\partial\vec{\mu}/\partial R_{D-I} > \partial\vec{\mu}/\partial R_{I-X}$. Since the charge redistribution due to complexation and during vibration is not known, predicting dipole moment changes is very difficult. It seems clear from the recent NQR data[15,16] that the halogen molecules in these complexes are considerably polarised and that the extent of charge-transfer may be smaller (about 20–30 %) than at one time thought. It seems clear that polarisation forces are also involved. Table 2 shows dipole moments induced in the iodine molecule by pyridine, using the simplest possible model[19], as a function of the average distance between the molecules. Pyridine is treated as a point dipole (of 2.2 Debye) and the polarisability of the iodine is taken as 17.5×10^{-24} cm^3 (ref. 17). On this basis the observed dipole moment of the complex (4.5 D)[18] corresponds to a distance of ~ 3.2 Å and the dipole moment change, $\partial\vec{\mu}/\partial R_{D-I}$, is 2.3 D $Å^{-1}$. For $k_{13} = 0.1$ mdyn $Å^{-1}$ this is considerably lower than the observed

TABLE 2

INDUCED DIPOLE MOMENTS AND TRANSITION MOMENTS $\partial\vec{\mu}/\partial R_{D-I}$ FOR THE PYRIDINE–I_2 SYSTEM

r (Å)	$\vec{\mu}_{ind}$[a] (Debye)	Total dipole moment[b] (Debye)	$\partial\vec{\mu}/\partial R_{D-I}$ (D $Å^{-1}$)
2.0	9.64	11.84	
2.5	4.92	7.12	
2.6	4.36	6.56	5.6
2.9	3.16	5.36	3.6
3.0	2.85	5.05	3.1
3.1	2.55	4.77	2.80
3.2	2.34	4.54	2.30
3.3	2.14	4.34	2.00
3.4	1.95	4.15	1.90
3.5	1.80	4.00	1.50
3.6	1.65	3.85	1.50
3.7	1.52	3.72	1.30
3.8	1.40	3.60	1.20
3.9	1.30	3.50	1.00
4.0	1.20	3.40	1.00

[a] The dipole moment induced in the iodine molecule by pyridine is

$$\mu = \frac{2\alpha\vec{\mu}_{pyr}}{r^3}$$

where α is the iodine polarisability and r is the average distance between the molecules[19].
[b] After adding pyridine dipole moment.

value. However, since the D–I distance in the solid complex is 2.3 Å[20] the relevant distance for calculation of the induced moment using the simple model is probably more like 3.5–3.6 Å. Here the dipole moment change is only about 1.5 D $Å^{-1}$. It would appear therefore that the effects of electron "delocalisation" during vibration are important at least in determining the infrared intensities. At present it is not, however, possible to be sure which transition moment should be the largest. We are currently working on a more sophisticated model for these complexes in an attempt to examine the effects of mixing of these two vibrations with skeletal vibrations of the pyridine ring.

Thanks are due to S.R.C. for a studentship (to G.W.B.) and for funds to purchase a far-infrared interferometer.

REFERENCES

1 A. I. Popov and R. H. Rygg, *J. Amer. Chem. Soc.*, 79 (1957) 4622.
2 H. D. Bist and W. B. Person, *J. Phys. Chem.*, 71 (1967) 2750.
3 S. G. W. Ginn and J. L. Wood, *Trans. Faraday Soc.*, 62 (1966) 777.
4 I. Haque and J. L. Wood, *Spectrochim. Acta*, 23A (1967) 959.
5 S. G. W. Ginn, I. Haque and J. L. Wood, *Spectrochim. Acta*, 24A (1968) 1531.
6 J. Yarwood, *Spectrochim. Acta*, 26A (1970) 2099; *Trans. Faraday Soc.*, 65 (1969) 934.
7 Y. Yagi, W. B. Person and A. I. Popov, *J. Phys. Chem.*, 71 (1967) 2439.
8 J. Yarwood and W. B. Person, *J. Amer. Chem. Soc.*, 90 (1968) 594, 3930.
9 A. G. Maki and R. Forneris, *Spectrochim. Acta*, 23A (1967) 867.
10 R. F. Lake and H. W. Thompson, *Proc. Roy. Soc. (London)*, A297 (1967) 440.
11 R. F. Lake and H. W. Thompson, *Spectrochim. Acta*, 24A (1968) 1321.
12 J. N. Gayles, *J. Chem. Phys.*, 49 (1968) 1840.
13 I. M. Mills, in M. Davies (Editor), *Infra-Red Spectroscopy and Molecular Structure*, Elsevier, Amsterdam, 1963, Chap. 5, p. 194.
14 F. Watari, *Spectrochim. Acta*, 23A (1967) 1917.
15 H. Creswell-Fleming and M. W. Hanna, *J. Amer. Chem. Soc.*, in press.
16 G. A. Bowmaker and S. Hacobian, *Aust. J. Chem.*, 22 (1969) 2047.
17 M. W. Hanna, *J. Amer. Chem. Soc.*, 90 (1968) 285.
18 K. Toyoda and W. B. Person, *J. Amer. Chem. Soc.*, 88 (1966) 1629.
19 M. Davies, *Some Electrical and Optical Aspects of Molecular Behaviour*, Pergamon, Oxford, 1965.
20 O. Hassel, Chr. Rømming and T. Tufte, *Acta Chem. Scand.*, 15 (1961) 967.

REFERENCES

1. F.B.J. Fourier, 'Theorie Analtique de la Chaleur', 1822.
2. A.A. Michelson, 'Light Waves and Their Uses', University of Chicago Press, 1902.
3. J.D. Strong and G.A. Vanasse, J. Opt. Soc. Amer., 1959, 49, 844.
4. P. Jacquinot, Rep. Prog. Phys., 1960, 23, 267.
5. J. Connes, Rev. Optique, 1961, 40, 45, 116, 171, 231.
6. L. Genzel, J. Mol. Spectroscopy, 1960, 4, 241.
7. R.J. Bell, 'Introductory Fourier Transform Spectroscopy', Academic Press, 1972.
8. J.W. Mellor, 'Comprehensive Treatise on Inorganic and Theoretical Chemistry', Longman Green and Co., London, 1922.
9. D.J. James and J. Ring 'Methodes Nouvelles de Spectroscopie Instrumentale', supplement of J. de Physique, 1967, 28, 22.
10. J.E. Chamberlain, Infrared Phys., 1966, 6, 195; J.E. Chamberlain, A.E. Costley and H.A. Gebbie, Spectrochim. Acta, 1967, 23A, 2255; J.E. Chamberlain and H.A. Gebbie, Appl. Optics, 1966, 5, 393.
11. M.J.E. Golay, Rev. Sci. Instrum., 1947, 18, 357.
12. J. Yarwood, 'Absolute Intensity Measurements in the Region 10 - 600 cm.$^{-1}$, Beckman-RIIC Ltd., 1971.
13. D.H. Martin (Editor) 'Spectroscopic Techniques', North Holland Publishing Company, 1967, Chapter 4.
14. R.B. Blackman and J.W. Tukey 'The Measurement of Power Spectra', Dover Publications, New York, 1959.
15. M.L. Forman, W.H. Steel, G.A. Vanasse, J. Opt. Soc. America, 1966, 56, 59.
16. J.W. Cooley and J.W. Tukey, Mathematics of Computation, 1965, 19, 195.
16. (a) W.J. Potts 'Chemical Infrared Spectroscopy', Vol. 1, J. Wiley and Sons, London, 1963, Chapter 6.

17. D.A. Ramsay, J. Amer. Chem. Soc., 1952, 74, 72.

18. J. Yarwood (Editor) 'Spectroscopy and Structure of Molecular Complexes', Planum Press, 1973, p.112.

19. J. Overend (Editor M.M. Davies) 'Infrared Spectroscopy and Molecular Structure', Elsevier Ltd., Amsterdam and London, 1963, Chapter 10.

20. E. Bright-Wilson and A.J. Wells, J. Chem. Phys., 1946, 14, 578.

21. G.J. Boobyer, Spectrochim. Acta, 1967, 23A, 335.

22. S. Maeda and P.N. Schatz, J. Chem. Phys., 1961, 35, 1617.

23. R.S. Mulliken, J. Amer. Chem. Soc., 1952, 74, 811.

24. S.M. Hasting, J.L. Franklin and J.C. Shiller, J. Amer. Chem. Soc., 1953, 75, 2901.

25. J.S. Ham, J.R. Platt and H. McConnell, J. Chem. Phys., 1951, 19, 1301.

26. E.E. Ferguson and F.A. Matsen, J. Chem. Phys., 1958, 29, 105; E.E. Ferguson and F.A. Matsen, J. Amer. Chem. Soc., 1960, 82, 3268.

27. E.E. Ferguson, J. Chim. Phys., 1964, 257.

28. R.S. Mulliken and W.B. Person 'Molecular Complexes - A lecture and preprint volume', Wiley-Interscience, New York, 1969.

29. W.B. Person, R.E. Humphrey and A.I. Popov, J. Amer. Chem. Soc., 1959, 81, 273.

30. J. Yarwood, Spectrochim. Acta, 1970, 26A, 2099.

31. H.C. Fleming and M.W. Hanna, J. Amer. Chem. Soc., 1971, 93, 5030.

32. S. Svenson, R. Nilsson, E. Basilier, U. Gelius, C. Nordling and K. Siegbahn, Chem. Phys. Letters, 1973, 23, 157.

33. (a) H.B. Friedrich and W.B. Person, J. Chem. Phys., 1966, 44, 2161.

33. (b) G.C. Pimentel and A.L. McClellan 'The Hydrogen Bond', W.H. Freeman and Co., San Francisco, 1960; A. Allerhand and P. von Rague Schleyer, J. Amer. Chem. Soc., 1963, 85, 1715.

34. H. Tsubomura, J. Chem. Phys., 1956, 24, 927.

35. J. Collin and L. D'Or, J. Chem. Phys., 1955, 23, 397.

36. W.B. Person (Ed. J. Yarwood) 'Spectroscopy and Structure of Molecular Complexes', Plenum Pub. Co., London, 1973, Chapter 1.

37. R.S. Drago 'Physical Methods in Inorganic Chemistry', Reinhold Pub. Co., New York, 1965, p.66.

38. R.L. Ward, J. Chem. Phys., 1963, 39, 852.

39. K.M.C. Davies and M.C.R. Symons, J. Chem. Soc., 1965, 2079.

40. S.G.W. Ginn and J.L. Wood, Trans. Faraday Soc., 1966, 62, 777.

41. J. Yarwood, Spectrochim. Acta, 1970, 26A, 2099.

42. R. Lake and H.W. Thompson, Spectrochim. Acta, 1968, 24A, 1321.

43. J.G. Kirkwood, J. Chem. Phys., 1937, 14, 5.

44. E. Bauer and M. Magat, J. Phys. Radium, 1938, 9, 319.

45. A.D. Buckingham, Proc. Roy. Soc., 1958, 248A, 169.

46. A.E. Baker and D.E. Bublitz, Spectrochim. Acta, 1966, 22, 1787.

47. T.D. Epley and R.S. Drago, J. Amer. Chem. Soc., 1967, 89, 5770.

48. M.D. Joesten and R.S. Drago, J. Amer. Chem. Soc., 1962, 84, 3817.

49. M.S. Nozari and R.S. Drago, J. Amer. Chem. Soc., 1970, 92, 7086.

50. T. Kitao and C.H. Jarboe, J. Org. Chem., 1967, 32, 407.

51. A. Hall, Ph.D. Thesis, University of London, 1969.

52. B.B. Wayland and R.S. Drago, J. Amer. Chem. Soc., 1964, 86, 5240.

53. S.K. Garg, H. Kilp and C.P. Smyth, Chem. Soc. Special Pub., No. 20, 83 (1966); R.A. Crump and A.H. Price, Trans. Faraday Soc., 1970, 66, 92.

54. J. Yarwood, Spectroscopy Lett., 1974, 7, 319.

55. M. Tamres (Ed. R. Foster) 'Molecular Complexes', Vol. 1 (Paul Elek Ltd., 1973), p.56.

56. C.N. Banwell, 'Fundamentals of Molecular Spectroscopy' McGraw-Hill Ltd., p.70.

57. W.J. Jones and N. Sheppard, Trans. Faraday Soc., 1960, 56, 625.

58. S.G. Lipson and H. Lipson, 'Optical Physics', Cambridge University Press.

59. P. Debye 'Polar Molecules', Chem. Catalog, New York, 1929.

60. J. Lamb, Trans. Faraday Soc., 1946, 42A, 242.

61. (a) S. Bratos, J. Rios and Y. Guissani, J. Chem. Phys., 1970, 52, 439.

(b) Y. Guissani, S. Bratos and J.C. Leicknam, C.R. Sci. Acad., B269, 1969, 137.

62. H. Morawitz and K.B. Eisenthal, J. Chem. Phys., 1971, 55, 887.

63. H. Dardy, V. Voltera and T.A. Litovitz, Faraday Symposium of Chem. Soc., 1972, No. 6, 71.

64. G.F. Pardoe, Trans. Faraday Soc., 1970, 66, 2699.

65. J. Yarwood, J. Chem. Soc., Faraday Transactions II, 1974 (in press).

66. (a) R.G. Gordon, J. Chem. Phys., 1963, 39, 2788.

(b) R.G. Gordon, J. Chem. Phys., 1964, 40, 1973.

(c) R.G. Gordon, J. Chem. Phys., 1965, 43, 1307.

(d) B.J. Benne, J. Jontner and R.G. Gordon, J. Chem. Phys., 1967, 47, 1600.

67. H. Shimizu, J. Chem. Phys., 1965, 43, 2453.

68. D. Steele 'Theory of Vibrational Spectroscopy', W.B. Saunders, London, 1971, Chapter 11.

69. J.H.R. Clarke and S. Miller, Chem. Phys. Lett., 1972, 13, 97.

70. H.W. Kroto and J. Teixeira Dias, Mol. Phys., 1970, 18, 773.

71. M. Scotto, J. Chem. Phys., 1968, 49, 5362.

72. C.H. Wang and P.A. Fleury, J. Chem. Phys., 1970, 53, 2243.

73. S. Bratos, Paper 15 at the Annual Re-Union Meeting of Societe de Chimie Physique, Paris, July 1973.

74. (a) M. Kakimoto and T. Fujiyama, Bull. Chem. Soc. Japan, 1972, 45, 2970.

(b) M. Kakimoto and T. Fujiyama, Bull. Chem. Soc. Japan, 1972, 45, 3021.

(c) H.E. Hallam, (Ed. M.M. Davies) 'Infrared Spectroscopy and Molecular Structure' (Elsevier, Amsterdam, 1964), Chapter 12.

75. M. Nelkon and P. Parker, 'Advanced Level Physics', Heinman Ltd., p.646.

76. C.H. Townes and A.L. Schawlow 'Microwave Spectroscopy', McGraw-Hill Ltd., New York, 1955.

77. G.W. Chantry 'Sub-Millimetre Spectroscopy', Academic Press, 1971, p.150.

78. J. Yarwood (Editor), 'The Spectroscopy and Structure of Molecular Complexes', Plenum Press, London, 1973, Chapters 2 and 3.

79. H.A. Benesi and J.H. Hildebrand, J. Amer. Chem. Soc., 1949, 71, 2703.

80. A.A. Ketelaar and C. van der Stolpe, Rec. Trav. Chim., 1952, 71, 1104.

81. R.S. Mulliken, J. Amer. Chem. Soc., 1952, 74, 811.

82. R.S. Mulliken, J. Phys. Chem., 1952, 56, 801.

83. R.S. Mulliken, J. Chim. Physique, 1964, 61, 20.

84. S. Kettle and A. Price, J. Chem. Soc., Faraday Trans. II, 1972, 68, 1306.

85. H. Rosen, Y.R. Shen and F. Stenman, Molecular Phys., 1971, 22, 33.

86. J.L. Lippert, M.W. Hanna and P.J. Trotter, J. Amer. Chem. Soc., 1969, 91, 4035.

87. D.L. Glusker, H.W. Thompson and R.S. Mulliken, J. Chem. Phys, 1953, 21, 1407.

88. D.L. Glusker and H.W. Thompson, J. Chem. Soc., 1955, 471.

89. S.G.W. Ginn, I. Haque and J.L. Wood, Spectrochimica Acta, 1968, 24A, 1531.

90. R.A. Zingaro and W.E. Tolberg, J. Amer. Chem. Soc., 1959, 81, 1353.

91. R.A. Zingaro and W.B. Witmer, J. Phys. Chem., 1960, 64, 1705.

92. F. Watari and S. Kinumaki, Sci. Reports Res. Inst. Tohoku University, 1962, A14, 64.

93. I. Haque and J.L. Wood, Spectrochimica Acta, 1967, 23A, 959, 2523.

94. A.V. Chekunov and P.A. Bazhulin, Teor. Eksperim. Akad. SSR., 1965, 1536 (Chem. Abstr., 1966, 64, 560g).

95. von R. Joeckle and R. Mecke, Ber. Bunsenges, Physik. Chem., 1967, 71, 165.

96. J. Yarwood, Trans. Faraday Soc., 1969, 65, 934.

97. A.I. Popov and R.H. Rygg, J. Amer. Chem. Soc., 1957, 79, 4622.

97 (a) J. Yarwood (Ed.), Spectroscopy and Structure of Molecular Complexes (Plenum Pub. Co. Ltd., 1973), Chapter 3.

98. R.D. Whittaker, J.R. Ambrose and C.W. Hickam, J. Inorg. Nucl. Chem., 1961, 17, 254.

99. L. Finar, Organic Chemistry, Volume 1, Longman Green and Co., p.138.

100. Second Year Honours Degree Lectures on Hückel Theory, Dr. D.T. Clark, University of Durham.

101. Y.A. Fialkov and I.D. Muzyka, Zhur. Obschchei Khim., 1948, 18, 1205.

102. R. Anderson and J.M. Prausnitz, J. Chem. Phys., 1963, 39, 1225.

103. L. Corrsin, B.J. Fax, R.C. Lord, J. Chem. Phys., 1953, 21, 1170.

104. D.A. Long, F.S. Murfin and E.L. Thomas, Trans. Faraday Soc., 1963, 59, 12.

105. D.H. Whiffen, J. Chem. Soc., 1956, 1350.

105. (a) G. Zerbi, B.L. Crawford and J. Overend, J. Chem. Phys., 1963, 38, 127.

106. H. Urey and C.A. Bradley, Phys. Rev., 1931, 38, 1969.

107. J.K. Wilmshurst and H.J. Bernstein, Can. J. Chem., 1957, 35, 1183.

108. J.P. McCullough, mentioned in 107.

109. (a) O. Hassel, T. Dahl and K. Sky, Acta Chem. Scand., 1967, 21, 592.

109. (b) O. Hassel and Ch. Rømming, Acta. Chem. Scand., 1956, 10, 696.

110. C.H. Kline and J. Turkevich, J. Chem. Phys., 1944, 12, 300.

111. G.C. Pimentel and A.L. McClellan, 'The Hydrogen Bond' (W.H. Freeman and Co., San Francisco, 1960); A. Allerhand and P. von Rague Schleyer, J. Amer. Chem. Soc., 1963, 85, 1715.

112. J.H.S. Green, W. Kynaston and H.M. Paisley, Spectrochimica Acta, 1963, 19, 549.

113. J.C. Duinker, Ph.D. Thesis, University of Amsterdam (1964).

114. G.A. Bowmaker and S. Hacobian, Aust. J. Chem., 1968, 21, 551.

115. R.T. Sanderson 'Inorganic Chemistry', Reinhold Inc., 1967, p.78.

116. C.E. Meloan and R.W. Kiser, Problems and Experiments in Instrumental Analysis, Charles E. Merril Books Inc., Columbus 16, Ohio, p.309.

117. E.E. Ferguson, J. Chem. Phys., 1956, 25, 577.
E.E. Ferguson, J. Chem. Phys., 1957, 26, 1357.
E.E. Ferguson, Spectrochimica Acta, 1958, 10, 123.

118. E.E. Ferguson and I.Y. Chang, J. Chem. Phys., 1961, 34, 628.

119. (a) M.W. Hanna, J. Amer. Chem. Soc., 1968, 90, 285.

119. (b) S.W. Benson 'The Foundations of Chemical Kinetics', McGraw Hill Inc., 1960, p.184.

119. (c) P.J. Trotter and D.A. Yphantis, J. Phys. Chem., 1970, 74, 1399.

119. (d) J.D. Childs, Ph.D. Thesis, Univ. of Oklahoma, 1971.

120. W.B. Person, J. Chem. Phys., 1963, 38, 115.

121. A.I. Popov, R.E. Humphrey and W.B. Person, J. Amer. Chem. Soc., 1960, 82, 1850.

122. (a) G. Briegleb, 'Elektronen-Donator-Acceptor-Komplexe', Springer-Verlag, Berlin, 1961.

122. (b) L.J. Andrews and R.M. Keefer 'Molecular Complexes in Organic Chemistry', Holden-Day, Inc., San Francisco, 1964.

122. (c) R.S. Mulliken and W.B. Person, Ann. Rev. Phys. Chem., 1962, 13, 107.

123. (a) H. Yada, J. Tanaka and S. Nagakura, J. Mol. Spectroscopy, 1962, 9, 461.

123. (b) F. Watari, Spectrochimica Acta, 1967, 23A, 1917.

123. (c) P. Klaboe, J. Amer. Chem. Soc., 1967, 89, 3667.

124. J. Yarwood and W.B. Person, J. Amer. Chem. Soc., 1968, 90, 3930.

125. (a) E.E. Ferguson, J. Chim. Physique, 1964, 61, 257.

(b) W.B. Person and J. Yarwood, J. Amer. Chem. Soc., 1968, 90, 594.

(c) G. Brownson and J. Yarwood, J. Mol. Struct., 1971, 10, 147.

126. J.L. Lippert, M.W. Hanna and P.J. Trotter, J. Amer. Chem. Soc., 1969, 91, 4035.

127. Spectrum published in Ref. 18, p.278.

128. G.F. Pardoe, Trans. Faraday Society, 1970, 66, 2699.

129. J. Ph. Poley, J. App. Sci., 1955, B4, 337; N.E. Hill, Proc. Phys. Soc., (London) 1963, 82, 723; N.E. Hill, Chem. Phys. Lett., 1968, 2, 5.

130. (a) R.G. Gordon, J. Chem. Phys., 1963, 38, 1724.

(b) G.W. Brownson and J. Yarwood, Spectroscopy Lett., 1972, 5, 185.

131. H. Tanaka, S. Higuchi and H. Kamada, Spectrochim Acta, 1972, 28A, 1721.

132. W.J. McKinney and A.I. Popov, J. Amer. Chem. Soc., 1969, 91, 5215.

133. B.L. Crawford and T. Fujiyama, J. Phys. Chem., 1969, 73, 4040.

133. (a) E.A. Moelwyn-Hughes, Physical Chemistry, Pergamon Press, 1961.

134. R.F. Lake and H.W. Thompson, Proc. Roy. Soc., 1967, A297, 440.

135. A.I. Popov and R.H. Rygg, J. Amer. Chem. Soc., 1957, 79, 4622.

136. K.R. Bhaskar and S. Singh, Spectrochimica Acta, 1967, 23A, 1155.

137. J. D'Hondt and Th. Zeegers-Huyskens, Mol. Struct., 1971, 10, 135.

138. S.G.W. Ginn, I. Haque and J.L. Wood, Spectrochimica Acta, 1968, 24A, 1531.

139. W.B. Person, R.E. Erickson and R.E. Buckles, J. Amer. Chem. Soc., 1960, 82, 29; W.B. Person, R.E. Erickson and R.E. Buckles, J. Chem. Phys., 1957, 27, 1211.

140. J.P. Jesson and H.W. Thompson, Spectrochimica Acta, 1958, 13, 217; G.L. Caldow, D. Cunliffe-Jones and H.W. Thompson, Proc. Roy. Soc., (London), 1959, 254A, 17.

141. E.J. Williams and J.A. Ladd, J. Mol. Struct., 1968, 2, 57.

142. B.H. Thomas and W.J. Orville-Thomas, J. Mol. Struct., 1971, 7, 123.

143. C.H. Townes and B.P. Dailey, J. Chem. Phys., 1949, 17, 782.

144. W.B. Person, R.E. Humphrey, W.A. Deskin and A.I. Popov, J. Amer. Chem. Soc., 1958, 80, 2049.

145. J. Yarwood, Spectroscopy Lett., 1972, 5, 193.

146. W.G. Rothschild
(a) Chem. Phys. Letters, 1971, 9, 149.
(b) J. Chem. Phys., 1971, 55, 1403.
(c) J. Chem. Phys., 1970, 53, 990.
(d) J. Chem. Phys., 1970, 53, 3265.
(e) Paper 22 at 24th Annual Reunion Meeting, Societe de Chimie Physique, Paris, July 1973.
(f) Paper given at Liége meeting on Molecular Dynamics of Complexes in Solution, Sept. 1974.

147. J.N. Murrel and V.M.S. Gil, Trans. Faraday Soc., 1965, 61, 402.

148. J.A. Ladd and V.I.P. Jones, Spectrochimica Acta, 1967, 23A, 2791; A.D. Buckingham, Can. J. Chem., 1960, 38, 300.

149. W.B. Person, R.E. Humphrey and A.I. Popov, 1959, 81, 273.

150. O.H. Ellestad, P. Klaboe and G. Hagen, Spectrochimica Acta, 1971, 27A, 1025.

151. R.S. Drago, J. Chem. Education, 1974, 5, 302.

152. R.G. Pearson
(a) J. Chem. Ed., 1968, 45, 58;
(b) J. Chem. Ed., 1968, 45, 643.

152. (c) R.G. Pearson and J. Songstad, J. Amer. Chem. Soc., 1967, 89, 1827.

153. M. Yamada, H. Saruyama, and K. Aida, Spectrochimica Acta, 1972, 28A, 439.

154. D.P. Craig, A. Maccoll, R.S. Nyholm, L.E. Orgel and L.E. Sutton, J. Chem. Soc., 1954, 332.

155. D.P. Craig and E.A. Magnusson, J. Chem. Soc., 1956, 4895.

156. D.P. Craig and C. Zauli, J. Chem. Phys., 1962, 37, 601.

157. M. Davies, G.W.F. Pardoe, J. Chamberlain, and H.A. Gebbie, Trans. Faraday Soc., 1970, 66, 273; S.K. Garg, J.E. Bertie, H. Kilp and C.P. Smyth, J. Chem. Phys., 1968, 49, 2551.

158. M. Davies, G.W.F. Pardoe, J.E. Chamberlain and H.A. Gebbie, Trans. Faraday Soc., 1968, 64, 847; S.G. Kroon and J. van der Elsken, Chem. Phys. Lett., 1967, 1, 285; Y. Leroy and E. Constant, C.R. Sci. Acad., 1966, 46, 396.

159. S.K. Garg, H. Kilp, C.P. Smyth, J. Chem. Phys., 1965, 43, 2341.

160. H.R. Wyss, R.D. Werder and Hs. H. Gunthard, Spectrochimica Acta, 1964, 20, 573; P. Delorme, J. Chim. Physique, 1964, 41, 437.

161. A. Mishra and A.D.E. Pullin, Aust. J. Chem., 1971, 24, 2493.

162. G.W. Chantry, 'Submillimetre Spectroscopy', Academic Press, New York and London, 1972, Chapter 11.

163. G.H. Wegdam, J.B. Tebeek, H. van der Linden and J. van der Elsken, J. Chem. Phys., 1971, 55, 5207.

164. R.M. Silverstein and G. Clayton Bassler, Spectrometric Identification of Organic Compounds, John Wiley and Sons Inc., New York, London.

165. D.H. Whiffen, Phil. Trans. Roy. Soc., 1955, A248, 131.

166. E.B. Wilson, J. Chem. Phys., 1939, 7, 1047.

167. E.B. Wilson, J. Chem. Phys., 1941, 9, 76.

168. E.B. Wilson, J.C. Decius and P.C. Cross, Molecular Vibrations, McGraw-Hill Inc., New York, 1955.

169. A.G. Maki and R. Forneris, Spectrochimica Acta, 1967, 23A, 867.

170. J.N. Gayles, J. Chem. Phys., 1968, 49, 1840.

171. J.R. Nielson and L.H. Berryman, J. Chem. Phys., 1949, 17, 659; E.L. Thomas, Ph.D. Thesis, University College Swansea, 1962.

172. B. Bak, L. Hansen-Nygard and J. Rastup-Andersen, J. Mol. Spectros., 1958, 2, 361.

173. B.L. Crawford and F.A. Miller, 1946, 14, 282.

174. J.H. Schachtschneider, Manual for G Matrix Evaluation Program; J.H. Schachtschneider and R.G. Snyder, Spectrochimica Acta, 1963, 19, 117.

175. M. Gussoni and G. Zerbi, J. Mol. Spectrosc., 1968, 26, 485.

176. W.J. Taylor, J. Chem. Phys., 1950, 18, 1301.

177. T. Magizawa, J. Chem. Phys., 1958, 29, 246.

178. G. Geiseler and G. Hanschmann, J. Mol. Struct., 1971, 8, 293.

179. M. Tranquille, P. Labarbe, M. Fouassier, and M.T. Forel, J. Mol. Struct., 1971, 8, 273.

180. R.D. Whittaker, J.R. Ambrose and C.W. Hickam, J. Inorg. Nucl. Chem., 1960, 17, 254; Journal of Inorg. Nucl. Chem., 1962, 24, 285-9.

181. R.D. Whittaker, J. Inorg. Nucl. Chem., 1964, 26, 1405.

182. O. Hassel and H. Hope, Acta. Chem. Scand., 1961, 15, 407.

183. J.A. Creighton, I. Haque and J.L. Wood, Chem. Comm., 1966, 229.